ABSTRACT

Title of Dissertation: FEEDBACK CONTROL OF BORDER COLLISION BIFURCATIONS IN PIECEWISE SMOOTH SYSTEMS

Monther A. Hasouneh, Doctor of Philosophy, 2003

Dissertation directed by: Professor Eyad H. Abed
Department of Electrical and Computer Engineering

Feedback control of border collision bifurcations in continuous piecewise smooth discrete-time systems is considered. These bifurcations occur when a fixed point or a periodic orbit of a piecewise smooth system crosses or collides with the border between two regions of smooth operation as a system parameter is quasistatically varied. The goal of the control effort in this work is to modify the bifurcation so that the bifurcated steady state is locally attracting and locally unique. In this way, the system's local behavior is ensured to remain stable and close to the original operating condition. Linear and piecewise linear feedbacks are used since the system linearization on the two sides of the border generically determines the type and stability properties of any border collision bifurcation.

A complete classification of possible border collision bifurcations is only available for one-dimensional maps. These classifications are used in the design of stabilizing feedback controls. For two dimensional piecewise smooth maps, sufficient conditions

for nonbifurcation with persistent stability are proved. The derived sufficient conditions are then used as a basis for the design of feedback controls to eliminate border collision bifurcations.

For higher dimensional piecewise smooth maps, only very general results on existence of certain types of border collision bifurcations are currently known. To address these problems Lyapunov techniques are used to find conditions for nonbifurcation with persistent local stability in general finite dimensional piecewise smooth discrete time systems depending on a parameter. A sufficient condition for nonbifurcation with persistent stability in PWS maps of any finite dimension is given in terms of linear matrix inequalities. This condition is then used as a basis for the design of feedback controls to eliminate border collision bifurcations in PWS maps and to produce desirable behavior. The Lyapunov-based methodology is used to consider the design of washout filter based controllers. These are dynamic feedback control laws that are designed so as not to alter a system's fixed points, even in the presence of model uncertainty. In addition, the Lyapunov-based approach is extended to allow nonmonotonically decreasing Lyapunov functions. Several examples are given to demonstrate the efficacy of the Lyapunov-based methods.

Finally, a two-dimensional example of using feedback to quench cardiac arrhythmia is considered. The cardiac model consists of a nonlinear discrete-time piecewise smooth system, and was previously used to show a link between cardiac alternans and period doubling bifurcation. In this work, it is first shown that the alternans exhibited by the model actually arise through a period doubling border collision bifurcation. The results of the thesis on feedback control of border collision bifurcation are then applied to the model, resulting in quenching of the bifurcation and hence in alternan suppression.

FEEDBACK CONTROL OF BORDER COLLISION

BIFURCATIONS IN PIECEWISE SMOOTH SYSTEMS

by

Monther A. Hasouneh

Dissertation submitted to the Faculty of the Graduate School of the
University of Maryland, College Park in partial fulfillment
of the requirements for the degree of
Doctor of Philosophy
2003

Advisory Committee:

Professor Eyad H. Abed, Chairman/Advisor
Associate Professor Raymond A. Adomaitis
Professor Balakumar Balachandran
Professor John S. Baras
Professor Edward Ott

DEDICATION

To my parents,

brothers and sisters

ACKNOWLEDGEMENTS

I would like to express my deepest gratitude to my advisor, Professor Eyad H. Abed, for his invaluable guidance, encouragement and support throughout my graduate studies at the University of Maryland. He has been a great source of inspiration throughout the years.

Thanks are also due to Professors Ramond A. Adomaitis, Balakumar Balachandran, John S. Baras and Edward Ott for serving on my Ph.D. dissertation committee. I am also grateful to Dr. David Elliott for his advice on research.

I would like to thank Dr. Helena E. Nusse of the University of Groningen for many helpful discussions on border collision bifurcations during her visits to College Park. I am also grateful to Dr. Soumitro Banerjee of IIT Kharagpur for helpful discussions during his visit to College Park in summer 2002.

This work was supported in part by the National Science Foundation under Grants ECS-01-15160, the Office of Naval Research under Grants CR4775430675 and N000140310103, and the Army Research Office under Grant DAAD190210319.

TABLE OF CONTENTS

LIST OF FIGURES

Chapter 1

Introduction

In this thesis, we develop stabilizing feedback control laws for piecewise smooth discrete-time systems exhibiting border collision bifurcations. By piecewise smooth systems we mean systems that are smooth everywhere except along borders separating regions of smooth behavior where the system is only continuous. Border collision bifurcations are bifurcations that occur when a fixed point (or a periodic orbit) of a piecewise smooth system crosses or collides with the border between two regions of smooth operation. In this work, the goal of the control effort is to modify the bifurcation so that the bifurcated steady state is locally unique and locally attracting. In this way, the system's local behavior is ensured to remain stable and close to the original operating condition. This is in the same spirit as local bifurcation control results for smooth systems, although the presence of a border complicates the bifurcation picture considerably. Indeed, a full classification of border collision bifurcations isn't available. So in this work, one of the main goals is to develop sufficient conditions for desirable (from a dynamical behavior viewpoint) cases.

The term border collision bifurcation was coined by Nusse and Yorke [61]. Border collision bifurcation had been studied in the Russian literature under the name

C-bifurcations by Feigin [27, 28]. Di Bernardo, Feigin, Hogan and Homer [23] introduced Feigin's results to the Western literature. Bifurcations in one-dimensional piecewise linear maps have been also studied by Hsu, Kreuzer and Kim [41]. Border collision bifurcations include bifurcations that are reminiscent of the classical bifurcations in smooth systems such as fold and period doubling bifurcations. Despite such resemblances, the classification of border collision bifurcations (BCBs) is far from complete, and certainly very preliminary in comparison to the results available in the smooth case. In smooth maps, a bifurcation occurs from a one-parameter family of fixed points when a real eigenvalue or a complex conjugate pair of eigenvalues crosses the unit circle. In piecewise smooth (PWS) maps, on the other hand, a border collision bifurcation can occur when a fixed point (or a periodic orbit) crosses or collides with the border between two regions of smooth behavior. This involves a discontinuous change in the eigenvalues of the Jacobian matrix evaluated at the fixed point (or at a periodic point) when the fixed point hits the border. As a result, border collision bifurcations for piecewise smooth systems in which the one-sided derivatives on the border are finite are classified based on the linearizations of the system on both sides of the border at criticality.

The classification of border collision bifurcations is complete only for one dimensional discrete-time systems [62, 73, 10]. Concerning two-dimensional piecewise smooth maps, Nusse and Yorke [61] and Nusse, Ott and Yorke [60] gave a general criterion for the occurrence of BCBs based on index theory. This criterion gives a sufficient condition for the occurrence of a border collision bifurcation. Moreover, a normal form for BCBs in two-dimensional PWS maps was derived [61]. Yuan [73] studied BCBs in dissipative PWS maps where it was assumed that the determinants of the Jacobian matrices on both sides of the border are equal. Banerjee and Gre-

bogi [9] proposed a classification for a class of two-dimensional (dissipative) maps undergoing border collision bifurcations by exploiting a normal form. However, the classification was largely based on heuristic arguments, and it will be shown in the thesis that some aspects of the classification do not hold. It has also recently been shown by Banerjee, Yorke and Grebogi [12] that the dynamics of two-dimensional piecewise-smooth (PWS) maps may feature so-called robust chaotic dynamics without parameter windows of periodic behavior. Dutta et al. [25] presented a novel analysis showing border collision bifurcations in which multiple coexisting attractors are created simultaneously causing the intriguing phenomenon that in the presence of arbitrarily small noise, the bifurcations lead to fundamentally unpredictable behavior as a system parameter is varied slowly through its bifurcation value. For higher dimensional systems, currently the known results are limited to very general results on existence of certain types of border collision bifurcations [60, 23].

Since the initial studies of border collision bifurcations, several researchers have studied bifurcations in PWS systems [60, 63, 7, 8, 74, 9, 10, 11, 23, 45, 52, 77, 76, 51, 24, 66]. PWS systems occur as models for switched systems, such as power electronic circuits (e.g., [74, 19, 45, 55, 66]) and impacting mechanical systems (e.g., [58, 33, 59, 18, 64, 52, 51]). They are usually modeled by piecewise smooth maps. In this work, we only consider piecewise smooth discrete-time systems with Jacobian matrices on both sides of the border having finite elements. This excludes piecewise smooth systems that have a singularity on the border, as in impacting mechanical systems.

Bifurcations in piecewise-smooth continuous-time systems were studied in [52]. Such bifurcations were called “discontinuous bifurcations.” It was demonstrated by examples that PWS systems exhibit a variety of possible border collision bifurca-

tions as equilibrium points or periodic orbits cross hypersurfaces separating regions of smooth behavior as a system parameter is slowly varied through a critical value. The discontinuous jump of the eigenvalues of the Jacobian matrix as a periodic orbit hits the border was conjectured to be a necessary condition for a bifurcation to occur [52]. These bifurcations are similar to border collision bifurcations observed in earlier work on PWS maps [61, 60, 62, 23]. Di Bernardo et al. [21] analyzed a so-called corner-collision bifurcation (which is a type of border-collision bifurcation) in piecewise-smooth systems of ordinary differential equations. Other examples of border collision bifurcations in continuous time PWS systems appeared in [77, 76]. In [77], it was shown that BCBs occur in relay control systems with hysteresis and dead zone nonlinearities.

Piecewise-smooth discrete time maps are used to model systems that are inherently discrete. For example, it has been recently shown that simple computer networks with Transmission Control Protocol (TCP) connections and implementing a Random Early Detection (RED) algorithm at the router end can be modeled as one-dimensional PWS maps [31]. Analysis of such models has revealed that various border collision bifurcations leading to oscillations and chaos occur as a system parameter is quasistatically varied [65]. Another example of a PWS discrete time computer network model was analyzed in [70]. It was shown that various kinds of BCBs occur in such a model. Other examples of PWS discrete time systems which have been shown to exhibit BCBs can be found in economics (e.g., [40]), biology (e.g., [69]) and in controlled linear discrete time systems with PWS nonlinearity (e.g., [7]). Piecewise smooth systems can of course exhibit classical smooth bifurcations, for example at a fixed point in a neighborhood of which the system is smooth. What is of interest therefore is the study of bifurcations in PWS systems that occur at the boundaries between regions of

smooth behavior, or that involve motions that include more than one such region.

In this work, the goal is to obtain feedback control laws to ensure a less severe form of border collision bifurcation than could otherwise occur. Since a full classification of possible border collision bifurcations isn't available, it is crucial that sufficient conditions for the desirable border collision bifurcations be derived. In particular, we are interested in obtaining sufficient conditions for *nonbifurcation with persistent stability*. That is, conditions under which the PWS map possesses a locally asymptotically stable fixed point which is also the locally unique attractor for all values of μ in a neighborhood of the critical value.

It should be emphasized that, while this work focuses on maps, the results have implications for switched continuous-time systems as well. Maps provide a concise representation that facilitates the investigation of system behavior and control design. They are also the natural models for many applications, as mentioned above. Even for a continuous-time piecewise smooth system, a control design derived using the map representation can be translated to a continuous controller either analytically or numerically.

There is little past work on control of BCBs [20, 22]. The control method of [20, 22] is based on the classification scheme of BCBs that was given by Feigin [23]. However, since Feigin didn't give conditions for specific scenarios, the results of [20, 22] do not address stabilization. Also, references [20, 22] use a trial and error approach that doesn't provide analytical conditions for existence of controllers. Moreover, the work in [20, 22] does not take into account the fact that the classification scheme of BCBs of Feigin, on which their control scheme is based, applies only to PWS maps that are continuous. Thus, the control they introduce may lead to unpredictable bifurcations if the control action introduces discontinuities into the map. In the present

work, a more careful analysis is performed to obtain sufficient conditions for desirable (from a dynamical behavior viewpoint) cases, which is then used in the design of stabilizing feedback controls.

The dissertation proceeds as follows. In the next chapter, theoretical background material employed in subsequent chapters is collected. The topics include bifurcations in smooth maps, bifurcation control, washout filters, border collision bifurcations and linear matrix inequalities.

In Chapter 3, a summary of possible border collision bifurcations in piecewise smooth maps of dimension one is given as well as some new results. In particular, we show that subcritical period doubling border collision can occur in one dimensional piecewise smooth maps. We also determine stability of the fixed point at criticality for all possible border collision bifurcations. The stability of the fixed point at criticality is then related to the nature of the border collision bifurcation that occurs.

In Chapter 4, the classification of border collision bifurcations presented in Chapter 3 is used in the design of stabilizing feedback control laws to modify the border collision bifurcation to one that is less severe. Linear and piecewise linear feedback control is used since the normal form for BCBs contains only linear terms. The feedback can either be applied on one side of the border and not the other, or on both sides of the border. Both approaches are considered. To achieve robustness to uncertainties in the location of the border, *simultaneous control* is considered— that is, controls are sought that function in exactly the same way on both sides of the border, while stabilizing the system's behavior. Not surprisingly, the conditions for existence of simultaneously stabilizing controls are more restrictive than for the existence of one sided controls.

In Chapter 5, we present new results on border collision bifurcations in two di-

mensional piecewise smooth maps. First, a new border collision bifurcation which we call "dangerous border collision bifurcation" is presented. This bifurcation occurs in two dimensional piecewise smooth maps in spite of the fact that the Jacobian matrices on both sides of the border are Schur stable. We then present examples of multiple attractor bifurcations that occur in two dimensional PWS maps even though the Jacobian matrices of the PWS system on both sides of the border are Schur stable. Sufficient conditions for nonbifurcation with persistent stability in two dimensional PWS maps are stated and proved.

In Chapter 6, the nonbifurcation with persistent stability results of Chapter 5 are used in the design of stabilizing feedback controls. Both Simultaneous control design (same control acting on both sides of the border) and switched control design are considered.

In Chapter 7, Lyapunov-based techniques are used in the analysis of finite dimensional piecewise smooth discrete time systems that depend on a parameter. The use of Lyapunov techniques facilitates the consideration of n-dimensional systems where n is not restricted to be 1 or 2 as in previous chapters. A sufficient condition for nonbifurcation with persistent stability in PWS maps of any finite dimension is given in terms of linear matrix inequalities. This condition is then used as a basis for the design of feedback controls to eliminate border collision bifurcations in PWS maps and to produce desirable behavior. The Lyapunov-based methodology is used to consider the design of washout filter based controllers. These are dynamic feedback control laws that are designed so as not to alter a system's fixed points, even in the presence of model uncertainty. In addition, the Lyapunov-based approach is extended to allow nonmonotonically decreasing Lyapunov functions. Several examples are given to demonstrate the efficacy of the Lyapunov-based methods.

In Chapter 8, the quenching of alternans (cardiac arrhythmia) exhibited as solutions of a cardiac conduction model is considered. The model consists of a nonlinear discrete-time piecewise smooth system, and was previously used to show a link between cardiac alternans and period doubling bifurcation. In this chapter, it is first shown that what actually occurs is a period doubling border collision bifurcation, and that it is this bifurcation that leads to the alternans. The results of the dissertation on feedback control of border collision bifurcation are then applied to the model, resulting in quenching of the bifurcation and hence in alternan suppression.

In Chapter 9, we collect concluding remarks and discuss possible directions for future research. Some of the results reported in this thesis were published in various journal and conference papers [37, 38, 36, 39].

Chapter 2

Preliminary Material

In this chapter, we collect theoretical background material that will be employed in the sequel. The topics we discuss include: bifurcations in smooth maps, bifurcation control, washout filters, border collision bifurcations and linear matrix inequalities.

2.1 Background on Bifurcation and Bifurcation Control in Smooth Maps

A bifurcation is a qualitative change in steady state behavior of a dynamical system resulting from small parameter changes. Thus, the number and/or type of steady state behaviors change at a critical value of the parameter, referred to as the bifurcation parameter. Bifurcation is closely tied to stability, since parameter changes that maintain asymptotic stability of an equilibrium point cannot lead to a bifurcation of the equilibrium.

Next, a brief summary of possible bifurcations in smooth discrete time systems is given. The purpose of presenting this summary here is that bifurcations in smooth discrete time systems can be compared with those in piecewise smooth systems. Details

on bifurcations in smooth discrete time systems and smooth continuous time systems can be found, for example, in [35, 71, 47].

Consider the case of an n-dimensional smooth discrete time system

$$x(k+1) \quad = \quad f(x(k),\mu) \tag{2.1}$$

where $f : \mathbb{R}^n \times \mathbb{R} \to \mathbb{R}^n$, $\mu \in \mathbb{R}$ is the bifurcation parameter and f is assumed smooth in x and μ. For a discrete time dynamical system which depends on a single parameter, there are three types of local bifurcation from a fixed point. (Local bifurcations involve qualitative changes occurring within a small neighborhood of a fixed point.) The first case occurs when a single eigenvalue crosses the unit circle through the point $+1$ (see Figure 2.1). This is called saddle-node bifurcation, tangent bifurcation or fold bifurcation. The second case occurs when one eigenvalue crosses the unit circle through the point -1 (see Figure 2.1). This case is called period doubling or flip bifurcation. The third case occurs when a complex conjugate pair of eigenvalues crosses the unit circle (see Figure 2.2). This is known as Neimark-Sacker bifurcation, secondary Hopf bifurcation, or Hopf bifurcation for maps.

2.1.1 Bifurcation Control

The simplest type of control for systems exhibiting bifurcations is the use of linear feedback to delay the onset of instability in a smooth control system. By delaying the instability, any associated bifurcation is also delayed. However, other goals can be pursued that are more closely tied to control of the nonlinear dynamic aspects of bifurcations. For example, using feedback to render supercritical an otherwise subcritical bifurcation was studied by Abed and Fu [4, 1] under the name local bifurcation control. A review of this and subsequent work on bifurcation control is available in [3].

In bifurcation control for smooth systems as discussed by Abed and Fu [4, 1], it was natural to use nonlinear feedback to alter the bifurcation characteristics of the system in the desired way. However, linear feedback plays the dominant role in control of border collision bifurcations because the map linearizations on both sides of the border determine the nature of the BCBs.

In this work, bifurcation control goals are pursued for border collision bifurcations in piecewise smooth maps. Because of the focus on piecewise smooth maps, the previous results on bifurcation control of smooth systems are not applicable here. However, the previous work provides useful motivation in the sense of stating appropriate control goals. In addition, some of the techniques found to be useful in controlling bifurcations in smooth systems are also employed here. In particular, washout filter-aided feedback is used to ensure that system operating points aren't moved by the feedback control even in the presence of model uncertainty.

2.1.2 Washout Filter-Aided Feedback

A washout filter (also sometimes called a washout circuit) is a high pass filter that washes out (rejects) steady state inputs, while passing transient inputs [13]. Washout filter-aided controllers for continuous time systems are discussed by Lee and Abed [50], Lee [49], and Wang and Abed [72]. A typical discrete-time washout filter is described by

$$w_{k+1} = x_k + (1-d)w_k \tag{2.2}$$

$$z_k = x_k - dw_k \tag{2.3}$$

where x_k is a state variable of a dynamical system (or map) to be controlled, w_k is the state of the corresponding washout filter, z_k is the output of the washout filter, and d

is the washout filter constant ($0 < d < 2$ for a stable filter). In general, the number of washout filters needed can be any number between 1 and the dimension of the system.

The control law is taken in the form of a static function of the washout filter output z_k, namely $u_k = u(z_k)$ with $u(0) = 0$. Note that since its by nature z_k vanishes at steady state, the fixed points of the map are not shifted by the control. Other advantages of using washout filters include automatic following of equilibrium points even in the presence of model uncertainty or parameter drift. For smooth maps, the function u often needs to include nonlinear terms to meet the control objectives. As mentioned above, however, for BCBs the linear terms in u are essential to ensuring that the bifurcation is of the desired type.

Washout filter-aided feedback was used in control design for smooth systems exhibiting bifurcation in references [2, 53, 50, 72].

2.2 Border Collision Bifurcations

In this section, we collect some known results on border collision bifurcations. First, the results of Nusse and Yorke [61] and Nusse, Ott and Yorke [60] on border collision bifurcation are summarized followed by the results of Feigin [23].

2.2.1 Border Collision Bifurcation: The Work of Nusse, Yorke and Ott

As discussed in the introduction, border collision bifurcations were named by Nusse and Yorke [61, 60]. They gave a general criterion for the occurrence of border collision bifurcations in PWS maps based on index theory. Next, we recall some definitions that are needed to state their border collision bifurcation theorem.

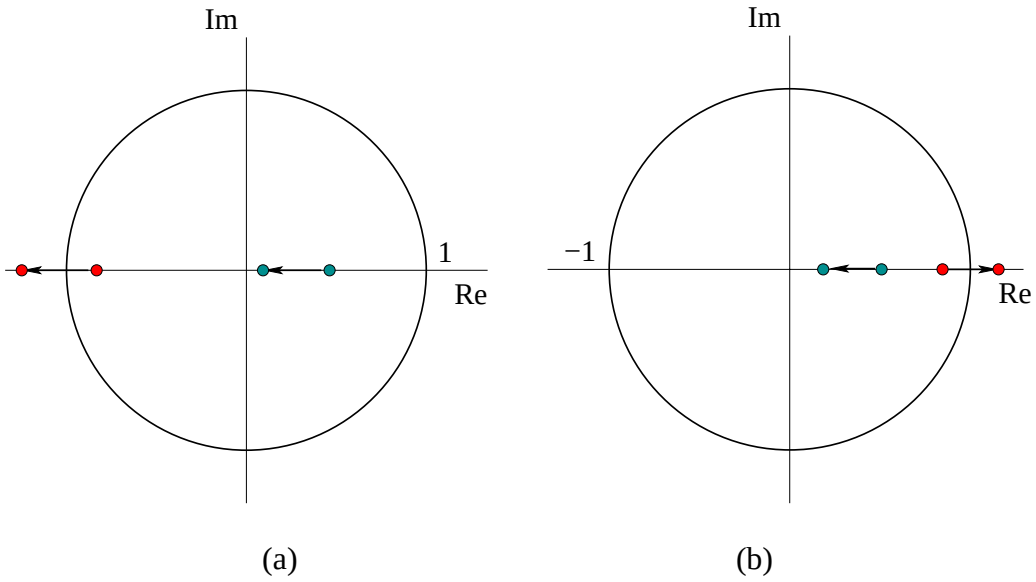

Figure 2.1: Eigenvalues change continuously as a bifurcation parameter is changed through a critical value in smooth maps. (a) Period-doubling bifurcation, (b) Saddle-node bifurcation.

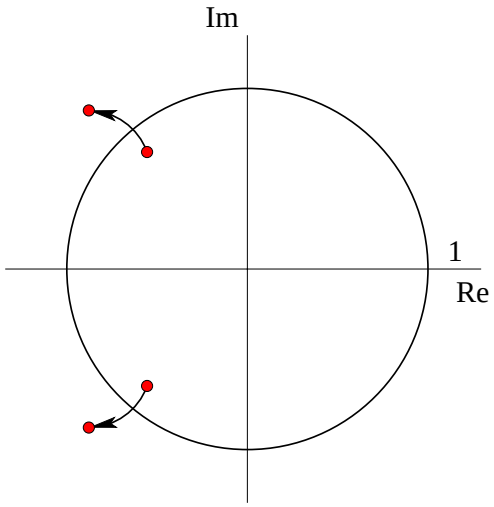

Figure 2.2: Eigenvalues change continuously at a Neimark-Sacker bifurcation as a bifurcation parameter is changed through a critical value in smooth maps.

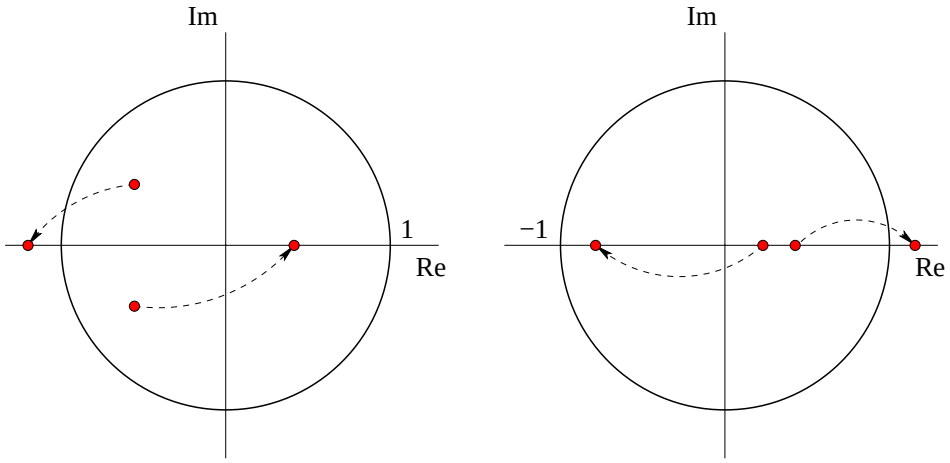

Figure 2.3: Eigenvalues undergoing a discontinuous jump as a bifurcation parameter is changed through a critical value in piecewise smooth maps (a) Period-doubling border collision bifurcation, (b) Saddle-node border collision bifurcation.

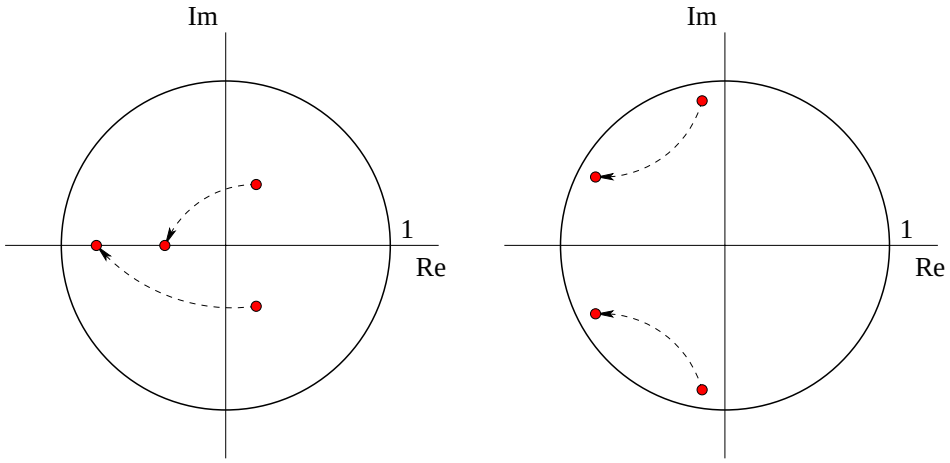

Figure 2.4: Eigenvalues undergoing a discontinuous jump as a bifurcation parameter is changed through a critical value in piecewise smooth maps. (a) Possible multiple attractor border collision bifurcation, (b) Possible dangerous border collision bifurcation.

Consider a PWS map that involves two regions of smooth behavior:

$$f(x,\mu) = \begin{cases} f_A(x,\mu), & x \in R_A \\ f_B(x,\mu), & x \in R_B \end{cases} \tag{2.4}$$

where $f : \mathbb{R}^n \times \mathbb{R} \to \mathbb{R}^n$ is piecewise smooth in x, smooth everywhere except on the border separating R_A and R_B, where it is continuous, f is smooth in the bifurcation parameter μ and R_A, R_B are two regions of smooth behavior separated by a smooth surface.

Let $x(\mu)$ be a fixed point of f and suppose that for $\mu = \mu_b$, $x(\mu_b)$ is on the border separating R_A and R_B. Assume without loss of generality that $\mu_b = 0$. Suppose also that $x(\mu)$ exists for $-\varepsilon < \mu < \varepsilon$. The fixed point $x(\mu)$ is called a border crossing fixed point [61, 60] if it crosses the border between R_A and R_B as μ is varied through 0.

Definition 2.1 ([61, 60]) An orbit of period-p is typical if its Jacobian matrix exists (i.e., the Jacobian matrix of the pth iterate of the map at a point of the orbit) and neither $+1$ nor -1 is an eigenvalue of this Jacobian matrix.

The orbit index is a number associated with a periodic orbit, and this number is useful in understanding patterns of bifurcations the orbit undergoes. For typical periodic orbits, the orbit index is -1, 0, or $+1$. The orbit index is a bifurcation invariant in the sense that if one examines the periodic orbits that collapse to the fixed point $x(\mu)$ as $\mu \to 0$, and adds the orbit indexes of the periodic orbits that exist just before a bifurcation, then that sum equals the corresponding sum just after that bifurcation [61].

Suppose a typical periodic orbit (PO) of a map f has a (minimum) period p. The orbit index of that orbit depends on the eigenvalues of the Jacobian matrix A_p of the map f^p (the pth iterate of f) at one of the points in PO.

Definition 2.2 ([61, 60]) Let I_{PO} be the orbit index of a PO. Let m be the number of real eigenvalues of A_p smaller than -1, and let n be the number of real eigenvalues of A_p greater than $+1$. The orbit index is defined by

$$I_{PO} = \begin{cases} 0, & \text{if } m \text{ is odd,} \\ -1, & \text{if } m \text{ is even and } n \text{ is odd,} \\ +1, & \text{if both } m \text{ and } n \text{ are even.} \end{cases} \tag{2.5}$$

Definition 2.3 ([61, 60]) A periodic orbit PO is an *isolated border crossing orbit* if (1) PO includes a point that is a border crossing fixed point under some iterate of the map, and (2) the orbit PO is isolated in phase space when $\mu = 0$. That is, in the plane there exists a neighborhood U of the orbit PO such that PO is the only periodic orbit in U when $\mu = 0$.

Next, we recall the border collision bifurcation theorem of Nusse and Yorke [61].

Theorem 2.1 ([61]) **Border Crossing Border Collision Bifurcation)**
For each two-dimensional piecewise smooth map that depends smoothly on a parameter μ, if the index of an isolated border crossing orbit changes as μ crosses 0, then at $\mu = 0$ a bifurcation occurs at this point, a bifurcation involving at least one additional periodic orbit.

The assertion of Theorem 2.1 apply to general piecewise smooth maps of dimension n [60].

Theorem 2.1 says that additional fixed points or periodic orbits must bifurcate from $x(\mu)$ at $\mu = 0$ if the orbit index changes. These bifurcating orbits need not be stable. As an example consider the supercritical period-doubling BCB. Suppose that for $\mu < 0$ there is a locally unique and locally attracting fixed point, the total index is

$+1$. Suppose also that for $\mu > 0$ there is a flip saddle (orbit index 0) and a period-2 attractor (orbit index $+1$). (Note that the two points of the period-2 orbit are collectively assigned $+1$.) Hence, the sum of the orbit indexes before and after the BCB is $+1$. In other words, a border collision bifurcation is a bifurcation at a fixed point (or periodic point) on the border of two regions when the orbit index of the fixed point (or periodic point) before the collision with the border is different from the orbit index of the fixed point after the collision.

We remark that Theorem 2.1 gives a sufficient condition for the occurrence of border collision bifurcation, and this condition is not necessary. One can easily find examples where border crossing border collision bifurcation occurs while the index of the crossing orbit does not change. For instance, if the eigenvalues of the Jacobian matrices of a two dimensional PWS map on both sides of the border are complex with absolute values less than one (i.e., the eigenvalue lie inside the unit circle), then the orbit index is zero before and after the bifurcation. This does not imply that no border collision bifurcation occurs. Indeed bifurcations of the form "fixed point attractor plus period-p_1 attractor to fixed point attractor plus period-p_2 attractor" are possible, where p_1, p_2 are positive integers greater than two (some examples of this type of BCB are given in Chapter 5). Moreover, Theorem 2.1 does not consider the case when the fixed point $x(\mu)$ exists on one side of the border only. In such a situation, the fixed point collides with the border (and possibly with other periodic orbits) and disappears. This is the case in a border collision pair bifurcation (or saddle node border collision bifurcation) where two fixed points on one side of the border merge at the border and disappear.

Nusse and Yorke [61] showed that for two-dimensional piecewise smooth maps, a

normal form for border collision bifurcation is given by

$$\begin{pmatrix} x_{k+1} \\ y_{k+1} \end{pmatrix} = \begin{cases} \begin{pmatrix} \tau_A & 1 \\ -\delta_A & 0 \end{pmatrix} \begin{pmatrix} x_k \\ y_k \end{pmatrix} + \begin{pmatrix} 1 \\ 0 \end{pmatrix} \mu, & x_k \leq 0 \\ \begin{pmatrix} \tau_B & 1 \\ -\delta_B & 0 \end{pmatrix} \begin{pmatrix} x_k \\ y_k \end{pmatrix} + \begin{pmatrix} 1 \\ 0 \end{pmatrix} \mu, & x_k > 0 \end{cases} \tag{2.6}$$

where τ_A and δ_A are the trace and the determinant of the limiting Jacobian matrix in R_A evaluated at a fixed point at the border. Similarly, τ_B and δ_B are the trace and the determinant of the limiting Jacobian matrix in R_B evaluated at a fixed point on the border. If the limiting Jacobian matrices with limits taken on both sides of the border have no eigenvalues on the unit circle, then border collision bifurcation that occurs in the original system before transformation can be studied by using the normal form [61, 9, 23]. Examples of various border collision bifurcations that can occur in two dimensional PWS maps can be found in [61]. The normal form (2.6) was used in [74, 9] to study BCBs in a class of two-dimensional PWS maps. It was demonstrated that, depending on the eigenvalues of the Jacobian matrices on both sides of the border, various possible BCBs occur [74, 9].

2.2.2 Border Collision Bifurcation (or C-bifurcation): The Work of Feigin

Border collision bifurcations have been studied in the Russian literature under the name *C*-bifurcation [27, 28, 23]. The letter *C* is derived from the Russian word *shivanije* meaning sewing [23]. Di Bernardo, Feigin, Hogan and Homer [23] introduced Feigin's results to the Western literature.

Below, the main results of Feigin are summarized. Consider the one parameter

family of piecewise smooth maps

$$f(x,\mu) \quad = \quad \begin{cases} f_A(x,\mu), & x \in R_A \\ f_B(x,\mu), & x \in R_B \end{cases} \tag{2.7}$$

where $f : \mathbb{R}^{n+1} \to \mathbb{R}^n$ is piecewise smooth in x; f is smooth in x everywhere except on the border (hypersurface Γ) separating R_A and R_B where it is only continuous, f is smooth in μ and R_A, R_B are the two (nonintersecting) regions of smooth behavior. In this work, we are interested in studying the dynamics of f at a fixed point (or a periodic orbit) near or at the border Γ. If the fixed point (or periodic orbit) is in R_A (respectively R_B) and is away from the border, then the dynamics is merely determined by the map f_A (respectively f_B). If on the other hand, the fixed point is close to the border, then jumps across the border can occur except in an extremely small neighborhood of the fixed point. Therefore, for operation close to the border, both f_A and f_B are needed in the study of the possible behavior. For a fixed point at or near the border, the dynamics is determined by the linearizations of the map on both sides of the border.

Border collision bifurcations occurring in the map (2.7) can be studied using the piecewise-linearized representation [23]

$$x(k+1) := F_\mu(x(k)) \quad = \quad \begin{cases} Ax(k) + b\mu, & x_1(k) \leq 0 \\ Bx(k) + b\mu, & x_1(k) > 0 \end{cases} \tag{2.8}$$

where A is the linearization of the PWS map f in R_A at a fixed point on the border approached from points in R_A near the border and B is the linearization of f at a fixed point on the border approached from points in R_B and b is the derivative of the map f with respect to μ. The coordinate system is chosen such that the sign of the first component of the vector x determines whether x is in R_A or R_B (a transformation to the form (2.8) is given in Appendix 9). If $x_1 = 0$, then x is on the border separating

R_A and R_B. The continuity of F_μ at the border implies that A and B differ only in their first columns.

The classification of border collision bifurcations (BCBs) depends on the eigenvalues of A and B [23]. A complete classification of BCBs is only available for one dimensional PWS maps. For two dimensional PWS maps, some results are available that only address a class of 2-D PWS maps [61, 73, 9].

Although Feigin [23] studied general n-dimensional PWS maps exhibiting border collisions, only very general conditions for existence of a fixed point and period-2 solutions before and after the border were given. The classification scheme of [23] does not give any information about stability or uniqueness of fixed points or period-2 orbits involved in the border collision bifurcation nor does it give information about higher period periodic orbits or chaos that might be involved in a border collision bifurcation.

Next, we recall the main results of [23]. Assume that $1 \notin \sigma(A)$, $1 \notin \sigma(B)$ (i.e., both $I-A$, $I-B$ are nonsingular). Formally solving for the fixed points of (2.8), we obtain $x_A(\mu) = (I-A)^{-1}b\mu$ and $x_B(\mu) = (I-B)^{-1}b\mu$. For $x_A(\mu)$ to actually occur, the first component of $x_A(\mu)$ must be nonpositive, i.e., $(e^1)^T\mu(I-A)^{-1}b \leq 0$. Similarly, for $x_B(\mu)$ to actually occur, we need $(e^1)^T\mu(I-B)^{-1}b > 0$. If on the other hand, the first component of $x_A(\mu)$ is positive (the first component of $x_B(\mu)$ is nonpositive), then the fixed point is called a virtual fixed point. Virtual fixed points are important in studying the dynamics of a PWS map near the border.

Let $p_A(\lambda)$ and $p_B(\lambda)$ be the characteristic polynomials of A and B, respectively. Then, $p_A(\lambda) = \det(\lambda I - A)$ and $p_B(\lambda) = \det(\lambda I - B)$.

Below, some definitions and notations are recalled from [23].

Definition 2.4 ([23]) Let

$\sigma_A^- :=$ number of real eigenvalues of A which are less than -1,

$\sigma_B^- :=$ number of real eigenvalues of B which are less than -1,

$\sigma_A^+ :=$ number of real eigenvalues of A which are greater than 1,

$\sigma_B^+ :=$ number of real eigenvalues of B which are greater than 1,

$\sigma_{AA}^+ :=$ number of real eigenvalues of A^2 which are greater than 1,

$\sigma_{AB}^+ :=$ number of real eigenvalues of AB which are greater than 1.

Three main events can take place as μ is increased (decreased) through zero [23]:

- A fixed point (periodic orbit) exists on one side of the border for $\mu < 0$ is smoothly changed into another fixed point (periodic orbit) on the other side of the border for $\mu > 0$ if

$$p_A(1)p_B(1) > 0 \iff \sigma_A^+ + \sigma_B^+ \text{ is even} \tag{2.9}$$

- Two fixed points (periodic orbits) exist on one side of the border for $\mu < 0$ (or $\mu > 0$) merge and annihilate each other as μ approaches zero if

$$p_A(1)p_B(1) < 0 \iff \sigma_A^+ + \sigma_B^+ \text{ is odd} \tag{2.10}$$

- A new period-2 solution bifurcates at $\mu = 0$ if

$$p_A(-1)p_B(-1) < 0 \iff \sigma_A^- + \sigma_B^- \text{ is odd} \tag{2.11}$$

The condition (2.10) is analogous to saddle node bifurcation in smooth maps, where two fixed points merge and disappear at the bifurcation.

From the summary on the theoretical results available to-date on border collision bifurcations, it is clear that the theory is general in nature and not much is available

in the way of clear sufficient conditions for the various types of BCBs either in the n-dimensional case or in the two-dimensional case. It is not our purpose in this work to fill in all the gaps in the mathematical theory of BCBs. Rather, since our ultimate goal in this thesis is the development of control techniques for BCBs, we are most interested in conditions guaranteeing the less severe forms of BCBs. In later chapters, we address the question of obtaining sufficient conditions for *nonbifurcation with persistent stability* . That is, conditions under which local asymptotic stability of the fixed point of a PWS map is maintained and no border collision bifurcation occurs as the bifurcation parameter is varied through its critical value.

2.3 Linear Matrix Inequalities (LMIs)

Linear matrix inequalities (LMIs) have attracted a lot of attention in recent years. They emerged as a powerful design tool in many areas including control engineering and structural design. The main reason that makes LMI techniques appealing is the development of many efficient algorithms for solving convex optimization problems [14]. LMIs are particularly useful in situations where no analytical solution is available. A large number of control problems have been recognized to be reducible to LMI-based optimization problems, and efficient software tools for solving these optimization problems exist (see [14, 34] and references therein).

A linear matrix inequality is any constraint of the form [14, 34]

$$A(x) := A_0 + x_1 A_1 + \cdots + x_m A_m < 0 \tag{2.12}$$

where

- $x = (x_1, x_2, \cdots, x_m)$ is a vector of unknown scalars usually called the decision or optimization variables.

- The matrices $A_0, A_1, \cdots, A_m$ are given symmetric matrices.
- The inequality sign "$<$" stands for negative definite. That is, $A(x) < 0 \iff u^T A(x) u < 0, \forall\, u \neq 0$. Equivalently, the largest eigenvalue of $A(x)$ is negative.

The solution set of the LMI (2.12) given by $S := \{x \in \mathbb{R}^m |\ A(x) < 0\}$ is convex and is called the feasible set (since (2.12) represents the constraints in an optimization problem). To see that S is convex, let $u, v \in S$ and $\lambda \in [0,1]$. Since $A(x)$ is affine in x, we have

$$A(\lambda u + (1-\lambda)v) = \lambda A(u) + (1-\lambda)A(v) < 0. \tag{2.13}$$

Below, we collect some useful properties of LMIs.

Intersection: If $G(x) < 0$ and $H(x) < 0$ are LMIs, then so is

$$\begin{pmatrix} G(x) & 0 \\ 0 & H(x) \end{pmatrix} < 0. \tag{2.14}$$

A point $x \in \mathbb{R}^n$ is feasible for the intersection of two LMIs if and only if it is feasible for each of the original LMIs.

Scaling: For $\alpha > 0$

$$G(x) < 0 \quad \iff \quad \alpha G(x) < 0 \tag{2.15}$$

Similarity: Suppose $G : \mathbb{R}^m \to \mathbb{R}^n$, and $H \in \mathbb{R}^{n \times p}$ has $ker(H) = \{0\}$. Then

$$G(x) < 0 \quad \iff \quad H^T G(x) H < 0 \tag{2.16}$$

Lemma 2.1 [14] **(Schur Complement)**

The following inequalities

$$R > 0 \tag{2.17}$$

$$Q - SR^{-1}S^T > 0 \tag{2.18}$$

where $Q = Q^T$ and $R = R^T$ are equivalent to

$$\begin{pmatrix} Q & S \\ S^T & R \end{pmatrix} > 0 \tag{2.19}$$

In other words, the set of nonlinear inequalities (2.17)-(2.18) can be represented as the LMI (2.19).

Lemma 2.2 [57] **(Schur Complement: Alternative Form)**

Inequalities (2.17)-(2.18) and (2.19) are equivalent to

$$Q > 0 \tag{2.20}$$

$$R - S^T Q^{-1} S > 0 \tag{2.21}$$

and

$$\begin{pmatrix} R & S^T \\ S & Q \end{pmatrix} > 0 \tag{2.22}$$

respectively.

Proof: Note that

$$\begin{pmatrix} R & S^T \\ S & Q \end{pmatrix} = \begin{pmatrix} 0 & I \\ I & 0 \end{pmatrix} \begin{pmatrix} Q & S \\ S^T & R \end{pmatrix} \begin{pmatrix} 0 & I \\ I & 0 \end{pmatrix} \tag{2.23}$$

The equivalence between (2.19) and (2.22) follows using the similarity property (2.16) of LMIs. The LMIs (2.20)-(2.21) follow from an application of the Schur complement to (2.22). ■

Linear Inequalities as LMIs [48]:

Let $x \in \mathbb{R}^n$, $b_i \in \mathbb{R}$ and $c_i \in \mathbb{R}^n$, $i = 1, \cdots, m$ be column vectors. The linear constraints

$$\begin{aligned} c_1^T x &< b_1 \\ c_2^T x &< b_2 \\ &\vdots \\ c_m^T x &< b_m \end{aligned}$$

can be expressed as a diagonal LMI

$$\begin{pmatrix} c_1^T x - b_1 & & & \\ & c_2^T x - b_2 & & \\ & & \ddots & \\ & & & c_m^T x - b_m \end{pmatrix} < 0. \tag{2.24}$$

Chapter 3

Border Collision Bifurcation in One Dimensional Maps

The purpose of this chapter is to provide a summary of known results on border collision bifurcation for one-dimensional (1-D) piecewise smooth (PWS) maps and to give several results on BCBs for 1-D maps that haven't been reported previously. These results will be used in Chapter 4 in designing stabilizing feedback controllers for 1-D maps.

3.1 Mathematical Setting and Normal Form

The analysis of border collision bifurcations (BCBs) in 1-D PWS maps is straightforward. There are two main ingredients in the analysis: (i) an observation about normal forms being affine (for fixed points on borders), and (ii) sketches that clarify how fixed points and periodic points depend on the bifurcation parameter for the scenarios associated with the various cases. For simplicity, a PWS map is considered that involves only two regions of smooth behavior.

Consider the 1-D PWS system

$$x_{k+1} = f(x_k, \mu) \tag{3.1}$$

where the map $f(x,\mu)$ takes the form

$$f(x,\mu) = \begin{cases} f_A(x,\mu), & x \le x_b \\ f_B(x,\mu), & x \ge x_b \end{cases} \tag{3.2}$$

and where μ is the bifurcation parameter. Since the system is one-dimensional, the border is just the point x_b. The map $f : \mathbb{R}\times\mathbb{R} \to \mathbb{R}$ is assumed to be PWS: f depends smoothly on x everywhere except at x_b, where it is continuous in x. It is also assumed that f depends smoothly on μ everywhere. Denote by R_A and R_B the two regions in state space separated by the border: $R_A := \{x :\ x \le x_b\}$ and $R_B := \{x :\ x > x_b\}$.

Let $x(\mu)$ be a path of fixed points of f; this path depends continuously on μ. Suppose also that the fixed point hits the boundary at a critical parameter value μ_b: $x(\mu_b) = x_b$. Below, conditions are recalled for the occurrence of various types of BCBs from x_b for μ near μ_b.

The normal form for the PWS map (3.1) at a fixed point on the border is a piecewise affine approximation of the map in the neighborhood of the border point x_b, in scaled coordinates [62, 23, 10]. For completeness, a derivation of the 1-D normal form is now recalled [10]. Letting $\bar{x} = x - x_b$ and $\bar{\mu} = \mu - \mu_b$, Eq. (3.2) becomes

$$\tilde{f}(\bar{x},\bar{\mu}) := f(\bar{x}+x_b, \bar{\mu}+\mu_b) = \begin{cases} f_A(\bar{x}+x_b, \bar{\mu}+\mu_b), & \bar{x} \le 0 \\ f_B(\bar{x}+x_b, \bar{\mu}+\mu_b), & \bar{x} \ge 0 \end{cases} \tag{3.3}$$

In these variables, the border is at $\bar{x} = 0$, and the state space is divided into two halves, $\mathbb{R}_- = (-\infty, 0]$ and $\mathbb{R}_+ = [0, \infty)$. Also, the fixed point of (3.1) is at the border for the parameter value $\bar{\mu} = 0$.

Expanding $\tilde{f}$ to first order about $(0,0)$ gives

$$\tilde{f}(\bar{x},\bar{\mu}) = \begin{cases} a\bar{x}+\bar{\mu}v+o(\bar{x},\bar{\mu}), & \bar{x}\leq 0 \\ b\bar{x}+\bar{\mu}v+o(\bar{x},\bar{\mu}), & \bar{x}\geq 0 \end{cases} \tag{3.4}$$

where

$$a = \lim_{\bar{x}\to 0^-}\frac{\partial}{\partial x}\tilde{f}(\bar{x},0), \quad b = \lim_{\bar{x}\to 0^+}\frac{\partial}{\partial x}\tilde{f}(\bar{x},0), \quad \text{and} \quad v = \lim_{\bar{x}\to 0}\frac{\partial}{\partial \mu}\tilde{f}(\bar{x},0).$$

(The last limit doesn't depend on the direction of approach of 0 by x, due to the assumed smoothness of f in μ.) Suppose $v \neq 0$, $|a| \neq 1$ and $|b| \neq 1$. The assumptions $|a| \neq 1$ and $|b| \neq 1$ imply that the nonlinear terms are negligible close to the border. The assumption $v \neq 0$ means that the fixed point crosses the border as μ is varied through its critical value. The 1-D normal form is therefore obtained by defining a new parameter $\bar{\bar{\mu}} = \bar{\mu}v$ and dropping the higher order terms [10]:

$$G_1(\bar{x},\bar{\bar{\mu}}) = \begin{cases} a\bar{x}+\bar{\bar{\mu}}, & \bar{x}\leq 0 \\ b\bar{x}+\bar{\bar{\mu}}, & \bar{x}\geq 0 \end{cases}$$

The normal form map $G_1(\cdot,\cdot)$ can be used to study local bifurcations of the original map $f(\cdot,\cdot)$ [62, 23, 10].

For simplicity of notation, below (x,μ) is used instead of $(\bar{x},\bar{\bar{\mu}})$. The normal form is therefore

$$x_{k+1} = G_1(x_k,\mu) = \begin{cases} ax_k+\mu, & x_k \leq 0 \\ bx_k+\mu, & x_k \geq 0 \end{cases} \tag{3.5}$$

Denote by $x_B(\mu)$ and $x_A(\mu)$ the fixed points of the system near the border to the right ($x > x_b$) and left ($x < x_b$) of the border, respectively. Then in the normal form (3.5), $x_B(\mu) = \frac{\mu}{1-b}$ and $x_A(\mu) = \frac{\mu}{1-a}$. For the fixed point $x_B(\mu)$ to actually occur, we need $\frac{\mu}{1-b} \geq 0$ which is satisfied if and only if either $\mu \geq 0$ and $b < 1$ or $\mu \leq 0$ and

$b > 1$. Similarly, for $x_A(\mu)$ to actually occur, we need $\frac{\mu}{1-a} \leq 0$ which is satisfied if and only if either $\mu \leq 0$ and $a < 1$ or $\mu \geq 0$ and $a > 1$.

Various combinations of the parameters a and b lead to different kinds of bifurcation behavior as μ is varied. Since the map G_1 is invariant under the transformation $x \to -x$, $\mu \to -\mu$, $a \rightleftharpoons b$, it suffices to consider only the case $a \geq b$.

The possible bifurcation scenarios are recalled next. Some of the language used below to describe the BCBs is introduced here to more easily convey the ideas. All the results below pertain to system (3.5).

3.2 Persistent Fixed Point (Scenario A)

In this scenario, a fixed point for $\mu < 0$ crosses the border and persists for $\mu > 0$. Two situations lead to this scenario. These are presented next.

Proposition 3.1 [73, 10] **(Scenario A1: Persistence of Stable Fixed Point)**

$$\textit{If} \quad -1 < b \leq a < 1 \tag{3.6}$$

then a stable fixed point for $\mu < 0$ persists and remains stable for $\mu > 0$.

Figure 3.1 illustrates the dependence of the map G_1 and its fixed points on μ near the border. The system has a single eigenvalue at the fixed point, which changes discontinuously at the border. The distinct eigenvalues are the slopes of the map on the two sides of the vertical axis in Figure 3.1.

Proposition 3.2 [73, 10] **(Scenario A2: Persistence of Unstable Fixed Point)**

$$\textit{If} \quad \textit{i)} \qquad 1 < b \leq a \tag{3.7}$$

$$\textit{or} \quad \textit{ii)} \qquad b \leq a < -1 \tag{3.8}$$

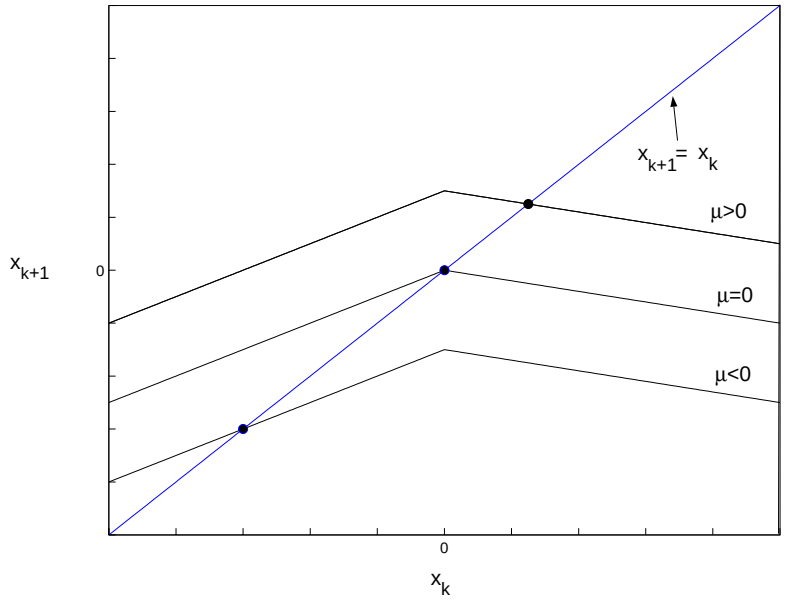

Figure 3.1: Dependence of first return map and its fixed point on μ for Scenario A1 ($-1 < b < a < 1$) is shown here. Intersections of the map with the line $x_{k+1} = x_k$ are the fixed points.

then an unstable fixed point for $\mu < 0$ *persists and remains unstable for* $\mu > 0$.

Figure 3.2 shows typical bifurcation diagrams for Scenario A1 and Scenario A2.

3.3 Border Collision Pair Bifurcation (Scenario B)

For other values of the parameters a and b, there are two main kinds of border collision bifurcation, namely, *border collision pair bifurcation* and *border crossing bifurcation*. Border collision pair bifurcation is similar to saddle node bifurcation in smooth systems, where two fixed points of the system collide and disappear at the bifurcation. Border crossing bifurcation, on the other hand, has some similarities with period doubling bifurcation in smooth maps as discussed below.

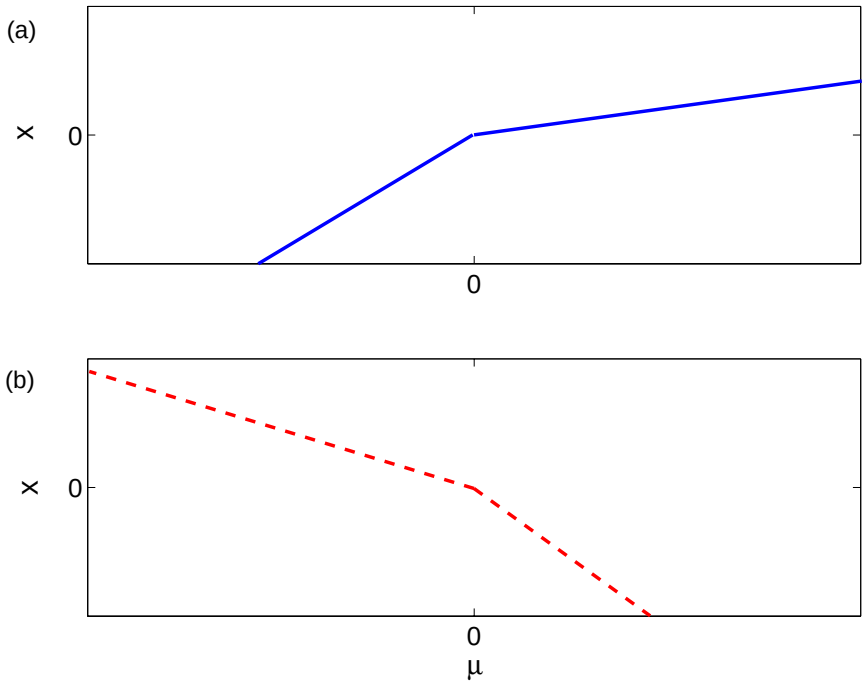

Figure 3.2: Bifurcation diagrams for Scenarios A1 and A2. A solid line represents a stable fixed point whereas a dashed line represents an unstable fixed point. (a) A typical bifurcation diagram for Scenario A1. (b) A typical bifurcation diagram for Scenario A2.

In border collision pair bifurcation, the map has two fixed points for positive (respectively, negative) values of μ, and no fixed points for negative (respectively, positive) values of μ. For the μ range that two fixed points exist, one fixed point is on one side of the border and the other fixed point is on the opposite side. The border collision pair bifurcation occurs if $b < 1 < a$. There are three situations that lead to this scenario. These are summarized next (see also Figure 3.3).

Proposition 3.3 [73, 10] **(Scenario B1: Merging and Annihilation of Stable and Unstable Fixed Points)**

$$If \quad -1 < b < 1 < a \tag{3.9}$$

then there is a bifurcation from no fixed point to two period-1 fixed points. In this case, there is no fixed point for $\mu < 0$ *while there are two fixed points* $x_A(\mu)$ *(unstable) and* $x_B(\mu)$ *(stable) for* $\mu \geq 0$.

A typical bifurcation diagram for Scenario B1 is depicted in Figure 3.3 (a). Scenario B1 is analogous to saddle-node bifurcation (or tangent bifurcation) in smooth maps.

Proposition 3.4 [73, 10] **(Scenario B2: Merging and Annihilation of Two Unstable Fixed Points, Plus Chaos)**

$$\textit{If} \quad a > 1 \quad \textit{and} \quad -\frac{a}{a-1} < b < -1 \tag{3.10}$$

then there is a bifurcation from no fixed point to two unstable fixed points plus a growing chaotic attractor as μ *is increased through zero.*

A typical bifurcation diagram for Scenario B2 is depicted in Figure 3.3 (b). A proof of this proposition is given in [73]. We point out that for the range of a and b given in (3.10), the normal form is basically a family of tent maps.

Proposition 3.5 [73, 10] **(Scenario B3: Merging and Annihilation of Two Unstable Fixed Points)**

$$\textit{If} \quad a > 1 \quad \textit{and} \quad b < -\frac{a}{a-1} \tag{3.11}$$

then there is a bifurcation from no fixed point to two unstable fixed points as μ *is increased through zero (see Figure 3.3 (c)). Also an unstable chaotic orbit exists for* $\mu > 0$. *The system trajectory diverges for all initial conditions.*

A typical bifurcation diagram for Scenario B3 is depicted in Figure 3.3 (c). A proof of this proposition is given in [73].

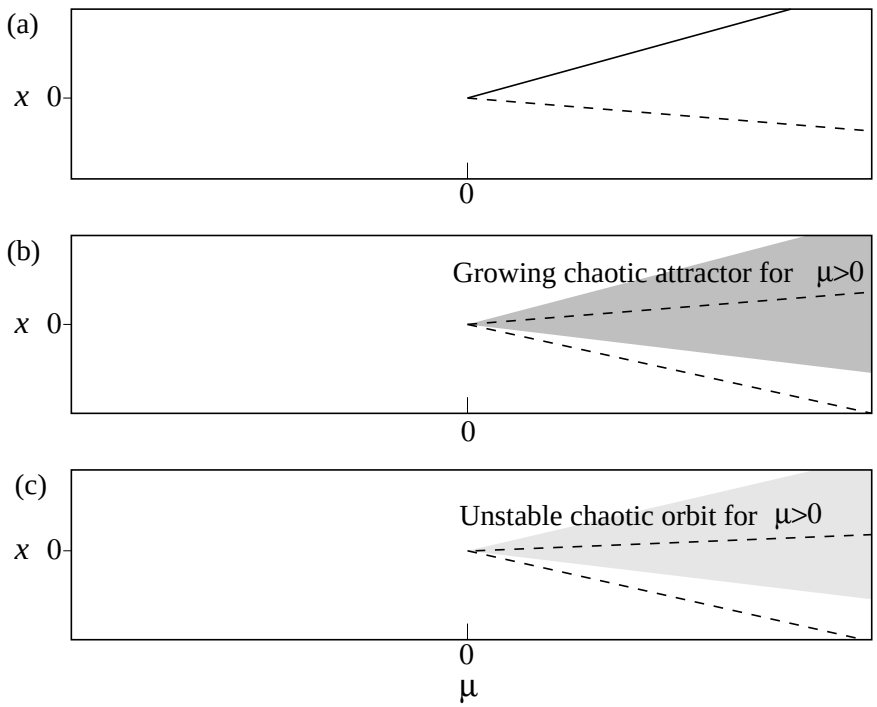

Figure 3.3: Bifurcation diagrams for Scenarios B1-B3. A solid line represents a stable fixed point whereas a dashed line represents an unstable fixed point. (a) A typical bifurcation diagram for Scenario B1. (b) A typical bifurcation diagram for Scenario B2. (c) A typical bifurcation diagram for Scenario B3.

3.4 Border Crossing Bifurcations (Scenario C)

In border crossing bifurcation, the fixed point persists and crosses the border as μ is varied through zero. Other attractors or repellers may appear or disappear as a result of the bifurcation. Border crossing bifurcation occurs if $-1 < a < 1$ and $b < -1$. There are three situations that lead to this scenario. These are summarized next.

Proposition 3.6 [73, 10] **(Scenario C1: Supercritical Period Doubling Border Collision Bifurcation)**

$$\textit{If} \quad b < -1 < a < 1 \quad \textit{and} \quad -1 < ab < 1 \tag{3.12}$$

then there is a bifurcation from a stable fixed point to an unstable fixed point plus a stable period-2 orbit as μ is increased through zero.

A typical bifurcation diagram for Scenario C1 is depicted in Figure 3.4(a). This bifurcation is analogous to supercritical period doubling bifurcation in smooth maps.

It is important to point out that a signature of BCBs is that the fixed points meet and form an acute angle (or a cusp) at the bifurcation point [73], which distinguishes BCBs in PWS maps from those occurring in smooth maps. This can be used as a signature of BCBs which may be useful in analysis of experimental data.

Proposition 3.7 (Scenario C2: Subcritical Period Doubling Border Collision Bifurcation)[1]

$$\textit{If} \quad b < -1 < a < 0 \quad \textit{and} \quad ab > 1 \tag{3.13}$$

then there is a bifurcation from a stable fixed point along with an unstable period-2 orbit to an unstable fixed point as μ is increased though zero.

A typical bifurcation diagram for Scenario C2 is depicted in Figure 3.4(b). This bifurcation is analogous to subcritical period doubling bifurcation in smooth maps.

To show the bifurcation of an unstable period-2 orbit for $\mu < 0$, consider the first and second return maps (for $\mu < 0$), given by

$$x_{k+1} = \begin{cases} ax_k + \mu, & x_k \leq 0 \\ bx_k + \mu, & x_k \geq 0 \end{cases} \tag{3.14}$$

$$x_{k+2} = \begin{cases} abx_k + \mu(1+b), & x_k \leq -\frac{\mu}{a} \\ a^2 x_k + \mu(1+a), & -\frac{\mu}{a} \leq x_k \leq 0 \\ abx_k + \mu(1+a), & x_k \geq 0 \end{cases} \tag{3.15}$$

[1] In [73, 10], the terminology *Period-1 $\rightarrow$ No Attractor* is used to describe this case, and the bifurcation of an unstable period-2 orbit is not mentioned.

respectively. The first return map has a stable fixed point, $x_A(\mu) = \frac{\mu}{1-a}$. The second return map has three fixed points one of which coincides with $x_A(\mu)$. The other two fixed points are given by $x_1^* = \frac{\mu(1+b)}{1-ab} < 0$ and $x_2^* = \frac{\mu(1+a)}{1-ab} > 0$. The fixed points x_1^* and x_2^* are unstable (since the slope of the second return map at both fixed points is $ab > 1$). Since x_1^* and x_2^* form a period-2 orbit for the first return map, it is concluded that the normal form has an unstable period-2 orbit in addition to the stable fixed point before the border (see Figure 3.4(b)). It remains to show that there is no period-2 orbit for $\mu > 0$. To this end, suppose that there is a period-2 orbit for $\mu > 0$ formed by $x_3^* < 0$ and $x_4^* > 0$. This means that if one starts at x_3^*, the next iterate is x_4^*. Applying the map one more time gives x_3^* and so on. It is straightforward to show that $x_3^* = \frac{\mu(1+a)}{1-ab}$ and $x_4^* = \frac{\mu(1+b)}{1-ab}$ with $\mu > 0$. Now we show that starting at x_3^* for example, and iterating the map twice gives $\frac{\mu(a^2b-ab^2+b+1)}{1-ab} \neq x_3^*$ and thus the map does not have a period-2 orbit for $\mu > 0$.

Proposition 3.8 [62] **(Scenario C3: Emergence of Periodic or Chaotic Attractor from Stable Fixed Point)**

$$\textit{If} \quad 0 < a < 1, \;\; b < -1 \;\; \textit{and} \;\; ab < -1 \tag{3.16}$$

then there is a bifurcation from a stable fixed point to an unstable fixed point plus a period-n attractor, $n \geq 2$ or a chaotic attractor as μ is increased through zero.

The specific scenario, period-n attractor or chaotic attractor, depends on the pair (a, b) as shown in Figure 3.5 (see [62] for details). The possible bifurcation scenarios for system (3.5) are summarized in Fig. 3.6, which expands on a similar figure in [10].

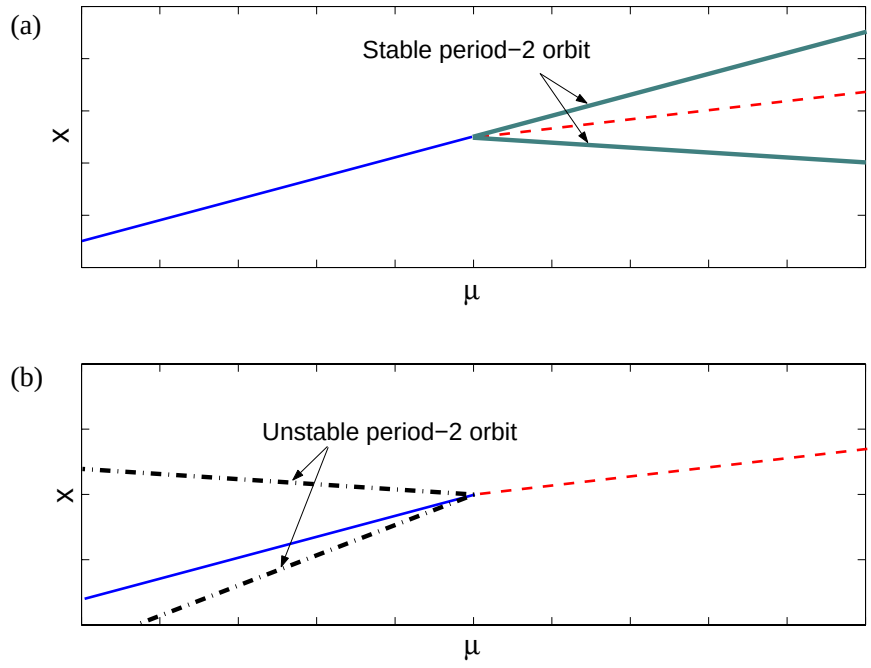

Figure 3.4: Typical bifurcation diagrams for Scenarios C1 and C2. A solid line represents a stable fixed point whereas a dashed line represents an unstable fixed point. (a) Supercritical period doubling border collision (Scenario C1, $b < -1 < a < 1$ and $-1 < ab < 1$), (b) Subcritical period doubling border collision (Scenario C2, $b < -1 < a < 0$ and $ab > 1$).

3.5 Stability of the Fixed Point at Criticality in Scenarios A-C

The following results give detailed statements relating stability of the fixed point at criticality with the nature of the BCB that occurs. These results, though not difficult to obtain, haven't previously been stated.

Proposition 3.9 *The origin of (3.5) at $\mu = 0$ is asymptotically stable if and only if any of (i)-(iii) below holds*

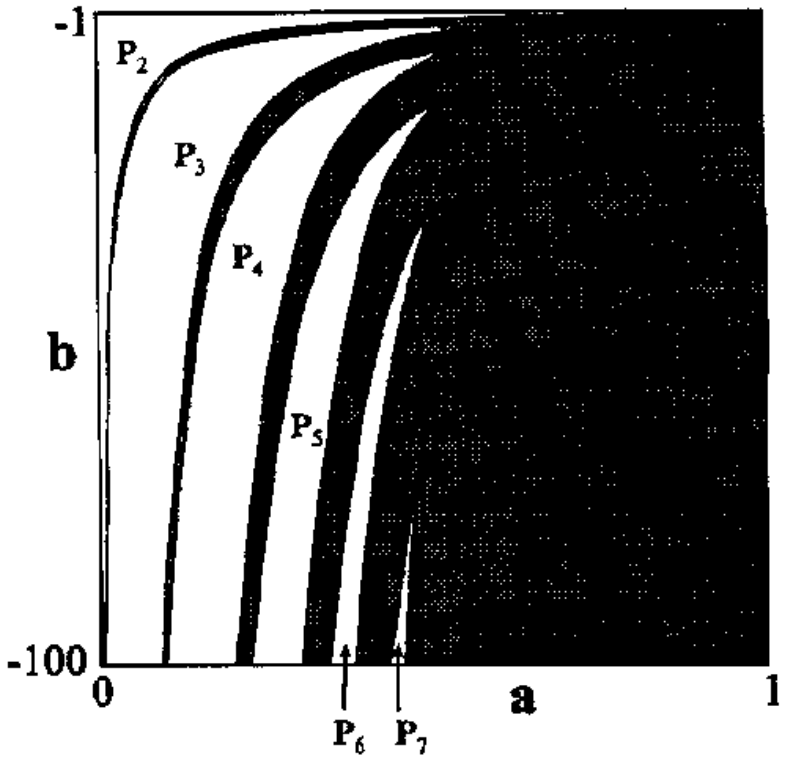

Figure 3.5: The bifurcation behavior describing Scenario C3 ($0 < a < 1$ and $b < -1$). Shaded regions indicate the existence of a chaotic attractor and a $P_n : \ n = 2, 3, \cdots, 7$, indicates the existence of a stable period-n attractor [62].

(i) $-1 < a < 1$ *and* $-1 < b < 1$

(ii) $\{0 < a < 1$ *and* $b < -1\}$ *or* $\{0 < b < 1$ *and* $a < -1\}$

(iii) $\{-1 < a < 0$, $b < -1$ *and* $ab < 1\}$ *or* $\{-1 < b < 0$, $a < -1$ *and* $ab < 1\}$.

The origin of (3.5) at $\mu = 0$ *is unstable iff any of (iv)-(vi) below holds*

(iv) $\{-1 < a < 1$ *and* $b > 1\}$ *or* $\{-1 < b < 1$ *and* $a > 1\}$

(v) $\{-1 < a < 0$, $b < -1$ *and* $ab > 1\}$ *or* $\{-1 < b < 0$, $a < -1$ *and* $ab > 1\}$

(vi) $|a| > 1$ *and* $|b| > 1$.

Proof (cases (i)-(iii)): Consider the piecewise quadratic Lyapunov function

$$V(x_k) = \begin{cases} p_1 x_k^2, & x_k \leq 0 \\ p_2 x_k^2, & x_k > 0 \end{cases} \tag{3.17}$$

where $p_1 > 0$ and $p_2 > 0$. Clearly, $V(x)$ is positive definite. To show asymptotic stability of the origin of (3.5) at criticality ($\mu = 0$), we need to show that the forward difference $\Delta V(x_k) := V(x_{k+1}) - V(x_k)$ is negative definite along the trajectories of (3.5) for all $x_k \neq 0$. There are two cases:

Case 1: $x_k < 0$

$$\begin{aligned} \Delta V(x_k) &= \begin{cases} p_1(x_{k+1}^2 - x_k^2), & x_{k+1} < 0 \\ p_2 x_{k+1}^2 - p_1 x_k^2, & x_{k+1} > 0 \end{cases} \\ &= \begin{cases} p_1 x_k^2(a^2 - 1), & x_{k+1} < 0 \\ x_k^2(p_2 a^2 - p_1), & x_{k+1} > 0 \end{cases} \end{aligned} \tag{3.18}$$

Case 2: $x_k > 0$

$$\begin{aligned} \Delta V(x_k) &= \begin{cases} p_2(x_{k+1}^2 - x_k^2), & x_{k+1} > 0 \\ p_1 x_{k+1}^2 - p_2 x_k^2, & x_{k+1} < 0 \end{cases} \\ &= \begin{cases} p_2 x_k^2(b^2 - 1), & x_{k+1} > 0 \\ x_k^2(p_1 b^2 - p_2), & x_{k+1} < 0 \end{cases} \end{aligned} \tag{3.19}$$

It remains to show that $\Delta V(x_k) < 0$ for all $x_k \neq 0$ in (i)-(iii).

(i) $-1 < a < 1$ and $-1 < b < 1$: Choose $p_1 = p_2 =: p > 0$. From (3.18), it follows that $\Delta V(x_k) = p x_k^2(a^2 - 1) < 0$ and from (3.19) it follows that $\Delta V(x_k) = p x_k^2(b^2 - 1) < 0$. Thus $\Delta V(x_k) < 0 \; \forall x_k \neq 0$.

(ii) $0 < a < 1$ and $b < -1$ (the proof for the symmetric case $0 < b < 1$ and $a < -1$ is similar and therefore omitted): Since $0 < a < 1$, if $x_k < 0$ then $x_{k+1} = a x_k < 0$.

From (3.18), $\Delta V(x_k) = p_1 x_k^2(a^2-1) < 0$. Since $b < -1$, if $x_k > 0$ then $x_{k+1} = bx_k < 0$. From (3.19), $\Delta V(x_k) = x_k^2(p_1 b^2 - p_2) < 0$ if and only if $p_2 > p_1 b^2 > 0$. Thus, choosing $p_1 > 0$ and $p_2 > p_1 b^2$ results in a positive definite V and a negative definite $\Delta V(x)$.

(iii) $-1 < a < 0$, $b < -1$ and $ab < 1$ (the proof for the symmetric case $-1 < b < 0$, $a < -1$ and $ab < 1$ is similar and therefore omitted): Since $-1 < a < 0$, if $x_k < 0$ then $x_{k+1} = ax_k > 0$. From (3.18), $\Delta V(x_k) = x_k^2(p_2 a^2 - p_1) < 0$ if and only if $p_1 > p_2 a^2$. Since $b < -1$, if $x_k > 0$ then $x_{k+1} = bx_k < 0$. From (3.19), $\Delta V(x_k) = x_k^2(p_1 b^2 - p_2) < 0$ if and only if $p_1 < \frac{p_2}{b^2}$. Thus, p_1 and p_2 must be chosen such that $p_2 a^2 < p_1 < \frac{p_2}{b^2}$. Clearly, any $p_2 > 0$ works. For $p_1 > 0$ to exist, we need $\frac{1}{b^2} > a^2$ which is satisfied since $ab < 1$ by hypothesis.

Proof (cases (iv)-(vi)): It suffices to show that no matter how close the initial condition is to the origin, the trajectory of (3.5) diverges.

(iv) $-1 < a < 1$ and $b > 1$ (the proof for the symmetric case $-1 < b < 1$ and $a > 1$ is similar and therefore omitted): Let $x_0 = \varepsilon > 0$. Then, $x_1 = b\varepsilon$, $x_2 = b^2\varepsilon$ and $x_k = b^k\varepsilon$. As $k \to \infty$, $x_k \to \infty$ no matter how small ε is.

(v) $-1 < a < 0$, $b < -1$ and $ab > 1$ (the proof for the symmetric case $-1 < b < 0$, $a < -1$ and $ab > 1$ is similar and therefore omitted): Let $x_0 = \varepsilon > 0$. It is straightforward to show that $x_{2k} = (ab)^k\varepsilon$. Since $ab > 1$, $x_{2k} \to \infty$ as $k \to \infty$, for any fixed ε.

(vi) Similar to the other cases proved above. ■

The assertions of the next theorem follow from relating the stability of the fixed point at criticality as given in Propositions 3.9 with the ensuing bifurcation for different regions in the (a,b) parameter space as discussed at length in this chapter.

Theorem 3.1 *1) If the fixed point of system (3.5) is asymptotically stable at criticality (i.e., at $\mu = 0$), then the border collision bifurcation is supercritical in the sense that*

no bifurcated orbits occur on the side of the border where the nominal fixed point is stable and the bifurcated solution on the unstable side is attracting.

2) If the fixed point of system (3.5) is unstable at criticality, then the border collision bifurcation is subcritical in the sense that there is no stable bifurcated orbit on one or both sides of the border.

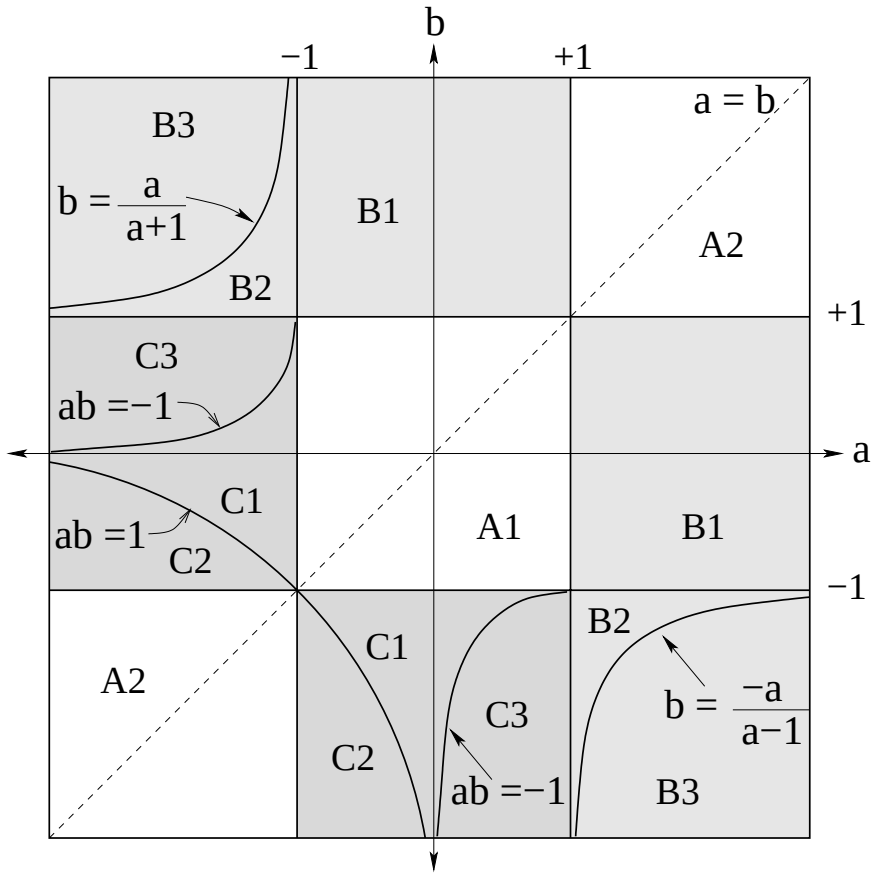

Figure 3.6: Partitioning of the parameter space into regions with the same qualitative phenomena. The labeling of regions refers to various bifurcation scenarios (associated parameter ranges are clear from the figure). *Scenario A1:* Persistence of stable fixed points (nonbifurcation), *Scenario A2:* Persistence of unstable fixed points, *Scenario B1:* Merging and annihilation of stable and unstable fixed points, *Scenario B2:* Merging and annihilation of two unstable fixed points plus chaos, *Scenario B3:* Merging and annihilation of two unstable fixed points, *Scenario C1:* Supercritical border collision period doubling, *Scenario C2:* Subcritical border collision period doubling, *Scenario C3:* Emergence of periodic or chaotic attractor from stable fixed point.

Chapter 4

Feedback Control of Border Collision Bifurcation in 1-D Maps

In this chapter, control of BCBs in PWS maps of dimension one is discussed. The goal of the control effort is to modify the bifurcation so that the bifurcated steady state is locally attracting. In this way, the system's local behavior is ensured to remain close to the original operating condition. Since the type and stability properties of a border collision bifurcation are determined (generically) by the system linearizations on both sides of the border, we employ linear and piecewise linear feedback laws.

Consider a general 1-D PWS map of the form

$$f(x,\mu) = \begin{cases} f_A(x,\mu), & x \leq x_b \\ f_B(x,\mu), & x \geq x_b \end{cases} \tag{4.1}$$

The sought linear or piecewise linear feedback can either be applied on one side of the border and not the other, or on both sides of the border. Both approaches are considered below. The issue of which approach to take and with what constraints is a delicate one. There are practical advantages to applying a feedback on only one side of the border, say the stable side. However, this requires knowledge of where the border lies, which is not necessarily the case in practice. An approach considered here that

doesn't require knowledge of the border is what we call *simultaneous stabilization*—here controls are sought that function in exactly the same way on both sides of the border. Not surprisingly, the conditions for existence of simultaneously stabilizing controls are more restrictive than for one sided controls.

All the developed control laws are developed for application to system models in normal form. To apply these control laws to a map not in normal form, inverse transformations need to be performed, and this is straightforward for 1-D maps.

We should emphasize that transforming a system to normal form is not needed when simultaneous feedback control is employed. All that is needed in this case is an estimate of the slopes of the map on both sides of the border.

4.1 Control of BCB in 1-D Maps Using Static Feedback

Consider the one-dimensional normal form (3.5) for a BCB, repeated here for convenience:

$$x_{k+1} = \begin{cases} ax_k + \mu, & x_k \leq 0 \\ bx_k + \mu, & x_k \geq 0 \end{cases} \tag{4.2}$$

Below, the control schemes described above are considered for the system (4.2), with a control signal u included in the dynamics as appropriate.

4.1.1 Control Applied on One Side of the Border

In the first control scheme, the feedback control is applied on one side of the border. Suppose that the system is operating at a stable fixed point on one side of the border, with the bifurcation parameter approaching its critical value. Without loss of generality, assume this region of stable operation is $\{x : x < 0\}$— that is, assume $-1 < a < 1$.

Since the control is applied only on one side of the border, a linear feedback will be applied either on the unstable side or the stable side of the border.

Linear feedback applied on unstable side of the border

Suppose that the fixed point is stable for $x(\mu) \in \mathbb{R}_-$ and unstable for $x(\mu) \in \mathbb{R}_+$. Applying additive linear state feedback only for $x \in \mathbb{R}_+$ leads to the closed-loop system

$$x_{k+1} = \begin{cases} ax_k + \mu, & x_k \leq 0 \\ bx_k + \mu + u_k, & x_k \geq 0 \end{cases} \tag{4.3}$$

$$u_k = \gamma x_k \tag{4.4}$$

The following proposition asserts stabilizability of the border collision bifurcation with this type of control policy.

Proposition 4.1 *Suppose (4.2) has a stable fixed point in $\mathbb{R}_-$ for $\mu < 0$ (i.e., $|a| < 1$) and that for $\mu > 0$, either there is an unstable fixed point in $\mathbb{R}_+$ (i.e., $b < -1$) or there is no fixed point (i.e., $b > 1$). Then there is a stabilizing linear feedback on the right side of the border. That is, a linear feedback exists resulting in a stable fixed point to the left and right of the border (i.e., achieving Scenario A1). Indeed, precisely those linear feedbacks $u_k = \gamma x_k$ with gain γ satisfying*

$$-1 - b < \gamma < 1 - b \tag{4.5}$$

are stabilizing.

Proof: With $u_k = \gamma x_k$, the closed loop system is

$$x_{k+1} = \begin{cases} ax_k + \mu, & x_k \leq 0 \\ (b+\gamma)x_k + \mu, & x_k \geq 0 \end{cases} \tag{4.6}$$

For $\mu > 0$, the fixed point is $\tilde{x}(\mu) = \frac{\mu}{1-(b+\gamma)}$. The fixed point $\tilde{x}(\mu) \in \mathbb{R}_+$ if $\gamma + b < 1$. The border collision bifurcation is eliminated if the eigenvalues of the closed loop

system on both sides of the border are in $(-1,1)$. This implies that the control gain γ must be chosen such that $|b+\gamma|<1$. ■

Rendering the bifurcation a supercritical period doubling BCB using linear feedback applied on the stable side of the border

For a linear feedback applied on the stable side of the border to be effective in ensuring an acceptable bifurcation, it turns out that one must assume that the open-loop system supports an unstable fixed point on the right side of the border. This is tantamount to assuming $b<-1$. Of course, the assumption $-1<a<1$ is still in force. Now, applying additive linear feedback in the $x<0$ region yields the closed-loop system

$$x_{k+1} = \begin{cases} ax_k+\mu+u_k, & x_k \le 0 \\ bx_k+\mu, & x_k \ge 0 \end{cases} \tag{4.7}$$

$$u_k = \gamma x_k \tag{4.8}$$

Note that such a control scheme does not stabilize the unstable fixed point on the right side of the border. This is because the control has no direct effect on the system for $x>0$. All is not lost, however. The next proposition asserts that such a control scheme may be used to stabilize the system to a period-2 solution after the border collision event.

Proposition 4.2 *Suppose that the fixed point of (4.2) is stable in $\mathbb{R}_-$ for $\mu<0$ and exists and is unstable in $\mathbb{R}_+$ for $\mu>0$ (i.e., $|a|<1$ and $b<-1$). Then there is a linear feedback that when applied to the left of the border (i) maintains a stable fixed point to the left of the border for $\mu<0$, and (ii) produces a stable period-2 orbit for $\mu>0$ (i.e., the feedback achieves Scenario C1). Indeed, precisely those linear feedbacks*

$u_k = \gamma x_k$ *with gain* γ *satisfying*

$$\frac{1}{b} - a < \gamma < -\frac{1}{b} - a \tag{4.9}$$

are stabilizing.

Proof: The closed-loop system is given by

$$x_{k+1} \quad = \quad \begin{cases} (a+\gamma)x_k + \mu, & x_k \leq 0 \\ bx_k + \mu, & x_k \geq 0 \end{cases}$$

The fixed point to the left of the border for $\mu < 0$ remains stable if and only if

$$|a+\gamma| < 1 \qquad \Longleftrightarrow \qquad -1-a < \gamma < 1-a \tag{4.10}$$

The fixed point to the right of the border for $\mu > 0$ remains unstable since the control is applied only in the $x < 0$ region. The closed-loop system bifurcates to a period-2 orbit as μ is increased through zero if and only if the fixed point of the second return map x_{k+2} for $\mu > 0$, which form a period-2 orbit for the first return map, is stable. That is, iff

$$|(a+\gamma)b| < 1 \qquad \Longleftrightarrow \qquad \frac{1}{b} - a < \gamma < -\frac{1}{b} - a \tag{4.11}$$

Combining conditions (4.10) and (4.11) yields

$$\max\left\{\frac{1}{b} - a, -1 - a\right\} < \gamma < \min\left\{-\frac{1}{b} - a, 1 - a\right\} \tag{4.12}$$

Since $b < -1 < a$, condition (4.12) is equivalent to $\frac{1}{b} - a < \gamma < -\frac{1}{b} - a$. This completes the proof. ■

4.1.2 Simultaneous Stabilization

In this method, the same linear feedback control is applied in both the $x < 0$ and $x > 0$ regions. This leads to the closed-loop system

$$x_{k+1} = \begin{cases} ax_k + \mu + u_k, & x_k \leq 0 \\ bx_k + \mu + u_k, & x_k \geq 0 \end{cases} \tag{4.13}$$

$$u_k = \gamma x_k \tag{4.14}$$

The following proposition gives a necessary and sufficient condition for existence of stabilizing simultaneous control.

Proposition 4.3 *The fixed points of the closed-loop system (4.13)-(4.14) on both sides of the border can be simultaneously stabilized using linear feedback control $u_k = \gamma x_k$ if and only if*

$$|a - b| < 2 \tag{4.15}$$

Indeed, precisely those linear feedbacks $u_k = \gamma x_k$ with gain γ satisfying

$$-1 - b < \gamma < 1 - a \tag{4.16}$$

are stabilizing.

Proof: The fixed points of the closed-loop system on both sides of the border are stabilized by the feedback control $u_k = \gamma x_k$ if and only if

$$-1 < \gamma + a < 1 \quad \text{and} \quad -1 < \gamma + b < 1$$

$$\iff \quad (-1-a,\ 1-a) \cap (-1-b,\ 1-b) \neq \emptyset$$

$$\iff \quad |a - b| < 2.$$

■.

Clearly, this condition is not met by all values of a and b. This condition might or might not be met for all scenarios of BCBs discussed in Chapter 3 above, except scenarios B2 and B3, in which it is definitely not met because $|a-b| \geq 2$.

Next, the case in which $|a-b| \geq 2$ is considered. Recall that, because of symmetry, $a-b \geq 2$ can be assumed to hold. The next proposition asserts that in this case a simultaneous linear feedback control exists that ensures the border collision bifurcation is from a stable fixed point to a stable period-2 solution (i.e., the feedback achieves Scenario C1, supercritical border collision period doubling).

Proposition 4.4 *Suppose $a-b \geq 2$. Then, there is a simultaneous control law that renders the BCB in the system (4.13)-(4.14) a supercritical border collision period doubling (Scenario C1). This is achieved precisely by the controls with control gain satisfying*

$$-1 < \gamma + a < 1 \quad \textit{and} \quad -1 < (\gamma + a)(\gamma + b) < 1 \tag{4.17}$$

One set of control gains satisfying (4.17) is $\gamma = -a + \varepsilon$ with ε sufficiently small.

Proof: The closed-loop system is given by

$$x_{k+1} = \begin{cases} (a+\gamma)x_k + \mu, & x_k \leq 0 \\ (b+\gamma)x_k + \mu, & x_k \geq 0 \end{cases} \tag{4.18}$$

The fixed point to the left of the border is stable if and only if

$$-1 < a + \gamma < 1 \tag{4.19}$$

Suppose the control gain γ is chosen such that (4.19) is satisfied. The closed loop system bifurcates to a period-2 orbit as μ is increased through zero if (i) the fixed

point to the right of the border for $\mu > 0$ is unstable, and (ii) the fixed points of the second return map x_{k+2} for $\mu > 0$, which form a period-2 orbit for the first return map, is stable. That is, if

$$|b+\gamma| \quad > \quad 1 \tag{4.20}$$

and

$$-1 < (a+\gamma)(b+\gamma) \quad < \quad 1 \tag{4.21}$$

Condition (4.20) is satisfied since $a-b \geq 2$ and $-1 < a+\gamma < 1$. Thus, the closed-loop system undergoes a bifurcation from a stable fixed point to a period-2 orbit at $\mu = 0$ if

$$-1 < \gamma + a < 1 \quad \text{and} \quad -1 < (\gamma+a)(\gamma+b) < 1 \tag{4.22}$$

Finally, if the control gain $\gamma = -a+\varepsilon$, then

$$a+\gamma \quad = \quad \varepsilon, \tag{4.23}$$

$$(a+\gamma)(b+\gamma) \quad = \quad \varepsilon(b-a+\varepsilon) \tag{4.24}$$

Thus, the stabilizability condition (4.22) is satisfied for a sufficiently small ε. ■

Note that if the system is known on the stable side but is uncertain on the unstable side (with $b < -1$), the conclusion of Proposition 4.4 still applies. This has important implications for robustly stabilizing the system. The next example illustrates the use of Proposition 4.4.

Example 4.1 (Robust Simultaneous Control)

Consider the following simple example in normal form for border collision bifurcation

$$x_{k+1} \quad = \quad \begin{cases} 0.5x_k + \mu, & x_k \leq 0 \\ bx_k + \mu, & x_k \geq 0 \end{cases} \tag{4.25}$$

A BCB occurs as μ is increased through zero. The resulting BCB depends on the value of b [60]. For $b = -4.15$, there is a bifurcation from a period-1 fixed point to a "six-piece " [60] chaotic attractor. For $b = -4.44$, there is a bifurcation from a period-1 fixed point to a "three-piece " chaotic attractor. Finally, for $b = -5.5$, a period-1 fixed point produces a one-piece chaotic attractor.

Figure 4.1 shows the bifurcation diagrams for the values of b above together with those of the controlled map using a simultaneous control achieving stable period doubling (with $\gamma = -0.51$ in all cases). Note that a persistent stable fixed point is not achievable because for each b values considered, $0.5 - b > 2$. ■

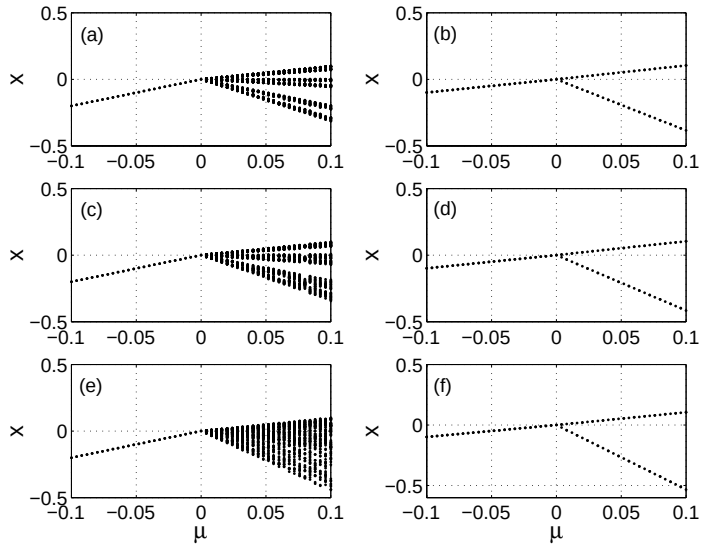

Figure 4.1: Bifurcation diagrams for Example 4.1. (a) $b = -4.15$ (c) $b = -4.44$, (e) $b = -5.5$, (b), (d) and (f) are bifurcation diagrams for the corresponding closed-loop system using the same control gain $\gamma = -0.51$ in all cases.

4.2 Discrete Control of a PWS Continuous-Time System: An Example

The next example, which builds on an example from [23], illustrates use of the foregoing theory to control BCB in a second order continuous-time PWS system. The system is such that its Poincaré map can be determined analytically.

Consider the second order PWS continuous time system

$$\dot{x} = y \tag{4.26}$$

$$\dot{y} = -(1+p_k^2)\,x + 2p_k\,y + v \tag{4.27}$$

where p_k is the piecewise smooth function

$$p_k = \begin{cases} \dfrac{1}{2\pi}\log\left(\dfrac{1+\alpha(Y_k-1)+\mu}{Y_k}\right), & \text{for } Y_k < 1 \\ \dfrac{1}{2\pi}\log\left(\dfrac{1+\beta(Y_k-1)+\mu}{Y_k}\right), & \text{for } Y_k > 1 \end{cases} \tag{4.28}$$

Y_k is the y-coordinate of the k-th intersection of the phase-plane trajectory with the positive y-axis ($x = 0$, $y > 0$), and v is a control to be designed. Next, a Poincaré map is used to obtain a discrete-time system for which the results of this chapter allow design of a discrete-time control u, and then a continuous-time feedback control v is obtained that agrees with u when sampled at the Poincaré crossings.

To study the open-loop dynamics of the system, set $v \equiv 0$. Take the Poincaré section to be the positive y-axis. The corresponding Poincaré map is evaluated in [23] as follows:

$$Y_{k+1} = e^{2\pi p_k} Y_k \tag{4.29}$$

which simplifies to yield

$$Y_{k+1} = \begin{cases} 1+\alpha(Y_k-1)+\mu, & \text{for } Y_k < 1 \\ 1+\beta(Y_k-1)+\mu, & \text{for } Y_k > 1 \end{cases} \tag{4.30}$$

Note that the Poincaré map is one dimensional. Letting $Z_k = Y_k - 1$, this map can be written as

$$Z_{k+1} = \begin{cases} \alpha Z_k + \mu, & Z_k < 0 \\ \beta Z_k + \mu, & Z_k > 0 \end{cases} \tag{4.31}$$

which, fortuitously, is in the normal form for border collision bifurcations in 1D maps. Clearly, (4.31) undergoes a border collision bifurcation at $Z^* = 0$ (equivalently, at $Y^* = 1$) as μ is increased through zero. The map (4.31) has a fixed point $Z_A(\mu) = \frac{\mu}{1-\alpha}$ that occurs for $Y < 1$ and a fixed point $Z_B(\mu) = \frac{\mu}{1-\beta}$ that occurs for $Y > 1$. The stability of these fixed points is determined by the values of α and β, respectively. Also, the BCB scenario depends on the pair (α, β) as discussed in detail in Chapter 3. For illustration purposes, the parameter values $\alpha = 0.4$ and $\beta = -8.0$ are considered [23]. For these values of the parameters, the continuous time system undergoes a BCB from a stable period-1 cycle to chaos as μ is increased through zero (see Figure 4.2). This can also be seen by looking at the Poincaré map in the normal form for BCB and observing that these parameters lead to Scenario C3.

Next, the results of this chapter are used to design controllers for the BCB. The three actuation modes (unstable side, stable side, and simultaneous) cannot all be addressed with a common control objective, as discussed previously. Static feedback will be designed for each of the static feedback design approaches of Section 4.1. The transformation between the continuous time system and the Poincaré map is used to design a controller for the continuous time system.

4.2.1 Control Applied on the Unstable Side

Proposition 4.1 is now used to design a static feedback of the form $u_k = \gamma Z_k = \gamma(Y_k - 1)$ which will be applied only on the unstable side of the border. The fixed point of the

Poincaré map is stabilized for $-1-\beta<\gamma<1-\beta$. From (4.28), p_k involves β but not α for $Y_k>1$, and it involves α but not β for $Y_k<1$. Since the feedback control affects the value of β but not that of α, it follows that the control affects p_k only in the region $Y_k>1$.

Consider the map obtained by applying a control u_k on the unstable side of (4.31):

$$Z_{k+1}=\begin{cases}\alpha Z_k+\mu, & Z_k<0\\ \beta Z_k+\mu+u_k, & Z_k>0\end{cases} \tag{4.32}$$

Taking $u_k=\gamma Z_k$, the controlled map is

$$Z_{k+1}=\begin{cases}\alpha Z_k+\mu, & Z_k<0\\ \underbrace{(\beta+\gamma)}_{\tilde{\beta}} Z_k+\mu, & Z_k>0\end{cases} \tag{4.33}$$

For $Y_k>1$, $\tilde{p}_k=\dfrac{1}{2\pi}\log\left(\dfrac{1+(\beta+\gamma)(Y_k-1)+\mu}{Y_k}\right)$ where a tilde is used to denote variables that pertain to the controlled system. It is straightforward to show that $\tilde{p}_k=p_k+\Delta p_k$, where

$$\Delta p_k=\frac{1}{2\pi}\log\left(1+\frac{\gamma(Y_k-1)}{1+\beta(Y_k-1)+\mu}\right) \tag{4.34}$$

Observe that $\Delta p_k=0$ if the control gain $\gamma=0$. Also, $\tilde{p}_k=p_k$ for $Y_k<1$. Thus $\tilde{p}_k$ can be written as $\tilde{p}_k=p_k+g_{1k}\Delta p_k$, where

$$g_{1k}=\begin{cases}0, & Y_k<1\\ 1, & Y_k>1\end{cases} \tag{4.35}$$

and p_k is given by (4.28).

To obtain a corresponding control that yields the same result when applied to the original continuous time system, we seek a feedback v that, when inserted in the continuous-time model (4.26),(4.27), gives the open-loop version of the same model

with p_k replaced by $\tilde{p}_k$. Substituting the formula $\tilde{p}_k = p_k + g_{1k}\Delta p_k$ in place of p_k in the open-loop version of (4.26),(4.27) gives

$$\dot{x} = y \tag{4.36}$$

$$\dot{y} = -(1+p_k^2)\,x + 2p_k\,y + v(x,y) \tag{4.37}$$

where

$$v(x,y) = -(2g_{1k}p_k\Delta p_k + g_{1k}^2\Delta p_k^2)\,x + 2g_{1k}\Delta p_k\,y \tag{4.38}$$

Verifying this is an easy computation.

To see how the feedback control $v(x,y)$ is evaluated and applied to the continuous time model, note that the coefficients of x, y (i.e., the control gains) indexed by k in the equation of $v(x,y)$ (4.38) are evaluated at every intersection of the phase-plane trajectory with the positive y-axis. The values of the coefficients evaluated at the k-th intersection are used in the feedback control $v(x,y)$ until the $k+1$ phase-plane intersection with the positive y-axis, and so on.

Consider the parameter values $\alpha = 0.4$ and $\beta = -8.0$. The uncontrolled system undergoes a BCB from a stable period-1 cycle to chaos (see Figure 4.2). As shown above, a stabilizing control gain γ must satisfy $-1-\beta < \gamma < 1-\beta$, i.e., $7 < \gamma < 9$. The phase plot for the controlled system with $\gamma = 7.6$ is depicted in Figure 4.3, which shows that the system has a stable limit cycle after the border collision.

4.2.2 Control Applied on the Stable Side

In this control scheme, the control is applied on the stable side of the border only. It is straightforward to show, using an argument analogous to that used for the case when the control was applied on the unstable side, that a static feedback control applied to

the stable side of the border of the Poincaré map results in a control applied to the original system as follows:

$$\dot{x} = y \tag{4.39}$$

$$\dot{y} = -(1+p_k^2)\,x + 2p_k\,y + v(x,y) \tag{4.40}$$

where

$$v(x,y) = -(2g_{2k}p_k\Delta p_k + g_{2k}^2\Delta p_k^2)\,x + 2g_{2k}\Delta p_k\,y, \tag{4.41}$$

$$\Delta p_k = \frac{1}{2\pi}\log\left(1+\frac{\gamma(Y_k-1)}{1+\alpha(Y_k-1)+\mu}\right) \tag{4.42}$$

and

$$g_{2k} = \begin{cases} 1, & Y_k < 1 \\ 0, & Y_k > 1 \end{cases} \tag{4.43}$$

For concreteness, a controller is designed for the parameter values considered before ($\alpha = 0.4, \beta = -8.0$). Recall that a controller applied to the stable side of the border can be used to render the BCB a supercritical period-doubling border collision bifurcation (see Proposition 4.2). Figure 4.4 shows the phase plots of the controlled system ($\alpha = 0.4$, $\beta = -8.0$) using this control method, exhibiting a stable period-2 orbit after the border collision. Note that the period-1 orbit of the controlled system for $\mu < 0$ is slightly changed as a result of the control action (compare Fig. 4.4(a) with Fig. 4.2(a)).

4.2.3 Simultaneous Control

A simultaneous control applied to the Poincaré map gives:

$$Z_{k+1} = \begin{cases} \underbrace{(\alpha+\gamma)}_{\tilde{\alpha}} Z_k + \mu, & Z_k < 0 \\ \underbrace{(\beta+\gamma)}_{\tilde{\beta}} Z_k + \mu, & Z_k > 0 \end{cases} \tag{4.44}$$

Using similar analysis as in the case when the control is applied on the unstable side, it is straightforward to show that the corresponding closed-loop continuous time system is given by

$$\dot{x} = y \tag{4.45}$$

$$\dot{y} = -(1+p_k^2)\,x + 2p_k\,y + v(x,y) \tag{4.46}$$

where

$$v(x,y) = -(2p_k\Delta p_k + \Delta p_k^2)\,x + 2p_k\Delta p_k\,y, \tag{4.47}$$

$$\Delta p_k = \begin{cases} \dfrac{1}{2\pi}\log\left(1+\dfrac{\gamma(Y_k-1)}{1+\alpha(Y_k-1)+\mu}\right), & Y_k < 1 \\ \dfrac{1}{2\pi}\log\left(1+\dfrac{\gamma(Y_k-1)}{1+\beta(Y_k-1)+\mu}\right), & Y_k > 1 \end{cases} \tag{4.48}$$

Next, a controller is designed for the parameter values considered before ($\alpha = 0.4$, $\beta = -8.0$). Since $|\alpha - \beta| = 8.4 > 2$, simultaneous control cannot be used to stabilize a period-1 orbit after the border collision. However, simultaneous control can be used to render the BCB a supercritical period-doubling border collision bifurcation (see Proposition 4.4). Figure 4.5 shows the phase plots of the controlled system ($\alpha = 0.4$, $\beta = -8.0$) using this control method.

4.2.4 Discussion

Note that in order to apply the proposed BCB control methods to continuous time systems one needs to relate the control action in continuous time $v(x,y)$ with the parameters of the normal form a and b. In some cases (as in the example above), this relationship may be derived analytically. In some situations, it may have to be determined numerically. A stable periodic orbit in continuous time is mapped to a stable

fixed point of a Poincaré section. By perturbing the initial condition away from the stable fixed point, and by observing the evolution of the subsequent iterates (or intersections with the Poincaré section), one can obtain the slope of the map (on the stable side) for any value of the control gain [67]. By repeating this procedure for various control gains, it is possible to establish a relationship between the controller gain in the continuous time system and the controller gain of the discrete time system. This technique can, however, be applied only for the cases where the control is applied on the stable side of the border or for simultaneous control. As demonstrated in the example above, a control applied on the stable side of the border and a simultaneous control stabilized the system behavior after the border to period-2 orbit. This is valuable in cases where the uncontrolled system has no local attractors after the border collision.

For applying control on the unstable side, one needs to establish a relationship between the slope of the map in the unstable side and the controller gain for the continuous time system. This is feasible if the system has a chaotic attractor after the border collision, but not feasible in cases where the system has no local attractors after the border collision.

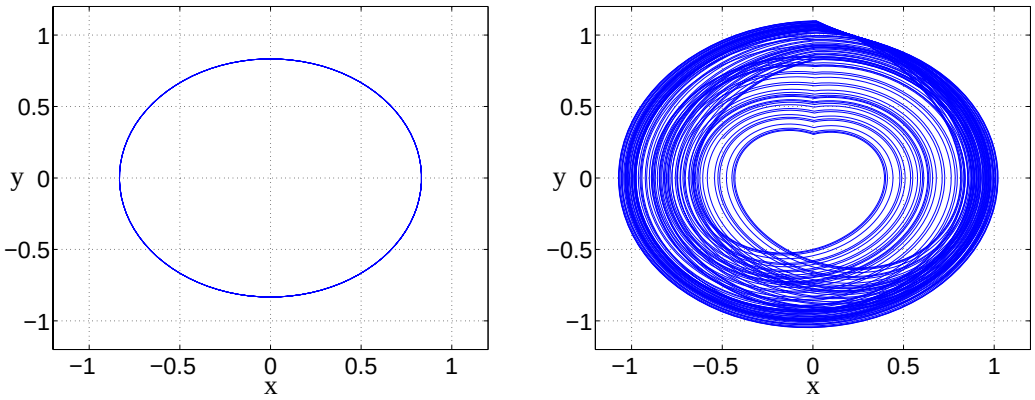

(a) $\mu = -0.1$ (b) $\mu = 0.1$

Figure 4.2: Phase plots of Example (4.26)-(4.27), uncontrolled system, $\alpha = 0.4$, $\beta = -8.0$. (a) before BCB ($\mu < 0$), (b) after BCB ($\mu > 0$).

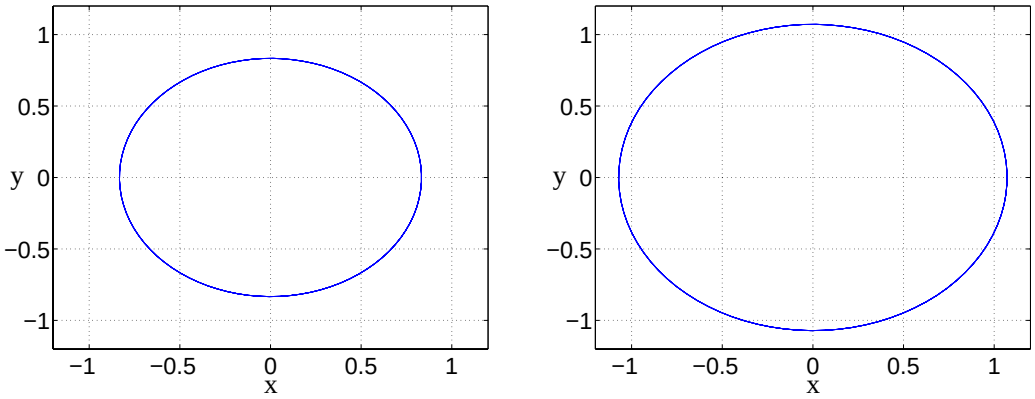

(a) $\mu = -0.1$ (b) $\mu = 0.1$

Figure 4.3: Controlled system (4.26)-(4.27), $\alpha = 0.4$, $\beta = -8.0$. Control applied in unstable side with control gain $\gamma = 7.6$.

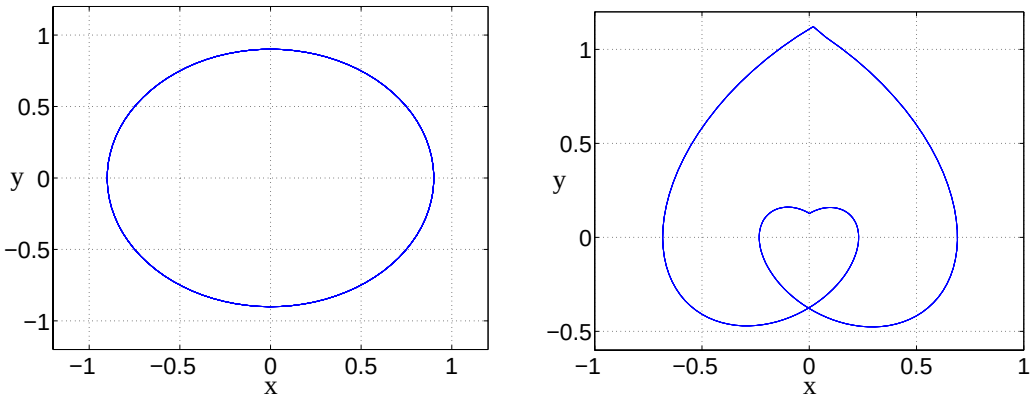

(a) $\mu = -0.1$ (b) $\mu = 0.1$

Figure 4.4: Controlled system (4.26)-(4.27), $\alpha = 0.4$, $\beta = -8.0$. Control applied in stable side with $\gamma = -0.41$.

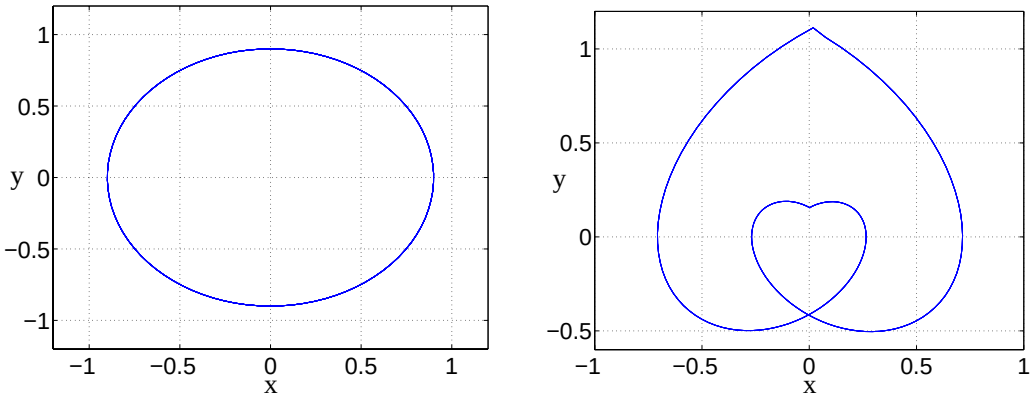

(a) $\mu = -0.1$ (b) $\mu = 0.1$

Figure 4.5: Controlled system (4.26)-(4.27), $\alpha = 0.4$, $\beta = -8.0$. Simultaneous control with $\gamma = -0.401$.

Chapter 5

Results on Border Collision Bifurcation in Two-Dimensional PWS Maps

As was pointed out in the summary given in Chapter 2 on the theoretical results available to-date on border collision bifurcations, the theory is general in nature and not much is available in the way of clear sufficient conditions for the various types of BCBs either in the *n*-dimensional case or in the two-dimensional case. It is not our purpose in this work to fill in all the gaps in the mathematical theory of BCBs. Rather, since our ultimate goal in this thesis is the development of control techniques for BCBs, we are most interested in conditions guaranteeing the less severe forms of BCBs. In this spirit, we undertake in the present chapter to address the question of sufficient conditions for *nonbifurcation with persistent stability* (defined in Chapters 1 and 2) for two dimensional systems undergoing border collision bifurcation. To illustrate the difficulty of determining such sufficient conditions, we begin the chapter with a discussion of an example of a new border collision phenomenon that we call "dangerous border collision bifurcation." We then present examples of multiple attractor bifurcations that occur in two dimensional PWS maps even though the Jacobian matrices of the PWS system on both sides of the border are Schur stable. Multiple attractor

bifurcations have been observed before [73, 9]. Finally, we state and prove sufficient conditions for nonbifurcation with persistent stability in two dimensional PWS maps. These results are applied to feedback control design in the next chapter.

5.1 Dangerous Border Collision Bifurcation

At the outset, it is tempting to conjecture that if the fixed points on either side of the border are asymptotically stable, then no BCB takes place and stability is maintained in a robust way as the fixed point crosses the border. To show that this conjecture is definitely false, we introduce a new border collision phenomenon in this section, that we refer to as dangerous border collision bifurcation [39]. This BCB doesn't occur in one-dimensional maps with two regions of smooth behavior, but can occur in piecewise smooth maps of dimension two and higher. In it, although the fixed points on either side of the border are certainly locally asymptotically stable, the stability is nonrobust as the border is crossed.

Consider the following two dimensional piecewise affine map:

$$\begin{pmatrix} x_{k+1} \\ y_{k+1} \end{pmatrix} = \begin{cases} \underbrace{\begin{pmatrix} -0.3 & 1 \\ -0.9 & 0 \end{pmatrix}}_{A} \begin{pmatrix} x_k \\ y_k \end{pmatrix} + \begin{pmatrix} 1 \\ 0 \end{pmatrix} \mu, & x_k \leq 0 \\ \underbrace{\begin{pmatrix} -1.6 & 1 \\ -0.9 & 0 \end{pmatrix}}_{B} \begin{pmatrix} x_k \\ y_k \end{pmatrix} + \begin{pmatrix} 1 \\ 0 \end{pmatrix} \mu, & x_k > 0 \end{cases} \tag{5.1}$$

The map is written in normal form for border collision bifurcation, and as usual μ represents the bifurcation parameter.

The eigenvalues of A are $\lambda_{A_{1,2}} = -0.15 \pm i0.9367$ and those of B are $\lambda_{B_{1,2}} = -0.80 \pm i0.5099$. Although the matrices A and B are Schur stable, it turns out that

the origin of the system with $\mu = 0$ is unstable. To see how the dynamics depends on μ, note that for $\mu < 0$, the fixed point is $(x_A(\mu), y_A(\mu)) = (\frac{1}{2.2}\mu, -\frac{0.9}{2.2}\mu)$, and that it is locally asymptotically stable as noted above. However, its region of attraction shrinks to the single point $(0,0)$ at $\mu = 0$. For $\mu > 0$, the fixed point is $(x_B(\mu), y_B(\mu)) = (\frac{1}{3.5}\mu, -\frac{0.9}{3.5}\mu)$ and is also locally asymptotically stable. Its regions of attraction shrinks to the single point $(0,0)$ at $\mu = 0$. Therefore, at $\mu = 0$, the trajectory of the map (5.1) diverges for any nonzero initial condition. A sample trajectory of x_k for $\mu = 0$ is shown in Figure 5.1 and a phase plot for y_k versus x_k for $\mu = 0$ is shown in Figure 5.2.

In Chapter 6, feedback control laws are designed to stabilize border collision bifurcations and this example is revisited where we show that feedback control can eliminate the bifurcation.

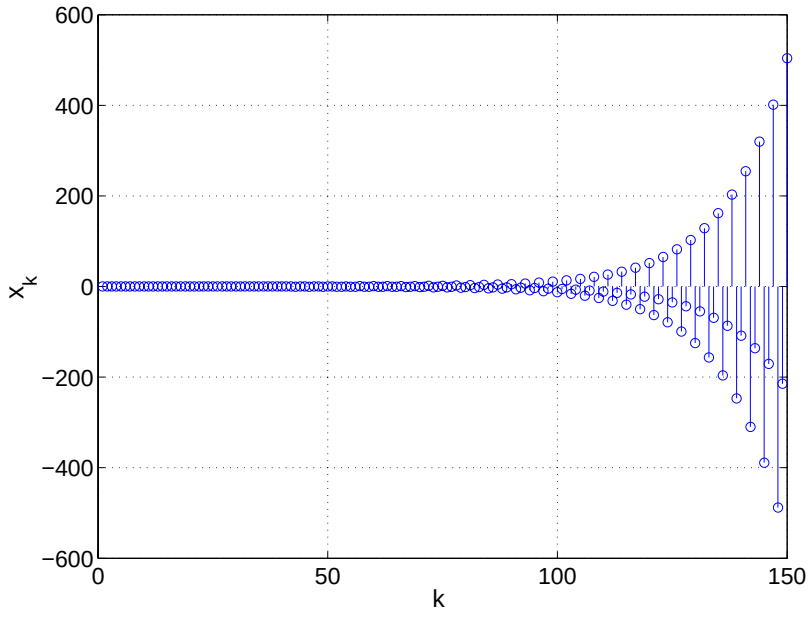

Figure 5.1: Time series for x_k for the example of dangerous border collision bifurcation given in (5.1) with $\mu = 0$ and initial condition $(x_0, y_0) = (-0.03, 0.01)$.

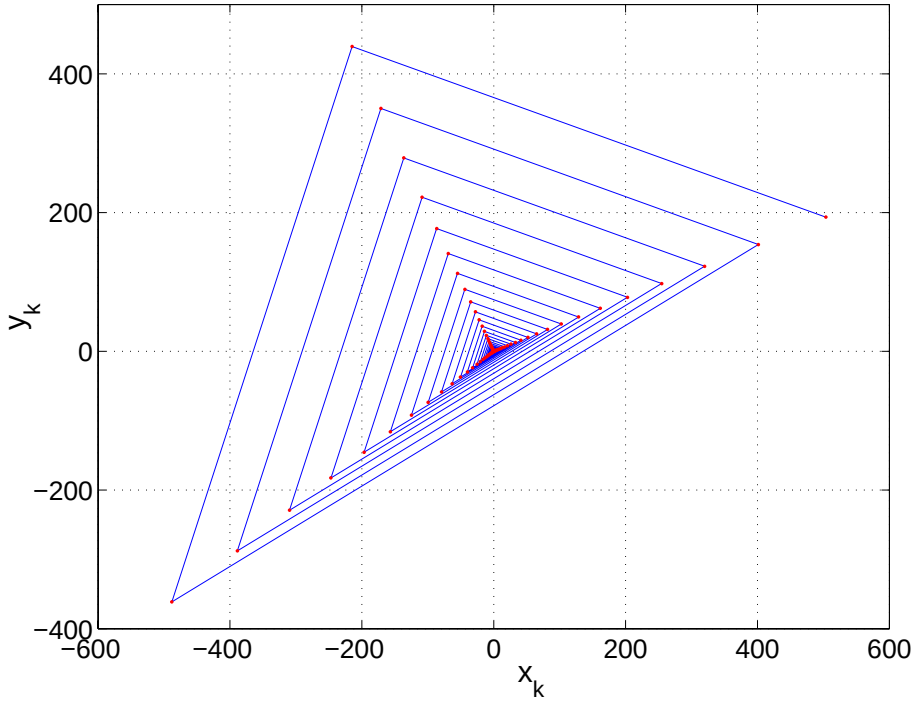

Figure 5.2: The phase plot for y_k versus x_k for the example of dangerous border collision bifurcation given in (5.1) with $\mu = 0$ and initial condition $(x_0, y_0) = (-0.03, 0.01)$.

5.2 Examples of Multiple Attractor BCB in 2-D Systems

In this section, we present new examples of multiple attractor border collision bifurcations. These examples show bifurcations of multiple attractors on one side or both sides of the border even though the fixed point is asymptotically stable on both sides of the border. Other examples demonstrating similar BCBs have appeared in [73, 9]. It is of interest to note that recently multiple attractor BCBs were shown to be a source of unpredictability in piecewise smooth systems [25]: the presence of arbitrarily small noise may lead to fundamentally unpredictable behavior of orbits as a bifurcation parameter is slowly varied through a critical value.

Example 5.1 Stable fixed point plus period-4 attractor bifurcating to stable fixed point plus period-3 attractor:

Consider the two-dimensional piecewise smooth map

$$\begin{pmatrix} x_{k+1} \\ y_{k+1} \end{pmatrix} = \begin{cases} \underbrace{\begin{pmatrix} 0.50 & 1 \\ -0.90 & 0 \end{pmatrix}}_{A} \begin{pmatrix} x_k \\ y_k \end{pmatrix} + \begin{pmatrix} 1 \\ 0 \end{pmatrix} \mu, & x_k \leq 0 \\ \underbrace{\begin{pmatrix} -1.22 & 1 \\ -0.36 & 0 \end{pmatrix}}_{B} \begin{pmatrix} x_k \\ y_k \end{pmatrix} + \begin{pmatrix} 1 \\ 0 \end{pmatrix} \mu, & x_k > 0 \end{cases} \tag{5.2}$$

This map undergoes a bifurcation in which a stable fixed point along with a period-4 attractor yield a stable fixed point and a period-3 attractor, as μ is increased through zero (see Figure 5.3). The eigenvalues of A are $\lambda_{A_{1,2}} = 0.25 \pm 0.9152\mathrm{i}$ and those of B are $\lambda_{B_1} = -0.5$, $\lambda_{B_2} = -0.72$.

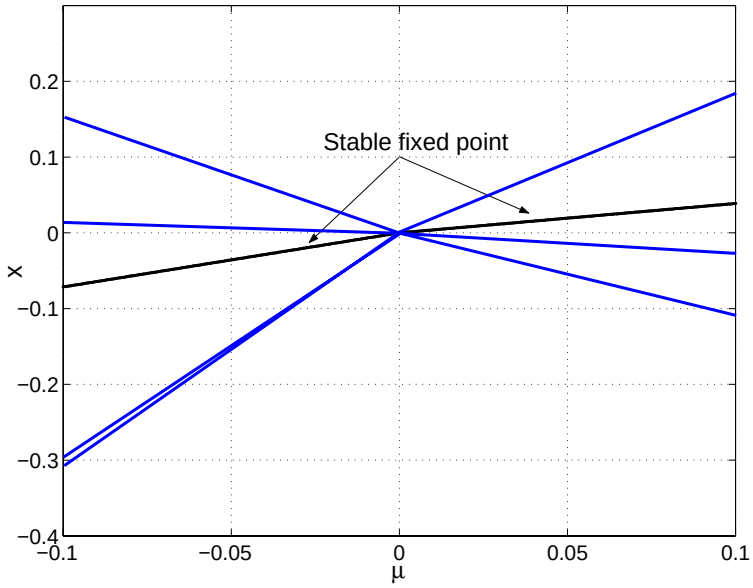

Figure 5.3: Bifurcation diagram for Example 5.1.

Example 5.2 Stable fixed point bifurcating to stable fixed point plus period-7 attractor:

Consider the two dimensional piecewise smooth map

$$\begin{pmatrix} x_{k+1} \\ y_{k+1} \end{pmatrix} = \begin{cases} \underbrace{\begin{pmatrix} 1.6 & 1 \\ -0.8 & 0 \end{pmatrix}}_{A} \begin{pmatrix} x_k \\ y_k \end{pmatrix} + \begin{pmatrix} 1 \\ 0 \end{pmatrix} \mu, & x_k \leq 0 \\ \underbrace{\begin{pmatrix} -1.4 & 1 \\ -0.6 & 0 \end{pmatrix}}_{B} \begin{pmatrix} x_k \\ y_k \end{pmatrix} + \begin{pmatrix} 1 \\ 0 \end{pmatrix} \mu, & x_k > 0 \end{cases} \tag{5.3}$$

This map undergoes a bifurcation in which a stable fixed point yields a stable fixed point along with a period-7 attractor, as μ is increased through zero (see Figure 5.4). The eigenvalues of A are $\lambda_{A_{1,2}} = 0.8 \pm 0.4\text{i}$ and those for B are $\lambda_{B_{1,2}} = -0.7 \pm 0.3317\text{i}$.

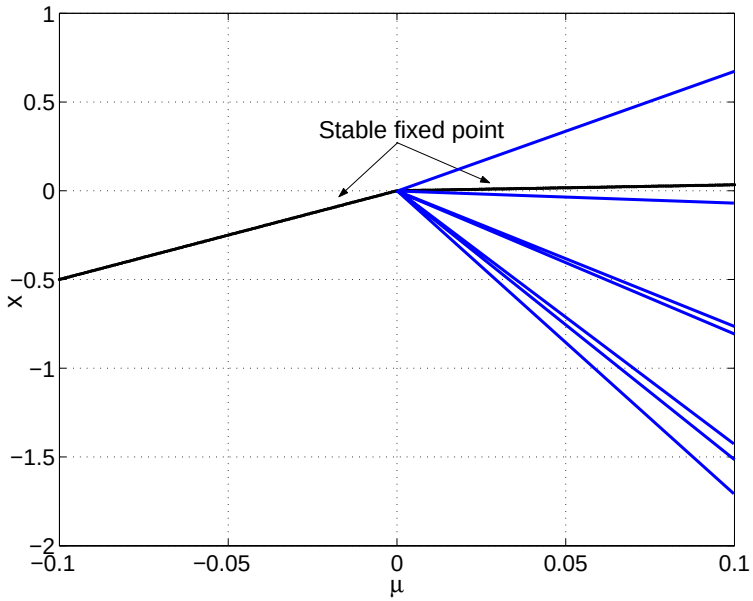

Figure 5.4: Bifurcation diagram for Example 5.2.

5.3 Sufficient Conditions for Nonbifurcation with Persistent Stability in Two-Dimensional PWS Maps

In this section, sufficient conditions for nonbifurcation with persistent stability in two dimensional PWS maps are stated and proved. Although, as mentioned earlier and illustrated by the foregoing examples, Schur stability of the Jacobian matrices on both sides of the border is insufficient for guaranteeing nonbifurcation with persistent stability, imposing a realness of eigenvalues condition along with Schur stability turns out to be a starting point for obtaining actual sufficient conditions. We have proved nonbifurcation with persistent stability results for some of the situations in which real and stable eigenvalues occur on both sides of the border, and the results are developed in detail below. The remaining cases left unproven at this time will be addressed in future work. It is important to point out that if a matrix has real distinct eigenvalues,

then a perturbed version of the matrix (with small perturbations) continues to have real eigenvalues.

Consider the one-parameter family of piecewise affine (PWA) maps (in normal form for BCB) $F_\mu : \mathbb{R}^2 \to \mathbb{R}^2$, where

$$F_\mu(x,y) = \begin{cases} \begin{pmatrix} \tau_A & 1 \\ -\delta_A & 0 \end{pmatrix} \begin{pmatrix} x \\ y \end{pmatrix} + \begin{pmatrix} 1 \\ 0 \end{pmatrix} \mu, & x \leq 0 \\ \begin{pmatrix} \tau_B & 1 \\ -\delta_B & 0 \end{pmatrix} \begin{pmatrix} x \\ y \end{pmatrix} + \begin{pmatrix} 1 \\ 0 \end{pmatrix} \mu, & x > 0 \end{cases} \tag{5.4}$$

Let $A := \begin{pmatrix} \tau_A & 1 \\ -\delta_A & 0 \end{pmatrix}$ and $B := \begin{pmatrix} \tau_B & 1 \\ -\delta_B & 0 \end{pmatrix}$. Denote the eigenvalues of A by $\lambda_A^{\pm}$ and the eigenvalues of B by $\lambda_B^{\pm}$. (For the case of real eigenvalues, the eigenvalue with a plus sign will be taken to be the larger of the two eigenvalues.)

As discussed in Chapter 2, the normal form can be used to study bifurcations in an original PWS map with nonlinear maps on either side of the border under generic conditions. In fact there are two such conditions, not usually explicated in the literature: 1) neither A nor B has eigenvalues on the unit circle; 2) the fixed point does not move along the border after the border collision event, i.e., either the fixed point crosses the border or it merges with another fixed point at the border collision and both fixed points disappear.

Next, we state and prove sufficient conditions for nonbifurcation with persistent stability. Each result is given in a separate subsection.

5.3.1 Positive Eigenvalues on Both Sides of the Border

In this subsection, we consider system (5.4) under the assumption that the eigenvalues of the matrices A and B lie in the open interval $(0,1)$. We show that this is a sufficient condition for nonbifurcation with persistent stability. We carry out the investigation of the dynamics of system (5.4) in two stages. First we prove global asymptotic stability for the system at criticality, i.e., for the system obtained upon setting $\mu = 0$ in (5.4). Then, we show a similar result for the system with $\mu < 0$ and with $\mu > 0$.

Proposition 5.1 (Global stability of fixed point attractor on border: positive eigenvalues)

Let the eigenvalues $\lambda_A^{\pm}$ of A and $\lambda_B^{\pm}$ of B satisfy $0 < \lambda_A^- < \lambda_A^+ < 1$ and $0 < \lambda_B^- < \lambda_B^+ < 1$. Then for $\mu = 0$, the map F_μ has a unique fixed point attractor $(x(\mu), y(\mu)) = (0,0)$ and this fixed point attractor is globally asymptotically stable. That is, for every initial condition (x_0, y_0), the resulting orbit converges to $(0,0)$, so $\lim_{n\to\infty} F_\mu^n(x_0,y_0) = (0,0)$.

Proof: Let the map F_μ satisfy the assumptions of Proposition 5.1. Note that the assumptions imply that $0 < \delta_A < 1$ and $0 < \delta_B < 1$. Denote by Γ the border $\{(x,y) |\ x = 0\}$ between the regions $R_A := \{(x,y) \in \mathbb{R}^2 |\ x \le 0\}$ and $R_B := \{(x,y) \in \mathbb{R}^2 |\ x \ge 0\}$. Denote by $L(\lambda_A^{\pm})$ the two half-lines determined by the eigenvectors of A corresponding to the eigenvalues $\lambda_A^{\pm}$, respectively, in region R_A, and by $L(\lambda_B^{\pm})$ the two half-lines determined by the eigenvectors of B corresponding to eigenvalues $\lambda_B^{\pm}$, respectively, in region R_B. These half-lines are given explicitly as follows:

$$L(\lambda_A^+) = \{(x,y) \in R_A \cup \Gamma :\ y = -\lambda_A^- x\}, \tag{5.5}$$

$$L(\lambda_A^-) = \{(x,y) \in R_A \cup \Gamma :\ y = -\lambda_A^+ x\}, \tag{5.6}$$

$$L(\lambda_B^+) = \{(x,y) \in R_B \cup \Gamma :\ y = -\lambda_B^- x\}, \tag{5.7}$$

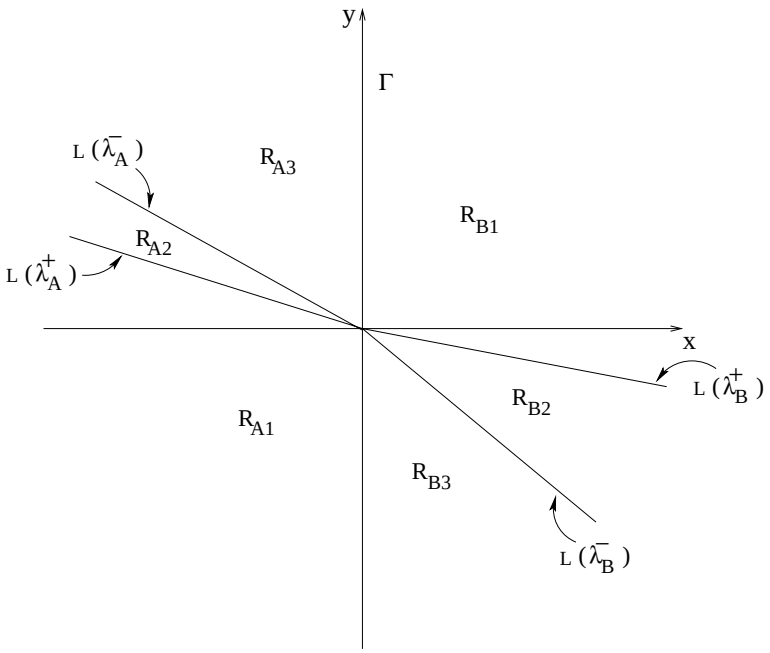

Figure 5.5: Schematic diagram showing the half-lines generated by eigenvectors and the regions R_{A1}, R_{A2}, R_{A3}, R_{B1}, R_{B2} and R_{B3} used in the proof of Proposition 5.1.

$$L(\lambda_B^-) \;=\; \{(x,y) \in R_B \cup \Gamma : \; y = -\lambda_B^+ x\}. \tag{5.8}$$

Note that the slopes of all four lines are negative. (Refer to Figure 5.5.) The half-lines $L(\lambda_A^+)$ and $L(\lambda_A^-)$ divide the region R_A into three subregions, denoted by R_{A1}, R_{A2} and R_{A3}. Similarly, the half-lines $L(\lambda_B^+)$ and $L(\lambda_B^-)$ divide the region R_B into three subregions, denoted by R_{B1}, R_{B2} and R_{B3}. The subregions of R_A are defined as follows: R_{A1} is the region bordered by Γ and $L(\lambda_A^+)$, R_{A2} is the region bordered by $L(\lambda_A^+)$ and $L(\lambda_A^-)$ and R_{A3} is the region bordered by $L(\lambda_A^-)$ and Γ. Similarly, subregions of R_B are defined in the following way: R_{B1} is the region bordered by Γ and $L(\lambda_B^+)$, R_{B2} is the region bordered by $L(\lambda_B^+)$ and $L(\lambda_B^-)$ and R_{B3} is the region bordered by $L(\lambda_B^-)$ and Γ (see Figure 5.5). Note that the subregions are numbered in a clockwise sense. Let $(x_0, y_0) \in \mathbb{R}^2$ be a given initial condition. Then, the following

facts are clear:

- If $(x_0,y_0) \in L(\lambda_A^+)$, then $\lim_{n\to\infty} F_\mu^n(x_0,y_0) = \lim_{n\to\infty}(\lambda_A^+)^n(x_0,y_0) = (0,0)$;
- If $(x_0,y_0) \in L(\lambda_A^-)$, then $\lim_{n\to\infty} F_\mu^n(x_0,y_0) = \lim_{n\to\infty}(\lambda_A^-)^n(x_0,y_0) = (0,0)$;
- If $(x_0,y_0) \in L(\lambda_B^+)$, then $\lim_{n\to\infty} F_\mu^n(x_0,y_0) = \lim_{n\to\infty}(\lambda_B^+)^n(x_0,y_0) = (0,0)$; and
- If $(x_0,y_0) \in L(\lambda_B^-)$, then $\lim_{n\to\infty} F_\mu^n(x_0,y_0) = \lim_{n\to\infty}(\lambda_B^-)^n(x_0,y_0) = (0,0)$.

The following facts, which assert positive invariance of the subregions R_{A1}, R_{A2}, R_{B1} and R_{B2}, follow from the expression for the solution of a general linear difference equation and the assumption that the eigenvalues lie in $(0,1)$:

- If $(x_0,y_0) \in R_{A1}$, then $F_\mu^n(x_0,y_0) \in R_{A1}\ \forall\ n$ and $\lim_{n\to\infty} F_\mu^n(x_0,y_0) = (0,0)$;
- If $(x_0,y_0) \in R_{A2}$, then $F_\mu^n(x_0,y_0) \in R_{A2}\ \forall\ n$ and $\lim_{n\to\infty} F_\mu^n(x_0,y_0) = (0,0)$;
- If $(x_0,y_0) \in R_{B1}$, then $F_\mu^n(x_0,y_0) \in R_{B1}\ \forall\ n$ and $\lim_{n\to\infty} F_\mu^n(x_0,y_0) = (0,0)$; and
- If $(x_0,y_0) \in R_{B2}$, then $F_\mu^n(x_0,y_0) \in R_{B2}\ \forall\ n$ and $\lim_{n\to\infty} F_\mu^n(x_0,y_0) = (0,0)$.

Hence, in the remainder of this proof, we assume that $(x_0,y_0) \notin R_{A1} \cup R_{A_2} \cup R_{B1} \cup R_{B2}$.

First, we consider the case $(x_0,y_0) \in \Gamma$. Denote by Γ^+ the positive y-axis $\{(x,y) \in \Gamma :\ y > 0\}$, and by Γ^- the negative y-axis $\{(x,y) \in \Gamma :\ y < 0\}$. If $(x_0,y_0) \in \Gamma^+$, then $F_\mu(x_0,y_0) = (y_0,0) \in R_{B1}$ and the positive invariance of R_{B1} implies that $F_\mu^n(x_0,y_0) \in R_{B1}\ \forall\, n \geq 1$ and $\lim_{n\to\infty} F_\mu^n(x_0,y_0) = (0,0)$. If $(x_0,y_0) \in \Gamma^-$, then $F_\mu(x_0,y_0) = (y_0,0) \in R_{A1}$ and the positive invariance of R_{A1} implies that $F_\mu^n(x_0,y_0) \in R_{A1}\ \forall\ n \geq 1$ and $\lim_{n\to\infty} F_\mu^n(x_0,y_0) = (0,0)$. It remains to consider the cases: (a) $(x_0,y_0) \in R_{A3}$ and (b) $(x_0,y_0) \in R_{B3}$.

Case (a). Assume that $(x_0,y_0) \in R_{A3}$. Define the map $G_A : \mathbb{R}^2 \to \mathbb{R}^2$ to be the affine extension of the left part of the map $F_\mu(x,y)$ to the whole plane: $G_A(x,y) = (\tau_A x + y, -\delta_A x)^T$. Since $0 < \delta_A < 1$, the map G_A is invertible, and $G_A^{-1}(x,y) = \left(-\frac{y}{\delta_A}, x + y\frac{\tau_A}{\delta_A}\right)^T$. Note that if $y > 0$, then $G_A^{-1}(0,y) = \left(-\frac{y}{\delta_A}, y\frac{\tau_A}{\delta_A}\right)^T \in R_{A3}$. Therefore, $G_A^{-1}(\Gamma^+)$ is contained in the subregion R_{A3}. By induction, one can show that for every $n \in \mathbb{N}$, $G_A^{-(n+1)}(\Gamma^+)$ is contained in the region bordered by $G_A^{-n}(\Gamma^+)$ and $L(\lambda_A^-)$. Furthermore, it is straightforward to show that the set $G_A^{-n}(\Gamma^+)$ asymptotically approaches the half-line $L(\lambda_A^-)$ as $n \to \infty$. Hence, there is a positive integer m such that either $(x_0,y_0) \in G_A^{-m}(\Gamma^+)$ or (x_0,y_0) is contained in the region bordered by $G_A^{-(m-1)}(\Gamma^+)$ and $G_A^{-m}(\Gamma^+)$. Hence, $F_\mu^{m+1}(x_0,y_0) \in R_{B1}$ and the positive invariance of R_{B1} implies that $F_\mu^{n+m}(x_0,y_0) \in R_{B1}\ \forall\ n \geq 1$ and $\lim_{n\to\infty} F_\mu^{n+m}(x_0,y_0) = (0,0)$.

Case (b). Assume that $(x_0,y_0) \in R_{B3}$. Define the map $G_B : \mathbb{R}^2 \to \mathbb{R}^2$ to be the affine extension of the right part of the map $F_\mu(x,y)$ to the whole plane: $G_B(x,y) = (\tau_B x + y, -\delta_B x)^T$. Since $0 < \delta_B < 1$, the map G_B is invertible, and $G_B^{-1}(x,y) = \left(-\frac{y}{\delta_B}, x + y\frac{\tau_B}{\delta_B}\right)^T$. Note that if $y < 0$, then $G_B^{-1}(0,y) = \left(-\frac{y}{\delta_B}, y\frac{\tau_B}{\delta_B}\right)^T \in R_{B3}$. Therefore, $G_B^{-1}(\Gamma^-)$ is contained in the subregion R_{B3}. By induction, one can show that for every $n \in \mathbb{N}$, $G_B^{-(n+1)}(\Gamma^-)$ is contained in the region bordered by $G_B^{-n}(\Gamma^-)$ and $L(\lambda_B^-)$. Furthermore, it is straightforward to show that the set $G_B^{-n}(\Gamma^-)$ asymptotically approaches the half-line $L(\lambda_B^-)$ as $n \to \infty$. Hence, there is a positive integer m such that either $(x_0,y_0) \in G_B^{-m}(\Gamma^-)$ or (x_0,y_0) is contained in the region bordered by $G_B^{-(m-1)}(\Gamma^-)$ and $G_B^{-m}(\Gamma^-)$. Hence, $F_\mu^{m+1}(x_0,y_0) \in R_{A1}$ and the positive invariance of R_{A1} implies that $F_\mu^{n+m}(x_0,y_0) \in R_{A1}\ \forall\ n \geq 1$ and $\lim_{n\to\infty} F_\mu^{n+m}(x_0,y_0) = (0,0)$.

All the cases have been exhausted and we conclude: if $\mu = 0$, then the map F_μ has a unique fixed point attractor at $(x(\mu),y(\mu)) = (0,0)$ and that this fixed point is globally asymptotically stable. This completes the proof of Proposition 5.1. ■

The next proposition asserts that the map (5.4) possesses a unique fixed point attractor for all values of μ if the eigenvalues of both A and B are in $(0,1)$.

Proposition 5.2 (Global stability of fixed point attractor: positive eigenvalues) *Let for $\mu \in \mathbb{R}$, the map $F_\mu : \mathbb{R}^2 \to \mathbb{R}^2$ be defined by (5.4). Let the eigenvalues $\lambda_A^{\pm}$ of A and $\lambda_B^{\pm}$ of B satisfy $0 < \lambda_A^- < \lambda_A^+ < 1$ and $0 < \lambda_B^- < \lambda_B^+ < 1$. Then for every $\mu \in \mathbb{R}$, the map F_μ has a unique fixed point attractor $(x(\mu), y(\mu))$ and this fixed point attractor is globally asymptotically stable. That is, for every initial condition $(x_0, y_0) \in \mathbb{R}^2$, the resulting orbit converges to $(x(\mu), y(\mu))$, so $\lim_{n\to\infty} F_\mu^n(x_0, y_0) = (x(\mu), y(\mu))$.*

Proof: Let the map F_μ satisfy the assumptions of Proposition 5.2. Denote by Γ the border $\{(x,y) \in \mathbb{R}^2 : \ x = 0\}$ between the regions R_A and R_B. For $\mu \in \mathbb{R}$, define the map $G_{\mu,A} : \mathbb{R}^2 \to \mathbb{R}^2$ to be the affine extension of the left part of the map $F_\mu(x,y)$ to the whole plane: $G_{\mu,A}(x,y) = (\tau_A x + y + \mu, -\delta_A x)^T$ and define the map $G_{\mu,B} : \mathbb{R}^2 \to \mathbb{R}^2$ to be the affine extension of the right part of the map $F_\mu(x,y)$ to the whole plane: $G_{\mu,B}(x,y) = (\tau_B x + y + \mu, -\delta_B x)^T$.

Denote by $\bar{P}_A(\mu) = (\bar{x}_A(\mu), \bar{y}_A(\mu))$ the fixed point of $G_{\mu,A}$, and by $\bar{P}_B(\mu) = (\bar{x}_B(\mu), \bar{y}_B(\mu))$ the fixed point of $G_{\mu,B}$. By the assumptions $0 < \delta_A < 1$ and $0 < \delta_B < 1$, the maps $G_{\mu,A}$ and $G_{\mu,B}$ are invertible. The inverse of the map $G_{\mu,A}$ is given by $G_{\mu,A}^{-1}(x,y) = \left(-\frac{y}{\delta_A}, x + y\frac{\tau_A}{\delta_A} - \mu\right)^T$, and the inverse of $G_{\mu,B}$ is given by $G_{\mu,B}^{-1}(x,y) = \left(-\frac{y}{\delta_B}, x + y\frac{\tau_B}{\delta_B} - \mu\right)^T$.

The proof of this proposition is divided by considering the following three cases: (1) $\mu = 0$, (2) $\mu < 0$ and (3) $\mu > 0$.

Case (1): $\mu = 0$. Follows from Proposition 5.1.

Case (2): $\mu < 0$. The map F_μ has a unique fixed point $P_A^*(\mu) = (x_A(\mu), y_A(\mu))$, where $x_A(\mu) = \frac{\mu}{1-\tau_A+\delta_A}$ and $y_A(\mu) = -\delta_A x_A(\mu)$. Note that: (a) the fixed point $\bar{P}_A(\mu)$ of $G_{\mu,A}$ is the fixed point $P_A^*(\mu) = (x_A(\mu), y_A(\mu))$ of F_μ, and (b) the fixed point $\bar{P}_B(\mu)$ of $G_{\mu,B}$

is the virtual fixed point of F_μ and this point is given by $\bar{x}_B(\mu) = \frac{\mu}{1-\tau_B+\delta_B}$ and $\bar{y}_B(\mu) = -\delta_B \bar{x}_B(\mu)$.

The map F_μ has four invariant half-lines: two invariant half-lines $L_\mu(\lambda_A^+)$ and $L_\mu(\lambda_A^-)$ in R_A corresponding to the fixed point $P_A^*(\mu)$ and two invariant half-lines $L_\mu(\lambda_B^+)$ and $L_\mu(\lambda_B^-)$ in R_B corresponding to the virtual fixed point $\bar{P}_B(\mu)$ (in R_A). The half-lines $L_\mu(\lambda_A^+)$ and $L_\mu(\lambda_A^-)$ are determined by the eigenvectors of A corresponding to eigenvalues λ_A^+ and λ_A^-, respectively, in the region R_A. Similarly, the half-lines $L_\mu(\lambda_B^+)$ and $L_\mu(\lambda_B^-)$ are determined by the eigenvectors of B corresponding to eigenvalues λ_B^+ and λ_B^-, respectively, in the region R_B. These half-lines are given explicitly as follows:

$$L_\mu(\lambda_A^+) = \{(x,y) \in R_A \cup \Gamma : y - y_A(\mu) = -\lambda_A^-(x - x_A(\mu))\}, \tag{5.9}$$

$$L_\mu(\lambda_A^-) = \{(x,y) \in R_A \cup \Gamma : y - y_A(\mu) = -\lambda_A^+(x - x_A(\mu))\}, \tag{5.10}$$

$$L_\mu(\lambda_B^+) = \{(x,y) \in R_B \cup \Gamma : y - \bar{y}_B(\mu) = -\lambda_B^-(x - \bar{x}_B(\mu))\}, \tag{5.11}$$

$$L_\mu(\lambda_B^-) = \{(x,y) \in R_B \cup \Gamma : y - \bar{y}_B(\mu) = -\lambda_B^+(x - \bar{x}_B(\mu))\}. \tag{5.12}$$

Note that the slopes of all four half-lines are negative. (Refer to Figure 5.6.) The two half-lines $L_\mu(\lambda_A^+)$ and $L_\mu(\lambda_A^-)$ divide the region R_A into four subregions denoted by R_{A1}, R_{A2}, R_{A3} and R_{A4}. Similarly, the half-lines $L_\mu(\lambda_B^+)$ and $L_\mu(\lambda_B^-)$ divide the region R_B into three subregions.

In order to define the four subregions of R_A and the subregions of R_B, we need the points of intersection of the four half-lines with the border Γ. The half-lines $L_\mu(\lambda_A^+)$, $L_\mu(\lambda_A^-)$, $L_\mu(\lambda_B^+)$, and $L_\mu(\lambda_B^-)$ intersect the border Γ at

$$y_\mu(\lambda_A^+) = \lambda_A^-(1-\lambda_A^+)x_A(\mu) = \frac{\mu\lambda_A^-}{1-\lambda_A^-}, \tag{5.13}$$

$$y_\mu(\lambda_A^-) = \lambda_A^+(1-\lambda_A^-)x_A(\mu) = \frac{\mu\lambda_A^+}{1-\lambda_A^+}, \tag{5.14}$$

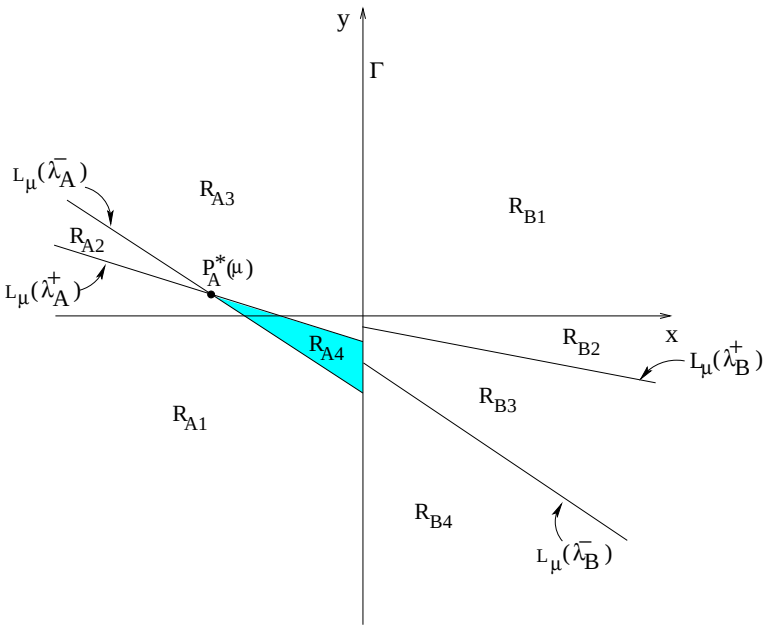

Figure 5.6: Schematic diagram showing the half-lines generated by eigenvectors and the regions R_{A1}, R_{A2}, R_{A3}, R_{A4}, R_{B1}, R_{B2}, R_{B3} and R_{B4} used in the proof of Proposition 5.2 for $\mu < 0$.

$$y_\mu(\lambda_B^+) = \lambda_B^-(1-\lambda_B^+)\bar{x}_B(\mu) = \frac{\mu\lambda_B^-}{1-\lambda_B^-}, \tag{5.15}$$

$$y_\mu(\lambda_B^-) = \lambda_B^+(1-\lambda_B^+)\bar{x}_B(\mu) = \frac{\mu\lambda_B^+}{1-\lambda_B^+}. \tag{5.16}$$

respectively. Furthermore, the half-lines $L_\mu(\lambda_A^+)$ and $L_\mu(\lambda_A^-)$ intersect the x-axis at

$$x_\mu(\lambda_A^+) = \frac{\mu}{1-\lambda_A^-}, \tag{5.17}$$

$$x_\mu(\lambda_A^-) = \frac{\mu}{1-\lambda_A^+}. \tag{5.18}$$

respectively. Note that $y_\mu(\lambda_A^-) < y_\mu(\lambda_A^+) < 0$, $y_\mu(\lambda_B^-) < y_\mu(\lambda_B^+) < 0$ and $x_\mu(\lambda_A^-) < x_\mu(\lambda_A^+) < 0$.

Denote by $\Gamma_\mu(\lambda_A^+) = (0, y_\mu(\lambda_A^+))$, $\Gamma_\mu(\lambda_A^-) = (0, y_\mu(\lambda_A^-))$, $\Gamma_\mu(\lambda_B^+) = (0, y_\mu(\lambda_B^+))$, $\Gamma_\mu(\lambda_B^-) = (0, y_\mu(\lambda_B^-))$, $S_\mu(\lambda_A^+) = (x_\mu(\lambda_A^+), 0)$, and $S_\mu(\lambda_A^-) = (x_\mu(\lambda_A^-), 0)$. It is straightforward to verify that, $F_\mu(\Gamma_\mu(\lambda_A^+)) = S_\mu(\lambda_A^+)$ and $F_\mu(\Gamma_\mu(\lambda_A^-)) = S_\mu(\lambda_A^-)$.

The subregions of R_A and R_B are defined as follows (for illustration see Figure 5.7): R_{A1} is the region bordered by Γ (the part of Γ below $\Gamma_\mu(\lambda_A^-)$), the segment $[\Gamma_\mu(\lambda_A^-), P_A^*(\mu)]$ on $L_\mu(\lambda_A^-)$, and the half-line $L_\mu(\lambda_A^+)$ from which the segment $[P_A^*(\mu), \Gamma_\mu(\lambda_A^+)]$ is deleted; R_{A2} is the region bordered by the half-lines $L_\mu(\lambda_A^+)$ and $L_\mu(\lambda_A^-)$ from which the segments $[P_A^*(\mu), \Gamma_\mu(\lambda_A^+)]$ and $[P_A^*(\mu), \Gamma_\mu(\lambda_A^-)]$, respectively, are deleted; R_{A3} is the region bordered by $L_\mu(\lambda_A^-)$ from which the segment $[P_A^*(\mu), \Gamma_\mu(\lambda_A^-)]$ is deleted, the segment $[P_A^*(\mu), \Gamma_\mu(\lambda_A^+)]$ on $L_\mu(\lambda_A^+)$ and the border Γ (in fact, the part of Γ above $\Gamma_\mu(\lambda_A^+)$); and R_{A4} is the region bordered by the segment $[P_A^*(\mu), \Gamma_\mu(\lambda_A^-)]$ on $L_\mu(\lambda_A^-)$, the segment $[P_A^*(\mu), \Gamma_\mu(\lambda_A^+)]$ on $L_\mu(\lambda_A^+)$ and the segment $[\Gamma_\mu(\lambda_A^-), \Gamma_\mu(\lambda_A^+)]$ on the border Γ. The region R_{A4} is bounded and it is the only subregion that is bounded. Similarly, R_{B1} is the region bordered by $\Gamma_{\mu,1} = \{(x,y) \in \Gamma : \ y \geq 0\}$ and the x-axis; R_{B2} is the region bordered by $L_\mu(\lambda_B^+)$, the segment $\Gamma_{\mu,2}$ on the border and the x-axis, where $\Gamma_{\mu,2} = \{(x,y) \in \Gamma : \ y_\mu(\lambda_B^+) \leq y \leq 0\}$; R_{B3} is the region bordered by $L_\mu(\lambda_B^+)$, $L_\mu(\lambda_B^-)$ and the segment $\Gamma_{\mu,3}$ on the border, where $\Gamma_{\mu,3} = \{(x,y) \in \Gamma : \ y_\mu(\lambda_B^-) \leq y \leq y_\mu(\lambda_B^+)\}$; and R_{B4} is the region bordered by $L_\mu(\lambda_B^-)$ and $\Gamma_{\mu,4} = \{(x,y) \in \Gamma : \ y \leq y_\mu(\lambda_B^-)\}$.

Consider the region $D_{A3} \subset R_{A3}$ defined as being the convex hull of the three points $P_A^*(\mu)$, $Q(\mu) = (0, -\mu)$ and $\Gamma_\mu(\lambda_A^+)$ (i.e., the filled-in triangle of which these three points are corner points, see Figure 5.7). The edges of this triangle are mapped by F_μ as follows: Denote by $O = (0,0)$ the origin. The segment $[P_A^*(\mu), Q(\mu)]$ is mapped onto the segment $[P_A^*(\mu), O] \subset D_{A3}$, the segment $[P_A^*(\mu), \Gamma_\mu(\lambda_A^+)]$ is mapped onto the segment $[P_A^*(\mu), S_\mu(\lambda_A^+)] \subset D_{A3}$, and the segment $[Q(\mu), \Gamma_\mu(\lambda_A^+)]$ is mapped onto the segment $[S_\mu(\lambda_A^+), O] \subset D_{A3}$. Since the map F_μ is continuous, it follows that the subregion D_{A3} is mapped into itself by F_μ, that is, D_{A3} is positively invariant: $F_\mu(D_{A3}) \subset D_{A3}$. From the theory of linear difference equations and the positive invariance of D_{A3}, it follows that if $(x_0, y_0) \in D_{A3}$, then $\lim_{n\to\infty} F_\mu^n(x_0, y_0) = P_A^*(\mu)$.

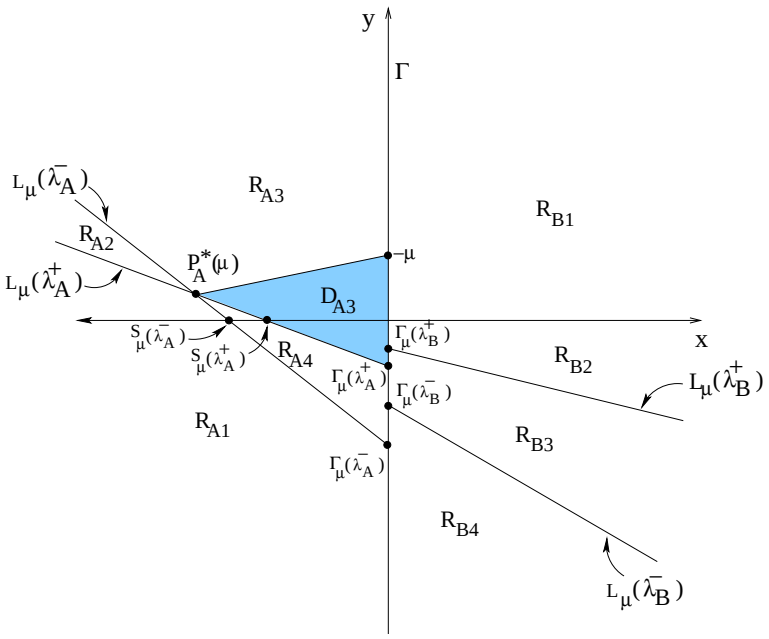

Figure 5.7: Schematic diagram showing the half-lines generated by the eigenvectors and the regions R_{A1}, R_{A2}, R_{A3}, R_{A4}, R_{B1}, R_{B2}, R_{B3}, R_{B4} and D_{A3} used in the proof of Proposition 5.2 for $\mu < 0$.

Denote by D_{A3}^* the union of all pre-images of D_{A3}, that is $D_{A3}^* = \cup_{n=0}^{\infty} G_{\mu,A}^{-n}(D_{A3})$. Hence, $D_{A3}^* = \{(x,y) \in R_{A3} : \ F_\mu^n(x,y) \in R_{A3} \ \forall n \in \mathbb{N}$ and there exists an integer $m \geq 0$ such that $F_\mu^m(x,y) \in D_{A3}\}$.

Let $(x_0,y_0) \in \mathbb{R}^2$ be a given initial condition. Then, the following fact is clear:

- If $(x_0,y_0) \in L_\mu(\lambda_A^+) \cup L_\mu(\lambda_A^-)$, then $\lim_{n\to\infty} F_\mu^n(x_0,y_0) = P_A^*(\mu)$.

The following facts, which assert positive invariance of the subregions R_{A1}, R_{A2} and R_{A4}, follow from the expression for the solution of a general linear difference equation and the assumption that the eigenvalues lie in $(0,1)$:

- If $(x_0,y_0) \in R_{A1}$, then $F_\mu^n(x_0,y_0) \in R_{A1} \ \forall n$ and $\lim_{n\to\infty} F_\mu^n(x_0,y_0) = P_A^*(\mu)$;

- If $(x_0,y_0) \in R_{A2}$, then $F_\mu^n(x_0,y_0) \in R_{A2} \ \forall n$ and $\lim_{n\to\infty} F_\mu^n(x_0,y_0) = P_A^*(\mu)$;

- If $(x_0,y_0) \in R_{A4}$, then $F_\mu^n(x_0,y_0) \in R_{A4}\ \forall n$ and $\lim_{n\to\infty} F_\mu^n(x_0,y_0) = P_A^*(\mu)$.

Denote by $\Gamma_\mu^+ = \{(x,y) \in \Gamma :\ y \geq -\mu\}$, $\Gamma_{\mu,A}^+ = G_{\mu,A}^{-1}(\Gamma_\mu^+)$, $\Gamma_\mu^- = \{(x,y) \in \Gamma :\ y < -\mu\}$ and $\Gamma_{\mu,B}^- = G_{\mu,B}^{-1}(\Gamma_\mu^-)$.

Consider initial conditions on the border Γ. If $(x_0,y_0) \in \Gamma$, then $F_\mu(x_0,y_0) = (y_0 + \mu, 0)$. It follows that if $(x_0,y_0) \in \Gamma_\mu^-$, then $F_\mu(x_0,y_0) = (y_0+\mu,0) \in D_{A3} \cup R_{A1} \cup R_{A2} \cup R_{A4}$ and the positive invariance of R_{A1}, R_{A2}, R_{A4} and D_{A3} implies that $F_\mu^{n+1}(x_0,y_0) \in D_{A3} \cup R_{A1} \cup R_{A2} \cup R_{A4} \forall n \in \mathbb{N}$ and $\lim_{n\to\infty} F_\mu^n(x_0,y_0) = P_A^*(\mu)$.

If $(x_0,y_0) \in L(\lambda_B^+)$, then there exists a positive integer m such that $F_\mu^m(x_0,y_0) \in D_{A3} \cup R_{A1} \cup R_{A2} \cup R_{A4}$ and the positive invariance of R_{A1}, R_{A2}, R_{A4} and D_{A3} implies that $F_\mu^{n+m}(x_0,y_0) \in D_{A3} \cup R_{A1} \cup R_{A2} \cup R_{A4} \forall n \in \mathbb{N}$, and $\lim_{n\to\infty} F_\mu^n(x_0,y_0) = P_A^*(\mu)$. Similarly, if $(x_0,y_0) \in L(\lambda_B^-)$, then there exists a positive integer m such that $F_\mu^m(x_0,y_0) \in D_{A3} \cup R_{A1} \cup R_{A2} \cup R_{A4}$ and the positive invariance of R_{A1}, R_{A2}, R_{A4} and D_{A3} implies that $F_\mu^{n+m}(x_0,y_0) \in D_{A3} \cup R_{A1} \cup R_{A2} \cup R_{A4} \forall n \in \mathbb{N}$, and $\lim_{n\to\infty} F_\mu^n(x_0,y_0) = P_A^*(\mu)$.

Consider initial conditions $(x_0,y_0) \in R_{B1}$. The next iterate $(x_1,y_1) = G_{\mu,B}(x_0,y_0) = (\tau_B x_0 + y_0 + \mu, -\delta_B x_0)^T$. Since $y_1 = -\delta_B x_0 < 0$, it follows that either, i) $(x_1,y_1) \in D_{A3} \cup R_{A1} \cup R_{A4}$ and the positive invariance of R_{A1}, R_{A4} and D_{A3} implies that $F_\mu^{n+1}(x_0,y_0) \in D_{A3} \cup R_{A1} \cup R_{A4} \forall n \in \mathbb{N}$, and $\lim_{n\to\infty} F_\mu^n(x_0,y_0) = P_A^*(\mu)$; or ii) $(x_1,y_1) \in R_{B2}$.

Consider initial conditions in R_{B2}. Let D_{B2} be the subregion of R_{B2} bordered by $L_\mu(\lambda_B^+)$, the border Γ, the x-axis and $\Gamma_{\mu,B}^-$, as shown in Figure 5.8. The region D_{B2} is a fundamental region for R_{B2}: if $(x_0,y_0) \in R_{B2}$ then there exists a nonnegative integer n such that $F_\mu^n(x_0,y_0)$ is in D_{B2} or on its border. In other words, $R_{B2} = \left(\cup_{n\geq 0} G_{\mu,B}^{-n}(\Gamma_{\mu,2} \cup D_{B2})\right) \cap R_{B2}$. By construction, the subregion D_{B2} is mapped into $D_{A3} \cup R_{A1} \cup R_{A2} \cup R_{A4}$ in one iterate, that is, $F_\mu(D_{B2}) \subset D_{A3} \cup R_{A1} \cup R_{A2} \cup R_{A4}$. The positive invariance of R_{A1}, R_{A2}, R_{A4} and D_{A3} implies that $F_\mu^{n+m}(x_0,y_0) \in D_{A3} \cup R_{A1} \cup R_{A2} \cup R_{A4} \forall n \in \mathbb{N}$, and $\lim_{n\to\infty} F_\mu^n(x_0,y_0) = P_A^*(\mu)$.

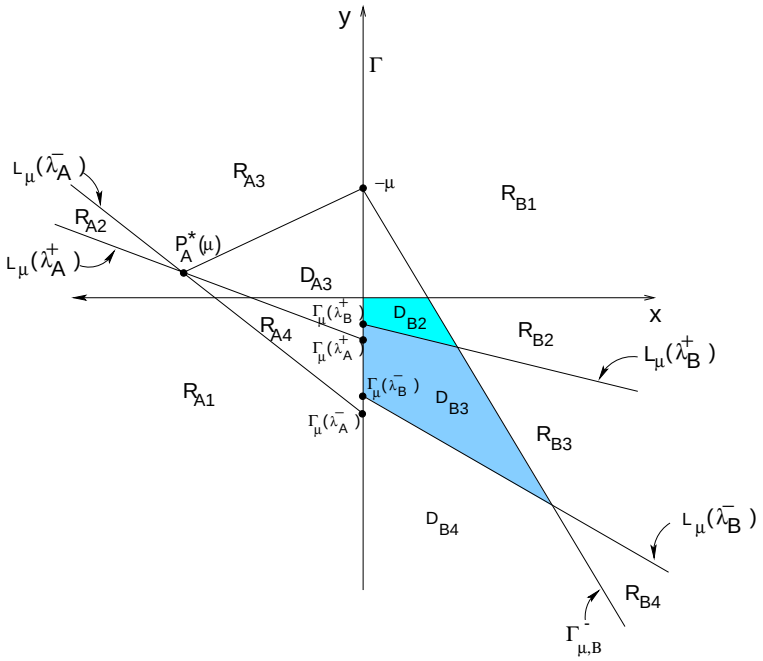

Figure 5.8: Schematic diagram showing the regions D_{B2}, D_{B3} and D_{B4} used in the proof of Proposition 5.2 for $\mu < 0$.

Consider initial conditions $(x_0, y_0) \in R_{B3}$. Let D_{B3} be the subregion of R_{B3} bordered by $L_\mu(\lambda_B^-)$, the border Γ, $L_\mu(\lambda_B^+)$ and $\Gamma_{\mu,B}^-$ (see Figure 5.8). The region D_{B3} is a fundamental region for R_{B3}: if $(x_0, y_0) \in R_{B3}$ then there exists a nonnegative integer n such that $F_\mu^n(x_0, y_0)$ is in D_{B3} or on its border. In other words, $R_{B3} = \cup_{n\geq 0} G_{\mu,B}^{-n}(\Gamma_{\mu,3} \cup D_{B3})$. By construction, the subregion D_{B3} is mapped into $D_{A3} \cup R_{A1} \cup R_{A2} \cup R_{A4}$ in one iterate, that is, $F_\mu(D_{B3}) \subset D_{A3} \cup R_{A1} \cup R_{A2} \cup R_{A4}$. Therefore, if $(x_0, y_0) \in R_{B3}$, then there exists a positive integer m such that $F_\mu^m(x_0, y_0) \in D_{A3} \cup R_{A1} \cup R_{A2} \cup R_{A4}$. The positive invariance of R_{A1}, R_{A2}, R_{A4} and D_{A3} implies that $F_\mu^{n+m}(x_0, y_0) \in D_{A3} \cup R_{A1} \cup R_{A2} \cup R_{A4} \forall n \in \mathbb{N}$, and $\lim_{n\to\infty} F_\mu^n(x_0, y_0) = P_A^*(\mu)$.

Consider initial conditions $(x_0, y_0) \in R_{B4}$. Let D_{B4} be the subregion of R_{B4} bordered by $L_\mu(\lambda_B^-)$, the border Γ and $\Gamma_{\mu,B}^-$ (see Figure 5.8). The region D_{B4} is a fundamental region for R_{B4}: if $(x_0, y_0) \in R_{B4}$ then there exists a nonnegative integer n such

that $F_\mu^n(x_0,y_0)$ is in D_{B4} or on its border. In other words, $R_{B4} = \cup_{n\geq 0} G_{\mu,B}^{-n}(\Gamma_{\mu,4} \cup D_{B4})$. By construction, the subregion D_{B4} is mapped into $D_{A3} \cup R_{A1} \cup R_{A2} \cup R_{A4}$, that is, $F_\mu(D_{B3}) \subset D_{A4} \cup R_{A1} \cup R_{A2} \cup R_{A4}$. Therefore, if $(x_0,y_0) \in R_{B4}$, then there exists a positive integer m such that $F_\mu^m(x_0,y_0) \in D_{A3} \cup R_{A1} \cup R_{A2} \cup R_{A4}$. The positive invariance of R_{A1}, R_{A2}, R_{A4} and D_{A3} implies that $F_\mu^{n+m}(x_0,y_0) \in D_{A3} \cup R_{A1} \cup R_{A2} \cup R_{A4} \forall n \in \mathbb{N}$, and $\lim_{n\to\infty} F_\mu^n(x_0,y_0) = P_A^*(\mu)$.

There is one case left, namely, $(x_0,y_0) \in R_{A3} \setminus D_{A3}^*$. Let $R_{A3}^* = R_{A3} \setminus D_{A3}^*$. Let U_{A3} be the subregion of R_{A3}^* bordered Γ and $\Gamma_{\mu,A}^+$. The region U_{A3}^* is a fundamental region for R_{A3}^*: if $(x_0,y_0) \in R_{A3}^*$ then there exists a nonnegative integer n such that $F_\mu^n(x_0,y_0)$ is in U_{A3} or on its border. In other words, $R_{A3} = \cup_{n\geq 0} G_{\mu,B}^{-n}(\Gamma_{\mu,A}^+ \cup U_{A3})$. By construction, the subregion U_{A3} is mapped into R_{B1}, that is, $F_\mu(U_{A3}) \subset R_{B1}$. Therefore, if $(x_0,y_0) \in R_{A3}^*$, then either there exists a positive integer $m \in \mathbb{N}$ such that $F_\mu^m(x_0,y_0) \in \Gamma_\mu^+$, or there exists $m \in \mathbb{N}$ such that $F_\mu^n(x_0,y_0) \in R_{B1}$. From the results above for the case $(x_0,y_0) \in R_{B1}$, it follows that $F_\mu^{n+m}(x_0,y_0) \in D_{A3} \cup R_{A1} \cup R_{A2} \cup R_{A4} \forall n \in \mathbb{N}$, and $\lim_{n\to\infty} F_\mu^n(x_0,y_0) = P_A^*(\mu)$.

All cases has been exhausted and we conclude: if $\mu < 0$, then the map F_μ has a unique fixed point attractor $P_A^*(\mu) = (x(\mu),y(\mu))$ which is globally asymptotically stable.

Case (3): $\mu > 0$. This case is similar to Case (2). They differ only in that the roles of regions R_A and R_B are interchanged.

We conclude that for every $\mu \in \mathbb{R}$, the map F_μ has a unique fixed point attractor $(x(\mu),y(\mu))$ and this fixed point attractor is globally asymptotically stable, that is, for every initial condition $(x_0,y_0) \in \mathbb{R}^2$, the resulting orbit converges to $(x(\mu),y(\mu))$, so $\lim_{n\to\infty} F_\mu^n(x_0,y_0) = (x(\mu),y(\mu))$. This completes the proof. ■

5.3.2 Negative Determinants on Both Sides of the Border

In this subsection, we consider system (5.4) under the assumption that the eigenvalues of the matrices A and B satisfy $-1 < \lambda_A^- < 0 < \lambda_A^+ < 1$ and $-1 < \lambda_B^- < 0 < \lambda_B^+ < 1$, respectively. We show that this is a sufficient condition for nonbifurcation with persistent stability. Before we state the proposition, some notation that will be used in the remainder of this section is given.

Definition 5.1 *Let*

- $\Gamma = \{(x,y) : \ x = 0\}$, *denote the border separating* R_A *and* R_B*;*
- $\Gamma_\mu^+ = \{(x,y) : x = 0, y \geq -\mu\}$*;*
- $\Gamma_\mu^- = \{(x,y) : x = 0, y \leq -\mu\}$*;*
- $\Gamma_{\mu,A}^- := \{x \leq 0, y = -\tau_A x - \mu\}$*; and*
- $\Gamma_{\mu,B}^- := \{x \geq 0, y = -\tau_B x - \mu\}$.

Definition 5.2 *Denote by* Q_1 *the first quadrant of the plane,* Q_2 *the second quadrant,* Q_3 *the third quadrant and* Q_4 *the fourth quadrant.*

Proposition 5.3 *Let for* $\mu \in \mathbb{R}$*, the map* $F_\mu : \mathbb{R}^2 \to \mathbb{R}^2$ *be defined by (5.4). Let the eigenvalues* $\lambda_A^\pm$ *of A and* $\lambda_B^\pm$ *of B satisfy* $-1 < \lambda_A^- < 0 < \lambda_A^+ < 1$ *and* $-1 < \lambda_B^- < 0 < \lambda_B^+ < 1$*. Then for every* $\mu \in \mathbb{R}$*, the map* F_μ *has a unique fixed point attractor* $(x(\mu), y(\mu))$ *and this fixed point attractor is globally asymptotically stable. That is, for every initial condition* (x_0, y_0)*, the resulting orbit converges to* $(x(\mu), y(\mu))$*, so* $\lim_{n\to\infty} F_\mu^n(x_0, y_0) = (x(\mu), y(\mu))$.

Proof: Let the map F_μ satisfy the assumptions of Proposition 5.3. Note that the assumptions imply that $-1 < \delta_A = \lambda_A^- \lambda_A^+ < 0$ and $-1 < \delta_B = \lambda_B^- \lambda_B^+ < 0$. Define the map $G_{\mu,A} : \mathbb{R}^2 \to \mathbb{R}^2$ to be the affine extension of the left part of the map $F_\mu(x,y)$ to the whole plane: $G_{\mu,A}(x,y) = (\tau_A x + y + \mu, -\delta_A x)^T$. Also define the map $G_{\mu,B}(x,y) = (\tau_B x + y + \mu, -\delta_B x)^T$ to be the affine extension of the right part of the map $F_\mu(x,y)$ to the whole plane. Denote by $\bar{P_A}(\mu) = (\bar{x_A}(\mu), \bar{y_A}(\mu))$ the fixed point of $G_{\mu,A}$, and by $\bar{P_B}(\mu) = (\bar{x_B}(\mu), \bar{y_B}(\mu))$ the fixed point of $G_{\mu,B}$. By the assumptions $-1 < \delta_A < 0$ and $-1 < \delta_B < 0$, the maps $G_{\mu,A}$ and $G_{\mu,B}$ are invertible. The inverse of the map $G_{\mu,A}$ is given by $G_{\mu,A}^{-1}(x,y) = \left(-\frac{y}{\delta_A}, x + y\frac{\tau_A}{\delta_A} - \mu\right)^T$, and the inverse of $G_{\mu,B}$ is given by $G_{\mu,B}^{-1}(x,y) = \left(-\frac{y}{\delta_B}, x + y\frac{\tau_B}{\delta_B} - \mu\right)^T$.

The half-lines generated by the eigenvector of A and B are defined in (5.9)-(5.12) above. The traces of A and B are given by $\tau_A = \lambda_A^- + \lambda_A^+$ and $\tau_B = \lambda_B^- + \lambda_B^+$, respectively. Depending on the signs of τ_A and τ_B, there are four cases:

- **Case 5.3.1:** $0 \leq \tau_A < 1$ and $0 \leq \tau_B < 1$;
- **Case 5.3.2:** $-1 < \tau_A \leq 0$ and $-1 < \tau_B \leq 0$;
- **Case 5.3.3:** $0 \leq \tau_A < 1$ and $-1 < \tau_B \leq 0$; and
- **Case 5.3.4:** $-1 < \tau_A \leq 0$ and $0 \leq \tau_B < 1$.

We will prove this proposition by considering each of the cases 5.3.1-5.3.4 separately. For each case, there are three scenarios: (i) $\mu = 0$, (ii) $\mu < 0$ and (iii) $\mu > 0$.

Case 5.3.1: $0 \leq \tau_A < 1$ and $0 \leq \tau_B < 1$.

(i) $\mu = 0$: The half-line $\Gamma_{\mu,A}^-$ divides R_A into two regions R_{A1} and R_{A2} (refer to Figure 5.9.) The region R_{A1} is bordered by Γ_μ^- and $\Gamma_{\mu,A}^-$. The region R_{A2} is bordered by Γ_μ^+ and $\Gamma_{\mu,A}^-$. Similarly, the half-line $\Gamma_{\mu,B}^-$ divides R_B into two regions R_{B1} and R_{B2}.

The region R_{B1} is bordered by Γ_{μ}^{+} and $\Gamma_{\mu,B}^{-}$. The region R_{B2} is bordered by Γ_{μ}^{-} and $\Gamma_{\mu,B}^{-}$.

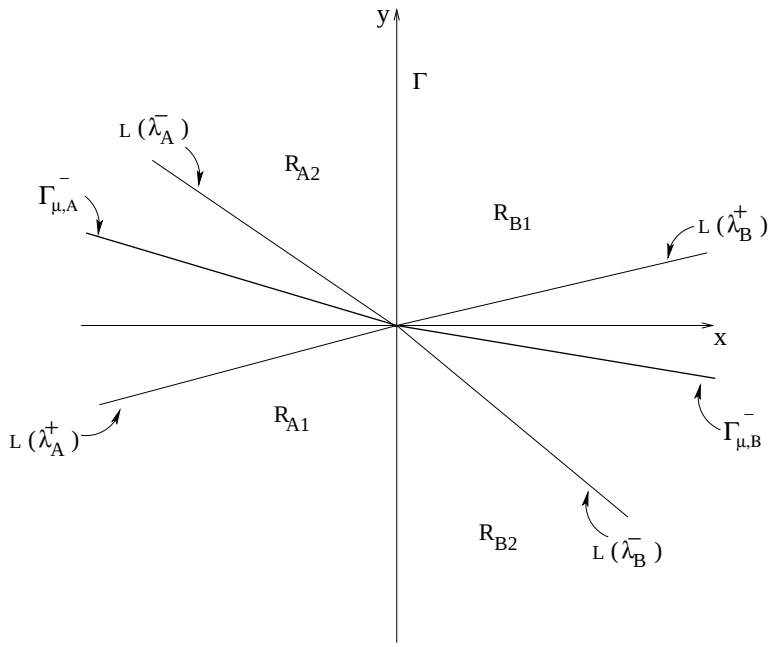

Figure 5.9: Schematic diagram showing the half-lines generated by the eigenvectors and the regions R_{A1}, R_{A2}, R_{B1} and R_{B2} used in the proof of Case 5.3.1 with $\mu = 0$.

Let $(x_0, y_0) \in \mathbb{R}^2$ be a given initial condition. If $(x_0, y_0) \in R_{A1}$, then $G_{\mu,A}(x_0, y_0) = (\underbrace{\tau_A x_0 + y_0}_{\leq 0}, \underbrace{-\delta_A x_0}_{\leq 0})^T \in Q_3 \subset R_{A1}$. Thus, R_{A1} is positively invariant. Since $(0,0) \in R_{A1}$ and A is Schur stable, it follows that $\lim_{n\to\infty} F_{\mu}^{n}(x_0, y_0) = (0,0)$.

If $(x_0, y_0) \in R_{B1}$, then $G_{\mu,B}(x_0, y_0) = (\underbrace{\tau_B x_0 + y_0}_{\geq 0}, \underbrace{-\delta_B x_0}_{\geq 0}) \in Q_1 \subset R_{B1}$. Thus, R_{B1} is positively invariant and it follows that $\lim_{n\to\infty} F_{\mu}^{n}(x_0, y_0) = (0,0)$.

If $(x_0, y_0) \in R_{A2}$, then $G_{\mu,A}(x_0, y_0) = (\underbrace{\tau_A x_0 + y_0}_{>0}, \underbrace{-\delta_A x_0}_{\leq 0})^T \in Q_4 \subset R_{B1} \cup R_{B2}$.

If $(x_0, y_0) \in R_{B2}$, then $G_{\mu,A}(x_0, y_0) = (\underbrace{\tau_B x_0 + y_0}_{<0}, \underbrace{-\delta_B x_0}_{\geq 0}) \in Q_2 \subset R_{A1} \cup R_{A2}$. Clearly, if $(x_0, y_0) \in R_{A2}$ or $(x_0, y_0) \in R_{B2}$, the trajectory starting at (x_0, y_0) may flip between the two regions. There are two possibilities: 1) there exists a positive integer m

such that $F_\mu^m(x_0,y_0) \in R_{A1} \cup R_{B1}$ and the positive invariance of R_{A1}, R_{B1} implies that $\lim_{n\to\infty} F_\mu^{n+m}(x_0,y_0) = (0,0)$; or 2) the trajectory keeps flipping between R_{A2} and R_{B2} and eventually converges to $(0,0)$ since AB (equivalently BA) is Schur stable, which can be seen as follows:

$$\begin{aligned} AB &= \begin{pmatrix} \tau_A & 1 \\ -\delta_A & 0 \end{pmatrix} \begin{pmatrix} \tau_B & 1 \\ -\delta_B & 0 \end{pmatrix} \\ &= \begin{pmatrix} \tau_A\tau_B - \delta_B & \tau_A \\ -\delta_A\tau_B & -\delta_A \end{pmatrix} \end{aligned} \tag{5.19}$$

Let $\delta_{AB} := \det(AB) = \delta_A\delta_B$ and $\tau_{AB} :=\text{trace}(AB) = \tau_A\tau_B - \delta_A - \delta_B$. By the Jury test for second order discrete-time systems [54], AB is Schur stable if and only if

$$\begin{aligned} -1 < \delta_{AB} &< 1 \\ -1-\delta_{AB} < \tau_{AB} &< 1+\delta_{AB} \end{aligned}$$

Equivalently,

$$-1 < \delta_A\delta_B < 1 \tag{5.20}$$

$$-(1-\delta_A)(1-\delta_B) < \tau_A\tau_B < (1+\delta_A)(1+\delta_B) \tag{5.21}$$

Inequality (5.20) is satisfied since $-1 < \delta_A < 0$ and $-1 < \delta_B < 0$. Since $0 < \tau_A < (1+\delta_A)$ and $0 < \tau_B < (1+\delta_B)$ by hypothesis, it follows that $0 < \tau_A\tau_B < (1+\delta_A)(1+\delta_B)$. This shows that inequality (5.21) is also satisfied. Therefore, AB is Schur stable.

(ii) $\mu < 0$: The map F_μ has a unique fixed point $P_A^*(\mu) = (x_A(\mu), y_A(\mu))$, where $x_A(\mu) = \frac{\mu}{1-\tau_A+\delta_A}$ and $y_A(\mu) = -\delta_A x_A(\mu)$. Note that: (a) the fixed point $\bar{P}_A(\mu)$ of $G_{\mu,A}$ is the fixed point $P_A^*(\mu) = (x_A(\mu), y_A(\mu))$ of F_μ, and (b) the fixed point $\bar{P}_B(\mu)$ of $G_{\mu,B}$ is the virtual fixed point of F_μ and this point is given by $\bar{x}_B(\mu) = \frac{\mu}{1-\tau_B+\delta_B}$ and $\bar{y}_B(\mu) = -\delta_B\bar{x}_B(\mu)$.

The map F_μ has four invariant half-lines generated by the eigenvectors of A and B. The equations for these half-lines are given in (5.9)-(5.12). These half-lines intersect the y-axis at the points defined by (5.13)-(5.16). Furthermore, the half-line $L_\mu(\lambda_A^+)$ intersects the x-axis at $x_\mu(\lambda_A^+) = \frac{\mu}{1-\lambda_A^-}$, and the half-line $L_\mu(\lambda_A^-)$ intersects the x-axis at $x_\mu(\lambda_A^-) = \frac{\mu}{1-\lambda_A^+}$. Note that $y_\mu(\lambda_A^-) < 0 < y_\mu(\lambda_A^+), y_\mu(\lambda_B^-) < 0 < y_\mu(\lambda_B^+)$ and $x_\mu(\lambda_A^-) < x_\mu(\lambda_A^+) < 0$.

Define R_{A1}, R_{A2}, R_{B1} and R_{B2} as in Figure 5.10 where $\Gamma_{\mu,A}^-$ divides R_A into two regions R_{A1}, R_{A2} and $\Gamma_{\mu,B}^-$ divides R_B into two regions R_{B1}, R_{B2}.

Next we show that for every initial condition $(x_0, y_0) \in \mathbb{R}^2$, $\lim_{n\to\infty} F_\mu^n(x_0, y_0) \to P_A^*(\mu)$.

If $(x_0, y_0) \in R_{A1}$, then $G_{\mu,A}(x_0, y_0) = (\underbrace{\tau_A x_0 + y_0 + \mu}_{\leq 0}, \underbrace{-\delta_A x_0}_{\leq 0})^T \in Q_3 \subset R_{A1}$. Thus, R_{A1} is positively invariant. Since $P_A^*(\mu) \in R_{A1}$ and the matrix A is Schur stable, it follows that $\lim_{n\to\infty} F_\mu^n(x_0, y_0) = P_A^*(\mu)$.

If $(x_0, y_0) \in R_{A2}$, then $G_{\mu,A}(x_0, y_0) = (\underbrace{\tau_A x_0 + y_0 + \mu}_{>0}, \underbrace{-\delta_A x_0}_{\leq 0})^T \in Q_4 \subset R_{B1} \cup R_{B2}$. If $(x_0, y_0) \in R_{B1}$, then $G_{\mu,B}(x_0, y_0) = (\underbrace{\tau_B x_0 + y_0 + \mu}_{\geq 0}, \underbrace{-\delta_B x_0}_{\geq 0}) \in Q_1 \subset R_{B1} \cup R_{B2}$. Since the fixed point of $G_{\mu,B}$ which is given by $\bar{P}_B(\mu)$ is in R_{A1} (is a virtual fixed point of F_μ and is stable), the trajectory starting at (x_0, y_0) approaches $\bar{P}_B(\mu)$ along the eigenvector $L_\mu(\lambda_B^+)$ and eventually enters D_{B2} or R_{B2}. That is, there exists $m > 0$ such that $G_{\mu,B}^m(x_0, y_0) \in D_{B2} \subset R_{B2}$, or $G_{\mu,B}^m(x_0, y_0) \in R_{B2} \setminus D_{B2}$. The subregion D_{B2} is bordered by Γ_μ^-, $\Gamma_{\mu,B}^-$ and $G_{\mu,B}^{-1}(\Gamma_{\mu,A}^-)$ (see Figure 5.10). The lines $\Gamma_{\mu,B}^-$ and $G_{\mu,B}^{-1}(\Gamma_{\mu,A}^-)$ intersect at the point $G_{\mu,B}^{-1}(0, -\mu) = (\frac{\mu}{\delta_B}, -\mu(1 + \frac{\tau_B}{\delta_B}))$. By construction, the subregion D_{B2} is mapped into R_{A1} in one step, i.e., $G_{\mu,B}(D_{B2}) \subset R_{A1}$.

If $(x_0, y_0) \in R_{B2} \setminus D_{B2}$, then $G_{\mu,B}(x_0, y_0) = (\underbrace{\tau_B x_0 + y_0 + \mu}_{<0}, \underbrace{-\delta_B x_0}_{\geq 0})^T \in R_{A2}$. Clearly, if $(x_0, y_0) \in R_{A2}$ or $(x_0, y_0) \in R_{B2} \setminus D_{B2}$, the trajectory starting at (x_0, y_0) may flip

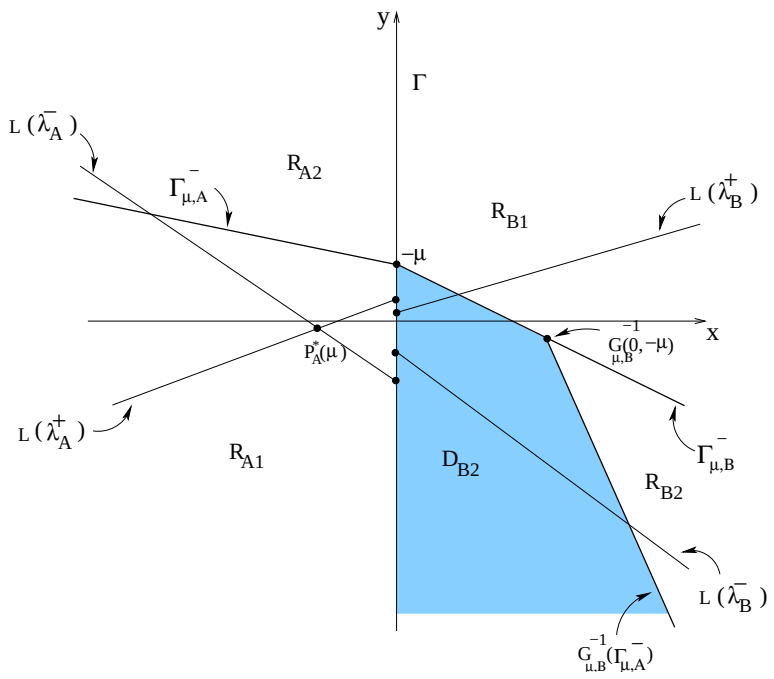

Figure 5.10: Schematic diagram showing the regions R_{A1}, R_{A2}, R_{B1} and R_{B2} used in the proof of Case 5.3.1 with $\mu < 0$.

between the two regions but eventually enters R_{A1} and is trapped there. To show that a trajectory starting at $(x_0, y_0) \in R_{A2} \cup R_{B2} \setminus D_{B2}$ has to enter R_{A1}, we show that $G_{\mu,B} \circ G_{\mu,A}$ has a stable fixed point in R_{A1}. Thus, the trajectory cannot flip between R_{A2} and R_{B2} for ever, it will enter R_{A1} after a finite number of iterates. It is straightforward to show that $(x_{AB}(\mu), y_{AB}(\mu)) = \left(\frac{\mu(1+\delta_B+\tau_B)}{(1+\delta_A)(1+\delta_B)-\tau_A\tau_B}, \frac{-\delta_B\tau_A x_{AB}(\mu)-\delta_B\mu}{1+\delta_B} \right) \in R_{A1}$ is a fixed point of $G_{\mu,B} \circ G_{\mu,A}$ and is stable since BA is Schur stable (see the proof for the case $\mu = 0$ above). We conclude that for every $(x_0, y_0) \in \mathbb{R}^2$, $\lim_{n\to\infty} F_\mu^n(x_0, y_0) = P_A^*(\mu)$.

(iii) $\mu > 0$: The proof for this case is similar to the symmetric case $\mu < 0$ discussed above and is therefore omitted.

Case 5.3.2: $-1 < \tau_A \leq 0$ and $-1 < \tau_B \leq 0$.

(i) $\mu = 0$: (Refer to Figure 5.11.) The half-line $\Gamma^-_{\mu,A}$ divides R_A into two regions R_{A1}

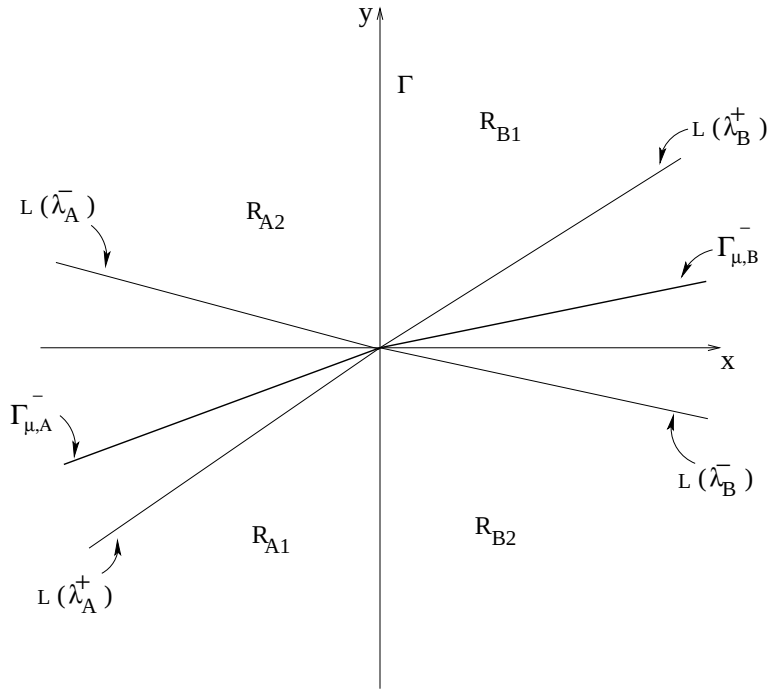

Figure 5.11: Schematic diagram showing the regions R_{A1}, R_{A2}, R_{B1} and R_{B2} used in the proof of Case 5.3.2 with $\mu = 0$.

and R_{A2}. The region R_{A1} is bordered by Γ_{μ}^{-} and $\Gamma_{\mu,A}^{-}$. The region R_{A2} is bordered by Γ_{μ}^{+} and $\Gamma_{\mu,A}^{-}$. Similarly, the half-line $\Gamma_{\mu,B}^{-}$ divides R_B into two regions R_{B1} and R_{B2}. The region R_{B1} is bordered by Γ_{μ}^{+} and $\Gamma_{\mu,B}^{-}$. The region R_{B2} is bordered by Γ_{μ}^{-} and $\Gamma_{\mu,B}^{-}$.

Let $(x_0, y_0) \in \mathbb{R}^2$ be a given initial condition. If $(x_0, y_0) \in R_{A1}$, then $G_{\mu,A}(x_0, y_0) = (\underbrace{\tau_A x_0 + y_0}_{\leq 0}, \underbrace{-\delta_A x_0}_{\leq 0})^T \in Q_3 \subset R_{A1} \cup R_{A2}$. There are two possibilities: 1) $G_{\mu,A}^n(x_0, y_0) \in R_{A1}$ $\forall n$, thus $\lim_{n\to\infty} G_{\mu,A}^n(x_0, y_0) = (0,0)$, or 2) There exists a positive integer m such that $G_{\mu,A}^m(x_0, y_0) \in R_{A2}$.

If $(x_0, y_0) \in R_{A2}$, then $G_{\mu,A}(x_0, y_0) = (\underbrace{\tau_A x_0 + y_0}_{>0}, \underbrace{-\delta_A x_0}_{\leq 0})^T \in Q_4 \subset R_{B2}$.

If $(x_0,y_0) \in R_{B1}$, then $G_{\mu,B}(x_0,y_0) = (\underbrace{\tau_B x_0 + y_0}_{\geq 0}, \underbrace{-\delta_B x_0}_{\geq 0})^T \in Q_1 \subset R_{B1} \cup R_{B2}$. Therefore, there are two possibilities: 1) $G^n_{\mu,B}(x_0,y_0) \in R_{B1}\ \forall n$, thus $\lim_{n\to\infty} G^n_{\mu,B}(x_0,y_0) = (0,0)$, or 2) There exists a positive integer m such that $G^m_{\mu,B}(x_0,y_0) \in R_{B2}$.

If $(x_0,y_0) \in R_{B2}$, then $G_{\mu,B}(x_0,y_0) = (\underbrace{\tau_B x_0 + y_0}_{<0}, \underbrace{-\delta_B x_0}_{\geq 0})^T \in Q_2 \subset R_{A2}$. Since $G_{\mu,B}(R_{B2}) \subset R_{A2}$ and $G_{\mu,A}(R_{A2}) \subset R_{B2}$, the trajectory starting at $(x_0,y_0) \in R_{A2} \cup R_{B2}$ flips between the two regions $RA2$ and R_{B2}. Since AB (equivalently, BA) is Schur stable, the trajectory starting at $(x_0,y_0) \in R_{A2} \cup R_{B2}$ eventually converges to $(0,0)$. This shows that $\lim_{n\to\infty} F^n_0(x_0,y_0) = (0,0)$, $\forall (x_0,y_0) \in \mathbb{R}^2$.

(ii) $\mu < 0$: The map F_μ has a unique fixed point $P^*_A(\mu) = (x_A(\mu), y_A(\mu))$, where $x_A(\mu) = \frac{\mu}{1-\tau_A+\delta_A}$ and $y_A(\mu) = -\delta_A x_A(\mu)$. Note that: (a) the fixed point $\bar{P}_A(\mu)$ of $G_{\mu,A}$ is the fixed point $P^*_A(\mu) = (x_A(\mu), y_A(\mu))$ of F_μ, and (b) the fixed point $\bar{P}_B(\mu)$ of $G_{\mu,B}$ is the virtual fixed point of F_μ and this point is given by $\bar{x}_B(\mu) = \frac{\mu}{1-\tau_B+\delta_B}$ and $\bar{y}_B(\mu) = -\delta_B \bar{x}_B(\mu)$.

Let R_{A1}, R_{A2}, R_{B1} and R_{B2} be defined as in Figure 5.12. Also, let $D_{A1} \subset R_{A1}$ be the triangle with corner points $(0,-\mu)$, $(-\frac{\mu}{\tau_A},0)$ and $G_{\mu,A}(-\frac{\mu}{\tau_A},0) = (0,\mu\frac{\delta_A}{\tau_A})$. The region D_{A1} is positively invariant. This follows from the continuity of the map F_μ and the observation that the edges of the D_{A1} are mapped inside D_{A1} as follows: the segment $(-\frac{\mu}{\tau_A},0)$, $(0,\mu\frac{\delta_A}{\tau_A})$ is mapped to the segment $(0,\mu\frac{\delta_A}{\tau_A})$, $(\mu(1+\frac{\delta_A}{\tau_A}),0) \subset D_{A1}$; the segment $(-\frac{\mu}{\tau_A},0)$, $(0,-\mu)$ is mapped to $(0,0)$, $(0,\mu\frac{\delta_A}{\tau_A}) \subset D_{A1}$; and the segment $(0,-\mu)$, $(0,\mu\frac{\delta_A}{\tau_A})$ is mapped to $(0,0)$, $(\mu(1+\frac{\delta_A}{\tau_A}),0) \subset D_{A1}$.

Let $D_{B2} \subset R_{B2}$ be the triangle with corner points $(0,-\mu)$, $(0,\mu\frac{\delta_A}{\tau_A})$ and $G^{-1}_{\mu,B}(0,-\mu) = (\frac{\mu}{\delta_B}, -\mu(1+\frac{\tau_B}{\delta_B}))$ (see Figure 5.12). By construction, D_{B2} is mapped to D_{A1}.

Let $(x_0,y_0) \in \mathbb{R}^2$ be a given initial condition. If $(x_0,y_0) \in R_{A1}$, then $G_{\mu,A}(x_0,y_0) \in Q_3 \subset R_{A1} \cup R_{A2}$. There are two possibilities: 1) $G^n_{\mu,A}(x_0,y_0) \in R_{A1}$, $\forall n \in \mathbb{N}$, thus $\lim_{n\to\infty} G^n_{\mu,A}(x_0,y_0) = P^*_A(\mu)$; or 2) There exists a positive integer m such that $G^m_{\mu,A}(x_0,y_0) \in$

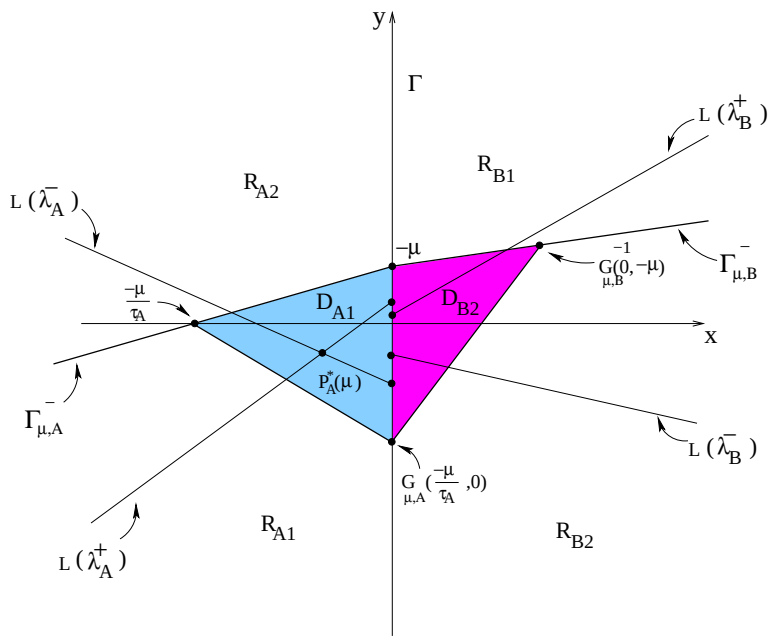

Figure 5.12: Schematic diagram showing the half-lines generated by the eigenvectors and the regions R_{A1}, R_{A2}, R_{B1} and R_{B2} used in the proof of Case 5.3.2 with $\mu < 0$.

R_{A2}.

If $(x_0,y_0) \in R_{A2}$, then $G_{\mu,A}(x_0,y_0) = (\underbrace{\tau_A x_0 + y_0}_{>0}, \underbrace{-\delta_A x_0}_{\leq 0}) \in Q_4 \subset R_{B2}$.

If $(x_0,y_0) \in R_{B1}$, then $G_{\mu,B}(x_0,y_0) = (\underbrace{\tau_B x_0 + y_0}_{\geq 0}, \underbrace{-\delta_B x_0}_{\geq 0}) \in Q_1 \subset R_{B1} \cup R_{B2}$. Since $\bar{P}_B(\mu) \in R_{A1}$ is stable, there exists a positive integer m such that $G^m_{\mu,B}(x_0,y_0) \in R_{B2}$. If $(x_0,y_0) \in D_{B2}$, then $G_{\mu,B}(x_0,y_0) \in D_{A1}$ and the trajectory converges to $P^*_A(\mu)$. If $(x_0,y_0) \in R_{B2} \setminus D_{B2}$, then $G_{\mu,B}(x_0,y_0) \in R_{A2}$.

Clearly, if $(x_0,y_0) \in R_{A2}$ or $(x_0,y_0) \in R_{B2} \setminus D_{B2}$, the trajectory starting at (x_0,y_0) may flip between the two regions but eventually enters R_{A1} and is trapped there. To show that a trajectory starting at $(x_0,y_0) \in R_{A2} \cup R_{B2} \setminus D_{B2}$ has to enter R_{A1}, we show that $G_{\mu,B} \circ G_{\mu,A}$ has a stable fixed point $(x_{AB}(\mu), y_{AB}(\mu)) \in R_{A1}$ with $-\frac{\mu}{\tau_A} < x_{AB}(\mu) < 0$. Thus, the trajectory cannot flip between R_{A2} and R_{B2} for ever, it will enter D_{A1} after a

finite number of iterates. The fixed point is given by

$$(x_{AB}(\mu), y_{AB}(\mu)) = \left(\frac{\mu(1+\delta_B+\tau_B)}{(1+\delta_A)(1+\delta_B)-\tau_A\tau_B}, \frac{-\delta_B\tau_A x_{AB}(\mu)-\delta_B\mu}{1+\delta_B} \right) \in R_{A1}$$

After simplification, $y_{AB}(\mu) = -\frac{\overbrace{\mu\delta_B}^{>0}\overbrace{(1+\delta_A+\tau_A)}^{>0}}{\underbrace{(1+\delta_A)(1+\delta_B)-\tau_A\tau_B}_{>0}} < 0$. But, the expression for $y_{AB}(\mu) = -\frac{\delta_B}{1+\delta_B}(\tau_A x_{AB}(\mu)+\mu) < 0$, implies that $(\tau_A x_{AB}(\mu)+\mu) < 0$ (since $-\frac{\delta_B}{1+\delta_B} > 0$), thus $-\frac{\mu}{\tau_A} < x_{AB}(\mu) < 0$.

This shows that $\lim_{n\to\infty} F_0^n(x_0,y_0) = P_A^*(\mu)$, $\forall (x_0,y_0) \in \mathbb{R}^2$.

(iii) $\mu > 0$: The proof for this case is similar to the symmetric case $\mu < 0$ above.

Case 5.3.3: $0 \le \tau_A < 1$ and $-1 < \tau_B \le 0$.

(i) $\mu = 0$: (Refer Figure 5.13.) The half-line $\Gamma^-_{\mu,A}$ divides R_A into two regions R_{A1} and R_{A2}. The region R_{A1} is bordered by Γ^-_μ and $\Gamma^-_{\mu,A}$. The region R_{A2} is bordered by Γ^+_μ and $\Gamma^-_{\mu,A}$. Similarly, the half-line $\Gamma^-_{\mu,B}$ divides R_B into two regions R_{B1} and R_{B2}. The region R_{B1} is bordered by Γ^+_μ and $\Gamma^-_{\mu,B}$. The region R_{B2} is bordered by Γ^-_μ and $\Gamma^-_{\mu,B}$.

Let $(x_0,y_0) \in \mathbb{R}^2$ be a given initial condition. If $(x_0,y_0) \in R_{A1}$, then $G_{\mu,A}(x_0,y_0) = (\underbrace{\tau_A x_0 + y_0}_{\le 0}, \underbrace{-\delta_A x_0}_{\le 0})^T \in Q_3 \subset R_{A1}$. Thus, R_{A1} is positively invariant and $\lim_{n\to\infty} G^n_{\mu,A}(x_0,y_0) = (0,0)$.

If $(x_0,y_0) \in R_{A2}$, then $G_{\mu,A}(x_0,y_0) = (\underbrace{\tau_A x_0 + y_0}_{>0}, \underbrace{-\delta_A x_0}_{\le 0})^T \in Q_4 \subset R_{B2}$.

If $(x_0,y_0) \in R_{B1}$, then $G_{\mu,B}(x_0,y_0) = (\underbrace{\tau_B x_0 + y_0}_{\ge 0}, \underbrace{-\delta_B x_0}_{\ge 0})^T \in Q_1 \subset R_{B1} \cup R_{B2}$. Therefore, there are two possibilities: 1) For all $n \in N$, $G^n_{\mu,B}(x_0,y_0) \in R_{B1}$, thus $\lim_{n\to\infty} G^n_{\mu,B}(x_0,y_0) = (0,0)$, or 2) There exists a positive integer m such that $G^m_{\mu,B}(x_0,y_0) \in R_{B2}$.

Let $D_{B2} \subset R_{B2}$ be the region bounded by $G^{-1}_{\mu,B}(\Gamma^-_{\mu,A})$ and Γ^-_μ, where $G^{-1}_{\mu,B}(\Gamma^-_{\mu,A}) = \{(x,y) \in R_{B2} : y = (\tau_B + \frac{\delta_B}{\tau_A})x\}$ is the pre-image of the half-line $\Gamma^-_{\mu,A}$ (see Figure 5.13). By construction, every point in D_{B2} is mapped into R_{A1} in one step. If $(x_0,y_0) \in$

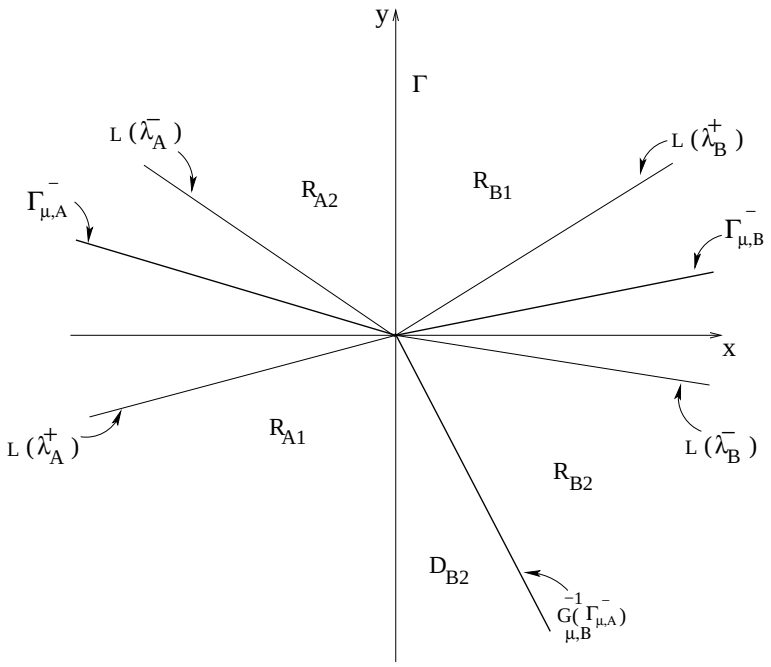

Figure 5.13: Schematic diagram showing the half-lines generated by the eigenvectors and the regions R_{A1}, R_{A2}, R_{B1} and R_{B2} used in the proof of Case 5.3.3 with $\mu = 0$.

$R_{B2} \setminus D_{B2}$, then $G_{\mu,B}(x_0,y_0) = (\underbrace{\tau_B x_0 + y_0}_{<0}, \underbrace{-\delta_B x_0}_{\geq 0})^T \in R_{A2}$. Recall from above that $G_{\mu,A}(R_{A2}) \subset R_{B2}$. Thus, if $(x_0,y_0) \in R_{A2} \cup R_{B2} \setminus D_{B2}$, the trajectory flips between the two regions R_{A2} and $R_{B2} \setminus D_{B2}$. Since the matrix product AB is Schur stable, the trajectory must enter D_{B2} which is then mapped into the positively invariant region R_{A1}. This shows that $\lim_{n\to\infty} F_0^n(x_0,y_0) = (0,0)$, $\forall (x_0,y_0) \in \mathbb{R}^2$.

(ii) $\mu < 0$: The map F_μ has a unique fixed point $P_A^*(\mu) = (x_A(\mu), y_A(\mu))$, where $x_A(\mu) = \frac{\mu}{1-\tau_A+\delta_A}$ and $y_A(\mu) = -\delta_A x_A(\mu)$. Note that: (a) the fixed point $\bar{P}_A(\mu)$ of $G_{\mu,A}$ is the fixed point $P_A^*(\mu) = (x_A(\mu), y_A(\mu))$ of F_μ, and (b) the fixed point $\bar{P}_B(\mu)$ of $G_{\mu,B}$ is the virtual fixed point of F_μ and this point is given by $\bar{x}_B(\mu) = \frac{\mu}{1-\tau_B+\delta_B}$ and $\bar{y}_B(\mu) = -\delta_B \bar{x}_B(\mu)$.

The map F_μ has four invariant half-lines as in Case 5.3.1 above. Define the sub-regions R_{A1}, R_{A2}, R_{B1} and R_{B2} as in Figure. 5.14. Next we will show that for every

$(x_0,y_0) \in \mathbb{R}^2$, $\lim_{n\to\infty} F_\mu^n(x_0,y_0) \to P_A^*(\mu)$.

Let $(x_0,y_0) \in \mathbb{R}^2$ be a given initial condition. If $(x_0,y_0) \in R_{A1}$, then $G_{\mu,A}(x_0,y_0) = (\underbrace{\tau_A x_0 + y_0 + \mu}_{\leq 0}, \underbrace{-\delta_A x_0}_{\leq 0})^T \in Q_3 \subset R_{A1}$. Thus, R_{A1} is positively invariant. Since $P_A^*(\mu) \in R_{A1}$ and the matrix A is Schur stable, it follows that $\lim_{n\to\infty} F_\mu^n(x_0,y_0) = P_A^*(\mu)$.

If $(x_0,y_0) \in R_{A2}$, then $G_{\mu,A}(x_0,y_0) = (\underbrace{\tau_A x_0 + y_0 + \mu}_{>0}, \underbrace{-\delta_A x_0}_{\leq 0})^T \in Q_4 \subset R_{B2}$.

If $(x_0,y_0) \in R_{B1}$, then $G_{\mu,B}(x_0,y_0) = (\underbrace{\tau_B x_0 + y_0 + \mu}_{\geq 0}, \underbrace{-\delta_B x_0}_{\geq 0})^T \in Q_1 \subset R_{B1} \cup R_{B2}$. Since the fixed point of $G_{\mu,B}$ which is given by $\bar{P}_B(\mu)$ is in R_{A1} (is a virtual fixed point of F_μ) and is stable, the trajectory starting at $(x_0,y_0) \in R_{B1}$ approaches $\bar{P}_B(\mu)$ along the eigenvector $L_\mu(\lambda_B^+)$ and eventually enters D_{B2} or R_{B2}, i.e., there exists $m > 0$ such that $G_{\mu,B}^m(x_0,y_0) \in R_{B2}$. The subregion D_{B2} is bordered by Γ_μ^-, $\Gamma_{\mu,B}^-$ and $G_{\mu,B}^{-1}(\Gamma_{\mu,A}^-)$. The lines $\Gamma_{\mu,B}^-$ and $G_{\mu,B}^{-1}(\Gamma_{\mu,A}^-)$ intersect at the point $G_{\mu,B}^{-1}(0,-\mu) = (\frac{\mu}{\delta_B}, -\mu(1+\frac{\tau_B}{\delta_B}))$. By construction, the subregion D_{B2} is mapped into R_{A1} in one step, i.e., $G_{\mu,B}(D_{B2}) \subset R_{A1}$.

If $(x_0,y_0) \in R_{B2} \setminus D_{B2}$, then $G_{\mu,B}(x_0,y_0) = (\underbrace{\tau_B x_0 + y_0 + \mu}_{<0}, \underbrace{-\delta_B x_0}_{\geq 0}) \in R_{A2}$. Clearly, if $(x_0,y_0) \in R_{A2}$ or $(x_0,y_0) \in R_{B2} \setminus D_{B2}$, the trajectory starting at (x_0,y_0) may flip between the two regions but eventually enters R_{A1} and is trapped there. To show that a trajectory starting at $(x_0,y_0) \in R_{A2} \cup R_{B2} \setminus D_{B2}$ eventually enters R_{A1}, we show that $G_{\mu,B} \circ G_{\mu,A}$ has a stable fixed point in R_{A1}. Thus, the trajectory cannot flip between R_{A2} and R_{B2} for ever, it enters R_{A1} after a finite number of iterates. It is straightforward to show that $(x_{AB}(\mu), y_{AB}(\mu)) = \left(\frac{\mu(1+\delta_B+\tau_B)}{(1+\delta_A)(1+\delta_B)-\tau_A\tau_B}, \frac{-\delta_B\tau_A x_{AB}(\mu)-\delta_B\mu}{1+\delta_B}\right) \in R_{A1}$ is a fixed point for $G_{\mu,B} \circ G_{\mu,A}$ and is stable since BA is Schur stable (see case 5.3.1 (ii) above). We conclude that for every $(x_0,y_0) \in \mathbb{R}^2$, $\lim_{n\to\infty} F_\mu^n(x_0,y_0) = P_A^*(\mu)$.

(iii) $\mu > 0$: The map F_μ has a unique fixed point $P_B^*(\mu) = (x_B(\mu), y_B(\mu))$, where $x_B(\mu) = \frac{\mu}{1-\tau_B+\delta_B}$ and $y_B(\mu) = -\delta_B x_B(\mu)$. Note that: (a) the fixed point $\bar{P}_B(\mu)$ of $G_{\mu,B}$ is the fixed point $P_B^*(\mu) = (x_B(\mu), y_B(\mu))$ of F_μ, and (b) the fixed point $\bar{P}_A(\mu)$ of $G_{\mu,A}$ is the virtual

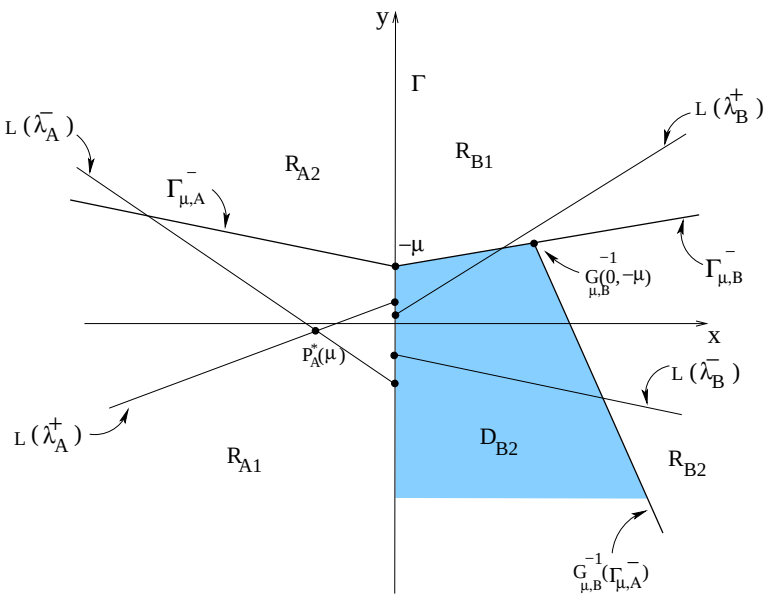

Figure 5.14: Schematic diagram showing the half-lines generated by the eigenvectors and the regions R_{A1}, R_{A2}, R_{B1} and R_{B2} used in the proof of Case 5.3.3 with $\mu < 0$.

fixed point of F_μ and this point is given by $\bar{x}_A(\mu) = \frac{\mu}{1-\tau_A+\delta_A}$ and $\bar{y}_A(\mu) = -\delta_A \bar{x}_A(\mu)$.

The subregions R_{A1}, R_{A2}, R_{B1} and R_{B2} are defined as for the case $\mu < 0$ (see Figure 5.15). Let $D_{A2} \subset R_{A2}$ be the triangle with corner points $(0,-\mu)$, $G^{-1}_{\mu,A}(0,-\mu)$ and $G^{-1}_{\mu,A}(-\frac{\mu}{\tau_B},0)$. Also let $D_{B1} \subset R_{B1}$ be the triangle with corner points $(0,-\mu)$, $G^{-1}_{\mu,A}(-\frac{\mu}{\tau_B},0)$ and $(-\frac{\mu}{\tau_B},0)$. Note that points in D_{A2} are mapped to D_{B1} in one step and D_{B1} is invariant. The fixed point $P^*_B(\mu) \in D_{B2}$. (This is easily shown by noting that the triangle D_{B2} contains the intersection of the half-lines with the x-axis and the y-axis, i.e., all the four points $y_\mu(\lambda^+_B)$, $y_\mu(\lambda^-_B)$, $x_\mu(\lambda^+_B)$, and $x_\mu(\lambda^-_B)$ are inside D_{B2} and $P^*_B(\mu)$ coincides with the intersection of the two half-lines in R_B (see Figure 5.15)).

Let $(x_0,y_0) \in \mathbb{R}^2$ be a given initial condition. If $(x_0,y_0) \in D_{B1}$, the positive invariance of D_{B1} implies that $F^n_\mu(x_0,y_0) = G^n_{\mu,B}(x_0,y_0) \in D_{B1}$ and $\lim_{n\to\infty} F^n_\mu(x_0,y_0) = P^*_B(\mu)$.

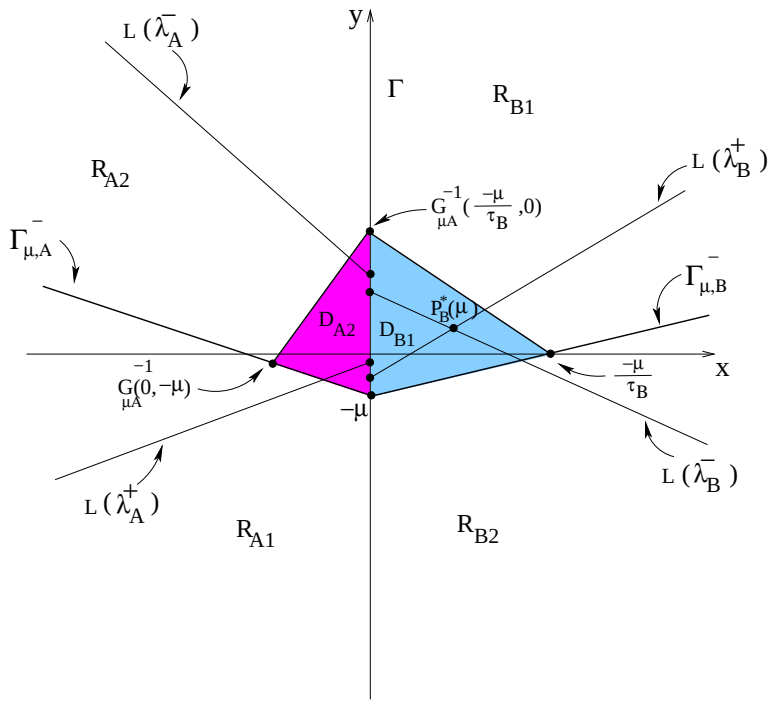

Figure 5.15: Schematic diagram showing the half-lines generated by the eigenvectors and the regions R_{A1}, R_{A2}, R_{B1} and R_{B2} used in the proof of Case 5.3.3 with $\mu > 0$.

If $(x_0, y_0) \in D_{A2}$, then $G_{\mu,A}(x_0, y_0) \in D_{B1}$ and thereafter the trajectory converges to $P_B^*(\mu)$.

If $(x_0, y_0) \in R_{A1}$, then $G_{\mu,A}(x_0, y_0) = (\underbrace{\tau_A x_0 + y_0 + \mu}_{\leq 0}, \underbrace{-\delta_A x_0}_{\leq 0})^T \in Q_3$. Since $\bar{P_A}(\mu) \in R_{B1}$ and is a stable fixed point of $G_{\mu,A}$, a trajectory starting in R_{A1} eventually enters R_{A2}. That is, there exists $m > 0$ such that $G_{\mu,A}^m(x_0, y_0) \in R_{A2}$. If $G_{\mu,A}^m(x_0, y_0) \in D_{A2}$, then $G_{\mu,A}^{(m+1)}(x_0, y_0) \in D_{B1}$ and hence the trajectory converges to $P_B^*(\mu)$. Otherwise, $G_{\mu,A}^{(m+1)}(x_0, y_0) \in R_{B2}$.

If $(x_0, y_0) \in R_{A2} \setminus D_{A2}$, then $G_{\mu,A}(x_0, y_0) = (\underbrace{\tau_A x_0 + y_0 + \mu}_{>0}, \underbrace{-\delta_A x_0}_{\leq 0})^T \in R_{B2}$.

If $(x_0, y_0) \in R_{B1}$, then $G_{\mu,B}(x_0, y_0) = (\underbrace{\tau_B x_0 + y_0 + \mu}_{\geq 0}, \underbrace{-\delta_B x_0}_{\geq 0})^T \in Q_1 \subset R_{B1} \cup R_{B2}$.

Clearly, if $(x_0,y_0) \in R_{B2}$ or $(x_0,y_0) \in R_{A2} \setminus D_{A2}$, the trajectory starting at (x_0,y_0) may flip between the two regions but eventually must enter D_{B1} and is trapped there.

To show that a trajectory starting at $(x_0,y_0) \in R_{A2} \cup R_{B2} \setminus D_{B2}$ has to enter D_{B1}, we show that $G_{\mu,A} \circ G_{\mu,B}$ has a stable fixed point in R_{B1}. Thus, the trajectory cannot flip between R_{A2} and R_{B2} for ever, it enters R_{B1} after a finite number of iterates. It is straightforward to show that $(x_{BA}(\mu), y_{BA}(\mu)) = \left(\frac{\mu(1+\delta_A+\tau_A)}{(1+\delta_A)(1+\delta_B)-\tau_A\tau_B}, \frac{-\delta_A\tau_B x_{BA}(\mu)-\delta_A\mu}{1+\delta_A} \right) \in R_{B1}$ is a fixed point of $G_{\mu,B} \circ G_{\mu,A}$ and is stable since AB is Schur stable (see above). By a similar argument as in Case 5.3.3 (ii), it is straightforward to show that $0 < x_{BA}(\mu) < -\frac{\mu}{\tau_B}$ and $y_{BA}(\mu) > 0$. We conclude that for every $(x_0,y_0) \in \mathbb{R}^2$, $\lim_{n\to\infty} F_\mu^n(x_0,y_0) = P_B^*(\mu)$.

Case 5.3.4: $-1 < \tau_A \leq 0$ and $0 \leq \tau_B < 1$.

The proof for this case is similar to Case 5.3.3.

This completes the proof of Proposition 5.3. ■

5.3.3 Positive Eigenvalues on One Side and Negative Determinant on Other Side of the Border

In this subsection, we consider system (5.4) under the assumption that the eigenvalues of the matrices A and B are real and satisfy (5.22) or (5.23). We show that this is a sufficient condition for nonbifurcation with persistent stability.

Proposition 5.4 *Let for $\mu \in \mathbb{R}$, the map $F_\mu : \mathbb{R}^2 \to \mathbb{R}^2$ be defined by (5.4). Let the eigenvalues $\lambda_A^\pm$ of A and $\lambda_B^\pm$ of B satisfy*

$$0 < \lambda_A^- < \lambda_A^+ < 1 \text{ and } -1 < \lambda_B^- < 0 < \lambda_B^+ < 1 \text{ with } \lambda_B^+ + \lambda_B^- > 0 \quad (5.22)$$

or $$0 < \lambda_B^- < \lambda_B^+ < 1 \text{ and } -1 < \lambda_A^- < 0 < \lambda_A^+ < 1 \text{ with } \lambda_A^+ + \lambda_A^- > 0 \quad (5.23)$$

Then for every $\mu \in \mathbb{R}$, the map F_μ has a unique fixed point attractor $(x(\mu), y(\mu))$ and this fixed point attractor is globally asymptotically stable. That is, for every initial condition (x_0, y_0), the resulting orbit converges to $(x(\mu), y(\mu))$, so $\lim_{n\to\infty} F_\mu^n(x_0, y_0) = (x(\mu), y(\mu))$.

Proof: Let the map F_μ satisfy the assumptions of Proposition 5.4. We will only prove the proposition when (5.22) is satisfied. The proof for the symmetric case (5.23) is similar. Assume (5.22) to hold. Note that assumption (5.22) implies that $0 < \delta_A = \lambda_A^- \lambda_A^+ < 1$ and $-1 < \delta_B = \lambda_B^- \lambda_B^+ < 0$. The traces of A and B are given by $\tau_A = \lambda_A^- + \lambda_A^+$ and $\tau_B = \lambda_B^- + \lambda_B^+$, respectively and both τ_A and τ_B are positive. There are three cases: (i) $\mu = 0$, (ii) $\mu < 0$ and (iii) $\mu > 0$.

(i) $\mu = 0$: (Refer to Figure 5.16.) The half-lines $L(\lambda_A^+)$ and $L(\lambda_A^+)$ defined in (5.5)-(5.6) divide R_A into three regions R_{A1}, R_{A2} and R_{A3}. The region R_{A1} is bordered by Γ_μ^- and $L(\lambda_A^+)$. The region R_{A2} is bordered by $L(\lambda_A^+)$ and $L(\lambda_A^-)$. The region R_{A3} is bordered by Γ_μ^+ and $L(\lambda_A^-)$. The half-line $\Gamma_{\mu,B}^- := \{(x,y) \in \mathbb{R}^2 |\ x \geq 0, y = -\tau_B x\}$ divides R_B into two regions R_{B1} and R_{B2}. The region R_{B1} is bordered by Γ_μ^+ and $\Gamma_{\mu,B}^-$. The region R_{B2} is bordered by Γ_μ^- and $\Gamma_{\mu,B}^-$.

The regions R_{A1} and R_{A2} are positively invariant (see the proof of Proposition 5.1). Thus, if $(x_0, y_0) \in R_{A1} \cup R_{A2}$, then $\lim_{n\to\infty} F_\mu^n(x_0, y_0) = (0,0)$. The region R_{A3} is mapped to Q_1 in a finite number of iterates (see the proof of Proposition 5.1).

If $(x_0, y_0) \in R_{B1}$, then $F_\mu(x_0, y_0) = G_{\mu,B}(x_0, y_0) = (\underbrace{\tau_B x_0 + y_0}_{\geq 0}, \underbrace{-\delta_B x_0}_{\geq 0})^T \in Q_1 \subset R_{B1}$. Thus, R_{B1} is positively invariant and $\lim_{n\to\infty} F_\mu^n(x_0, y_0) = (0,0)$.

If $(x_0, y_0) \in R_{B2}$, then $F_\mu(x_0, y_0) = G_{\mu,B}(x_0, y_0) = (\underbrace{\tau_B x_0 + y_0}_{<0}, \underbrace{-\delta_B x_0}_{\geq 0})^T \in Q_2 \subset R_A$.

If $G_{\mu,B}(x_0, y_0) \in R_{A3}$, then the trajectory is mapped to R_{B1} after a finite number of iterates. That is, there exists a positive integer m such that $G_{\mu,A}^m(x_0, y_0) \in R_{B1}$. The

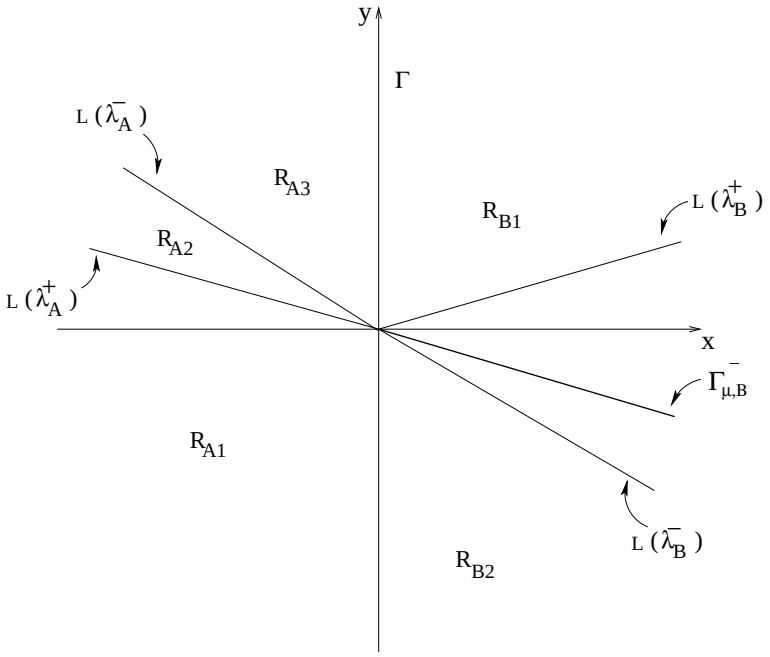

Figure 5.16: Schematic diagram the regions R_{A1}, R_{A2}, R_{A3}, R_{B1} and R_{B2} used in the proof of Proposition 5.4 with $\mu = 0$.

positive invariance of R_{B1} implies that $\lim_{n\to\infty} F_\mu^{n+m}(x_0,y_0) = (0,0)$.

We conclude that, $\forall (x_0,y_0) \in \mathbb{R}^2$, $\lim_{n\to\infty} F_\mu^n(x_0,y_0) = (0,0)$.

(ii) $\mu < 0$: The map F_μ has a unique fixed point $P_A^*(\mu) = (x_A(\mu), y_A(\mu))$, where $x_A(\mu) = \frac{\mu}{1-\tau_A+\delta_A}$ and $y_A(\mu) = -\delta_A x_A(\mu)$. Note that: (a) the fixed point $\bar{P}_A(\mu)$ of $G_{\mu,A}$ is the fixed point $P_A^*(\mu) = (x_A(\mu), y_A(\mu))$ of F_μ, and (b) the fixed point $\bar{P}_B(\mu)$ of $G_{\mu,B}$ is the virtual fixed point of F_μ and this point is given by $\bar{x}_B(\mu) = \frac{\mu}{1-\tau_B+\delta_B}$ and $\bar{y}_B(\mu) = -\delta_B \bar{x}_B(\mu)$.

Define R_{A1}, R_{A2}, R_{A3}, R_{A4}, R_{B1} and R_{B2} as in Figure 5.17. Next we will show that for every $(x_0,y_0) \in \mathbb{R}^2$, $\lim_{n\to\infty} F_\mu^n(x_0,y_0) \to P_A^*(\mu)$.

Let $(x_0,y_0) \in \mathbb{R}^2$ be a given initial condition. The regions R_{A1}, R_{A2} and R_{A4} are positively invariant (see the proof of Proposition 5.2). Thus, if $(x_0,y_0) \in R_{A1} \cup R_{A2} \cup R_{A4}$, then $\lim_{n\to\infty} F_\mu^n(x_0,y_0) = P_A^*(\mu)$.

Define $D_{A3} \subset R_{A3}$ to be the area inside the triangle with corner points $(0,-\mu)$, $(0,y_\mu(\lambda_A^+))$ and P, where P is any point on the half-line $L_\mu(\lambda_A^-)$ to the left of $P_A^*(\mu)$. The region $D_{A3} \subset R_{A3}$ is also positively invariant (easy to see, since all the edges are mapped inside the region and the map is continuous).

If $(x_0,y_0) \in R_{A3} \setminus D_{A3}$, then there are two possibilities: 1) there exists an $m > 0$ such that $G_{\mu,A}^m(x_0,y_0) \in D_{A3}$ or 2) there exists an $m > 0$ such that $G_{\mu,A}^m(x_0,y_0) \in Q_1 \subset R_{B1} \cup R_{B2}$ (see the proof of Proposition 5.2).

If $(x_0,y_0) \in R_{B1}$, then $G_{\mu,B}(x_0,y_0) = (\underbrace{\tau_B x_0 + y_0 + \mu}_{\geq 0}, \underbrace{-\delta_B x_0}_{\geq 0})^T \in Q_1 \subset R_{B1} \cup R_{B2}$. Since the fixed point of $G_{\mu,B}$ which is given by $\bar{P}_B(\mu)$ is in R_{A1} (is a virtual fixed point of F_μ) and is stable, the trajectory starting at (x_0,y_0) approaches $\bar{P}_B(\mu)$ along the eigenvector $L_\mu(\lambda_B^+)$ and eventually enters D_{B2}. The subregion D_{B2} is bordered by Γ_μ^-, $\Gamma_{\mu,B}^-$ and $G_{\mu,B}^{-1}(L_P)$. The lines $\Gamma_{\mu,B}^-$ and $G_{\mu,B}^{-1}(L_P)$ intersect at the point $G_{\mu,B}^{-1}(0,-\mu) = (\frac{\mu}{\delta_B}, -\mu(1+\frac{\tau_B}{\delta_B}))$. By construction, the subregion D_{B2} is mapped to $R_{A1} \cup R_{A2} \cup R_{A4} \cup D_{A3}$ in one step. If $(x_0,y_0) \in R_{B2} \setminus D_{B2}$, then $G_{\mu,B}(x_0,y_0) = (\underbrace{\tau_B x_0 + y_0 + \mu}_{<0}, \underbrace{-\delta_B x_0}_{\geq 0}) \in Q_2$. Then, either 1) $G_{\mu,B}(x_0,y_0) \in R_{A1} \cup R_{A2} \cup R_{A4} \cup D_{A3}$, and $\lim_{n\to\infty} F_\mu^n(x_0,y_0) = P_A^*(\mu)$ or 2) $G_{\mu,B}(x_0,y_0) \in R_{A3}$. The possibility that the trajectory flips continuously between $R_{A3} \setminus D_{A3}$ and $R_{B2} \setminus D_{B2}$ is ruled out since the matrix product AB is Schur stable (see the proof of Proposition 5.3).

We conclude that for every $(x_0,y_0) \in \mathbb{R}^2$, $\lim_{n\to\infty} F_\mu^n(x_0,y_0) = P_A^*(\mu)$.

(iii) $\mu > 0$: The proof is similar to the proof of Proposition 5.3, Case 5.3.1.

This completes the proof. ■

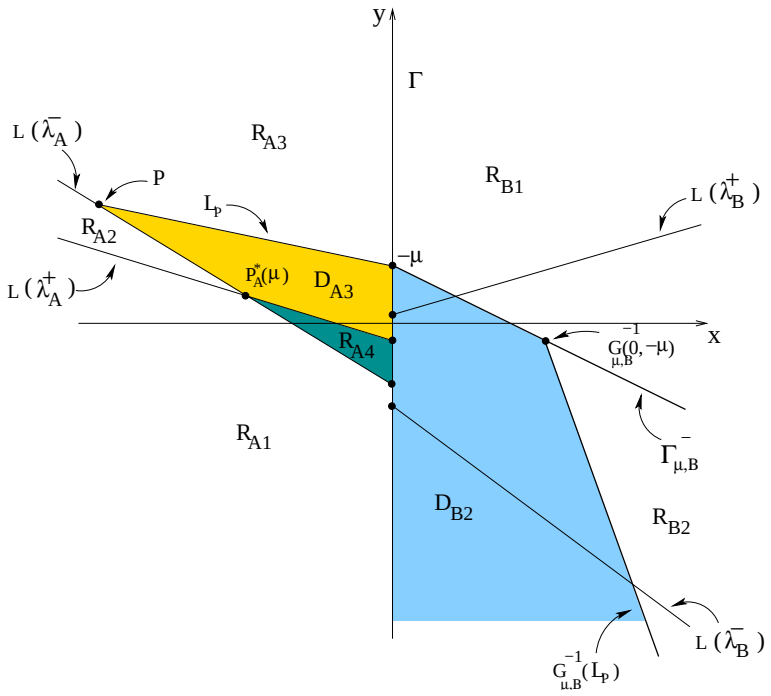

Figure 5.17: Schematic diagram showing the half-lines generated by the eigenvectors and the regions R_{A1}, R_{A2}, R_{A3}, R_{A4}, R_{B1} and R_{B2} used in the proof of Proposition 5.4 with $\mu < 0$.

Chapter 6

Feedback Control of Border Collision Bifurcation in Two-Dimensional PWS maps

In this chapter, feedback control of border collision bifurcations is considered for two-dimensional piecewise smooth discrete-time systems. As discussed before, these are bifurcations that occur when a fixed point of a piecewise smooth system crosses or collides with the border between two regions of smooth operation. The goal of the control effort is to modify the bifurcation so that the bifurcated steady state is locally unique and locally attracting. In this way, the system's local behavior is ensured to remain close to the original operating condition. The sufficient conditions for nonbifurcation with persistent stability in 2-D PWS maps derived in the previous chapter are used as a basis for feedback control design. The analysis leads to sufficient conditions that are in the form of systems of inequalities. These inequalities are either linear or can be approximated as linear. The feasibility of the resulting inequalities can be easily verified using available software packages such as MATLAB.

6.1 Mathematical Setting and Change of Coordinates

In this section, a transformation that sets the border of a two-dimensional PWS map at $x = 0$ is performed. This is an initial step that is performed prior to applying control. Consider a general 2-D PWS map of the form

$$\bar{f}(\bar{x},\bar{y},\mu) = \begin{cases} \bar{f}_A(\bar{x},\bar{y},\mu), & (\bar{x},\bar{y}) \in R_A \\ \bar{f}_B(\bar{x},\bar{y},\mu), & (\bar{x},\bar{y}) \in R_B \end{cases} \tag{6.1}$$

where μ is the bifurcation parameter and R_A, R_B are two regions of smooth behavior separated by a smooth curve (the border)— $\bar{x} = h(\bar{y})$. The map $\bar{f}(\cdot,\cdot,\cdot)$ is assumed to be PWS: $\bar{f}_A(\bar{x},\bar{y},\mu) := \begin{pmatrix} \bar{f}_{A_1}(\bar{x},\bar{y},\mu) \\ \bar{f}_{A_2}(\bar{x},\bar{y},\mu) \end{pmatrix}$ is smooth on R_A, $\bar{f}_B(\bar{x},\bar{y},\mu) := \begin{pmatrix} \bar{f}_{B_1}(\bar{x},\bar{y},\mu) \\ \bar{f}_{B_2}(\bar{x},\bar{y},\mu) \end{pmatrix}$ is smooth on R_B and f is continuous in $(\bar{x},\bar{y})$ and depends smoothly on μ everywhere. Let $(\bar{x}(\mu),\bar{y}(\mu))$ be a path of fixed points of $\bar{f}$; this path depends continuously on μ. Suppose also that the fixed point hits the border at a critical parameter value μ_b. Assume without loss of generality that $\mu_b = 0$. Suppose that the coordinate system is chosen such that $(\bar{x}(0),\bar{y}(0)) = (0,0)$.

Next, we make a change of variable to set the border at $x = 0$ (i.e., the y-axis). Let $x = \bar{x} - h(\bar{y})$ and $y = \bar{y}$. (The Jacobian of the transformation is $\begin{pmatrix} 1 & -\partial h/\partial \bar{y} \\ 0 & 1 \end{pmatrix}$, which is invertible and therefore is a similarity transformation.)

In the new coordinates, the map is given by

$$\bar{f}(x+h(y),y,\mu) = \begin{cases} \bar{f}_A(x+h(y),y,\mu), & x \le 0 \\ \bar{f}_B(x+h(y),y,\mu), & x > 0 \end{cases} \tag{6.2}$$

Letting $f(x,y,\mu) := \bar{f}(x+h(y),y,\mu)$, (6.2) can be written as

$$f(x,y,\mu) = \begin{cases} f_A(x,y,\mu), & x \leq 0 \\ f_B(x,y,\mu), & x > 0 \end{cases} \tag{6.3}$$

Expanding (6.3) in a Taylor series near the fixed point $(0,0,0)$ gives

$$f(x,y,\mu) = \begin{cases} A\begin{pmatrix} x \\ y \end{pmatrix} + \begin{pmatrix} b_1 \\ b_2 \end{pmatrix}\mu + HOT, & x \leq 0 \\ B\begin{pmatrix} x \\ y \end{pmatrix} + \begin{pmatrix} b_1 \\ b_2 \end{pmatrix}\mu + HOT, & x > 0 \end{cases} \tag{6.4}$$

where A and B are the limiting Jacobians of f and $(b_1,\ b_2)^T$ is the derivative of f with respect to μ, and HOT denotes higher order terms. The quantities in (6.4) are thus:

$$A = \lim_{(x,y)\to(0^-,0)} \begin{pmatrix} \dfrac{\partial f_{A_1}(x,y,0)}{\partial x} & \dfrac{\partial f_{A_1}(x,y,0)}{\partial y} \\ \dfrac{\partial f_{A_2}(x,y)}{\partial x} & \dfrac{\partial f_{A_2}(x,y,0)}{\partial y} \end{pmatrix}, \tag{6.5}$$

$$B = \lim_{(x,y)\to(0^+,0)} \begin{pmatrix} \dfrac{\partial f_{B_1}(x,y,0)}{\partial x} & \dfrac{\partial f_{B_1}(x,y,0)}{\partial y} \\ \dfrac{\partial f_{B_2}(x,y)}{\partial x} & \dfrac{\partial f_{B_2}(x,y,0)}{\partial y} \end{pmatrix}, \tag{6.6}$$

and

$$\begin{pmatrix} b_1 \\ b_2 \end{pmatrix} = \lim_{(x,y)\to(0,0)} \begin{pmatrix} \dfrac{\partial f_{A_1}(x,y,0)}{\partial \mu} \\ \dfrac{\partial f_{A_2}(x,y,0)}{\partial \mu} \end{pmatrix} = \lim_{(x,y)\to(0,0)} \begin{pmatrix} \dfrac{\partial f_{B_1}(x,y,0)}{\partial \mu} \\ \dfrac{\partial f_{B_2}(x,y,0)}{\partial \mu} \end{pmatrix}. \tag{6.7}$$

Note that the limit in (6.7) is independent of the direction of approach to the origin since f is smooth in μ.

6.2 Control Constraints for Maintaining BCB

The fact that the normal form for BCBs contains only linear terms in the state leads one to seek linear feedback controllers to modify the system's bifurcation characteristics. The linear feedback can either be applied on only one side of the border or on both sides of the border. However, one must keep in mind that, for our approach to apply, the control action should not introduce discontinuity in the map. This is because, as summarized in Chapter 2, the definition of BCBs requires that the system map be continuous at the border, and thus our results on nonbifurcation with persistent stability also apply only under this condition. Therefore, to maintain continuity of the map after control is applied, we assume that the input vectors on both sides of the border are equal. In this work, the input vectors are taken to be equal to b (the derivative of the map with respect to the bifurcation parameter.) Also some constraints are placed on the control gains so as to maintain continuity of the map, as will be elaborated below. We consider the following possibilities for applying the feedback control:

- Switched feedback, where different controls are applied on each side of the border;
- Simultaneous feedback, where the same control is applied on both sides of the border;
- One sided feedback, where the control is applied on one side of the border but not the other.

The issue of which type of actuation to use is a delicate one. There are practical advantages to applying a switched feedback (different feedback on each side of the border) or one sided feedback. However, this requires knowledge of where the border

lies, which is not necessarily available in practice. Simultaneous control is used to ensure robustness with respect to uncertainty in knowledge of the border, as was done for 1-D maps. Moreover, the use of simultaneous feedback control alleviates the need to transform the system to the normal form. Not surprisingly, the conditions for existence of simultaneously stabilizing controls are more restrictive than for the existence of switched controls.

All the control laws are developed based on the map linearizations as the fixed point is approached on both sides of the border. It is important to emphasize that we do not assume the system to be in normal form (see Section 2.2). This alleviates the need to include state transformations in the design of control laws except for the transformation setting the border to lie on the y-axis. Thus, in the remainder of this chapter, we consider the following 2-D piecewise affine map

$$f_\mu(x,y) = \begin{cases} \underbrace{\begin{pmatrix} a_{11} & a_{12} \\ a_{13} & a_{14} \end{pmatrix}}_{A} \begin{pmatrix} x \\ y \end{pmatrix} + \begin{pmatrix} b_1 \\ b_2 \end{pmatrix} \mu, & x \leq 0 \\ \underbrace{\begin{pmatrix} a_{21} & a_{22} \\ a_{23} & a_{24} \end{pmatrix}}_{B} \begin{pmatrix} x \\ y \end{pmatrix} + \begin{pmatrix} b_1 \\ b_2 \end{pmatrix} \mu, & x > 0 \end{cases} \tag{6.8}$$

where μ is the bifurcation parameter and f_μ is assumed continuous in $\mathbb{R}^2$ but nonsmooth at the border. Since the map f_μ is not differentiable at the border $x = 0$, $A \neq B$. The continuity of f_μ at the border implies that the second column of A equals the second column of B, i.e., $a_{12} = a_{22} =: a_2$ and $a_{14} = a_{24} =: a_4$. Let $\tau_A :=\text{trace}(A) = a_{11} + a_4$, $\delta_A :=\det(A) = a_{11}a_4 - a_2a_{13}$, $\tau_B :=\text{trace}(B) = a_{21} + a_4$ and $\delta_B :=\det(B) = a_{21}a_4 - a_2a_{23}$.

Note that the map (6.8) in general represents the linearizations of a two-dimensional PWS map near a fixed point on the border separating two regions of smooth behavior R_A and R_B as shown above. System (6.8) undergoes a variety of border collision bifurcations depending on the values of the parameters τ_A, δ_A, τ_B and δ_B [61, 9, 23] as discussed at length in Section 2.2.

The fixed points of the map (6.8) on both sides of the border are given by

$$\begin{aligned}(x_A(\mu), y_A(\mu)) &= \left(\frac{(b_1 - b_1a_4 + a_2b_2)\mu}{1-\tau_A+\delta_A}, \frac{(a_{13}b_1 + b_2 - b_2a_{11})\mu}{1-\tau_A+\delta_A}\right), \\ (x_B(\mu), y_B(\mu)) &= \left(\frac{(b_1 - b_1a_4 + a_2b_2)\mu}{1-\tau_B+\delta_B}, \frac{(a_{23}b_1 + b_2 - b_2a_{21})\mu}{1-\tau_B+\delta_B}\right).\end{aligned}$$

Assume that $b_1 - b_1a_4 + a_2b_2 \neq 0$, so that the fixed point does not move along the border as μ is varied through zero. Without loss of generality, assume $b_1 - b_1a_4 + a_2b_2 > 0$ (if $b_1 - b_1a_4 + a_2b_2 < 0$, just replace μ by $-\mu$).

Below, the sufficient conditions for nonbifurcation with persistent stability derived in Chapter 5 are used as a basis in synthesizing stabilizing feedback controls. We begin with switched feedback control design, then we consider simultaneous feedback control design and we end this chapter with one sided feedback control design. In all the cases, we make sure that the feedback control does not introduce discontinuity into the map.

6.3 Switched Feedback Control Design

In this method, different controls are applied on each side of the border. This leads to the closed-loop system

$$\begin{pmatrix} x_{k+1} \\ y_{k+1} \end{pmatrix} = \begin{cases} \begin{pmatrix} a_{11} & a_2 \\ a_{13} & a_4 \end{pmatrix} \begin{pmatrix} x_k \\ y_k \end{pmatrix} + \begin{pmatrix} b_1 \\ b_2 \end{pmatrix} \mu + \begin{pmatrix} b_1 \\ b_2 \end{pmatrix} u_{1_k}, & x_k \leq 0 \\ \begin{pmatrix} a_{21} & a_2 \\ a_{23} & a_4 \end{pmatrix} \begin{pmatrix} x_k \\ y_k \end{pmatrix} + \begin{pmatrix} b_1 \\ b_2 \end{pmatrix} \mu + \begin{pmatrix} b_1 \\ b_2 \end{pmatrix} u_{2_k}, & x_k > 0 \end{cases} \tag{6.9}$$

$$u_{1_k} = (\gamma_{11}\ \gamma_2) \begin{pmatrix} x_k \\ y_k \end{pmatrix} = \gamma_{11} x_k + \gamma_2 y_k \tag{6.10}$$

$$u_{2_k} = (\gamma_{21}\ \gamma_2) \begin{pmatrix} x_k \\ y_k \end{pmatrix} = \gamma_{21} x_k + \gamma_2 y_k \tag{6.11}$$

where γ_{11}, γ_2 and γ_{21} are the control gains. Note that the control gain γ_2 multiplying y_k is the same in both u_{1_k} and u_{2_k} in order to maintain continuity along the border in the controlled system. Suppose that the fixed point to the left of the border for $\mu < 0$ is stable— that is, assume $-(1+\delta_A) < \tau_A < (1+\delta_A)$. Suppose also that as μ is increased through zero, a BCB occurs.

The closed-loop system can be written as

$$\begin{pmatrix} x_{k+1} \\ y_{k+1} \end{pmatrix} = \begin{cases} \begin{pmatrix} a_{11}+b_1\gamma_{11} & a_2+b_1\gamma_2 \\ a_{13}+b_2\gamma_{11} & a_4+b_2\gamma_2 \end{pmatrix} \begin{pmatrix} x_k \\ y_k \end{pmatrix} + \begin{pmatrix} b_1 \\ b_2 \end{pmatrix} \mu, & x_k \leq 0 \\ \begin{pmatrix} a_{21}+b_1\gamma_{21} & a_2+b_1\gamma_2 \\ a_{23}+b_2\gamma_{21} & a_4+b_2\gamma_2 \end{pmatrix} \begin{pmatrix} x_k \\ y_k \end{pmatrix} + \begin{pmatrix} b_1 \\ b_2 \end{pmatrix} \mu, & x_k > 0 \end{cases} \tag{6.12}$$

The characteristic polynomials of the closed loop system to the left and right of the

border are given by

$$\begin{aligned}\tilde{p}_A(\lambda) &= \lambda^2 - \underbrace{(\tau_A + b_1\gamma_{11} + b_2\gamma_2)}_{\tilde{\tau}_A}\lambda \\ &+ \underbrace{\delta_A + (b_1a_4 - b_2a_2)\gamma_{11} + (a_{11}b_2 - a_{13}b_1)\gamma_2}_{\tilde{\delta}_A} \end{aligned} \tag{6.13}$$

and

$$\begin{aligned}\tilde{p}_B(\lambda) &= \lambda^2 - \underbrace{(\tau_B + b_1\gamma_{21} + b_2\gamma_2)}_{\tilde{\tau}_B}\lambda \\ &+ \underbrace{\delta_B + (b_1a_4 - b_2a_2)\gamma_{21} + (a_{21}b_2 - a_{23}b_1)\gamma_2}_{\tilde{\delta}_B} \end{aligned} \tag{6.14}$$

respectively, where a tilde is used to denote closed-loop quantities.

Next, the nonbifurcation results derived in Chapter 5 are used to find conditions for stabilizing control laws.

Feedback Control Design Based on Proposition 5.3:

Using Proposition 5.3, the following conditions on the controlled system Jacobian matrices are derived:

$$-1 < \tilde{\delta}_A < 0 \tag{6.15}$$

$$1 + \tilde{\tau}_A + \tilde{\delta}_A > 0 \tag{6.16}$$

$$1 - \tilde{\tau}_A + \tilde{\delta}_A > 0 \tag{6.17}$$

and

$$-1 < \tilde{\delta}_B < 0 \tag{6.18}$$

$$1 + \tilde{\tau}_B + \tilde{\delta}_B > 0 \tag{6.19}$$

$$1 - \tilde{\tau}_B + \tilde{\delta}_B > 0 \tag{6.20}$$

Substituting the expressions for $\tilde{\delta}_A$, $\tilde{\tau}_A$, $\tilde{\delta}_B$ and $\tilde{\tau}_B$ in (6.15)-(6.20) yields

$$\begin{aligned}
(b_1a_4 - a_2b_2)\gamma_{11} &< -(a_{11}b_2 - a_{13}b_1)\gamma_2 - \delta_A && (6.21)\\
(b_1a_4 - a_2b_2)\gamma_{11} &> -(a_{11}b_2 - a_{13}b_1)\gamma_2 - \delta_A - 1 && (6.22)\\
(b_1a_4 - a_2b_2 + b_1)\gamma_{11} &> -(b_2 + a_{11}b_2 - a_{13}b_1)\gamma_2 - (1 + \tau_A + \delta_A) && (6.23)\\
(b_1a_4 - a_2b_2 - b_1)\gamma_{11} &> -(-b_2 + a_{11}b_2 - a_{13}b_1)\gamma_2 - (1 - \tau_A + \delta_A) && (6.24)
\end{aligned}$$

and

$$\begin{aligned}
(b_1a_4 - a_2b_2)\gamma_{21} &< -(a_{21}b_2 - a_{23}b_1)\gamma_2 - \delta_B && (6.25)\\
(b_1a_4 - a_2b_2)\gamma_{21} &> -(a_{21}b_2 - a_{23}b_1)\gamma_2 - \delta_B - 1 && (6.26)\\
(b_1a_4 - a_2b_2 + b_1)\gamma_{21} &> -(b_2 + a_{21}b_2 - a_{23}b_1)\gamma_2 - (1 + \tau_B + \delta_B) && (6.27)\\
(b_1a_4 - a_2b_2 - b_1)\gamma_{21} &> -(-b_2 + a_{21}b_2 - a_{23}b_1)\gamma_2 - (1 - \tau_B + \delta_B) && (6.28)
\end{aligned}$$

Stabilizing control laws exist if inequalities (6.21)-(6.28) are feasible which is easy to check.

Feedback Control Design Based on Proposition 5.4:

Below, we seek control gains such that the eigenvalues of the controlled system (6.12) satisfy Proposition 5.4:

$$\begin{aligned}
0 < \tilde{\delta}_A &< 1, && (6.29)\\
2\sqrt{\tilde{\delta}_A} < \tilde{\tau}_A &< (1 + \tilde{\delta}_A), && (6.30)
\end{aligned}$$

and

$$\begin{aligned}
-1 < \tilde{\delta}_B &< 0, && (6.31)\\
0 < \tilde{\tau}_B &< 1 + \tilde{\delta}_B. && (6.32)
\end{aligned}$$

Inequalities (6.29)-(6.32) give a sufficient condition for nonbifurcation with persistent stability in the controlled system. Let $\varepsilon \in (0,1)$ be a small parameter. Then, the conditions $0 < \tilde{\delta}_A < 1$ and $2\sqrt{\tilde{\delta}_A} < \tilde{\tau}_A < (1+\tilde{\delta}_A)$ are satisfied if

$$0 < \tilde{\delta}_A < \varepsilon, \tag{6.33}$$

and

$$2\sqrt{\varepsilon} < \tilde{\tau}_A < (1+\tilde{\delta}_A), \qquad 0 < \varepsilon < 1 \tag{6.34}$$

Writing (6.29)-(6.32) explicitly together with (6.33)-(6.34) yields

$$(b_1a_4 - a_2b_2)\gamma_1 < -(a_{11}b_2 - a_{13}b_1)\gamma_2 - \delta_A + \varepsilon \tag{6.35}$$

$$(b_1a_4 - a_2b_2)\gamma_1 > -(a_{11}b_2 - a_{13}b_1)\gamma_2 - \delta_A \tag{6.36}$$

$$b_1\gamma_1 > -b_2\gamma_2 + 2\sqrt{\varepsilon} - \tau_A \tag{6.37}$$

$$(b_1a_4 - a_2b_2 - b_1)\gamma_1 > -(-b_2 + a_{11}b_2 - a_{13}b_1)\gamma_2 - (1 - \tau_A + \delta_A) \tag{6.38}$$

and

$$(b_1a_4 - a_2b_2)\gamma_1 < -(a_{21}b_2 - a_{23}b_1)\gamma_2 - \delta_B \tag{6.39}$$

$$(b_1a_4 - a_2b_2)\gamma_1 > -(a_{21}b_2 - a_{23}b_1)\gamma_2 - \delta_B - 1 \tag{6.40}$$

$$b_1\gamma_1 > -b_2\gamma_2 - \tau_B \tag{6.41}$$

$$(b_1a_4 - a_2b_2 - b_1)\gamma_1 > -(-b_2 + a_{21}b_2 - a_{23}b_1)\gamma_2 - (1 - \tau_B + \delta_B) \tag{6.42}$$

Again, checking the feasibility of the linear inequalities (6.35)-(6.42) is an easy task. Similar conditions can be obtained using Proposition 5.2.

6.4 Simultaneous Stabilization

In this control method, the same feedback control is applied on both sides of the border. This leads to the closed-loop system

$$\begin{pmatrix} x_{k+1} \\ y_{k+1} \end{pmatrix} = \begin{cases} \begin{pmatrix} a_{11} & a_2 \\ a_{13} & a_4 \end{pmatrix} \begin{pmatrix} x_k \\ y_k \end{pmatrix} + \begin{pmatrix} b_1 \\ b_2 \end{pmatrix} \mu + \begin{pmatrix} b_1 \\ b_2 \end{pmatrix} u_k, & x_k \leq 0 \\ \begin{pmatrix} a_{21} & a_2 \\ a_{23} & a_4 \end{pmatrix} \begin{pmatrix} x_k \\ y_k \end{pmatrix} + \begin{pmatrix} b_1 \\ b_2 \end{pmatrix} \mu + \begin{pmatrix} b_1 \\ b_2 \end{pmatrix} u_k, & x_k > 0 \end{cases} \tag{6.43}$$

$$u_k = (\gamma_1 \ \gamma_2) \begin{pmatrix} x_k \\ y_k \end{pmatrix} = \gamma_1 x_k + \gamma_2 y_k \tag{6.44}$$

where γ_1 and γ_2 are the control gains.

The following proposition asserts stabilizability of the border collision bifurcation with this type of control policy. The conditions are based on Proposition 5.3.

Proposition 6.1 If the following inequalities

$$(b_1a_4 - a_2b_2)\gamma_1 < -(a_{11}b_2 - a_{13}b_1)\gamma_2 - \delta_A \tag{6.45}$$

$$(b_1a_4 - a_2b_2)\gamma_1 > -(a_{11}b_2 - a_{13}b_1)\gamma_2 - \delta_A - 1 \tag{6.46}$$

$$(b_1a_4 - a_2b_2 + b_1)\gamma_1 > -(b_2 + a_{11}b_2 - a_{13}b_1)\gamma_2 - (1 + \tau_A + \delta_A) \tag{6.47}$$

$$(b_1a_4 - a_2b_2 - b_1)\gamma_1 > -(-b_2 + a_{11}b_2 - a_{13}b_1)\gamma_2 - (1 - \tau_A + \delta_A) \tag{6.48}$$

and

$$(b_1a_4 - a_2b_2)\gamma_1 < -(a_{21}b_2 - a_{23}b_1)\gamma_2 - \delta_B \tag{6.49}$$

$$(b_1a_4 - a_2b_2)\gamma_1 > -(a_{21}b_2 - a_{23}b_1)\gamma_2 - \delta_B - 1 \tag{6.50}$$

$$(b_1a_4 - a_2b_2 + b_1)\gamma_1 > -(b_2 + a_{21}b_2 - a_{23}b_1)\gamma_2 - (1 + \tau_B + \delta_B) \tag{6.51}$$

$$(b_1a_4 - a_2b_2 - b_1)\gamma_1 > -(-b_2 + a_{21}b_2 - a_{23}b_1)\gamma_2 - (1 - \tau_B + \delta_B) \tag{6.52}$$

are feasible, then a stabilizing simultaneous feedback control exists. Any (γ_1, γ_2) satisfying (6.45)-(6.52) are stabilizing.

Proof: Follows from (6.21)-(6.28) after setting $\gamma_{11} = \gamma_{21} =: \gamma_2$.

The following proposition asserts stabilizability of the border collision bifurcation using simultaneous feedback control based on Proposition 5.4.

Proposition 6.2 If inequalities (6.35)-(6.42) are feasible with $\gamma_{11} = \gamma_{21} =: \gamma_1$, then a stabilizing simultaneous feedback control exists. Any (γ_1, γ_2) satisfying (6.35)-(6.42) are stabilizing.

Remark 6.1 *It is important to point out that simultaneous control (same control applied on both sides of the border) is robust to uncertainty in location of border. Moreover transforming a system to normal form is not needed when simultaneous feedback control is employed. All that is needed in this case is an estimate of the Jacobian matrices of the map on both sides of the border.*

6.5 One-Sided Feedback Control

In this control method, the feedback is applied on one side of the border only. We will only consider applying the control on the unstable side of the border. Control applied on the stable side of the border is not considered here, because sufficient conditions for it to work are not currently available.

Assume that A is Schur Stable with eigenvalues $\lambda_A^{\pm}$ satisfying, either $0 < \lambda_A^- < \lambda_A^+ < 1$, or $-1 < \lambda_A^- < 0 < \lambda_A^+$. This implies that the system possesses an asymptotically stable fixed point in the left half plane for $\mu < 0$. Assume that the system without control undergoes a BCB as μ is increased through zero. Applying feedback control

on the unstable side (the right half plane) yields the closed-loop system

$$\begin{pmatrix} x_{k+1} \\ y_{k+1} \end{pmatrix} = \begin{cases} \begin{pmatrix} a_{11} & a_2 \\ a_{13} & a_4 \end{pmatrix} \begin{pmatrix} x_k \\ y_k \end{pmatrix} + \begin{pmatrix} b_1 \\ b_2 \end{pmatrix} \mu, & x_k \leq 0 \\ \begin{pmatrix} a_{21} & a_2 \\ a_{23} & a_4 \end{pmatrix} \begin{pmatrix} x_k \\ y_k \end{pmatrix} + \begin{pmatrix} b_1 \\ b_2 \end{pmatrix} \mu + \begin{pmatrix} b_1 \\ b_2 \end{pmatrix} u_k, & x_k > 0 \end{cases} \tag{6.53}$$

$$u_k = \gamma_1 x_k \tag{6.54}$$

where γ_1 is the control gain. Note that only x_k is used in the feedback to maintain continuity of the controlled map along the border $x = 0$. One sided control is a special case of switched feedback control considered in Section 6.3 after setting $\gamma_{11} = \gamma_{12} = \gamma_{22} = 0$. Thus, a stabilizing one sided control as in (6.53),(6.54) exists if a switched feedback exists with $\gamma_{11} = \gamma_{12} = \gamma_{22} = 0$.

6.6 Numerical Examples

In this section, numerical examples are given to illustrate how the developed control laws above can be used to eliminate border collision bifurcation and produce desirable behavior.

Example 6.1 Border collision pair bifurcation (saddle node bifurcation)

Consider the two-dimensional piecewise smooth map

$$\begin{pmatrix} x_{k+1} \\ y_{k+1} \end{pmatrix} = \begin{cases} \underbrace{\begin{pmatrix} 1 & 1 \\ -0.5 & 0 \end{pmatrix}}_{A} \begin{pmatrix} x_k \\ y_k \end{pmatrix} + \begin{pmatrix} 1 \\ 0 \end{pmatrix} \mu + \begin{pmatrix} 1 \\ 0 \end{pmatrix} u_k, & x_k \leq 0 \\ \underbrace{\begin{pmatrix} 2.5 & 1 \\ -0.7 & 0 \end{pmatrix}}_{B} \begin{pmatrix} x_k \\ y_k \end{pmatrix} + \begin{pmatrix} 1 \\ 0 \end{pmatrix} \mu + \begin{pmatrix} 1 \\ 0 \end{pmatrix} u_k, & x_k > 0 \end{cases} \tag{6.55}$$

$$u_k = \gamma_1 x_k + \gamma_2 y_k \tag{6.56}$$

This map with $u_k = 0$ undergoes a border collision pair bifurcation (saddle node bifurcation), where a stable and an unstable fixed point merge and disappear as μ is increased through zero (see Figure 6.1). This is an example of a "dangerous" bifurcation because there are no local attractors for values of μ beyond the critical value. For this example, $a_{11} = 1$, $a_2 = 1$, $a_{13} = -0.5$, $a_4 = 0$, $a_{21} = 2.5$, $a_{23} = -0.7$, $b_1 = 1$ and $b_2 = 0$. The eigenvalues of A are $\lambda_{A_{1,2}} = 0.5 \pm 0.5i$ and those of B are $\lambda_{B_1} = 2.1787$ and $\lambda_{B_2} = 0.3213$.

Next, the control methods developed above are applied to control the BCB in (6.55) so that the closed loop system possesses a locally unique and attracting fixed point on both sides of the border.

Simultaneous control

For this example, it is straightforward to check that inequalities (6.45)-(6.52) are feasible. Thus, a stabilizing simultaneous feedback control exists. A set of stabilizing control gain pairs (γ_1,γ_2) is obtained from inequalities (6.45)-(6.52) and is depicted in Figure 6.2. The bifurcation diagram of the controlled system with $\gamma_1 = -1.95$ and $\gamma_2 = -1.05$ is shown in Figure 6.3.

Example 6.2 (Dangerous Border Collision Bifurcation, Example Revisited)

We revisit the example of Section 5.1, and show that the control methods presented above can be used to eliminate the instability and produce a locally unique fixed point attractor on both sides of the border. The map (5.1) is repeated here with control

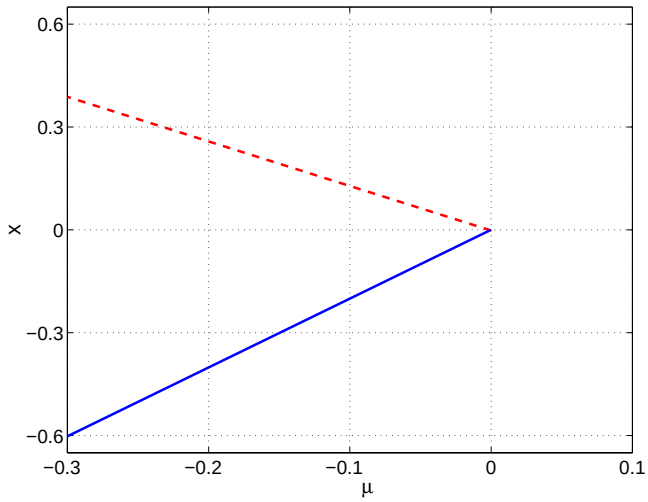

Figure 6.1: Bifurcation diagram for Example 6.1 without control. The solid line represents a path of stable fixed points whereas the dashed line represents a path of unstable fixed points.

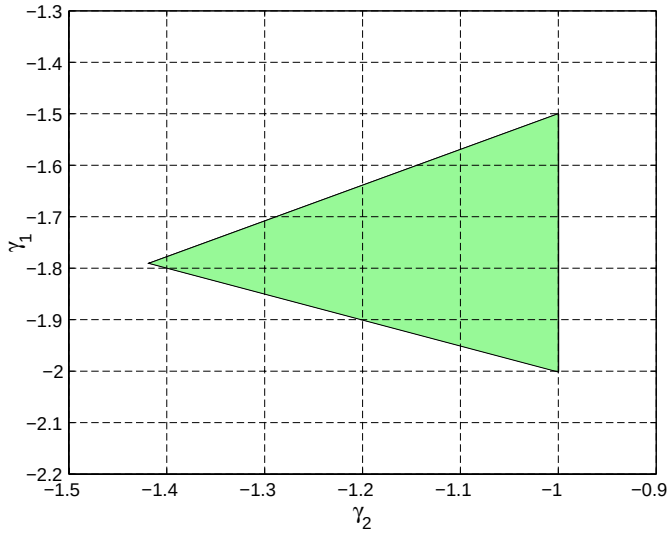

Figure 6.2: The interior of the triangle gives simultaneously stabilizing control gains for Example 6.1.

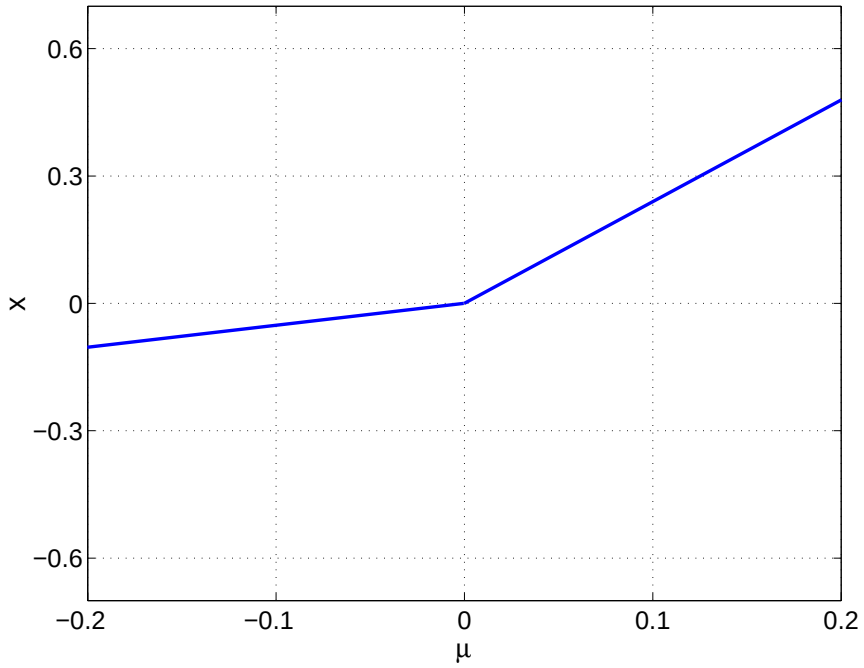

Figure 6.3: Bifurcation diagram for Example 6.1 with simultaneous control using $\gamma_1 = -1.95$ and $\gamma_2 = -1.05$ (A locally unique and stable fixed point exists on both sides of the border).

signal included:

$$\begin{pmatrix} x_{k+1} \\ y_{k+1} \end{pmatrix} = \begin{cases} \underbrace{\begin{pmatrix} -0.3 & 1 \\ -0.9 & 0 \end{pmatrix}}_{A} \begin{pmatrix} x_k \\ y_k \end{pmatrix} + \begin{pmatrix} 1 \\ 0 \end{pmatrix} \mu + \begin{pmatrix} 1 \\ 0 \end{pmatrix} u_k, & x_k \leq 0 \\ \underbrace{\begin{pmatrix} -1.6 & 1 \\ -0.9 & 0 \end{pmatrix}}_{B} \begin{pmatrix} x_k \\ y_k \end{pmatrix} + \begin{pmatrix} 1 \\ 0 \end{pmatrix} \mu + \begin{pmatrix} 1 \\ 0 \end{pmatrix} u_k, & x_k > 0 \end{cases}$$

$$u_k = \underbrace{(\gamma_1 \ \gamma_2)}_{g} \begin{pmatrix} x_k \\ y_k \end{pmatrix}$$

A simple check shows that a simultaneous feedback control based on Proposition 6.1 exists. One stabilizing control gain vector is given by $g = (1 \quad -1.1)$. This yields the

closed-loop matrices

$$\begin{aligned} A_c &= A + bg \\ &= \begin{pmatrix} 0.7 & -0.1 \\ -0.9 & 0 \end{pmatrix} \end{aligned}$$

and

$$\begin{aligned} B_c &= B + bg \\ &= \begin{pmatrix} -0.6 & -0.1 \\ -0.9 & 0 \end{pmatrix} \end{aligned}$$

The eigenvalues of A_c and B_c are given by $\{0.811, -0.111\}$ and $\{-0.7243, 0.1243\}$, respectively. The bifurcation diagram of the closed-loop system is similar to that shown in Figure 6.3.

Chapter 7

Lyapunov-Based Stability Analysis and Feedback Control of Piecewise Smooth Discrete-Time Systems

In this chapter, Lyapunov techniques are used in the analysis of finite dimensional piecewise smooth discrete-time systems that depend on a parameter. The use of Lyapunov techniques facilitates the consideration of n-dimensional systems where n is not restricted to be 1 or 2 as in previous chapters. A sufficient condition for nonbifurcation with persistent stability in PWS maps of dimension n is derived. The derived condition is in terms of linear matrix inequalities (LMIs). This condition is then used as a basis for the design of feedback controls to eliminate border collision bifurcations in PWS maps and to produce desirable behavior. The Lyapunov-based methodology is used to consider the design of washout filter based controllers. These are dynamic feedback control laws that are designed so as not to alter a system's fixed points, even in the presence of model uncertainty. In addition, the Lyapunov-based approach is extended to allow nonmonotonically decreasing Lyapunov functions.

7.1 Introduction

Recently, many researchers have studied stability of a fixed point of switched discrete-time linear systems (e.g., [44, 57, 30, 29, 46]) as well as continuous time switched systems (e.g.,[43, 42]). In all the referenced studies, Lyapunov techniques were used to obtain sufficient conditions for stability of the fixed point (or equilibrium point) of a piecewise linear system. For instance, in [42, 57, 30], quadratic as well as piecewise quadratic Lyapunov functions were used in the analysis of stability of switched systems and also in the synthesis of stabilizing controls. In [46], piecewise linear Lyapunov functions were used to obtain stabilizing switching sequences. The author is unaware of any previous study using Lyapunov methods to analyze the dynamics of switched systems depending on a parameter. Here, we use quadratic Lyapunov functions to study border collision bifurcations in PWS maps and to obtain sufficient conditions for nonbifurcation with persistent stability in such maps.

7.2 Lyapunov-Based Analysis of PWS Maps

In this section, we consider Lyapunov-based stability and bifurcation analysis of n-dimensional PWS maps. Consider the one-parameter family of piecewise affine (PWA) maps $f_\mu : \mathbb{R}^n \to \mathbb{R}^n$ in normal form for BCB given by

$$f_\mu(x(k)) = \begin{cases} Ax(k) + \mu b, & \text{if } x_1(k) \leq 0 \\ Bx(k) + \mu b, & \text{if } x_1(k) > 0 \end{cases}$$

We start with scalar systems to illustrate the ideas and then we proceed to multi-dimensional systems.

7.2.1 Scalar Systems

For scalar systems, the normal form is given by

$$x(k+1) = f_\mu(x(k)) = \begin{cases} ax(k)+\mu, & \text{if } x(k) \le 0 \\ bx(k)+\mu, & \text{if } x(k) > 0 \end{cases} \tag{7.1}$$

The possible fixed points are given by: $x_B(\mu) = \frac{\mu}{1-b}$ and $x_A(\mu) = \frac{\mu}{1-a}$. For the fixed point $x_B(\mu)$ to actually occur, we need $\frac{\mu}{1-b} \ge 0$ which is satisfied if and only if $\mu \ge 0$ and $b < 1$ or $\mu \le 0$ and $b > 1$. Similarly, for $x_A(\mu)$ to actually occur, we need $\frac{\mu}{1-a} \le 0$ which is satisfied if and only if $\mu \le 0$ and $a < 1$ or $\mu \ge 0$ and $a > 1$.

Case 1): $\mu \le 0$ *and* $a < 1$, *scalar systems*. Here, the fixed point of f_μ is $x_A(\mu) = \frac{\mu}{1-a}$. Changing the state variable to $z = x - x_A(\mu)$, we have

$$\begin{aligned} z(k+1) &= \begin{cases} a(z(k)+x_A(\mu))+\mu-x_A(\mu), & \text{if } z(k) \le -x_A(\mu) \\ b(z(k)+x_A(\mu))+\mu-x_A(\mu), & \text{if } z(k) > -x_A(\mu) \end{cases} \\ &= \begin{cases} az(k), & \text{if } z(k) \le -x_A(\mu) \\ bz(k)+\frac{b-a}{1-a}\mu, & \text{if } z(k) > -x_A(\mu) \end{cases} \end{aligned} \tag{7.2}$$

In the new coordinates, $z = 0$ is a fixed point for $\mu \le 0$. (Note that the border point $z_{border} = -\frac{\mu}{1-a}$ varies as a function of μ.)

Consider the quadratic Lyapunov function candidate

$$V(z) = pz^2, \quad \text{where } p > 0 \tag{7.3}$$

The forward difference of V along the trajectories of (7.2) is $\Delta V(z(k)) = V(z(k+1) - V(z(k))$. There are two cases: $z(k) \le -x_A(\mu)$ and $z(k) > -x_A(\mu)$.

Case 1.1): $z(k) \le -x_A(\mu)$. In this case, we use a subscript L to indicate calculations to the "left" of the border.

$$\Delta V_L(z(k)) = V(z(k+1)) - V(z(k))$$

$$
\begin{aligned}
&= p(az(k))^2 - pz^2(k) \\
&= p(a^2-1)z^2(k) \qquad (7.4)
\end{aligned}
$$

Note that $\Delta V(z(k))$ in (7.4) is negative if and only if $-1 < a < 1$.

Case 1.2: $z(k) > -x_A(\mu)$. In this case, we use a subscript R to indicate calculations to the "right" of the border.

$$
\begin{aligned}
\Delta V_R(z(k)) &= V(z(k+1)) - V(z(k)) \\
&= p\left(bz(k) + \frac{b-a}{1-a}\mu\right)^2 - pz^2(k) \\
&= p(b^2-1)z^2(k) + 2pb\mu\frac{b-a}{1-a}z(k) + p\left(\frac{b-a}{1-a}\right)^2\mu^2. \qquad (7.5)
\end{aligned}
$$

Combining (7.4) and (7.5) yields

$$
\Delta V(z(k)) = \begin{cases} p(a^2-1)z^2(k), & z(k) \le -x_A(\mu) \\ p(b^2-1)z^2(k) + 2pb\mu\frac{b-a}{1-a}z(k) + p\left(\frac{b-a}{1-a}\right)^2\mu^2, & z(k) > -x_A(\mu) \end{cases} \qquad (7.6)
$$

The next proposition asserts that $\Delta V(z(k))$ in (7.6) is negative definite if and only if $|a| < 1$ and $|b| < 1$.

Proposition 7.1 *The forward difference of V given in (7.6) is negative definite if and only if $|a| < 1$ and $|b| < 1$.*

Proof: The necessity part is clear from (7.4) and (7.5); if $|a| \ge 1$ then $\Delta V > 0$ in (7.4), similarly, if $|b| \ge 1$ then $\Delta V > 0$ in (7.5) for large z.

To prove the sufficiency part, assume $|a| < 1$ and $|b| < 1$. Note that $\Delta V(z(k))$ is continuous $\forall z \in \mathbb{R}$. Continuity of ΔV follows from the continuity of V and the continuity of the map (7.2). Since $\Delta V(z(k)) < 0$ for all $z \le -x_A(\mu)$ (by (7.4) $\Delta V(z) = 0$ only if $z = 0$) and ΔV is continuous $\forall z$, it follows that $\Delta V(z) < 0$ at the point $z = -x_A(\mu)$. It remains to show that $\Delta V(z) < 0$ for all $z > -x_A(\mu)$ (note that $-x_A(\mu) > 0$).

To this end, we use (7.5) to show that $\Delta V(z)$ is decreasing in z in the region $z > -x_A(\mu)$:

$$\frac{d\Delta V}{dz} = 2p(b^2-1)z + 2pb(b-a)x_A(\mu), \qquad z > -x_A(\mu) > 0 \tag{7.7}$$

Since $z > -x_A(\mu)$, we can express z as: $z = -x_A(\mu) + w$, where $w > 0$. Then

$$\begin{aligned} \frac{d\Delta V}{dz} &= 2p(b^2-1)(-x_A(\mu)+w) + 2pb(b-a)x_A(\mu) \\ &= \underbrace{2p(b^2-1)}_{<0} w + 2p\underbrace{x_A(\mu)}_{\leq 0}\underbrace{(1-ab)}_{>0} < 0 \end{aligned} \tag{7.8}$$

Thus, $\Delta V(z) < 0$ for all $z > -x_A(\mu)$. We conclude that $\Delta V(z(k)) < 0$ for all $z(k) \neq 0$ and $\Delta V(z(k)) = 0$ for $z(k) = 0$. ■

Case 2): $\mu > 0$ *and* $b < 1$, *scalar systems*. In this case, the fixed point of f_μ is $x_B(\mu) = \frac{\mu}{1-b}$. Changing the state variable to $z = x - x_B(\mu)$, we have

$$\begin{aligned} z(k+1) &= \begin{cases} a(z(k)+x_B(\mu)) + \mu - x_B(\mu), & \text{if } z(k) \leq -x_B(\mu) \\ b(z(k)+x_B(\mu)) + \mu - x_B(\mu), & \text{if } z(k) > -x_B(\mu) \end{cases} \\ &= \begin{cases} az(k) + \frac{a-b}{1-b}\mu, & \text{if } z(k) \leq -x_B(\mu) \\ bz(k), & \text{if } z(k) > -x_B(\mu) \end{cases} \end{aligned} \tag{7.9}$$

Consider the same quadratic Lyapunov function candidate as in (7.3) above:

$$V(z) = pz^2, \qquad \text{where } p > 0$$

The forward difference of V along the trajectories of (7.9) is $\Delta V(z(k)) = V(z(k+1) - V(z(k))$ and is given by

$$\Delta V(z(k)) = \begin{cases} p(a^2-1)z^2(k) + 2pa\mu\frac{a-b}{1-b}z(k) + p\left(\frac{a-b}{1-b}\right)^2\mu^2, & z(k) \leq -x_B(\mu) \\ p(b^2-1)z^2(k), & z(k) > -x_B(\mu) \end{cases} \tag{7.10}$$

The following proposition summarizes the result for this case. The derivation is similar to that of Proposition 7.1 above.

Proposition 7.2 *The forward difference of V given in (7.10) is negative definite if and only if $|a| < 1$ and $|b| < 1$.*

Combining Propositions 7.1 and 7.2 yields that the map (7.1) has a globally asymptotically stable fixed point for all $\mu \in \mathbb{R}$ if $|a| < 1$ and $|b| < 1$. The following proposition summarizes this result.

Proposition 7.3 (Nonbifurcation with Persistent Stability in 1-D PWS Maps) The PWS map (7.1) has a globally asymptotically stable fixed point for all $\mu \in \mathbb{R}$ if $|a| < 1$ and $|b| < 1$.

This result is in agreement with the known results discussed in Chapter 3.

7.2.2 Multidimensional Systems

We now consider Lyapunov-based stability and bifurcation analysis for n-dimensional PWS maps. Consider the one-parameter family of piecewise smooth maps

$$f(x,\mu) = \begin{cases} f_A(x,\mu), & x \in R_A \\ f_B(x,\mu), & x \in R_B \end{cases} \tag{7.11}$$

where $f : \mathbb{R}^{n+1} \to \mathbb{R}^n$ is piecewise smooth in x; f is smooth in x everywhere except on the border (hypersurface Γ) separating R_A and R_B where it is only continuous, f is smooth in μ and R_A, R_B are the two (nonintersecting) regions of smooth behavior. We are interested in studying the dynamics of f at a fixed point (or a periodic orbit) near or at the border Γ. If the fixed point (or periodic orbit) is in R_A (respectively R_B) and is away from the border, then the local dynamics is determined by the single map f_A (respectively f_B). If, on the other hand, the fixed point is close to the border, then jumps across the border can occur except in an extremely small neighborhood of the

fixed point. Therefore, for operation close to the border, both f_A and f_B are needed in the study of the possible behavior. For a fixed point at or near the border, the dynamics is determined by the linearizations of the map on both sides of the border, as was discussed at length in Section 2.2.

Consider the piecewise-linearized representation of (7.11) [23]

$$x(k+1) = f_\mu(x(k)) = \begin{cases} Ax(k)+\mu b, & \text{if } x_1(k) \le 0 \\ Bx(k)+\mu b, & \text{if } x_1(k) > 0 \end{cases} \tag{7.12}$$

where A is the linearization of the PWS map f in R_A at a fixed point on the border approached from points in R_A near the border; B is the linearization of f at a fixed point on the border approached from points in R_B; and b is the derivative of the map f with respect to μ. The sign of the first component of the vector x determines whether x is in R_A or in R_B. If $x_1 = 0$, then x is on the border separating R_A and R_B. Note that the assumed continuity of f_μ at the border implies that A and B differ only in their first columns. That is, $a_{ij} = b_{ij}$, for $j \neq 1$, where $A = [a_{ij}]$ and $B = [b_{ij}]$.

Assume that $1 \notin \sigma(A)$ and $1 \notin \sigma(B)$ (i.e., both $I-A$, $I-B$ are nonsingular). Formally solving for the fixed points of (7.12), we obtain $x_A(\mu) = (I-A)^{-1}b\mu$ and $x_B(\mu) = (I-B)^{-1}b\mu$. For $x_A(\mu)$ to actually occur as a fixed point, the first component of $x_A(\mu)$ must be nonpositive. That is,

$$x_{A_1}(\mu) \;=\; (e^1)^T \mu (I-A)^{-1} b \le 0 \tag{7.13}$$

where $(e^1)^T = (1\ 0\ \cdots\ 0)$. Similarly, for $x_B(\mu)$ to actually occur as a fixed point, we need

$$x_{B_1}(\mu) \;=\; (e^1)^T \mu (I-B)^{-1} b > 0 \tag{7.14}$$

If, on the other hand, the first component of $x_A(\mu)$ is positive (the first component of

$x_B(\mu)$ is nonpositive), then the fixed point is called a virtual fixed point. Virtual fixed points are important in studying the dynamics of a PWS map at or near the border.

Let $p_A(\lambda)$ and $p_B(\lambda)$ be the characteristic polynomials of A and B, respectively. Then $p_A(\lambda) = \det(\lambda I - A)$ and $p_B(\lambda) = \det(\lambda I - B)$.

The fixed points can be written as

$$\begin{aligned} x_A(\mu) &= (I-A)^{-1}b\mu \\ &= \frac{\text{adj}(I-A)b\mu}{\det(I-A)} \\ &= \frac{\bar{b}_A}{p_A(1)}\mu, \end{aligned} \tag{7.15}$$

$$\begin{aligned} x_B(\mu) &= (I-B)^{-1}b\mu \\ &= \frac{\text{adj}(I-B)b\mu}{\det(I-B)} \\ &= \frac{\bar{b}_B}{p_B(1)}\mu. \end{aligned} \tag{7.16}$$

where $\bar{b}_A$ =adj$(I-A)b$ and $\bar{b}_B$ =adj$(I-B)b$. It can be shown that $\bar{b}_{A_1} = \bar{b}_{B_1} =: \bar{b}_1$ [23]. To see this, recall that A and B differ only in their first columns and adj$(I-A) = (cof(I-A))^T$. Thus, the first row of adj$(I-A)$ is equal to the first row of adj$(I-B)$, which implies that $(e^1)^T adj(I-A)b = (e^1)^T adj(I-B)b =: \bar{b}_1$. Thus, the first component of $x_A(\mu)$ is $x_{A_1}(\mu) = \frac{\bar{b}_1}{p_A(1)}\mu$ and the first component of $x_B(\mu)$ is $x_{B_1}(\mu) = \frac{\bar{b}_1}{p_B(1)}\mu$. For the fixed point $x_A(\mu)$ to occur for $\mu \leq 0$, we need $x_{A_1}(\mu) \leq 0$, i.e., $\frac{\bar{b}_1}{p_A(1)}\mu \leq 0$, or, equivalently, $\frac{\bar{b}_1}{p_A(1)} > 0$. Similarly, for the fixed point $x_B(\mu)$ to occur for $\mu > 0$, we need $x_{B_1}(\mu) > 0$, i.e., $\frac{\bar{b}_1}{p_B(1)}\mu > 0$, or, equivalently, $\frac{\bar{b}_1}{p_B(1)} > 0$. Therefore, a necessary and sufficient condition to have a fixed point for all μ is $p_A(1)p_B(1) > 0$, which is assumed to be in force in the remainder of the discussion.

As we did for scalar systems, we perform a change of variables to simplify the analysis.

Case 1): $\underline{\mu \leq 0,\ \textit{n-dimensional systems.}}$ The fixed point of f_μ is $x_A(\mu)$. Changing the state vector to $z = x - x_A(\mu)$, we have

$$\begin{aligned} z(k+1) &= \begin{cases} A(z(k)+x_A(\mu))+b\mu-x_A(\mu), & \text{if } z_1(k) \leq -x_{A_1}(\mu) \\ B(z(k)+x_A(\mu))+b\mu-x_A(\mu), & \text{if } z_1(k) > -x_{A_1}(\mu) \end{cases} \\ &= \begin{cases} Az(k), & \text{if } z_1(k) \leq -x_{A_1}(\mu) \\ Bz(k)+(I-(I-B)(I-A)^{-1})b\mu, & \text{if } z_1(k) > -x_{A_1}(\mu) \end{cases} \\ &= \begin{cases} Az(k), & \text{if } z_1(k) \leq -x_{A_1}(\mu) \\ Bz(k)+\underbrace{(B-A)(I-A)^{-1})b}_{=:c}\mu, & \text{if } z_1(k) > -x_{A_1}(\mu) \end{cases} \end{aligned} \tag{7.17}$$

In the new coordinates, $z = 0$ is a fixed point for all $\mu \leq 0$. (Note that the border $z_{border} = \{z : z_1 = -x_{A_1}(\mu)\}$, varies as a function of μ.) Note that since B and A differ only in their first columns, all elements of $B-A$ are zero except for the first column. Thus, $c\mu = (B-A)(I-A)^{-1}b\mu = (B-A)x_A(\mu) = x_{A_1}(\mu)(B^1 - A^1)$, where A^1 (resp. B^1) denotes the first column of the matrix A (resp. B).

Consider the quadratic Lyapunov function candidate

$$V(z) = z^T P z, \quad \text{where } P = P^T > 0 \tag{7.18}$$

The forward difference of V along trajectories of (7.17) is $\Delta V(z(k)) = V(z(k+1) - V(z(k))$. There are two cases: $z_1(k) \leq -x_{A_1}(\mu)$ and $z_1(k) > -x_{A_1}(\mu)$.

Case 1.1): $z_1(k) \leq -x_{A_1}(\mu)$

$$\begin{aligned} \Delta V_L(z(k)) &= V(z(k+1)) - V(z(k)) \\ &= (Az(k))^T PAz(k) - z(k)^T Pz(k) \\ &= z(k)^T (A^T PA - P) z(k) \end{aligned} \tag{7.19}$$

Case 1.2): $z_1(k) > -x_{A_1}(\mu)$

$$\Delta V_R(z(k)) = V(z(k+1)) - V(z(k))$$

$$
\begin{aligned}
&= (Bz(k)+c\mu)^T P(Bz(k)+c\mu) - z(k)^T Pz(k) \\
&= z(k)^T (B^T PB - P)z(k) + 2\mu c^T PBz(k) + \mu^2 c^T Pc \\
&= z(k)^T (B^T PB - P)z(k) + 2x_{A_1}(\mu)(B^1 - A^1)^T PBz(k) \\
&+ x_{A_1}^2(\mu)(B^1 - A^1)^T P(B^1 - A^1) \qquad (7.20)
\end{aligned}
$$

Combining (7.19) and (7.20) yields

$$
\Delta V(z(k)) = \begin{cases} \Delta V_L(z(k)), & \text{if } z_1(k) \leq -x_{A_1}(\mu) \\ \Delta V_R(z(k)), & \text{if } z_1(k) > -x_{A_1}(\mu) \end{cases} \qquad (7.21)
$$

From (7.19) and (7.20), a necessary condition for $\Delta V(z(k))$ to be negative definite is that the following two matrix inequalities hold:

$$A^T PA - P < 0 \qquad (7.22)$$

$$B^T PB - P < 0 \qquad (7.23)$$

Moreover, we have the following claim, which asserts sufficiency of (7.22),(7.23) for negative definiteness of $\Delta V(z(k))$.

Claim: (Sufficiency of LMIs (7.22)-(7.23) for a Decreasing Lyapunov Function) If the matrix inequalities (7.22)-(7.23) are satisfied with $P = P^T > 0$, then $\Delta V(z(k))$ given by (7.21) is negative definite.

Proof: Assume that there is a $P = P^T > 0$ such that (7.22)-(7.23) are satisfied. Then $\Delta V_L(z) = z^T(A^T PA - P)z < 0 \ \forall z \neq 0$. It remains to show that $\Delta V_R(z) < 0$. Let $z = (z_1, z_2)^T$, where $z_1 \in \mathbb{R}$ and $z_2 \in \mathbb{R}^{n-1}$. Note that $\Delta V(z)$ is continuous for all z. Continuity of $\Delta V(z)$ follows from the continuity of $V(z)$ and continuity of the map (7.17). Since $\Delta V_L(z) < 0$ ($\Delta V_L(z) = 0$ if and only if $z = 0$) and $\Delta V(z)$ is continuous for all z, it follows that $\Delta V_R(z) < 0$ at the border $\{z_1 = -x_{A_1}(\mu)\}$ (since

$\lim_{(z_1,z_2)\to(-x_{A1}^-(\mu),z_2)} \Delta V_L = \lim_{(z_1,z_2)\to(-x_{A1}^+(\mu),z_2)} \Delta V_R$). It remains to show that $\Delta V_R(z) < 0$ for all z in the region $z_1 > -x_{A_1}(\mu)$ (note that $-x_{A_1}(\mu) > 0$). Completing the squares in (7.20) allows us to write $\Delta V_R(z)$ as follows:

$$\begin{aligned}\Delta V_R(z) &= z^T(B^TPB-P)z + 2x_{A_1}(\mu)(B^1-A^1)^TPBz + x_{A_1}^2(\mu)(B^1-A^1)^TP(B^1-A^1) \\ &= (z-\alpha)^T(B^TPB-P)(z-\alpha) - \alpha^T(B^TPB-P)\alpha \\ &+ x_{A_1}^2(\mu)(B^1-A^1)^TP(B^1-A^1) \qquad (7.24)\end{aligned}$$

where $\alpha = -x_{A_1}(\mu)(B^TPB-P)^{-1}B^TP(B^1-A^1)$. Let $N \subset \mathbb{R}^n$ such that N is convex and contains the origin (for example, a ball). Since the fixed point $x_A(\mu)$ is close to the origin for small μ, the hyperplane $z_1 = -x_{A_1}(\mu)$ slices the neighborhood N. Consider $\Delta V_R(z)$ restricted to N. The second derivative of $\Delta V_R(z)$ with respect to z (i.e., its Hessian matrix) is $\nabla^2 \Delta V_R = 2(B^TPB-P) < 0$. Thus, $\Delta V_R(z)$ is strictly concave on N, i.e., for every $z, y \in N$, and $\theta \in (0,1)$, $\Delta V_R(\theta z + (1-\theta)y) > \theta \Delta V_R(z) + (1-\theta)\Delta V_R(y)$. Note that $\Delta V_R(0) = x_{A_1}^2(\mu)(B^1-A^1)^TP(B^1-A^1) > 0$. Now, we show that $\Delta V_R < 0$ $\forall z \in N$ with $z_1 > -x_{A_1}(\mu)$. By way of contradiction, suppose there is a $y \in N$, with $y_1 > -x_{A1}(\mu)$, such that $\Delta V_R(y) > 0$. Since $\Delta V_R(z)$ is strictly concave, it follows that $\Delta V_R(z)$ is positive along the line segment connecting 0 and y: $\Delta V_R(\theta \cdot 0 + (1-\theta)y) > \theta \underbrace{\Delta V_R(0)}_{>0} + (1-\theta)\underbrace{\Delta V_R(y)}_{>0} > 0$, $\forall \theta \in (0,1)$. But, along the line connecting $z = 0$ with $z = y$, there is a point z^* with $z_1^* = -x_{A_1}(\mu)$ where $\Delta V_R(z^*) < 0$, which is a contradiction. Thus, $\Delta V_R(z) < 0$ for all $z \in N$ with $z_1 > -x_{A_1}(\mu) > 0$. ■

Remark 7.1 *If the piecewise smooth map is affine as in (7.12), then the result above applies globally. That is, if the origin of a piecewise affine map is quadratically stable (i.e., can be proved stable using a common quadratic Lyapunov function), then the map has a globally asymptotically stable fixed point for all $\mu \leq 0$. This is easily seen*

in the proof above by using a global argument (the neighborhood N can be taken as $\mathbb{R}^n$).

The following proposition summarizes the results so far.

Proposition 7.4 *The forward difference of $V = z^T Pz$, with $P = P^T > 0$, along trajectories of (7.17) with $\mu \leq 0$ is negative definite (i.e., $\Delta V(z) < 0$) if and only if the following matrix inequalities hold:*

$$A^T PA - P < 0 \tag{7.25}$$

$$B^T PB - P < 0 \tag{7.26}$$

Case 2): $\underline{\mu > 0,\ n\text{-dimensional systems.}}$ The fixed point of f_μ is $x_B(\mu)$. Changing the state vector to $z = x - x_B(\mu)$, we have

$$\begin{aligned} z(k+1) &= \begin{cases} A(z(k)+x_B(\mu))+b\mu-x_B(\mu), & \text{if } z_1(k) \leq -x_{B_1}(\mu) \\ B(z(k)+x_B(\mu))+b\mu-x_B(\mu), & \text{if } z_1(k) > -x_{B_1}(\mu) \end{cases} \\ &= \begin{cases} Az(k)+(I-(I-A)(I-B)^{-1})b\mu, & \text{if } z_1(k) \leq -x_{B_1}(\mu) \\ Bz(k), & \text{if } z_1(k) > -x_{B_1}(\mu) \end{cases} \\ &= \begin{cases} Az(k)+\underbrace{(A-B)(I-B)^{-1})b}_{=:c}\mu, & \text{if } z_1(k) \leq -x_{B_1}(\mu) \\ Bz(k), & \text{if } z_1(k) > -x_{B_1}(\mu) \end{cases} \end{aligned} \tag{7.27}$$

In the new coordinates, $z = 0$ is a fixed point for all $\mu > 0$. (Note that the border $z_{border} = \{z : z_1 = -x_{B_1}(\mu)\}$, varies as a function of μ.) Note that since B and A differ only in their first columns, all elements of $A - B$ are zero except for the first column. Thus, $c\mu = (A-B)(I-B)^{-1}b\mu = (A-B)x_B(\mu) = x_{B_1}(\mu)(A^1 - B^1)$.

Consider the same quadratic Lyapunov function candidate as in (7.18) above:

$$V(z) = z^T P z, \quad \text{where } P = P^T > 0$$

The forward difference of V along trajectories of (7.27) is $\Delta V(z(k)) = V(z(k+1) - V(z(k))$. There are two cases: $z_1(k) \leq -x_{B_1}(\mu)$ and $z_1(k) > -x_{B_1}(\mu)$. (Note that $x_{B1}(\mu) > 0$ from (7.14).)

Case 2.1): $z_1(k) \leq -x_{B_1}(\mu)$

$$\begin{aligned}
\Delta V_L(z(k)) &= V(z(k+1)) - V(z(k)) \\
&= (Az(k) + c\mu)^T P(Az(k) + c\mu) - z(k)^T P z(k) \\
&= z(k)^T (A^T PA - P) z(k) + 2\mu c^T PAz(k) + \mu^2 c^T Pc \\
&= z(k)^T (A^T PA - P) z(k) + 2x_{B_1}(\mu)(A^1 - B^1)^T PAz(k) \\
&+ x_{B_1}^2(\mu)(A^1 - B^1)^T P(A^1 - B^1) \qquad (7.28)
\end{aligned}$$

Case 2.2): $z_1(k) > -x_{B_1}(\mu)$

$$\begin{aligned}
\Delta V_R(z(k)) &= V(z(k+1)) - V(z(k)) \\
&= (Bz(k))^T PBz(k) - z(k)^T Pz(k) \\
&= z(k)^T (B^T PB - P) z(k) \qquad (7.29)
\end{aligned}$$

Combining (7.28) and (7.29) yields

$$\Delta V(z(k)) = \begin{cases} \Delta V_L(z(k)), & \text{if } z(k) \leq -x_{B_1}(\mu) \\ \Delta V_R(z(k)), & \text{if } z(k) > -x_{B_1}(\mu) \end{cases} \qquad (7.30)$$

Proposition 7.5 (Necessary and Sufficient Conditions for a Decreasing Lyapunov Function)

The forward difference of $V = z^T Pz$, with $P = P^T > 0$, along trajectories of (7.27) with $\mu \geq 0$ is negative definite (i.e., $\Delta V(z) < 0$) if and only if the following matrix inequalities hold:

$$A^T PA - P < 0 \tag{7.31}$$

$$B^T PB - P < 0 \tag{7.32}$$

Proof: Necessity follows from (7.28) and (7.29), and the proof for sufficiency is similar to that for the case $\mu \leq 0$ above. ■

By combining Proposition 7.4 and Proposition 7.5, we obtain the main result of this chapter.

Proposition 7.6 (Sufficient Condition for Nonbifurcation with Persistent Stability in n-D PWS Maps)

Consider the system (7.12). If there is a $P = P^T > 0$ such that

$$A^T PA - P < 0,$$

$$B^T PB - P < 0,$$

then system (7.12) has a globally asymptotically stable fixed point for all $\mu \in \mathbb{R}$.

Corollary 7.1 *If at $\mu = 0$ the origin of the map (7.12) is quadratically stable, i.e., using a quadratic Lyapunov function $V = x^T Px$, with $P > 0$, then the fixed point depending on μ on both sides of the border is attracting and no bifurcation occurs from the origin as μ is varied through zero.*

Proposition 7.7 (Necessary Condition for Existence of a CQLF) [57]

A necessary condition for the existence of a common quadratic Lyapunov function (CQLF) for the two systems in (7.12) is that the matrix product AB is Schur stable (and, by symmetry, that BA is Schur stable).

Proof: Suppose that a CQLF exists for A and B. That is,

$$A^T PA - P < 0,$$

$$B^T PB - P < 0.$$

Equivalently,

$$P > A^T PA, \tag{7.33}$$

$$P > B^T PB. \tag{7.34}$$

Using the property that $X > Y \Longrightarrow C^T XC \geq C^T YC$, we have

$$P > A^T PA \Longrightarrow B^T PB \geq B^T A^T PAB$$

Using (7.34), we get

$$P > B^T A^T PAB$$

Thus, AB must be Schur stable. Similarly,

$$P > B^T PB \Longrightarrow A^T PA \geq A^T B^T PBA$$

Using (7.33), we get

$$P > A^T B^T PBA$$

Thus BA must be Schur stable. ■

Remark 7.2 *A necessary and sufficient condition for existence of a CQLF that shows Schur stability of a pair of second order discrete time systems with matrices A and B was given by Akar and Narendra [6]. The condition is based on Schur stability of two matrix pencils of A and B. Mason and Shorten [56] give other necessary conditions for existence of a CQLF for two discrete-time systems of dimension n. The necessary conditions are also defined in terms of invertibility of two matrix pencils of A and B.*

7.2.3 Numerical Examples

In this subsection, we give numerical examples to demonstrate how the Lyapunov-based techniques considered in the previous section can be used in the stability and bifurcation analysis.

Example 7.1 Consider the two-dimensional piecewise affine (PWA) map

$$x(k+1) = \begin{cases} \underbrace{\begin{pmatrix} 0.10 & 1 \\ 0.72 & 0 \end{pmatrix}}_{A} x(k) + \begin{pmatrix} 1 \\ 0 \end{pmatrix} \mu, & x_1(k) \leq 0 \\ \underbrace{\begin{pmatrix} 1.6 & 1 \\ -0.73 & 0 \end{pmatrix}}_{B} x(k) + \begin{pmatrix} 1 \\ 0 \end{pmatrix} \mu, & x_1(k) > 0 \end{cases} \tag{7.35}$$

The eigenvalues of A are $\lambda_{A_1} = -0.8$, $\lambda_{A_2} = 0.9$ and the eigenvalues of B are $\lambda_{B_{1,2}} = 0.8 \pm j\ 0.3$. Although the eigenvalues of A and B are inside the unit circle, we cannot conclude that no bifurcation for (7.35) occurs at $\mu = 0$.

A simple check shows that AB is Schur stable ($\sigma(AB) = \{-0.6539, 0.8039\}$), thus the necessary condition for existence of a CQLF given in Proposition 7.7 is satisfied. The next step is to check whether a CQLF exists for this example or not. A common quadratic Lyapunov function $V = x^T P x$, with $P = P^T > 0$ that satisfies the conditions

of Proposition 7.6 exists for this example. To wit:

$$P = \begin{pmatrix} 0.8556 & 0.8552 \\ 0.8552 & 1.1158 \end{pmatrix}$$

is obtained using the MATLAB LMI toolbox. Thus, the PWA map (7.35) has a unique attracting fixed point for all μ. This is also validated by calculating the bifurcation diagram, depicted in Figure 7.1.

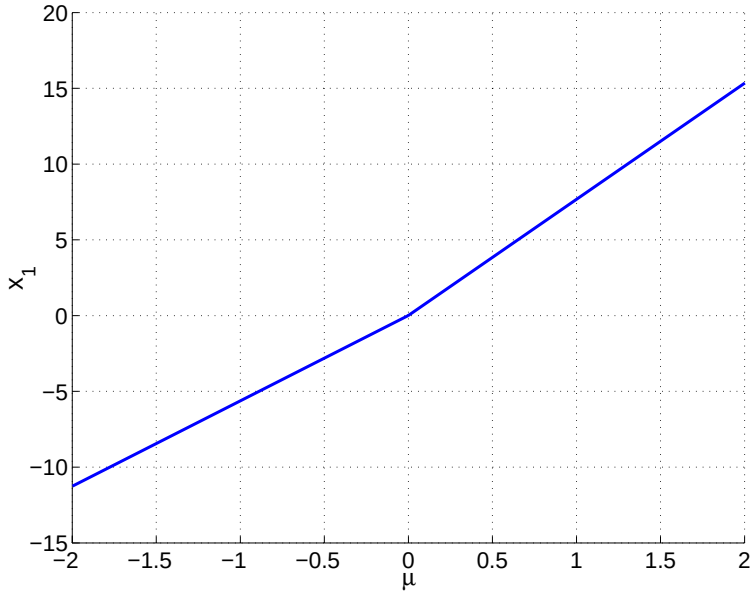

Figure 7.1: Bifurcation diagram for Example 7.1. Each solid line represents a path of stable fixed points.

Example 7.2 Consider the two-dimensional PWA map

$$x(k+1) = \begin{cases} \underbrace{\begin{pmatrix} -0.8 & 1 \\ -0.17 & 0 \end{pmatrix}}_{A} x(k) + \begin{pmatrix} 1 \\ 0 \end{pmatrix} \mu, & x_1(k) \leq 0 \\ \underbrace{\begin{pmatrix} 0.4 & 1 \\ -0.13 & 0 \end{pmatrix}}_{B} x(k) + \begin{pmatrix} 1 \\ 0 \end{pmatrix} \mu, & x_1(k) > 0 \end{cases} \tag{7.36}$$

The eigenvalues of A are $\lambda_{A_{1,2}} = -0.4 \pm j\,0.1$ and the eigenvalues of B are $\lambda_{B_{1,2}} = 0.2 \pm j0.3$. Although both A and B are stable matrices, we cannot conclude that no bifurcation for (7.36) occurs at $\mu = 0$.

A common quadratic Lyapunov function $V = x^T P x$, with $P = P^T > 0$ that satisfies the conditions of Proposition 7.6 exists for this example, with:

$$P = \begin{pmatrix} 0.5929 & -0.1022 \\ -0.1022 & 1.4391 \end{pmatrix}.$$

This matrix was found using the MATLAB LMI toolbox. Thus, the PWA map (7.36) has a unique attracting fixed point for all μ. The bifurcation diagram is given in Figure 7.2.

Example 7.3 Consider the three-dimensinal PWA map

$$x(k+1) = \begin{cases} Ax(k) + b\mu, & x_1(k) \leq 0 \\ Bx(k) + b\mu, & x_1(k) > 0 \end{cases} \tag{7.37}$$

where

$$A = \begin{pmatrix} 0.4192 & 0.3514 & 0.3473 \\ 0.2840 & -0.2733 & -0.3107 \\ 0.1852 & -0.2224 & -0.3974 \end{pmatrix},$$

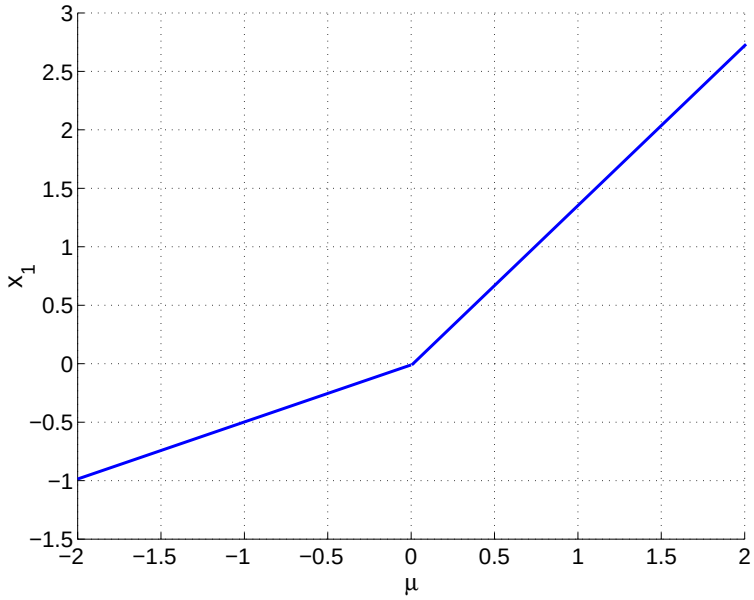

Figure 7.2: Bifurcation diagram for Example 7.2. Each solid line represents a path of stable fixed points.

$$B = \begin{pmatrix} -0.60 & 0.3514 & 0.3473 \\ 0.56 & -0.2733 & -0.3107 \\ -0.90 & -0.2224 & -0.3974 \end{pmatrix} \text{ and } b = \begin{pmatrix} 1 \\ 0 \\ 0 \end{pmatrix}.$$

The eigenvalues of A and B are $\sigma(A) = \{0.5653, -0.7413, -0.0755\}$ and $\sigma(B) = \{0.0395, -0.6551 \pm j\ 0.4246\}$, respectively. Although both A and B are Schur stable matrices, we cannot conclude that no bifurcation for (7.37) occurs at $\mu = 0$.

A common quadratic Lyapunov function $V = x^T P x$, with $P = P^T > 0$ that satisfies the conditions of Proposition 7.6 exists for this example. To wit:

$$P = \begin{pmatrix} 1.6304 & 0.1559 & -0.1313 \\ 0.1559 & 1.3200 & 0.4436 \\ -0.1313 & 0.4436 & 1.3266 \end{pmatrix}$$

is found using the MATLAB LMI toolbox. Thus, the PWA map (7.37) has a unique attracting fixed point for all μ. Figure 7.3 depicts the bifurcation diagram for the three state variables of this system.

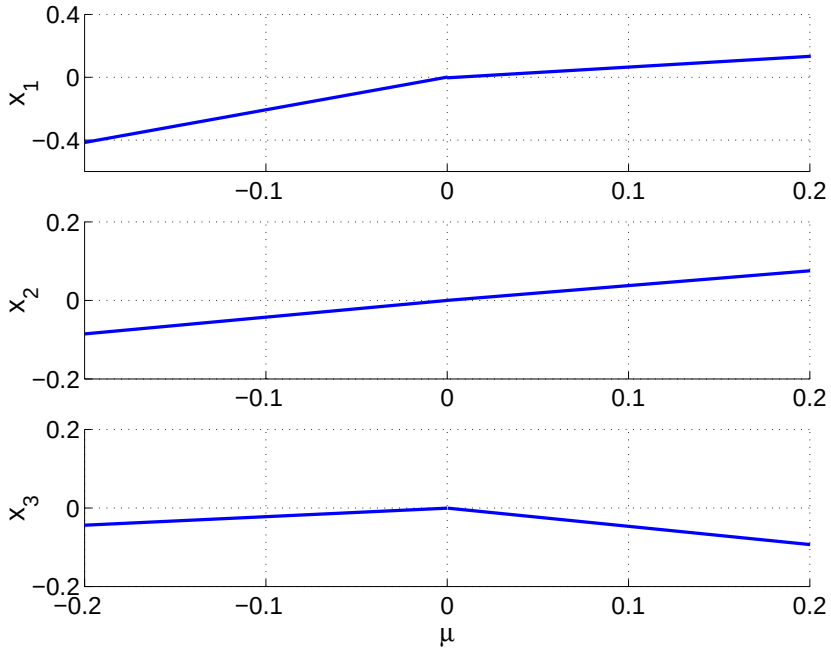

Figure 7.3: Bifurcation diagram for Example 7.3. Each solid line represents a path of stable fixed points.

7.3 Lyapunov-Based Feedback Control Design

In this section, we use the results of Section 7.2 in the design of stabilizing feedback control laws. We emphasize that (as was discussed in Chapter 6) for our approach to apply, the control action should not introduce discontinuity in the map. This is because, as summarized in Chapter 2, the definition of BCBs requires that the system map be continuous at the border, and thus our results on nonbifurcation with persistent

stability also apply only under this condition. Therefore, to maintain continuity of the map after control is applied, we assume that the input vectors on both sides of the border are equal. In this work, the input vectors are taken to be equal to b (the derivative of the map with respect to the bifurcation parameter.)

Simultaneous feedback control is considered first, followed by switched feedback control design.

7.3.1 Simultaneous Feedback Control Design

In this control method, the same control is applied on both sides of the border. The purpose of pursuing stabilizing feedback acting on both sides of the border is to ensure robustness with respect to modeling uncertainty. Moreover, transformation to the normal form is not required when simultaneous control is used. All that is needed is a good estimate of the Jacobian matrices on both sides of the border.

Consider the closed-loop system using static linear state feedback

$$x(k+1) = \begin{cases} Ax(k)+b\mu+bu(k), & \text{if } x_1(k) \leq 0 \\ Bx(k)+b\mu+bu(k), & \text{if } x_1(k) > 0 \end{cases} \tag{7.38}$$

$$u(k) = gx(k) \tag{7.39}$$

where g is the control gain (row) vector.

The following proposition gives stabilizability condition for the border collision bifurcation with this type of control policy.

Proposition 7.8 *If there exist a $P = P^T > 0$, and a feedback gain (row) vector g such that*

$$P-(A+bg)^T P(A+bg) > 0 \tag{7.40}$$

$$P-(B+bg)^T P(B+bg) > 0 \tag{7.41}$$

then any border collision bifurcation that occurs in the open-loop system ($u \equiv 0$) of (7.38) can be eliminated using simultaneous feedback (7.39) and persistent stability is guaranteed using simultaneous feedback (7.39). Equivalently, if there exist a Q and y such that

$$\begin{pmatrix} Q & AQ+by \\ (AQ+by)^T & Q \end{pmatrix} > 0, \tag{7.42}$$

$$\begin{pmatrix} Q & BQ+by \\ (BQ+by)^T & Q \end{pmatrix} > 0, \tag{7.43}$$

then any border collision bifurcation that occurs in (7.38) can be eliminated using simultaneous feedback (7.39). Here $Q = P^{-1}$ and the feedback gain is given by $g = yP$.

Proof: The closed-loop system is given by

$$x(k+1) = \begin{cases} (A+bg)x(k)+\mu b, & \text{if } x_1(k) \le 0 \\ (B+bg)x(k)+\mu b, & \text{if } x_1(k) > 0 \end{cases} \tag{7.44}$$

Using Proposition 7.6, a sufficient condition to eliminate the BCB is the existence of a $P = P^T > 0$ such that

$$P-(A+bg)^T P(A+bg) > 0 \tag{7.45}$$

$$P-(B+bg)^T P(B+bg) > 0 \tag{7.46}$$

where g is the control gain to be chosen.

Next, we show that (7.45)-(7.46) are equivalent to (7.42)-(7.43). Using Lemma 2.1 and Lemma 2.2, it is straightforward to show that

$$P-(A+bg)^T P(A+bg) > 0 \iff P^{-1}-(A+bg)P^{-1}(A+bg)^T > 0,$$

$$P-(B+bg)^T P(B+bg) > 0 \iff P^{-1}-(B+bg)P^{-1}(B+bg)^T > 0.$$

The nonlinear matrix inequalities above are transformed into LMIs using Lemma 2.2:

$$\begin{aligned} P^{-1}-(A+bg)P^{-1}(A+bg)^T &= P^{-1}-(A+bg)P^{-1}PP^{-1}(A+bg)^T \\ &= P^{-1}-(AP^{-1}+bgP^{-1})P(AP^{-1}+bgP^{-1})^T>0 \\ \iff & \begin{pmatrix} P^{-1} & AP^{-1}+by \\ (AP^{-1}+by)^T & P^{-1} \end{pmatrix} > 0 \end{aligned}$$

Similarly,

$$\begin{aligned} & P-(B+bg)^TP(B+bg) > 0 \\ \iff & \begin{pmatrix} P^{-1} & BP^{-1}+by \\ (BP^{-1}+by)^T & P^{-1} \end{pmatrix} > 0 \end{aligned}$$

by similar reasoning. ■

Below, we show that if a CQLF exists in one coordinate system, another CQLF exists in a different coordinate system arrived at using a simultaneous similarity transformation applied to both A and B.

Proposition 7.9 (CQLF and Similarity Transformations)

Suppose $V = x^TPx$ (with $P = P^T > 0$) is a common quadratic Lyapunov function for both of the matrices A and B (i.e., $A^TPA - P < 0$ and $B^TPB - P < 0$). Then $\tilde{V} = x^T\tilde{P}x$ with $\tilde{P} = (T^{-1})^TPT^{-1} = \tilde{P}^T > 0$ is a common quadratic Lyapunov function for $\tilde{A} = TAT^{-1}$ and $\tilde{B} = TBT^{-1}$ (i.e. $\tilde{A}^T\tilde{P}\tilde{A} - \tilde{P} < 0$ and $\tilde{B}^T\tilde{P}\tilde{B} - \tilde{P} < 0$). In other words, if a CQLF exists in one coordinate system, another CQLF exists if a simultaneous change of coordinates is applied to both A and B.

Proof: Since $V = x^TPx$ is a CQLF for both A and B, we have

$$A^TPA - P < 0, \tag{7.47}$$

and

$$B^TPB - P < 0. \tag{7.48}$$

Pre-multiply (7.47) by $(T^{-1})^T$ and post-multiply by T^{-1} yields

$$\begin{aligned} & (T^{-1})^T A^T P A T^{-1} - (T^{-1})^T P T^{-1} < 0 \\ \iff \quad & \underbrace{(T^{-1})^T A^T T^T}_{\tilde{A}^T} \underbrace{(T^{-1})^T P T^{-1}}_{\tilde{P}} \underbrace{T A T^{-1}}_{\tilde{A}} - \underbrace{(T^{-1})^T P T^{-1}}_{\tilde{P}} < 0, \quad (7.49) \end{aligned}$$

Similarly, pre-multiply (7.48) by $(T^{-1})^T$ and post-multiply by T^{-1} yields

$$\begin{aligned} & (T^{-1})^T B^T P B T^{-1} - (T^{-1})^T P T^{-1} < 0 \\ \iff \quad & \underbrace{(T^{-1})^T B^T T^T}_{\tilde{B}^T} \underbrace{(T^{-1})^T P T^{-1}}_{\tilde{P}} \underbrace{T B T^{-1}}_{\tilde{B}} - \underbrace{(T^{-1})^T P T^{-1}}_{\tilde{P}} < 0. \quad (7.50) \end{aligned}$$

Thus, $\tilde{V} = x^T \tilde{P} x$ is a CQLF for both $\tilde{A}$ and $\tilde{B}$, which completes the proof. ■

Remark 7.3 *The switched control design presented above does not depend on the border separating the two regions of smooth behavior. Thus, transformation to the normal form is not required before the control design.*

7.3.2 Switched Feedback Control Design

Consider the closed-loop system using static piecewise linear state feedback

$$f_\mu(x(k)) = \begin{cases} Ax(k) + b\mu + bu(k), & \text{if } x_1(k) \leq 0 \\ Bx(k) + b\mu + bu(k), & \text{if } x_1(k) > 0 \end{cases} \tag{7.51}$$

where

$$u(k) = \begin{cases} g_1 x(k), & x_1(k) \leq 0 \\ g_2 x(k), & x_1(k) > 0 \end{cases} \tag{7.52}$$

with the restriction that g_1 and g_2 may only differ in their first component, i.e., $g_{1i} = g_{2i}$, $i = 2, 3, \cdots, n$. This condition is imposed to maintain continuity along the border $\{x : x_1 = 0\}$.

Proposition 7.10 *If there exist a $P = P^T > 0$, and feedback gains g_1 and g_2 with $g_{1i} = g_{2i}$, $i = 2,3,\cdots,n$ such that*

$$P - (A+bg_1)^T P(A+bg_1) \;>\; 0 \tag{7.53}$$

$$P - (B+bg_2)^T P(B+bg_2) \;>\; 0 \tag{7.54}$$

then any border collision bifurcation that occurs in the open-loop system ($u \equiv 0$) of (7.51) can be eliminated using switched feedback (7.52). Equivalently, if there exist a Q, y_1 and $\alpha \in \mathbb{R}$ such that

$$\begin{pmatrix} Q & AQ+by_1 \\ (AQ+by_1)^T & Q \end{pmatrix} > 0, \tag{7.55}$$

$$\begin{pmatrix} Q & BQ+by_1 \\ (BQ+by_1)^T & Q \end{pmatrix} - \alpha \begin{pmatrix} 0 & b(e^1)^T Q \\ Qe^1 b^T & 0 \end{pmatrix} > 0. \tag{7.56}$$

then any border collision bifurcation that occurs in (7.51) can be eliminated using switched feedback (7.52). Here, $Q = P^{-1}$ and the feedback gains are given by $g_1 = y_1 P$ and $g_2 = g_1 - \alpha(e^1)^T$.

Proof: The closed-loop system is given by

$$x(k+1) = \begin{cases} (A+bg_1)x(k) + \mu b, & \text{if } x_1(k) \le 0 \\ (B+bg_2)x(k) + \mu b, & \text{if } x_1(k) > 0 \end{cases} \tag{7.57}$$

Using Proposition 7.6, a sufficient condition to eliminate the BCB is the existence of a $P = P^T > 0$ such that

$$P - (A+bg_1)^T P(A+bg_1) \;>\; 0 \tag{7.58}$$

$$P - (B+bg_2)^T P(B+bg_2) \;>\; 0 \tag{7.59}$$

where g_1, g_2 are the control gains to be chosen. Inequalities (7.58),(7.59) are equivalent to

$$\begin{pmatrix} Q & AQ+by_1 \\ (AQ+by_1)^T & Q \end{pmatrix} > 0 \tag{7.60}$$

$$\begin{pmatrix} Q & BQ+by_2 \\ (BQ+by_2)^T & Q \end{pmatrix} > 0 \tag{7.61}$$

respectively, where $Q = P^{-1}$, $g_1 = y_1 P$ and $g_2 = y_2 P$. This equivalence can be shown using similar reasoning as that in the proof of Proposition 7.8.

But, $g_{1i} = g_{2i}$, $i = 2, 3, \cdots, n$. This restriction on g_1 and g_2 can be written as

$$g_2 = g_1 - \alpha(e^1)^T \tag{7.62}$$

where $\alpha \in \mathbb{R}$. Therefore,

$$\begin{aligned} y_1 - y_2 &= g_1 Q - g_2 Q \\ &= (g_1 - g_2)Q \\ &= \alpha(e^1)^T Q \end{aligned} \tag{7.63}$$

Substituting $y_2 = y_1 - \alpha(e^1)^T Q$ in (7.61) yields (7.56). This completes the proof. ■

Note that if $\alpha = 0$ in (7.56), then the switched feedback control (7.52) becomes simultaneous control.

Remark 7.4 *We remark that switched control design (with no restriction on feedback gains) was used in [57] for stabilization of the origin of discrete time switched systems. No bifurcation control was considered in the referenced work.*

7.3.3 Numerical Examples

In this subsection, we present numerical examples to demonstrate the feedback control methods of the previous section.

Example 7.4 (Fixed point attractor bifurcating to instantaneous chaos)
Consider the three-dimensional PWA map

$$x(k+1) = \begin{cases} Ax(k)+b\mu, & x_1(k) \leq 0 \\ Bx(k)+b\mu, & x_1(k) > 0 \end{cases} \tag{7.64}$$

where

$$A = \begin{pmatrix} 0.0334 & 1.7874 & -0.1705 \\ -0.4588 & -0.4430 & -0.8282 \\ 0.0474 & -0.0416 & 0.8000 \end{pmatrix},$$

$$B = \begin{pmatrix} 0.8384 & 1.7874 & -0.1705 \\ -0.8180 & -0.4430 & -0.8282 \\ 0.6602 & -0.0416 & 0.8000 \end{pmatrix} \text{ and } b = \begin{pmatrix} 1 \\ 0 \\ 0 \end{pmatrix}.$$

The eigenvalues of A and B are $\sigma(A) = \{0.766, -0.1878 \pm j\ 0.8389\}$ and $\sigma(B) = \{-0.1157, 0.6555 \pm j\ 1.0987\}$, respectively. Note that A is Schur stable, but B is unstable. Simulation results show that (7.64) undergoes a border collision bifurcation from a fixed point attractor to instantaneous chaos at $\mu = 0$ (see Figure 7.4).

Feedback control design: Using the results of Proposition 7.8, a symmetric and positive definite matrix Q and a feedback control gain vector g that satisfy the LMIs (7.42)-(7.43) are sought. The following solution to (7.42)-(7.43) is obtained using the MAT-

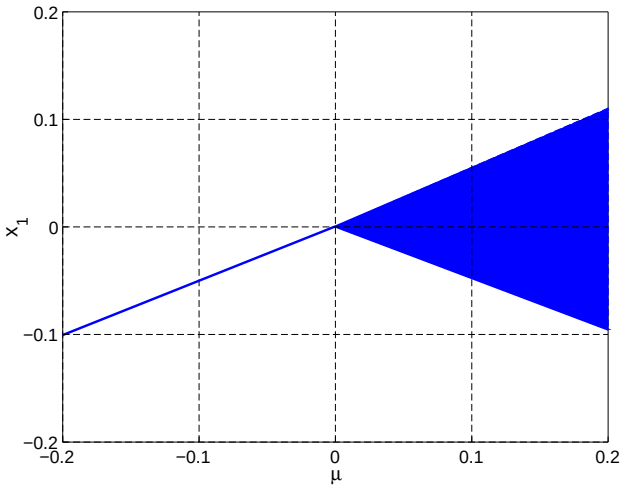

Figure 7.4: Bifurcation diagram for Example 7.4. The solid line represents a path of stable fixed points and the shaded region represents a one piece chaotic attractor growing out of the fixed point at $\mu = 0$.

LAB LMI toolbox:

$$Q = \begin{pmatrix} 0.4753 & -0.0428 & -0.1694 \\ -0.0428 & 0.8821 & -0.1647 \\ -0.1694 & -0.1647 & 0.5041 \end{pmatrix}, \tag{7.65}$$

$$y = \begin{pmatrix} -0.1601 & -1.4937 & 0.3356 \end{pmatrix}, \tag{7.66}$$

$$\begin{aligned} g &= yQ^{-1} \\ &= \begin{pmatrix} -0.5193 & -1.7324 & -0.0747 \end{pmatrix}. \end{aligned} \tag{7.67}$$

The closed-loop matrices are given by

$$\begin{aligned} A_c &= A + bg \\ &= \begin{pmatrix} -0.4859 & 0.0550 & -0.2452 \\ -0.4588 & -0.4430 & -0.8282 \\ 0.0474 & -0.0416 & 0.8000 \end{pmatrix}, \end{aligned}$$

$$
\begin{aligned}
B_c &= B + bg \\
&= \begin{pmatrix} 0.3191 & 0.0550 & -0.2452 \\ -0.8180 & -0.4430 & -0.8282 \\ 0.6602 & -0.0416 & 0.8000 \end{pmatrix}.
\end{aligned}
$$

Their eigenvalues are:

$\sigma(A_c) = \{0.8141, -0.4715 \pm j\, 0.1409\}$ and $\sigma(B_c) = \{-0.4507, 0.5634 \pm j\, 0.3498\}$.

The bifurcation diagram of the closed-loop system is depicted in Figure 7.5.

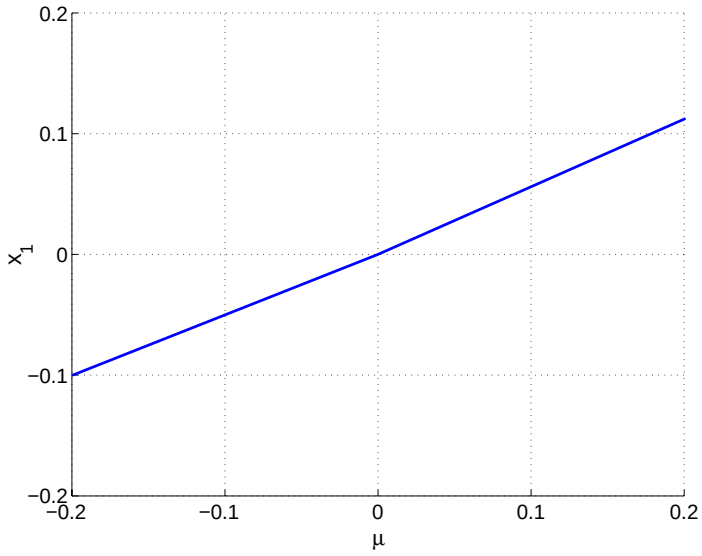

Figure 7.5: Bifurcation diagram for Example 7.4 with simultaneous feedback control $u(k) = gx(k)$. The solid lines represent a path of stable fixed points.

Example 7.5 (Saddle-node border collision bifurcation)

Consider the three-dimensional PWA map

$$
x(k+1) = \begin{cases} Ax(k) + b\mu, & x_1(k) \leq 0 \\ Bx(k) + b\mu, & x_1(k) > 0 \end{cases} \tag{7.68}
$$

where

$$A = \begin{pmatrix} 0.0350 & -0.2280 & -0.9385 \\ -0.3123 & -0.0029 & 0.9191 \\ -0.3825 & -0.5107 & 0.5553 \end{pmatrix},$$

$$B = \begin{pmatrix} 3.3000 & -0.2280 & -0.9385 \\ -0.6299 & -0.0029 & 0.9191 \\ 0.3705 & -0.5107 & 0.5553 \end{pmatrix} \text{ and } b = \begin{pmatrix} 1 \\ 0 \\ 0 \end{pmatrix}.$$

The eigenvalues of A and B are $\sigma(A) = \{-0.2921, 0.4397 \pm j\ 0.3470\}$ and $\sigma(B) = \{3.1739, 0.3392 \pm j\ 0.4756\}$, respectively. Note that A is Schur stable, but B is unstable. Simulation results show that (7.68) undergoes a saddle node border collision bifurcation where a stable and an unstable fixed point collide and disappear as μ is increased through zero (see Figure 7.6).

Feedback control design: We note that a simultaneous stabilizing feedback control based on Proposition 7.8 does not exist for this example. Therefore, we seek a stabilizing control using Proposition 7.10. Using the LMI toolbox in MATLAB, a symmetric and positive definite matrix Q and a feedback control gain vectors g_1 and g_2 that satisfy the LMIs (7.55)-(7.56) are obtained:

$$\alpha = 3.0972 \tag{7.69}$$

$$Q = \begin{pmatrix} 25.3606 & 4.5507 & 7.9810 \\ 4.5507 & 43.0961 & 9.8713 \\ 7.9810 & 9.8713 & 30.8840 \end{pmatrix}, \tag{7.70}$$

$$y_1 = \begin{pmatrix} 5.7709 & 14.8260 & 34.4887 \end{pmatrix}, \tag{7.71}$$

$$g_1 = y_1 Q^{-1}$$

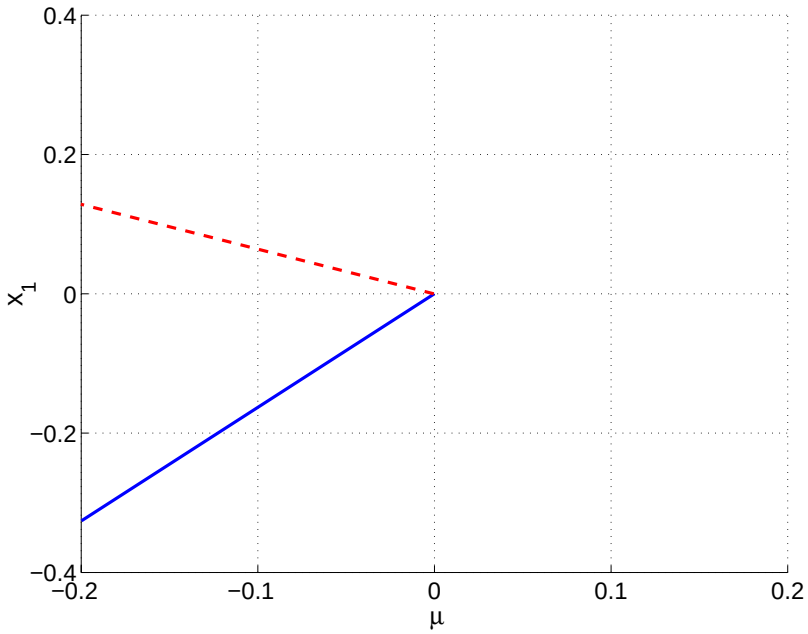

Figure 7.6: Bifurcation diagram for Example 7.5 without control. The solid line represents a path of stable fixed points and the dashed line represents a path of unstable fixed points.

$$= \begin{pmatrix} -0.1436 & 0.1024 & 1.1211 \end{pmatrix}, \tag{7.72}$$

$$g_2 = g_1 - \alpha(e^1)^T$$

$$= \begin{pmatrix} -3.2408 & 0.1024 & 1.1211 \end{pmatrix}. \tag{7.73}$$

The closed-loop matrices are given by

$$A_c = A + bg_1$$

$$= \begin{pmatrix} -0.1086 & -0.1256 & 0.1826 \\ -0.3123 & -0.0029 & 0.9191 \\ -0.3825 & -0.5107 & 0.5553 \end{pmatrix},$$

$$B_c = B + bg_2$$

$$= \begin{pmatrix} 0.0592 & -0.1256 & 0.1826 \\ -0.6299 & -0.0029 & 0.9191 \\ 0.3705 & -0.5107 & 0.5553 \end{pmatrix}.$$

Their eigenvalues are:

$\sigma(A_c) = \{0.0011, 0.2213 \pm j\ 0.6236\}$ and $\sigma(B_c) = \{-0.0002, 0.3059 \pm j\ 0.5102\}$.

The bifurcation diagram of the closed-loop system is depicted in Figure 7.7.

7.3.4 Washout Filter-Aided Feedback Control Design

In this section, washout filter-aided feedback control is used. As discussed in Section 2.1, washout filter-aided feedback has advantages over static feedback in that it maintains the fixed points of the open loop system even in the presence of model uncertainty. Moreover, it provides automatic following of the fixed point to be stabilized which alleviates the need for providing an estimate of the unstable fixed point to the controller. This is particularly useful in situations where the system model is uncertain and/or cases where there is parameter drift.

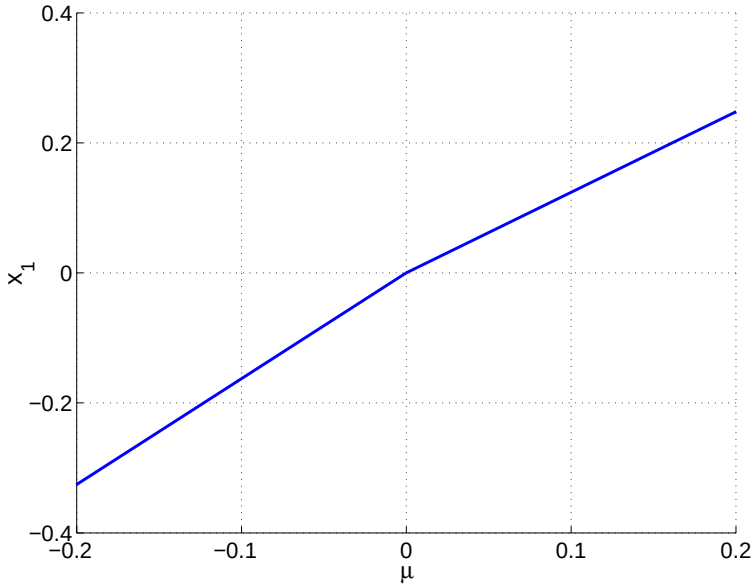

Figure 7.7: Bifurcation diagram for Example 7.5 with switched feedback control $u(k)$ as in (7.52) . The solid line represents a path of stable fixed points.

Using simultaneous washout filter-aided feedback control applied to (7.12) leads to the closed-loop system

$$x(k+1) = \begin{cases} Ax(k)+\mu b+bu(k), & \text{if } x(k)\in R_A \\ Bx(k)+\mu b+bu(k), & \text{if } x(k)\in R_B \end{cases} \tag{7.74}$$

$$w(k+1) = Dx(k)+(I-D)w(k) \tag{7.75}$$

$$u(k) = g(x(k)-w(k)) \tag{7.76}$$

where $D\in\mathbb{R}^{n\times n}$ is a nonsingular matrix such that $I-D$ is Schur stable, $g\in\mathbb{R}^{1\times n}$ is the control gain vector and $w\in\mathbb{R}^{n\times 1}$ is the washout filters' state vector. The closed-loop system can be written as

$$\begin{pmatrix} x(k+1) \\ w(k+1) \end{pmatrix} = \begin{cases} \begin{pmatrix} A+bg & -bg \\ D & I-D \end{pmatrix}\begin{pmatrix} x(k) \\ w(k) \end{pmatrix}+\begin{pmatrix} b \\ 0 \end{pmatrix}\mu, & \text{if } x(k)\in R_A \\ \begin{pmatrix} B+bg & -bg \\ D & I-D \end{pmatrix}\begin{pmatrix} x(k) \\ w(k) \end{pmatrix}+\begin{pmatrix} b \\ 0 \end{pmatrix}\mu, & \text{if } x(k)\in R_B \end{cases} \tag{7.77}$$

Now the question is: Are there g and D such that the closed-loop system of (7.77) is stabilized in the sense that a BCB that may occur in the open loop system is eliminated and local persistent stability produced?

Let $A_c = \begin{pmatrix} A+bg & -bg \\ D & I-D \end{pmatrix}$ and $B_c = \begin{pmatrix} B+bg & -bg \\ D & I-D \end{pmatrix}$. Consider the quadratic Lyapunov function candidate

$$V = z^T P z, \tag{7.78}$$

where $P \in \mathbb{R}^{2n\times 2n}$, with $P = P^T > 0$.

Proposition 7.11 *If there exist a $P = P^T > 0$, $g \in \mathbb{R}^{1\times n}$ and $D \in \mathbb{R}^{n\times n}$ such that*

$$A_c^T P A_c - P < 0 \tag{7.79}$$

$$B_c^T P B_c - P < 0 \tag{7.80}$$

then any border collision bifurcation that can occur in the open loop system (7.74) (with $u \equiv 0$) can be eliminated. The matrix inequalities (7.79)-(7.80) are equivalent to the bilinear matrix inequalities (BMIs)

$$\begin{pmatrix} P & A_c^T P \\ PA_c & P \end{pmatrix} > 0, \tag{7.81}$$

$$\begin{pmatrix} P & B_c^T P \\ PB_c & P \end{pmatrix} > 0. \tag{7.82}$$

Washout filter-aided feedback results in bilinear matrix inequalities. This is not surprising since washout filter-aided feedback is a form of output feedback and in general, Lyapunov-based output feedback control design results in matrix inequalities

that are bilinear. In recent years, there has been a growing interest in developing algorithms to solve BMIs (e.g., [68, 75])

The closed-loop system with washout filter-aided feedback can be written as an output feedback problem as follows:

$$\begin{pmatrix} x(k+1) \\ w(k+1) \end{pmatrix} = \begin{cases} \begin{pmatrix} A & 0 \\ D & I-D \\ B & 0 \\ D & I-D \end{pmatrix} \begin{pmatrix} x(k) \\ w(k) \\ x(k) \\ w(k) \end{pmatrix} + \begin{pmatrix} b \\ 0 \\ b \\ 0 \end{pmatrix} \mu + \begin{pmatrix} b \\ 0 \\ b \\ 0 \end{pmatrix} u(k), & x(k) \in R_A \\ \\ \begin{pmatrix} A & 0 \\ D & I-D \\ B & 0 \\ D & I-D \end{pmatrix} \begin{pmatrix} x(k) \\ w(k) \\ x(k) \\ w(k) \end{pmatrix} + \begin{pmatrix} b \\ 0 \\ b \\ 0 \end{pmatrix} \mu + \begin{pmatrix} b \\ 0 \\ b \\ 0 \end{pmatrix} u(k), & x(k) \in R_B \end{cases} \tag{7.83}$$

$$y(k) = (I \quad -I) \begin{pmatrix} x(k) \\ w(k) \end{pmatrix} \tag{7.84}$$

$$u(k) = gy(k) \tag{7.85}$$

Moreover, the closed-loop system can be also viewed as state feedback with gain matrix having a special structure

$$\tilde{x}(k+1) = \begin{cases} \tilde{A}\tilde{x}(k) + \tilde{b}\mu + B_u u(k), & x(k) \in R_A \\ \tilde{B}\tilde{x}(k) + \tilde{b}\mu + B_u u(k), & x(k) \in R_B \end{cases} \tag{7.86}$$

$$u(k) = G\tilde{x}(k) \tag{7.87}$$

where

$$\tilde{A} = \begin{pmatrix} A & 0 \\ 0 & 0 \end{pmatrix}, \tilde{B} = \begin{pmatrix} B & 0 \\ 0 & 0 \end{pmatrix}, \tilde{b} = \begin{pmatrix} b \\ 0 \end{pmatrix}, B_u = \begin{pmatrix} 0 & b \\ I & 0 \end{pmatrix} \text{ and}$$

$$G = \begin{pmatrix} D & I-D \\ g & -g \end{pmatrix}.$$

The problem of finding quadratic stabilizing controllers (controllers based on a quadratic Lyapunov function) has been recently addressed in [68], and some algorithms for solving the resulting BMIs were proposed.

As mentioned in Section 2.1, depending on the structure of the system to be controlled, sometimes the number of washout filters needed is smaller than the dimension of the system. In some cases, one or two washout filters suffice. In such a case, a stabilizing controller can be found (if one exists) numerically by performing a search over the control parameters (say γ, d). For fixed values of γ, d, the matrix inequalities are linear, and can therefore be solved using standard LMI solvers (see Section 8.2.3 for an example).

In this work, we leave the study of more general problems related to use of washout filter-aided feedback to future research.

7.4 Stability and Stabilization of Fixed Points at Criticality

In this section, stability and stabilization of fixed points at criticality of a switched discrete-time system are studied using Lyapunov-based techniques. We use results from the literature on stabilization of fixed point of a switched system [57].

Below, piecewise quadratic Lyapunov functions are used to develop less conservative sufficient conditions for asymptotic stability of fixed points at criticality than the ones developed in the previous sections using quadratic Lyapunov functions. However, the conditions derived in this section only consider the stability of the fixed point at criticality. The results provide no information on the type of border collision bifurcation that can occur in the system. Nonetheless, these results may be useful in situations where the sufficient condition for nonbifurcation with persistent stability derived in the previous sections is not satisfied. In such a case, the least one can do is to stabilize the fixed point at criticality. Numerical simulation can be used to study

the dynamics of the system with a parameter. We point out that since only stability and stabilization of fixed points at criticality are considered in this section, there is no restriction on the control gains or the input vectors as in previous sections.

7.4.1 Analysis of Stability at Criticality Using Piecewise Quadratic Lyapunov Functions

A piecewise smooth system at criticality can be approximated using a piecewise linear system of the form

$$x(k+1) = \begin{cases} A_1 x(k), & \text{if } x(k) \in R_1 \\ A_2 x(k), & \text{if } x(k) \in R_2 \end{cases} \tag{7.88}$$

where $x \in \mathbb{R}^n$, $A_i \in \mathbb{R}^{n\times n}$, $i = 1,2$ and $R_i \subset \mathbb{R}^n$, $i = 1,2$. Here, without loss of generality, we have considered only two regions in the state space. The results can be easily extended to the case where the state space is divided into m regions, where $m > 2$ and finite.

Consider the piecewise quadratic (PWQ) Lyapunov function candidate

$$V(x) = \begin{cases} x^T P_1 x, & x \in R_1 \\ x^T P_2 x, & x \in R_2 \end{cases} \tag{7.89}$$

where $P_1 = P_1^T > 0$ and $P_2 = P_2^T > 0$.

Proposition 7.12 *[57] The origin of (7.88) is asymptotically stable if there exists a PWQ Lyapunov function (7.89) such that the following matrix inequalities are satisfied:*

$$P_i > 0, \quad i = 1,2 \tag{7.90}$$

$$A_i^T P_j A_i - P_i < 0, \quad (i,j) \in \{(1,1),(1,2),(2,1),(2,2)\} \tag{7.91}$$

Proof: Assume $x(k) \in R_i$ and $x(k+1) \in R_j$, $i, j \in \{1,2\}$. Then

$$\begin{aligned} \Delta V(x(k)) &= x(k+1)^T P_j x(k+1) - x(k)^T P_i x(k) \\ &= x(k)^T (A_i^T P_j A_i - P_i) x(k) \end{aligned} \tag{7.92}$$

From (7.90) and (7.91) it follows that $V(x(k))$ is positive definite and ΔV is negative definite along the trajectories of the system. Thus, the origin of (7.88) is asymptotically stable. ■

7.4.2 Feedback Control Design

The results of the previous subsection are now used to develop stabilizing switched feedback controls. Using switched feedback control applied to (7.88) leads to the closed-loop system

$$x(k+1) = \begin{cases} A_1 x(k) + B_1 u(k), & \text{if } x(k) \in R_1 \\ A_2 x(k) + B_2 u(k), & \text{if } x(k) \in R_2 \end{cases} \tag{7.93}$$

$$u(k) = \begin{cases} G_1 x(k), & x(k) \in R_1 \\ G_2 x(k), & x(k) \in R_2 \end{cases} \tag{7.94}$$

where B_1 and B_2 are the input matrices (of appropriate dimensions) for the system in R_1 and R_2, respectively and G_1, G_2 are the control gains. In general, $B_1 \neq B_2$ and they depend on the available means of actuation for a given system.

Proposition 7.13 *[57] Suppose there exist $P_i = P_i^T > 0$ and G_i, $i = 1,2$ such that*

$$(A_j + B_j G_j)^T P_i (A_j + B_j G_j) - P_j < 0, \;\; (i,j) \in \{(1,1),(1,2),(2,1),(2,2)\} \tag{7.95}$$

Then the origin of the closed-loop system (7.93)-(7.94) is asymptotically stable. Equivalently, (7.93)-(7.94) is asymptotically stable, if there exist $Q_i = Q_i^T > 0$ *and* Y_i, $i = 1,2$ *such that*

$$\begin{pmatrix} Q_i & A_jQ_j + B_jY_j \\ (A_jQ_j + B_jY_j)^T & Q_j \end{pmatrix} > 0, \quad (i,j) \in \{(1,1),(1,2),(2,1),(2,2)\} \tag{7.96}$$

where $Q_i = P_i^{-1}$ *and* $Y_i = G_iP_i^{-1}$, $i = 1,2$.

Proof: The proof of (7.95) follows from the proof of Proposition 7.12 by replacing A_i with $A_i + B_iG_i$, $i = 1,2$. The equivalence between (7.95) and (7.96) follows by a straightforward application of the Schur complement.

7.5 Stability Analysis Using Nonmonotonically Decreasing Lyapunov Functions

Recently, Aeyels and Peuteman [5] reported a new sufficient condition for asymptotic stability of finite dimensional ordinary differential equations and finite dimensional difference equations. They showed that, unlike in the classical Lyapunov theory, a stability condition can be stated in which the time derivative (forward difference) of a Lyapunov function candidate along trajectories of the system may have positive and negative values [5]. We will show that this weaker condition on the forward difference of a Lyapunov function candidate can be used to derive less conservative sufficient conditions for asymptotic stability of fixed points at criticality of PWS discrete-time systems.

Consider the discrete-time system

$$x(k+1) \quad = \quad f(x(k)) \tag{7.97}$$

where $f : W \to \mathbb{R}^n$ is locally Lipschitz, where $W \subset \mathbb{R}^n$ is open. Let $f(0) = 0$ and $0 \in W$. Below, we recall the theorem from [5] stated here for time invariant systems.

Theorem 7.1 [5] *Consider a function $V : U \to \mathbb{R}$ with $U \subset W$ an open neighborhood of the origin. Assume:*

i) $V(x)$ is positive definite.

ii) There exists a finite $m \in Z$, $m > 0$ and an open set $U' \subset U$ that contains the origin such that $\forall x \in U' \setminus \{0\}$ and $\forall k \in Z$

$$V(x(k+m)) - V(x(k)) < 0$$

Then the equilibrium point $x = 0$ of (7.97) is asymptotically stable.

Definition 7.1 Define the *m*th step forward difference of a Lyapunov function V along trajectories of a discrete time system by

$$\Delta V_m = V(x(k+m)) - V(x(k))$$

where m is a positive integer.

Proposition 7.14 (Sufficient Conditions for Stability at Criticality Using Non-monotonically Decreasing Common Quadratic Lyapunov Function)

Consider the switched system (7.12) with $\mu = 0$ and a common quadratic Lyapunov function $V(x) = x^T Px$, with $P > 0$.

1) $\Delta V_1(x)$ is negative definite iff

$$A^T PA - P < 0 \tag{7.98}$$

$$B^T PB - P < 0 \tag{7.99}$$

2) $\Delta V_2(x)$ *is negative definite iff*

$$(A^2)^T PA^2 - P < 0 \tag{7.100}$$

$$A^T B^T PBA - P < 0 \tag{7.101}$$

$$B^T A^T PAB - P < 0 \tag{7.102}$$

$$(B^2)^T PB^2 - P < 0 \tag{7.103}$$

3) $\Delta V_3(x)$ *is negative definite iff*

$$(A^3)^T PA^3 - P < 0 \tag{7.104}$$

$$(A^2)^T B^T PBA^2 - P < 0 \tag{7.105}$$

$$A^T B^T A^T PABA - P < 0 \tag{7.106}$$

$$A^T (B^2)^T PB^2 A - P < 0 \tag{7.107}$$

$$B^T (A^2)^T PA^2 B - P < 0 \tag{7.108}$$

$$B^T A^T B^T PBAB - P < 0 \tag{7.109}$$

$$(B^2)^T A^T PAB^2 - P < 0 \tag{7.110}$$

$$(B^3)^T PB^3 - P < 0 \tag{7.111}$$

Moreover, the origin of (7.12) is asymptotically stable if $\Delta V_m < 0$*, for some* $m > 0$*.*

Proof: Follows by a straightforward application of Theorem 7.1.

It is easy to see that $\Delta V_m(x) < 0 \Longrightarrow \Delta V_q(x) < 0$ for $q > m$, while the converse does not hold.

The following example illustrates the use of Proposition 7.14.

Example 7.6 Consider the piecewise linear discrete-time system (7.12) with $\mu = 0$

and with A and B given by

$$A = \begin{pmatrix} 0.5 & 1 \\ -0.3 & 0 \end{pmatrix}, \quad B = \begin{pmatrix} -1 & 1 \\ -0.1 & 0 \end{pmatrix}$$

Note that the system is continuous at the border $x = 0$ but not differentiable. The eigenvalues of A are $\lambda_{A_{1,2}} = 0.2500 \pm j\ 0.4873$ and those of B are $\lambda_{B_1} = -0.8873$ and $\lambda_{B_2} = -0.1127$.

It can be checked (for example using the LMI package in MATLAB) that a common quadratic Lyapunov function that shows stability of the origin does not exist (i.e.,$\Delta V_1(x(k)) = V(x(k+1)) - V(x(k)) > 0$ for some values of $k > 0$). However, using Proposition 7.14 and the LMI solver in Matlab, it is shown that $\Delta V_2 = V(x(k+2)) - v(x(k)) < 0\ \forall k > 0$ with $V(x) = x^T P x$ and

$$P = \begin{pmatrix} 1.1479 & -0.3215 \\ -0.3215 & 5.0917 \end{pmatrix}.$$

Numerical studies show that for this example no bifurcation occurs in (7.12) as μ is varied through zero.

Proposition 7.15 (Sufficient Conditions for Stability at Criticality Using Non-monotonically Decreasing Piecewise Quadratic Lyapunov Function)

Consider the switched system (7.12) with $\mu = 0$ and the PWQ Lyapunov function candidate

$$V(x) = \begin{cases} x^T P_1 x, & x \in R_A \\ x^T P_2 x, & x \in R_B \end{cases}$$

with $P_1 > 0$ and $P_2 > 0$.

1) $\Delta V_1(x)$ is negative definite iff

$$A_1^T P_1 A_1 - P_1 \ < \ 0 \tag{7.112}$$

$$A_1^T P_2 A_1 - P_1 < 0 \tag{7.113}$$

$$A_2^T P_1 A_2 - P_2 < 0 \tag{7.114}$$

$$A_2^T P_1 A_2 - P_2 < 0 \tag{7.115}$$

2) $\Delta V_2(x)$ *is negative definite iff*

$$(A_1^2)^T P_1 A_1^2 - P_1 < 0 \tag{7.116}$$

$$(A_1^2)^T P_2 A_1^2 - P_1 < 0 \tag{7.117}$$

$$(A_2 A1)^T P_1 A_2 A_1 - P_1 < 0 \tag{7.118}$$

$$(A_2 A1)^T P_2 A_2 A_1 - P_1 < 0 \tag{7.119}$$

$$(A_2^2)^T P_2 A_2^2 - P_2 < 0 \tag{7.120}$$

$$(A_2^2)^T P_1 A_2^2 - P_2 < 0 \tag{7.121}$$

$$(A_1 A2)^T P_2 A_1 A_2 - P_2 < 0 \tag{7.122}$$

$$(A_1 A2)^T P_1 A_1 A_2 - P_2 < 0 \tag{7.123}$$

Moreover, the origin of (7.12) is asymptotically stable if $\Delta V_m(x) < 0$*, for some* $m > 0$*.*

The following example illustrates the use of Proposition 7.15.

Example 7.7 *Consider the piecewise linear discrete-time system (7.12) with* $\mu = 0$ *and with A and B given by*

$$A = \begin{pmatrix} 0.5 & 1 \\ -0.3 & 0 \end{pmatrix}, \quad B = \begin{pmatrix} -1 & 1 \\ -0.27 & 0 \end{pmatrix}$$

The eigenvalues of A are $\lambda_{A_{1,2}} = 0.2500 \pm j\, 0.4873$ *and those of B are* $\lambda_{B_{1,2}} = -0.5000 \pm j\, 0.1414$*.*

It can be checked (for example using the LMI package in MATLAB) that a common quadratic Lyapunov function that shows stability of the origin does not exist

based on Proposition 7.14. Moreover, a PWQ Lyapunov function with negative one step forward difference does not exist. However, a PWQ Lyapunov function with $\Delta V_2(x(k)) = V(x(k+2)) - v(x(k))) < 0$ *exists and can be calculated using the LMI toolbox in MATLAB. A particular such Lyapunov function has*

$$P_1 = \begin{pmatrix} 1.3467 & 1.0642 \\ 1.0642 & 4.0967 \end{pmatrix}, \quad P_2 = \begin{pmatrix} 2.2299 & -1.2542 \\ -1.2542 & 2.7764 \end{pmatrix}.$$

Thus, using Proposition 7.15, we conclude that the origin of (7.12) is asymptotically stable.

Chapter 8

Quenching of Alternans in a Cardiac Conduction Model

The quenching of alternans exhibited as solutions of a cardiac conduction model is considered. The model consists of a nonlinear discrete-time piecewise smooth system, and was previously used to show a link between cardiac alternans and period doubling bifurcation. In this work, it is first shown that the model indeed admits a period doubling border collision bifurcation, and that it is this bifurcation that leads to the alternan solutions. No smooth period doubling bifurcation occurs in the parameter region of interest. Next, the results of the previous chapters on feedback control of border collision bifurcation are applied to the model, resulting in quenching of the period doubling border collision bifurcation and hence in alternan suppression.

8.1 Introduction

In this chapter, we revisit the cardiac conduction model proposed by Sun, Amellal, Glass and Billette [69] with two aims in mind. These aims relate first to a detailed analysis of the model, and second to control of the bifurcation as will be elaborated

below. The model is formulated as two dimensional piecewise smooth map. The model incorporates physiological concepts of recovery, facilitation and fatigue. It predicts a variety of experimentally observed complex rhythms of nodal conduction. In particular, alternans, in which there is an alternation in conduction time from beat to beat, were associated in [69] with a period-doubling bifurcation in the theoretical model.

As mentioned above, our first aim in this chapter is to perform a more detailed study of the instability or bifurcation mechanism that leads to alternan solutions. Second, we are interested in applying the control laws developed in this thesis for suppressing the alternans in the model. This work demonstrates that the instability mechanism giving rise to cardiac alternans is in fact not a smooth period doubling bifurcation as earlier hypothesized, but rather its nonsmooth cousin, the period doubling border collision bifurcation.

Several researchers studied the model of [69] and developed control techniques to eliminate the period-2 rhythm and stabilize the underlying period-1 rhythm (e.g., [17, 15, 16]). With the exception of [16], all the studies of this model reported in the literature viewed the border collision period doubling bifurcation in this system as if it were an ordinary period doubling bifurcation in a smooth dynamical system. In [16], the bifurcation in the cardiac model was identified as a border collision bifurcation based on numerical evidence. However, no analysis was given to prove this claim. The authors of [16] also investigated the feedback control of the BCB detected in the alternan model, but the feedback design was largely based on trial and error, and did not involve a detailed consideration of the border collision bifurcation. In [15], the authors propose the use of delayed linear feedback to suppress the period doubling bifurcation. In [17], the authors apply a technique for control of chaos to suppress the

alternation resulting from the period doubling bifurcation. In [26], a smooth one dimensional map was used as a model for cardiac conduction. A form of linear dynamic feedback where the unstable fixed point corresponding to the unstable rhythm is estimated as the average value of two consecutive beats was used to achieve alternan quenching [26]. The control gain was determined by trial and error.

In this work, the results on feedback control of border collision bifurcations developed in the previous chapters are used to quench the period doubling border collision bifurcation which consequently suppresses the alternans. The feedback can be either linear or piecewise linear. Both static and washout filter-aided feedbacks are considered. Washout filter-aided feedback has certain advantages over static feedback: it maintains the fixed points of the open-loop system even in the presence of model uncertainty, and it provides automatic following of the fixed point to be stabilized which alleviates the need for providing an estimate of the unstable fixed point to the controller. This is particularly useful in situations where the system model is uncertain and/or cases where there is parameter drift.

It is important to realize that, since border collision bifurcations arise at the border separating regions of smooth operation, a linear feedback that seems to "delay" a border collision bifurcation to occur away from the border actually does no such thing. If a BCB seems to have been delayed by feedback, what actually is happening is that the feedback has changed the BCB to a type that replaces the nominal fixed point by a new one (fixed point to fixed point BCB), and a new smooth bifurcation has been created elsewhere (away from the border). Thus, concepts and methods developed in the control of smooth bifurcations cannot be carried over in a direct way to the nonsmooth case.

8.2 The Cardiac Conduction Model

In this section, we consider a cardiac conduction model of [69]. The model incorporates physiological concepts of recovery, facilitation and fatigue. It is formulated as a two-dimensional PWS map. Two factors determine the atrioventricular (AV) nodal conduction time: the time interval from the atrial activation to the activation of the Bundle of His and the history of activation of the node. The model predicts a variety of experimentally observed complex rhythms of nodal conduction. In particular, alternans, in which there is an alternation in conduction time from beat to beat, are associated with period-doubling bifurcation in the theoretical model.

The authors first define the atrial His interval, A, to be that between cardiac impulse excitation of the lower interatrial septum and the Bundle of His. (See [69] for definitions.) The model is

$$\begin{pmatrix} A_{n+1} \\ R_{n+1} \end{pmatrix} = f(A_n, R_n, H_n)$$

where

$$f(A_n,R_n,H_n) = \begin{cases} \begin{pmatrix} A_{min}+R_{n+1}+(201-0.7A_n)e^{-H_n/\tau_{rec}} \\ R_n e^{-(A_n+H_n)/\tau_{fat}}+\gamma e^{-H_n/\tau_{fat}} \end{pmatrix}, & \text{for } A_n \le 130 \\ \begin{pmatrix} A_{min}+R_{n+1}+(500-3.0A_n)e^{-H_n/\tau_{rec}} \\ R_n e^{-(A_n+H_n)/\tau_{fat}}+\gamma e^{-H_n/\tau_{fat}} \end{pmatrix}, & \text{for } A_n > 130 \end{cases} \tag{8.1}$$

with $R_0 = \gamma exp(-H_0/\tau_{fat})$. Here H_0 is the initial H interval and the parameters A_{min}, τ_{fat}, γ and τ_{rec} are positive constants. The variable H_n represents the interval between bundle of His activation and the subsequent activation (the AV nodal recovery time) and is usually taken as the bifurcation parameter. The variable R_n represents a drift in the nodal conduction time, and is sometimes taken to be constant. In this work, we

consider R_n as a variable as in [69]. Note that the map f is piecewise smooth and is continuous at the border $A_b := 130$ms.

8.2.1 Analysis of the Border Collision Bifurcation

Numerical simulations indicate that the map (8.1) undergoes (some type of) supercritical period doubling bifurcation as the bifurcation parameter $S := H_n$ is decreased through a critical value (see Figures 8.1-8.2). We show that this bifurcation is in fact a supercritical period doubling BCB which occurs when the fixed point of the map hits the border $A_b = 130$.

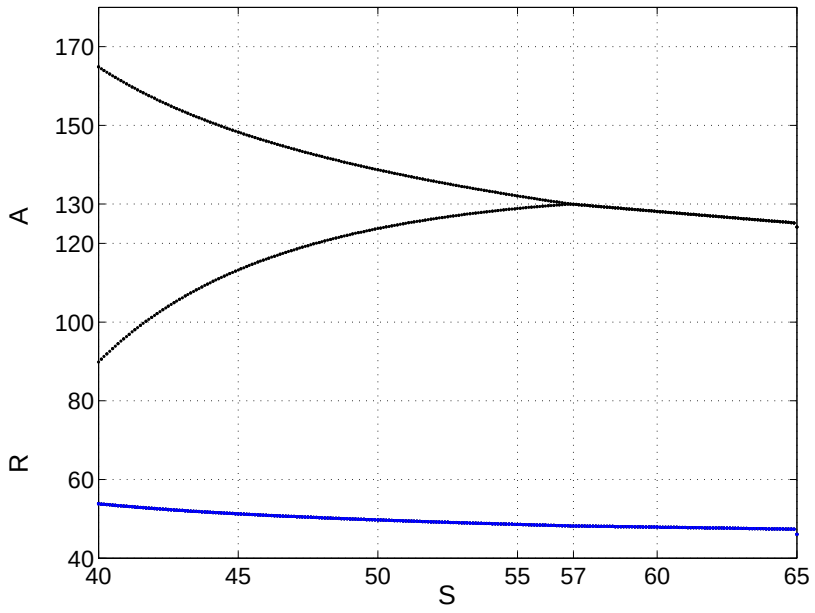

Figure 8.1: Joint bifurcation diagram for A_n and for R_n for (8.1) with S as bifurcation parameter and $\tau_{rec} = 70$ms, $\tau_{fat} = 30000$ms, $A_{min} = 33$ms and $\gamma = 0.3$ms.

Let the fixed points of the map (8.1) be given by $(A^*_-(S), R^*_-(S))$ for $A_n < A_b$ and $(A^*_+(S), R^*_+(S))$ for $A_n > A_b$. Under normal conditions, the fixed point $(A^*_-(S), R^*_-(S))$ is stable and it loses stability as S is decreased through a critical value $S = S_b$ where

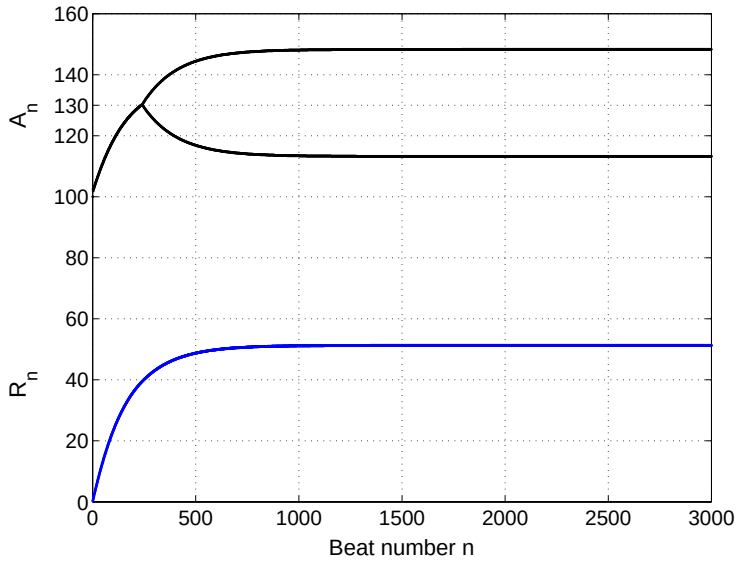

Figure 8.2: Iterations of map showing the alternation in A_n as a result of period doubling bifurcation. The parameter values are: $\tau_{rec} = 70$ms, $\tau_{fat} = 30000$ms, $A_{min} = 33$ms, $\gamma = 0.3$ms and $S = 45$ms.

$A^*_- = A_b$. Denote by R_b the value of R^*_- at criticality ($S = S_b$).

Next, we calculate the limiting Jacobian matrices on both sides of the border:

$$J_L = \begin{pmatrix} -0.7e^{\frac{-S_b}{\tau_{rec}}} - \frac{R_b}{\tau_{fat}} e^{\frac{-(130+S_b)}{\tau_{fat}}} & e^{\frac{-(130+S_b)}{\tau_{fat}}} \\ -\frac{R_b}{\tau_{fat}} e^{\frac{-(130+S_b)}{\tau_{fat}}} & e^{\frac{-(130+S_b)}{\tau_{fat}}} \end{pmatrix} \tag{8.2}$$

and

$$J_R = \begin{pmatrix} -3.0e^{\frac{-S_b}{\tau_{rec}}} - \frac{R_b}{\tau_{fat}} e^{\frac{-(130+S_b)}{\tau_{fat}}} & e^{\frac{-(130+S_b)}{\tau_{fat}}} \\ -\frac{R_b}{\tau_{fat}} e^{\frac{-(130+S_b)}{\tau_{fat}}} & e^{\frac{-(130+S_b)}{\tau_{fat}}} \end{pmatrix} \tag{8.3}$$

Also, the derivative of f with respect to S at (A_b, R_b, S_b) is

$$\begin{pmatrix} b_1 \\ b_2 \end{pmatrix} = \begin{pmatrix} -\frac{110}{\tau_{rec}} e^{\frac{-S_b}{\tau_{rec}}} - \frac{\gamma}{\tau_{fat}} e^{\frac{-S_b}{\tau_{fat}}} - \frac{R_b}{\tau_{fat}} e^{\frac{-(130+S_b)}{\tau_{fat}}} \\ -\frac{\gamma}{\tau_{fat}} e^{\frac{-S_b}{\tau_{fat}}} - \frac{R_b}{\tau_{fat}} e^{\frac{-(130+S_b)}{\tau_{fat}}} \end{pmatrix} \tag{8.4}$$

Next, the following parameter values are assumed (borrowed from [69]): $\tau_{rec} =$ 70ms, $\tau_{fat} = 30000$ms, $A_{min} = 33$ms, $\gamma = 0.3$ms. For these parameter values, $S_b =$ 56.9078ms, $R_b = 48.2108$ms and

$$J_L = \begin{pmatrix} -0.31208 & 0.99379 \\ -0.001597 & 0.99379 \end{pmatrix}, \quad J_R = \begin{pmatrix} -1.33223 & 0.99379 \\ -0.001597 & 0.99379 \end{pmatrix}$$

and $$\begin{pmatrix} b_1 \\ b_2 \end{pmatrix} = \begin{pmatrix} -0.69861 \\ -0.001607 \end{pmatrix}.$$

The eigenvalues of J_L are $\lambda_{L1} = -0.3109$, $\lambda_{L2} = 0.9926$ ($\tau_L = 0.6817$, $\delta_L = -0.3086$) and those of J_R are $\lambda_{R1} = -1.3315$, $\lambda_{R2} = 0.9931$ ($\tau_R = -0.3384$ and $\delta_R = -1.3224$). Note that there is a discontinuous jump in the eigenvalues of the Jacobian matrix when the fixed point hits the border at the critical parameter values $S = S_b$. The occurrence of a border collision bifurcation at S_b is now ascertained by applying Theorem 2.1. The fixed point attractor for $S < S_b$ becomes unstable for $S > S_b$ and a period-2 solution is born. The stability of the period-2 orbit with one point in $\{(A,R) \in \mathbb{R}^2 : A \leq 130\}$ and the other point in $\{(A,R) \in \mathbb{R}^2 : A > 130\}$ is determined by looking at the eigenvalues of $J_{LR} := J_L J_R$. These eigenvalues are $\lambda_{LR_1} = 0.4135$ and $\lambda_{LR_2} = 0.9867$. This implies that a stable period-2 orbit is born after the border collision. The supercritical period doubling BCB is shown in the bifurcation diagram in Figure 8.1. In the figure, the bifurcated solution departs in a nonsmooth way from the nominal fixed point branch.

8.2.2 Static Feedback Control of the Period Doubling BCB

In past studies of control of the cardiac conduction model considered here, the control is usually applied as a perturbation to the bifurcation parameter (the nodal recovery

time) S [17, 16]. The state A_n has been used in the feedback loop by other researchers who developed control laws for this model (e.g., [15, 16]). We use the same measured signal in our feedback design. Below, the control methods of Chapter 6 are used to quench the period doubling bifurcation, replacing the period doubled orbit by a stable fixed point. First, feedback applied on the unstable side is considered followed by simultaneous control.

Feedback applied on unstable side

Applying linear state feedback on the unstable side only ($A_n > 130$) as a perturbation to the bifurcation parameter S yields the closed loop system

$$\begin{pmatrix} A_{n+1} \\ R_{n+1} \end{pmatrix} = \begin{cases} \begin{pmatrix} A_{min} + R_{n+1} + (201 - 0.7A_n)e^{-S/\tau_{rec}} \\ R_n e^{-(A_n+S)/\tau_{fat}} + \gamma e^{-S/\tau_{fat}} \end{pmatrix}, & \text{for } A_n \leq 130 \\ \begin{pmatrix} A_{min} + R_{n+1} + (500 - 3.0A_n)e^{-(S+u_n)/\tau_{rec}} \\ R_n e^{-(A_n+(S+u_n))/\tau_{fat}} + \gamma e^{-(S+u_n)/\tau_{fat}} \end{pmatrix}, & \text{for } A_n > 130 \end{cases} \tag{8.5}$$

$$u_n = (\gamma_1 \ \gamma_2) \begin{pmatrix} A_n - A_b \\ R_n - R_b \end{pmatrix} = \gamma_1(A_n - A_b) + \gamma_2(R_n - R_b) \tag{8.6}$$

For the assumed parameter values, the Jacobians of the closed loop system for $A_n \leq 130$ and $A_n > 130$ are

$$\tilde{J_L} = J_L = \begin{pmatrix} -0.31208 & 0.99379 \\ -0.001597 & 0.99379 \end{pmatrix},$$

and

$$\tilde{J_R} = \begin{pmatrix} -1.33223 - 0.69860\gamma_1 & 0.99379 - 0.69860\gamma_2 \\ -0.001597 - 0.001607\gamma_1 & 0.99379 - 0.001607\gamma_2 \end{pmatrix}$$

$$= \underbrace{\begin{pmatrix} -1.33223 & 0.99379 \\ -0.001597 & 0.99379 \end{pmatrix}}_{J_R} + \underbrace{\begin{pmatrix} -0.69860 \\ -0.001607 \end{pmatrix}}_{\mathbf{b}} \begin{pmatrix} \gamma_1 & \gamma_2 \end{pmatrix}$$

respectively. Now, we seek $\gamma_1, \gamma_2 \equiv 0$ such that the eigenvalues of the linearizations of the closed-loop system satisfy Proposition 5.3. It is straightforward to verify that $(\gamma_1, \gamma_2) = (-1, 0)$ is stabilizing. Figure 8.3 shows the bifurcation diagram of the controlled system with $(\gamma_1, \gamma_2) = (-1, 0)$. Note that by setting $\gamma_2 = 0$, only A_n is used in the feedback. In practice, the conduction time of the nth beat A_n, can be measured and it has been used in the feedback loop by other researchers who developed control laws for this model (e.g., [15, 16]).

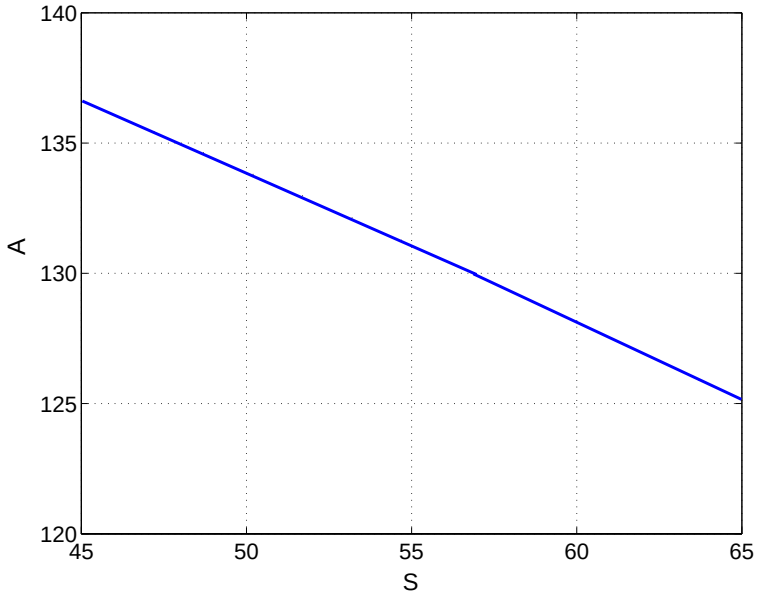

Figure 8.3: Bifurcation diagram of controlled system using linear state feedback applied on unstable region ($A_n > 130$) with control gains$(\gamma_1, \gamma_2) = (-1, 0)$.

Simultaneous feedback control

Applying the same linear state feedback on both sides of the border as a perturbation to the bifurcation parameter yields the closed loop system

$$\begin{pmatrix} A_{n+1} \\ R_{n+1} \end{pmatrix} = \begin{cases} \begin{pmatrix} A_{min} + R_{n+1} + (201 - 0.7A_n)e^{-(S+u_n)/\tau_{rec}} \\ R_n e^{-(A_n+(S+u_n))/\tau_{fat}} + \gamma e^{-(S+u_n)/\tau_{fat}} \end{pmatrix}, & \text{for } A_n \leq 130 \\ \begin{pmatrix} A_{min} + R_{n+1} + (500 - 3.0A_n)e^{-(S+u_n)/\tau_{rec}} \\ R_n e^{-(A_n+(S+u_n))/\tau_{fat}} + \gamma e^{-(S+u_n)/\tau_{fat}} \end{pmatrix}, & \text{for } A_n > 130 \end{cases} \tag{8.7}$$

$$u_n = (\gamma_1 \ \gamma_2) \begin{pmatrix} A_n - A_b \\ R_n - R_b \end{pmatrix} = \gamma_1(A_n - A_b) + \gamma_2(R_n - R_b) \tag{8.8}$$

The Jacobians of the controlled system to the left and right of the border are given by

$$\begin{aligned} \tilde{J_L} &= \begin{pmatrix} -0.31208 - 0.69860\gamma_1 & 0.99379 - 0.69860\gamma_2 \\ -0.001597 - 0.001607\gamma_1 & 0.99379 - 0.001607\gamma_2 \end{pmatrix} \\ &= \underbrace{\begin{pmatrix} -0.31208 & 0.99379 \\ -0.001597 & 0.99379 \end{pmatrix}}_{J_L} + \underbrace{\begin{pmatrix} -0.69860 \\ -0.001607 \end{pmatrix}}_{\mathbf{b}} \begin{pmatrix} \gamma_1 & \gamma_2 \end{pmatrix} \end{aligned}$$

and

$$\begin{aligned} \tilde{J_R} &= \begin{pmatrix} -1.33223 - 0.69860\gamma_1 & 0.99379 - 0.69860\gamma_2 \\ -0.001597 - 0.001607\gamma_1 & 0.99379 - 0.001607\gamma_2 \end{pmatrix} \\ &= \underbrace{\begin{pmatrix} -1.33223 & 0.99379 \\ -0.001597 & 0.99379 \end{pmatrix}}_{J_R} + \begin{pmatrix} -0.69860 \\ -0.001607 \end{pmatrix} \begin{pmatrix} \gamma_1 & \gamma_2 \end{pmatrix} \end{aligned}$$

respectively. Using the results of Section 6.4, stabilizing control gains (γ_1, γ_2) are obtained by solving (6.45)-(6.52). Figure 8.4 shows all stabilizing gains (γ_1, γ_2) that

satisfy (6.45)-(6.52), and Figure 8.5 shows the bifurcation diagram of the controlled system with $(\gamma_1, \gamma_2) = (-1, 0)$. Figure 8.6 shows the effectiveness of the control in quenching the period-2 orbit and simultaneously stabilizing the unstable fixed point. The robustness of the control law with respect to noise is demonstrated in Figure 8.7.

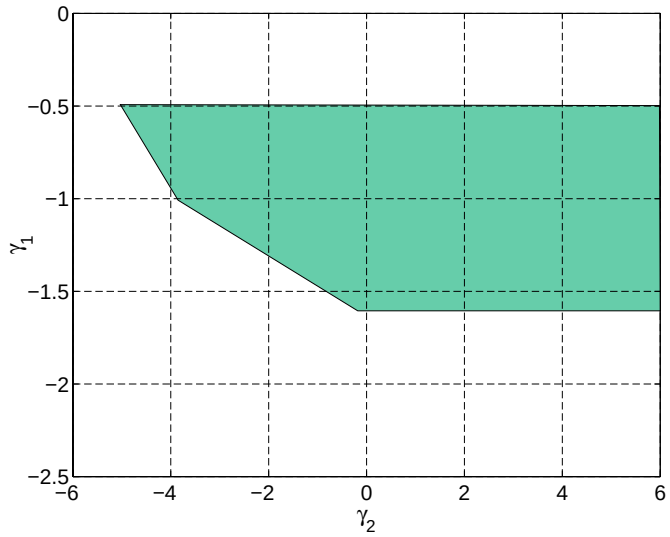

Figure 8.4: Stabilizing control gain pairs based on Proposition 6.2 are within the shaded region in the figure , with simultaneous linear state feedback control.

Lyapunov-based simultaneous feedback control design

The linearization of the cardiac model at a fixed point on the border is given by

$$\begin{pmatrix} A(k+1) \\ R(k+1) \end{pmatrix} = \begin{cases} J_L \begin{pmatrix} A(k) \\ R(k) \end{pmatrix} + b\mu + bu(k), & \text{if } A(k) \leq 130\text{ms} \\ J_R \begin{pmatrix} A(k) \\ R(k) \end{pmatrix} + b\mu + bu(k), & \text{if } A(k) > 130\text{ms} \end{cases} \tag{8.9}$$

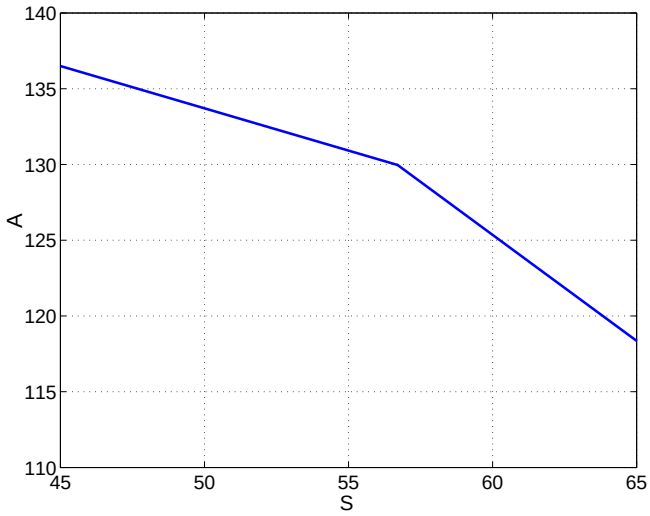

Figure 8.5: Bifurcation diagram of the controlled system using simultaneous linear state feedback with control gains $(\gamma_1, \gamma_2) = (-1, 0)$.

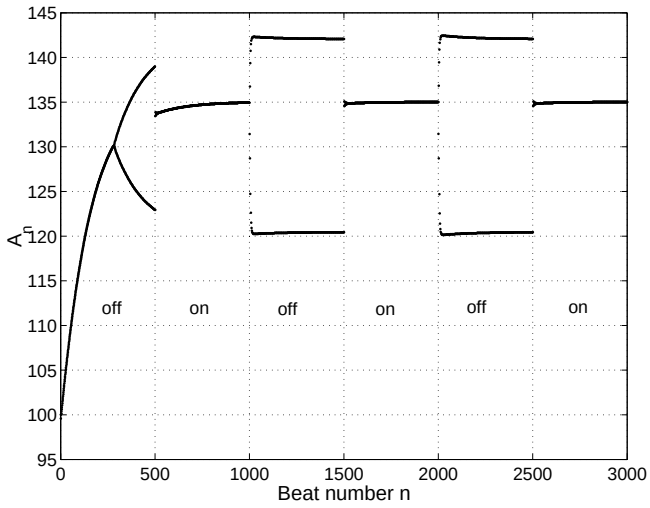

Figure 8.6: Iterations of map. Simultaneous linear state feedback control applied at beat number $n = 500$. The control is switched off and on every 500 beats to show the effectiveness of the controller ($S = 48$ms and $(\gamma_1, \gamma_2) = (-1, 0)$).

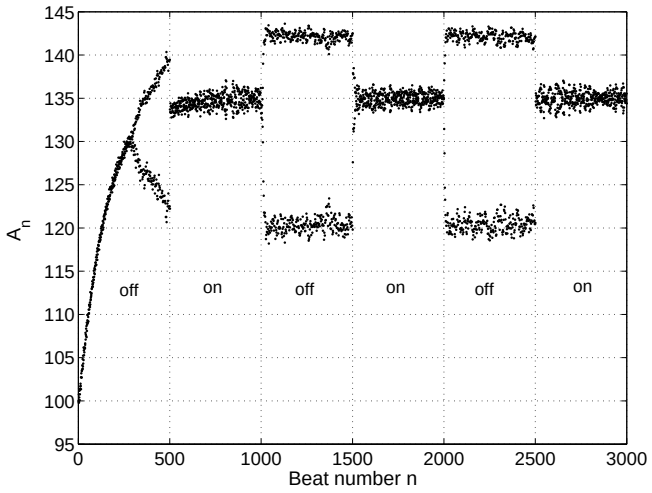

Figure 8.7: Iterations of map. Simultaneous linear state feedback control applied at beat number $n = 500$. The control is switched off and on every 500 beats to show the effectiveness of the controller ($S = 48$ms and $(\gamma_1, \gamma_2) = (-1, 0)$) when zero mean, $\sigma = 0.5$ms white Gaussian noise added to S.

where

$$J_L = \begin{pmatrix} -0.3121 & 0.9938 \\ -0.0016 & 0.9938 \end{pmatrix}, \; J_R = \begin{pmatrix} -1.3322 & 0.9938 \\ -0.0016 & 0.9938 \end{pmatrix} \text{ and } b = \begin{pmatrix} -0.69861 \\ -0.00161 \end{pmatrix}.$$

Next, we use Proposition 7.8 to seek a simultaneous feedback control that eliminates the period doubling BCB and achieve alternans quenching. The LMI package in Matlab yields

$$Q = \begin{pmatrix} 0.8499 & -0.0011 \\ -0.0011 & 0.4879 \end{pmatrix}, \tag{8.10}$$

$$y = \begin{pmatrix} -1.0018 & 0.6983 \end{pmatrix}, \tag{8.11}$$

$$\begin{aligned} g &= yQ^{-1} \\ &= \begin{pmatrix} -1.1768 & 1.4288 \end{pmatrix}. \end{aligned} \tag{8.12}$$

The limiting Jacobians of the closed-loop system are given by

$$\begin{aligned} J_{L_c} &= J_R + bg \\ &= \begin{pmatrix} 0.5100 & -0.0043 \\ 0.0003 & 0.9915 \end{pmatrix}, \\ J_{R_c} &= J_L + bg \\ &= \begin{pmatrix} -0.5101 & -0.0043 \\ 0.0003 & 0.9915 \end{pmatrix}. \end{aligned}$$

The eigenvalues of the closed-loop Jacobians are: $\sigma(J_{L_c}) = \{0.51, 0.9915\}$ and $\sigma(J_{R_c}) = \{-0.5101, 0.9915\}$. The bifurcation diagram of the open-loop and closed loop system is depicted in Figure 8.8.

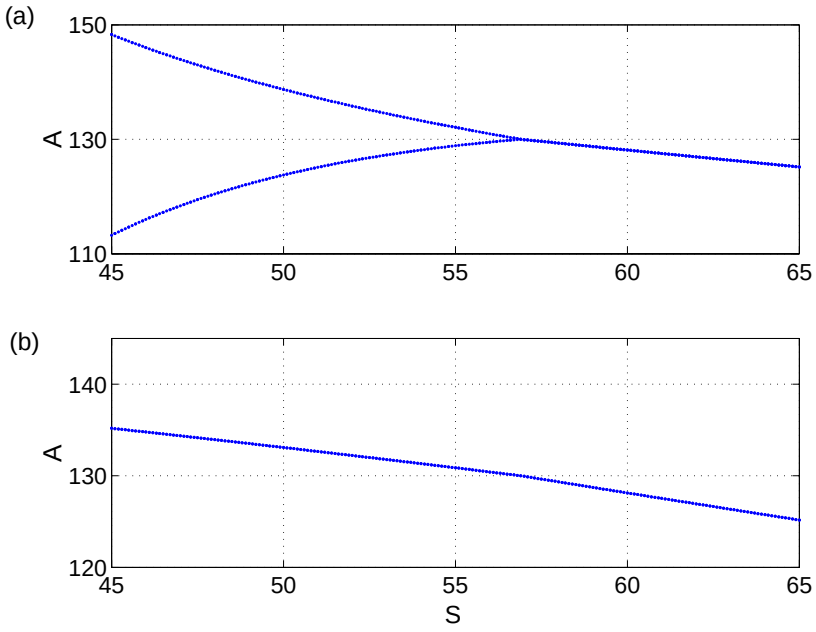

Figure 8.8: Bifurcation diagram for cardiac model ($\tau_{rec} = 70$ms, $\tau_{fat} = 30000$ms, $A_{min} = 33$ms and $\gamma = 0.3$ms). (a) Open-loop, (b) Closed-loop using simultaneous feedback control.

8.2.3 Washout Filter-Aided Feedback Control of the Period Doubling BCB

In Section 8.2.2, control of period doubling border collision bifurcation using static feedback was considered. Static linear feedback changes the operating conditions (fixed points) of the open-loop system. This results in wasted control effort and may also result in degrading system performance. Washout filter-aided linear feedback, on the other hand, does not change the value of the fixed points of the open-loop system since the control vanishes by nature at steady state. Adding a washout filter in the feedback loop provides automatic tracking of the fixed point to be stabilized even in the presence of model uncertainty or small parameter variations. This is valuable in applications where the parameters may drift, which is particularly useful for the cardiac arrhythmia model considered in this chapter. A brief summary on washout filters and their use in control applications is given Section 2.1.

Consider the cardiac model with simultaneous washout filter-aided feedback

$$\begin{pmatrix} A_{n+1} \\ R_{n+1} \end{pmatrix} = \begin{cases} \begin{pmatrix} A_{min} + R_{n+1} + (201 - 0.7A_n)e^{-(S+u_n)/\tau_{rec}} \\ R_n e^{-(A_n+(S+u_n))/\tau_{fat}} + \gamma e^{-(S+u_n)/\tau_{fat}} \end{pmatrix}, & \text{for } A_n \leq 130 \\ \begin{pmatrix} A_{min} + R_{n+1} + (500 - 3.0A_n)e^{-(S+u_n)/\tau_{rec}} \\ R_n e^{-(A_n+(S+u_n))/\tau_{fat}} + \gamma e^{-(S+u_n)/\tau_{fat}} \end{pmatrix}, & \text{for } A_n > 130 \end{cases} \tag{8.13}$$

$$w_{n+1} = A_n + (1-d)w_n \tag{8.14}$$

$$z_n = A_n - dw_n \tag{8.15}$$

$$u_n = \gamma_1 z_n \tag{8.16}$$

The Jacobians of the controlled system to the left and right of the border are given by

$$\tilde{J}_L = \begin{pmatrix} -0.31208 - 0.69860\gamma_1 & 0.99379 & 0.69860\gamma_1 d \\ -0.001597 - 0.001607\gamma_1 & 0.99379 & 0.001607\gamma_1 d \\ 1 & 0 & 1-d \end{pmatrix}$$

and

$$\tilde{J}_R = \begin{pmatrix} -1.33223 - 0.69860\gamma_1 & 0.99379 & 0.69860\gamma_1 d \\ -0.001597 - 0.001607\gamma_1 & 0.99379 & 0.001607\gamma_1 d \\ 1 & 0 & 1-d \end{pmatrix}$$

respectively. Note that only one washout filter was used in the feedback loop. In general, the number of washout filters needed is between one and the the dimension of the system. In some cases, such as the cardiac model considered here, one washout filter suffices.

Stabilizing washout filter-aided feedback parameters are obtained using the result of Proposition 7.10. Figure 8.9 shows the region of stabilizing control parameters γ_1, d, which was obtained using the LMI toolbox in Matlab.

Next, simultaneous static feedback and simultaneous washout filter-aided feedback are compared. Figure 8.10 shows the bifurcation diagram of the closed loop system for both simultaneous static feedback and simultaneous washout filter-aided feedback. Note that the (stabilized) fixed point of the closed loop system using washout filter-aided feedback coincides with the open loop (unstable) fixed point. However, the (stabilized) fixed point of the closed loop system using static state feedback is different from the open loop (unstable) fixed point. This is also evident from Figure 8.11 and Figure 8.12 which show that the control effort becomes zero in steady state when a washout filter is employed, whereas when static state feedback is used, the control effort approaches a constant value different from zero.

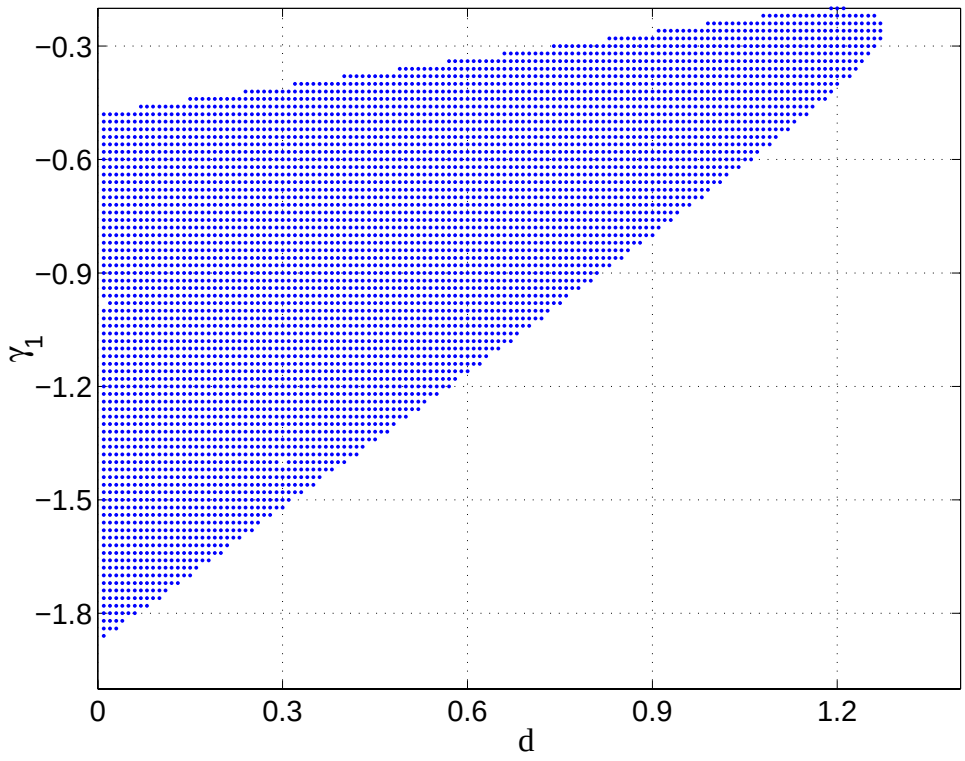

Figure 8.9: Stabilizing simultaneous washout filter-aided feedback control parameters are within the shaded region.

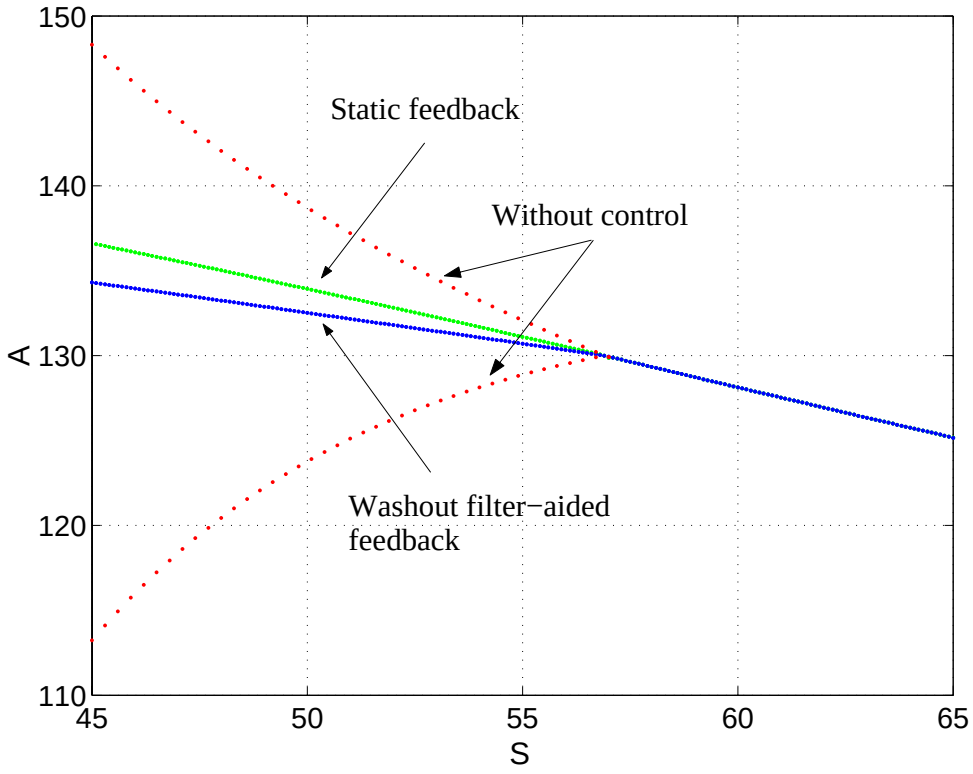

Figure 8.10: Bifurcation diagram of closed loop system, comparing static feedback control ($\gamma_1 = -1$, $\gamma_2 = 0$) with washout filter-aided feedback control ($\gamma_1 = -1$, $d = 0.1$). The (red) dotted lines represent the open loop bifurcation diagram.

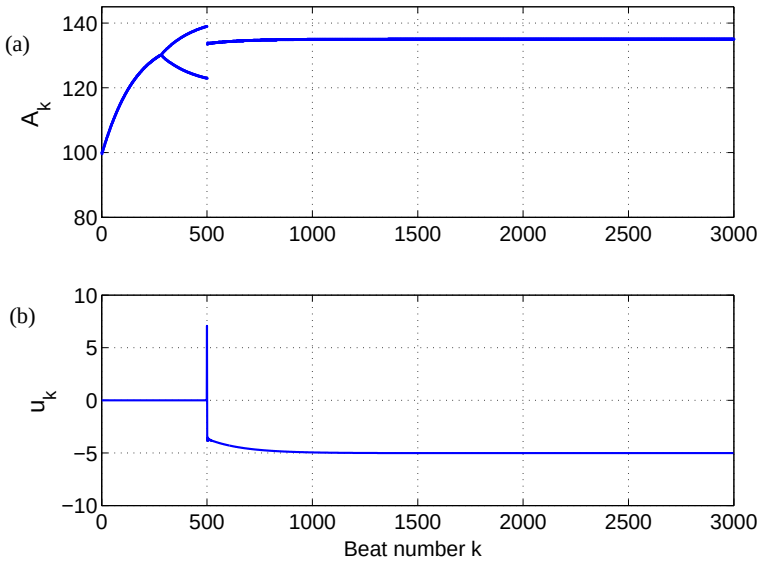

Figure 8.11: Time series of closed-loop system with static state feedback applied at beat number 500 ($\gamma_1 = -1$, $\gamma_2 = 0$ and $S = 48$), (a) Conduction time A_n, (b) Control input u_n.

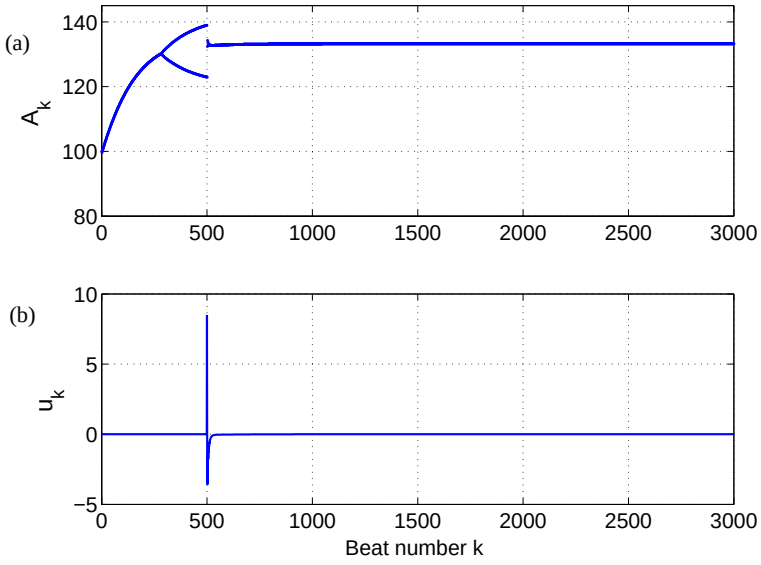

Figure 8.12: Time series of closed-loop system with washout filter-aided feedback applied at beat number 500 ($\gamma_1 = -1$, $d = 0.1$ and $S = 48$), (a) Conduction time A_n, (b) Control input u_n.

Chapter 9

Conclusions and Suggestions for Future Work

In this dissertation, feedback control of border collision bifurcation in piecewise smooth discrete-time systems was studied. First, the available results on BCBs in one dimensional PWS maps were summarized and used in the feedback control design. For two dimensional PWS maps, we have derived sufficient conditions for nonbifurcation with persistent stability. The derived conditions were then used to design stabilizing feedback control laws.

Lyapunov-based techniques were used to derive a sufficient condition for nonbifurcation with persistent stability in PWS maps of dimension n, where n is finite. The use of Lyapunov techniques facilitates the consideration of n-dimensional systems where n is not restricted to be 1 or 2. The derived condition is in terms of linear matrix inequalities (LMIs). This condition is then used as a basis for the design of feedback controls to eliminate border collision bifurcations in PWS maps and to produce desirable behavior. Both simultaneous and switched feedback control design were considered. We have shown that when simultaneous feedback control is used, only the linearizations of the PWS map on both sides of the border are needed. This alleviates the need for transformations to set the system in a normal form. Moreover,

simultaneous feedback control is robust to uncertainties in the border. The conditions on the control gains are in terms of linear matrix inequalities which can be efficiently solved using LMI solvers.

Washout filter-aided feedback was used to ensure that the fixed points of the open-loop system are not moved by the feedback action. Other advantages of washout filters include automatic fixed point following even in the presence of model uncertainty and small parameter variations. The use of washout filters was shown to lead to sufficient conditions of nonbifurcation that are in terms of bilinear matrix inequalities (BMIs). However, depending on the structure of the system under study, sometimes one washout filter is enough to stabilize the system. In such a case, the BMIs can be reduced to LMIs and solved for the control parameters.

A two-dimensional example on quenching of cardiac arrhythmia was considered. The cardiac model consists of a nonlinear discrete-time piecewise smooth system. We have shown that a period doubling border collision bifurcation occurs in the model, and that it is this bifurcation that leads to the alternan solutions. This is contrary to what has been hypothesized that a smooth period-doubling bifurcation in the model leads to the alternans. The results of the dissertation on feedback control of border collision bifurcation were applied to the model, resulting in quenching of the period doubling border collision bifurcation and hence in alternan suppression. It has been shown that washout filter-aided feedback can be used to achieve alternan quenching. The use of a washout filter facilitates stabilization of the exact value of the unstable fixed point (which corresponds to the period-1 rhythm) to be stabilized.

In the remainder of this chapter, we outline some interesting problems for future research.

It was pointed out that the basic theory of BCBs is incomplete and needs further

development in order for control problems to be adequately addressed. Among the many open problems of interest are the following:

- Detailed classification of BCBs: As was pointed out in this dissertation, the theory of border collision bifurcation for nonscalar maps is incomplete and certainly very preliminary in comparison to the results available for smooth systems. Therefore, there are a lot of gaps that need to be filled.

- Order reduction principles for BCBs: It would be very useful both for analysis and feedback control design to obtain order reduction principles for BCBs so that the study of the dynamics of multidimensional systems can be reduced to the study systems of lower dimension.

- Exchange of stability/stability of critical systems for n-dimensional PWS discrete-time systems

- Relation of critical system dynamics to multiple bifurcating attractor phenomenon.

- Performance analysis using Lyapunov techniques.

- Detailed analysis of washout filter-aided feedback control of border collision bifurcations.

APPENDIX A

Transformation to Normal Form in n-Dimensional PWS Maps

Consider the one parameter family of piecewise smooth maps

$$f(x,\mu) \quad = \quad \begin{cases} f_A(x,\mu), & x \in R_A^n \\ f_B(x,\mu), & x \in R_B^n \end{cases} \tag{9.1}$$

where $f : \mathbb{R}^{n+1} \to \mathbb{R}^n$ is piecewise smooth in x (f is smooth everywhere except on the border (hypersurface) $\Gamma(x)$ separating R_A^n and R_B^n where it is only continuous), f is smooth in μ and R_A^n, R_B^n are two regions of smooth behavior. Suppose that at $\mu = \mu_b$, a fixed point of f is at the border separating R_A and R_B, i.e., $\Gamma(x_0(\mu)) = 0$. Assume without loss of generality that $\mu_b = 0$ and $x_0(0) = 0$. We also assume that the hypersurface $\Gamma(x)$ is smooth around 0. Suppose that $\frac{\partial \Gamma(0)}{\partial x_1} \neq 0$, then using the implicit function theorem (see for instance [32, p. 408]), one can solve for x_1 in terms of x_i, $i = 2, \cdots, n$. That is, there exists a neighborhood $N \subset \mathbb{R}^{n-1}$ containing the origin and a continuously differentiable mapping $G : N \to \mathbb{R}$ such that $\Gamma(G(x_2, x_3, \cdots, x_n), x_2, x_3, \cdots, x_n) = 0$, $\forall x \in N$ and whenever $x \in N$ and $\Gamma(x) = 0$, then $x_1 = G(x_2, x_3, \cdots, x_n)$.

Now consider the following state transformation:

$$v_1 \quad := \quad x_1 - G(x_2, x_3, \cdots, x_n) \tag{9.2}$$

$$v_i \quad := \quad x_i, \; i = 2, \cdots, n. \tag{9.3}$$

This transformation is invertible. To see this, we calculate the Jacobian of the transformation:

$$\begin{pmatrix} \frac{\partial v_1}{\partial x_1} & \frac{\partial v_1}{\partial x_2} & \cdots & \frac{\partial v_1}{\partial x_n} \\ \vdots & \vdots & \ddots & \vdots \\ \frac{\partial v_n}{\partial x_1} & \frac{\partial v_n}{\partial x_2} & \cdots & \frac{\partial v_n}{\partial x_n} \end{pmatrix} = \begin{pmatrix} 1 & \frac{\partial G}{\partial x_2} & \cdots & \cdots & \frac{\partial G}{\partial x_n} \\ 0 & 1 & 0 & \cdots & 0 \\ \vdots & 0 & \ddots & 1 & 0 \\ 0 & 0 & \cdots & 0 & 1 \end{pmatrix}. \tag{9.4}$$

Thus, the transformation to the normal for is a similarity transformation, hence the eigenvalues are preserved. In the new coordinates, the border is the hyperplane $v_1 = 0$. Thus, the normal form for BCBs in n-dimension follows

$$v(k+1) = \begin{cases} Av(k) + \mu b, & \text{if } v_1(k) \leq 0 \\ Bv(k) + \mu b, & \text{if } v_1(k) > 0 \end{cases} \tag{9.5}$$

where A and B are the linearizations of the PWS map after transformation on both sides of the border, respectively and b is the derivative of the map with respect to μ.

BIBLIOGRAPHY

[1] E. H. Abed and J.-H. Fu. Local feedback stabilization and bifurcation control, II. Hopf bifurcation. *Systems and Control Letters*, 8(5):467–473, May 1987.

[2] E. H. Abed, H. O. Wang, and R. C. Chen. Stabilization of period-doubling bifurcations and implications for control of chaos. *Physica D*, 70(1-2):154–164, Jan 1994.

[3] E. H. Abed, H. O. Wang, and A. Tesi. Control of bifurcations and chaos. In W.S. Levine, editor, *The Control Handbook*, chapter 56.7, pages 951–966. CRC Press, Boca Raton, FL, 1996.

[4] E.H. Abed and J.-H. Fu. Local feedback stabilization and bifurcation control, I. Hopf bifurcation. *Systems and Control Letters*, 7(1):11–17, Feb 1986.

[5] D. Aeyels and J. Peuteman. A new asymptotic stability criterion for nonlinear time-variant differential equations. *IEEE Transactions on Automatic Control*, 43(7):968–971, July 1998.

[6] M. Akar and K. S. Narendra. On the existence of a common quadratic Lyapunov function for two stable second order LTI discrete-time systems. In *Proceedings of the American Control Conference*, pages 2572–2577, Arlington, VA, June 2001.

[7] J. Alvarez-Ramirez. Dynamics of controlled-linear discrete time systems with a dead-zone nonlinearity. In *American Control Conference*, volume 1, pages 761–765, 1994.

[8] J. Alvarez-Ramirez. Border-collision crises in a two-dimensional map. *International Journal of Bifurcation and Chaos*, 5(1):275–279, 1995.

[9] S. Banerjee and C. Grebogi. Border collision bifurcations in two-dimensional piecewise smooth maps. *Physical Review E*, 59(4):4052–4061, 1999.

[10] S. Banerjee, M. S. Karthik, G. H. Yuan, and J. A. Yorke. Bifurcations in one-dimensional piecewise smooth maps- theory and applications in switching systems. *IEEE Transactions on Circuits and Systems I*, 47(3):389–394, 2000.

[11] S. Banerjee, P. Ranjan, and C. Grebogi. Bifurcations in two-dimensional piecewise smooth maps — theory and applications in switching circuits. *IEEE Transactions on Circuits and Systems-I*, 47(5):633–643, 2000.

[12] S. Banerjee, J. A. Yorke, and C. Grebogi. Robust chaos. *Physical Review Letters*, 80:3049–3052, April 1998.

[13] J. H. Blakelock. *Automatic Control of Aircraft and Missiles*. Wiley, New York, 1965.

[14] S. Boyd, L.El Ghaoui, E.Feron, and V.Balakrishnan. *Linear Matrix Inequalities in System and Control Theory*. SIAM, 1994.

[15] M. E. Brandt, H. T. Shih, and G. Chen. Linear time-delay feedback control of a pathological rhythm in a cardiac conduction model. *Physical Review E*, 56(2):R1334–R1337, Aug 1997.

[16] D. Chen, H.O. Wang, and W. Chin. Suppressing cardiac alternans: Analysis and control of a border-collision bifurcation in a cardiac conduction model. In *IEEE International Symposium on Circuits and Systems*, volume 3, pages 635–638, 1998.

[17] D. J. Christini and J. J. Collins. Using chaos control and tracking to suppress a pathological nonchaotic rhytms in cardiac model. *Physical Review E*, 53(1):R49–R51, Jan 1996.

[18] H. Dankowicz and A. B. Nordmark. On the origin and bifurcations of stick-slip oscillations. *Physica D*, 136(3-4):280–302, Feb 2000.

[19] M. di Bernardo. The complex behavior of switching devices. *IEEE CAS Newsletter*, 10(4), Dec 1999.

[20] M. di Bernardo. Controlling switching systems: a bifurcation approach. *IEEE International Symposium on Circuits and Systems*, 2:377–380, 2000.

[21] M. di Bernardo, C. J. Budd, and A. R. Champneys. Corner collision implies border-collision bifurcation. *Physica D*, 154:171–194, 2001.

[22] M. di Bernardo and G. Chen. Controlling bifurcations in nonsmooth dynamical systems. In G. Chen and X. Dong, editors, *Controlling Chaos and Bifurcations in Engineering Systems*, chapter 18, pages 391–412. CRC Press, Boca Raton, FL, 2000.

[23] M. di Bernardo, M. I. Feigin, S. J. Hogan, and M. E. Homer. Local analysis of *C*-bifurcations in *n*-dimensional piecewise smooth dynamical systems. *Chaos, Solitons & Fractals*, 10(11):1881–1908, 1999.

[24] M. di Bernardo, F. Garofalo, L. Iannelli, and F. Vasca. Bifurcations in piecewise-smooth feedback systems. *International Journal of Control*, 75(16/17):1243–1259, 2002.

[25] M. Dutta, H. E. Nusse, E. Ott, J. A. Yorke, and G. H. Yuan. Multiple attractor bifurcations: A source of unpredictability in piecewise smooth systems. *Physical Review Letters*, 83(21):4281–4284, Nov 1999.

[26] K. Hall et al. Dynamic control of cardiac alternans. *Physical Review Letters*, 78:4518–4521, 1997.

[27] M. I. Feigin. Doubling of the oscillation period with C-bifurcations in piecewise continuous systems. *Prikladnaya Matematika i Mechanika*, 34:861–869, 1970.

[28] M. I. Feigin. The increasingly complex structure of the bifurcation tree of a piecewise-smooth system. *Journal of Applied Mathematics and Mechanics*, 59(6):853–863, 1995.

[29] G. Feng. Stability analysis of piecewise discrete-time linear systems. *IEEE Transactions on Automatic Control*, 47(7):1108–1112, July 2002.

[30] G. Ferrari-Trecate, F. A. Cuzzola, D. Mignone, and M. Morari. Analysis of discrete-time piecewise affine and hybrid systems. *Automatica*, 38:2139–2146, Dec 2002.

[31] V. Firoiu and M. Borden. A study of active queue management for congestion control. *Proceedings of INFOCOM*, 3:1435–1444, 2000.

[32] P. M. Fitzpatrick. *Advanced Calculus: A course in mathematical analysis*. ITP, Boston, MA, 1996.

[33] M. H. Frederiksson and A. B. Nordmark. Bifuractions caused by grazing incidence in many degrees of freedom impact oscillators. *Proc. Royal Soc. Lond. A*, 453:1261–1276, June 1997.

[34] P. Gahinet, A. Nemirovski, A. L. Laub, and M. Chilali. *LMI Control Toolbox*. The Math Works Inc., Natick, MA, 1995.

[35] J. Guckenheimer and P. Holmes. *Nonlinear Oscillations, Dynamical Systems, and Bifurcations of Vector Fields*. Springer-Verlag, New York, 1983.

[36] M. A. Hassouneh and E. H. Abed. Border collision bifurcation control of cardiac alternans. In *Proceedings of the American Control Conference*, pages 459–464, Denver, CO, June 2003.

[37] M. A. Hassouneh and E. H. Abed. Control of border collision bifurcations. In W. Kang, M. Xiao, and C. Borges, editors, *New Trends in Nonlinear Dynamics and Control, and Their Applications*, volume 295, pages 49–64. Springer-Verlag, 2003.

[38] M. A. Hassouneh and E. H. Abed. Border collision bifurcation control of cardiac alternans. *International Journal of Bifurcation and Chaos*, 14(9), Sept. 2004. to appear.

[39] M. A. Hassouneh, E. H. Abed, and H. E. Nusse. Robust dangerous border-collision bifurcations in piecewise smooth systems. submitted for publication.

[40] C. H. Hommes and H. E. Nusse. Period 3 to period 2 bifurcation for piecewise linear-models. *Journal of Economics*, 54(2):157–169, 1991.

[41] C. S. Hsu, E. Kreuzer, and M. C. Kim. Bifurcation characteristics of piecewise linear mappings and their applications. *Dynamics and Stability of Systems*, 5(4):227–254, 1990.

[42] M. Johansson. *Piecewise Linear Control Systems*. Ph.D. thesis, Lund Institute of Technology, Lund, Sweden, 1999.

[43] M. Johansson and A. Rantzer. Computation of piecewise quadratic Lyapunov functions for hybrid systems. *IEEE Transactions on Automatic Control*, 43:555–559, April 1998.

[44] M. Kantner. Robust stability of piecewise linear discrete time systems. In *Proceedings of the American Control Conference*, pages 1241–1245, Albuquerque, NM, June 1997.

[45] T. Kousaka, T. Kido, T. Ueta, H. Kawakami, and M. Abe. Analysis of border-collision bifurcation in a simple circuit. In *IEEE International Symposium on Circuits and Systems*, volume 2, pages 481–484, Geneva, Switzerland, May 2000.

[46] X. D. Koutsoukos and P. J. Antsaklis. Design of stabilizing switching control laws for discrete- and continuous-time linear systems using piecewise-linear Lyapunov functions. *International Journal of Control*, 75(12):932–945, August 2002.

[47] Y. A. Kuznetsov. *Elements of Applied Bifurcation Theory*, volume 112. Springer, 2nd edition, 1995.

[48] S. Lall. Lecture notes on robust control analysis and synthesis. Stanford University, 2002.

[49] H. -C. Lee. *Robust Control of Bifurcating Nonlinear Systems with Applications*. PhD thesis, University of Maryland, College Park, USA, 1991.

[50] H. C. Lee and E. H. Abed. Washout filters in the bifurcation control of high alpha flight dynamics. In *Proceedings of the American Control Conference*, pages 206–211, Boston, MA, 1991.

[51] R. I. Leine and D. H. Van Campen. Discontinuous fold bifurcations in mechanical systems. *Archive of Applied Mechanics*, 72:138–146, 2002.

[52] R. I. Leine, D. H. Van Campen, and B. L. Van de Vrande. Bifurcations in nonlinear discontinuous systems. *Nonlinear Dynamics*, 23:105–164, 2000.

[53] D.-C. Liaw and E. H. Abed. Active control of compressor stall inception: a bifurcation-theoretic approach. *Automatica*, 32(1):109–115, 1996.

[54] D. P. Lindorff. *Theory of Sampled-Data Control Systems*. Wiley, New York, 1965.

[55] G. M. Maggio, M. di Bernardo, and M. P. Kennedy. Nonsmooth bifurcations in a piecewise-linear model of the collpitts oscillator. *IEEE Transactions on Circuits and Systems-I*, 47(8):1160–1177, August 2000.

[56] O. Mason and R. Shorten. On common quadratic Lyapunov functions for stable discrete-time LTI systems. Preprint, 2003.

[57] D. Mignone, G. Ferrari-Trecate, and M. Morari. Stability and stabilization of piecewise affine and hybrid systems: an LMI approach. In *Conference on Decision and Control*, volume 1, pages 504–509, Sydney, Australia, Dec 2000.

[58] A. B. Nordmark. Non-periodic motion caused by grazing incidence in impact oscillators. *Journal of Sound and Vibration*, 2:279–297, 1991.

[59] A. B. Nordmark. Universal limit mapping in grazing bifurcations. *Physical Review E*, 55:266–270, 1997.

[60] H. E. Nusse, E. Ott, and J. A. Yorke. Border-collision bifurcation: An explanation for an observed phenomena. *Physical Review E*, 201:197–204, 1994.

[61] H. E. Nusse and J. A. Yorke. Border-collision bifurcations including "period two to period three" for piecewise smooth maps. *Physica D*, 57:39–57, 1992.

[62] H. E. Nusse and J. A. Yorke. Border-collision bifurcations for piecewise smooth one-dimensional maps. *International Journal of Bifurcation & Chaos*, 5:189–207, 1995.

[63] M. Ohnishi and N. Inaba. A singular bifurcation into instant chaos in piecewise-linear circuit. *IEEE Transactions on Circuits and Systems I Communications and Computer Sciences*, 41(6), June 1994.

[64] F. Peterka and T. Kotera. Four ways from periodic to chaotic motions in the impact oscillator. *Machine Vibration*, 5:71–82, 1996.

[65] P. Ranjan, E. H. Abed, and R. J. La. Nonlinear instabilities in TCP-RED. In *INFOCOM*, volume 1, pages 249–258, New York, NY, 2002.

[66] B. Robert and C. Robert. Border collision bifurcations in a one-dimensional piecewise smooth map for a PWM current programmed h-bridge inverter. *International Journal of Control*, 75(16/17):1356–1367, 2002.

[67] T. Shinbrot, C. Grebogi, E. Ott, and J.A. Yorke. Using small perturbations to control chaos. *Nature*, 363(3):411–417, 1993.

[68] O. Slupphaug and B. A. Foss. Constrained quadratic stabilization of discrete-time uncertain non-linear multi-model systems using piecewise affine state-feedback. *International Journal of Control*, 72(7-8):686–701, May 1999.

[69] J. Sun, F. Amellal, L. Glass, and J. Billette. Alternans and period-doubling bifurcations in atrioventricular nodal conduction. *Journal Theoretical Biology*, 173:79–91, 1995.

[70] H. Tanaka and T. Ushio. Analysis of border-collision bifurcations in a flow model of a switching system. *IEICE Transactions on Fundamentals of Electronics, Communications and Computer Sciences*, E85-A(4):734–739, 2002.

[71] J. M. T. Thompson and H. B. Stewart. *Nonlinear Dynamics and Chaos*. John Wiley and Sons, UK, 1986.

[72] H. O. Wang and E. H. Abed. Bifurcation control of a chaotic system. *Automatica*, 31(9):1213–1226, Sep 1995.

[73] G. H. Yuan. *Shipboard Crane Control, Simulated Data Generation and Border Collision Bifurcations*. PhD thesis, University of Maryland, College Park, USA, 1997.

[74] G. H. Yuan, S. Banerjee, E. Ott, and J. A. Yorke. Border collision bifurcations in the buck converter. *IEEE Transactions on Circuits and Systems-I*, 45(7):707–716, 1998.

[75] F. Zheng, Q.-G. Wang, and T. H. Lee. A heuristic approach to solving a class of bilinear matrix inequality problems. *Systems and Control Letters*, 47:111–119, 2002.

[76] Z. T. Zhusubaliyev, E. A. Soukhoterin, and E. Mosekilde. Border-collision bifurcations and chaotic oscillations in a piecewise-smooth dynamical system. *International Journal of Bifurcation and Chaos*, 11(12):2977–3001, Dec 2001.

[77] Z. T. Zhusubaliyev and V. S. Titov. C-bifurcations in the dynamics of control system with pulse-width modulation. In *Proceedings of 2nd International Conference*, volume 1, pages 203–204, 2000.